

2D ELASTO-PLASTIC FINITE ELEMENT ANALYSIS OF TUNNELS IN DUBAI,
UAE

by

Nasser Al Hai

A Thesis Presented to the Faculty of the
American University of Sharjah
College of Engineering
in Partial Fulfillment
of the Requirements
for the Degree of
Master of Science in
Civil Engineering

Sharjah, United Arab Emirates

June 2012

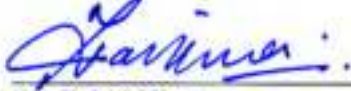
Approval Signatures

We, the undersigned, approve the Master's Thesis of Nasser Al Hai.

Thesis Title: 2DElasto-Plastic finite element analysis of tunnels in Dubai, UAE

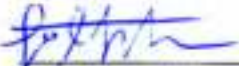
Signature

Date of Signature



Dr. Zahid Khan
Assistant Professor
Department of Civil Engineering
Thesis Advisor

06-06-2012.



Dr. Mousa Attom
Professor
Department of Civil Engineering
Thesis Committee Member

06/06/2012



Dr. Farid Abed
Associate Professor
Department of Civil Engineering
Thesis Committee Member

06-06-2012



Dr. Maher Omar
Associate Professor,
Department of Civil Engineering, University of Sharjah
Thesis Committee Member

06-06-2012



Dr. Jamal El-Din Abdalla
Head, Department of Civil Engineering

10/6/2012



Dr. Hany El Kadi
Associate Dean, College of Engineering

19/6/2012



Dr. Yousef Al-Assaf
Dean of College of Engineering

19/6/12



Dr. Khaled Assaleh
Director of Graduate Studies

21/06/2012

Acknowledgements

During the long work, planning and preparation of this thesis, I have incurred indebtedness to many people. First of all, I would like to express my sincere gratitude and deep appreciation to Dr. Zahid Hamid Khan, College of Engineering, Civil Engineering Department, American University of Sharjah for his direct, kind and effective supervision, valuable guidance, helpful discussions, encouragement, and valuable advice throughout all phases of this work.

The author is indebted with great favor to Prof. Dr. Jamal Abdalla, Professor and Head of Civil Engineering Department, American University of Sharjah for his helpful advice, appreciable guidance and support, discussions, companionship, and enormous contribution in all my post graduate studies.

My appreciation is also extended to the members of my examining committee, Dr. Farid Abed, Assistant Professor and Dr. Basil Darras, Assistant Professor, Civil Engineering Department, American University of Sharjah.

I would also like to thank Eng. Mohammad Serhan, and his staff for their continuous co-operation and offering all facilities during all stages of research work.

I wish also to express my sincere thanks to my colleagues and friends in Permit Section, Posts, Customs & Free Zone Corporation, Trakhees. In particular Eng. Wael Mohammad, for his effort and co-operation in selection the soil model, the numerical analysis software, and valuable discussions during finite element analysis. His constructive suggestions and valuable criticism are to be deeply acknowledged. I also extend my appreciation to Eng. Abdullah Belhoul, for helping me during the stage of data collection, wishing them the best of luck in their walk of life.

This work would not have been possible without the support, patience, love in all times, and understanding of my mother.

Deeds not words, with my great pleasure, I dedicate this work to my mother and to the Al Hai family.

Dedication

I dedicate this thesis to my mother and to the Al Hai family.

Abstract

Major cities in UAE in general and Dubai in particular are facing significant challenges in terms of traffic flow patterns. Tunnels are being considered as viable option to alleviate the problems faced by transportation networks. The construction of tunnels at different depths requires insight into the behavior of regional soils to avoid unfavorable effects on surface settlements. This research is an attempt to evaluate the effect of geotechnical properties of regional soil, tunnel diameter, and overburden depth on the deformation around the tunnel and ground surface. The study involved finite element modeling of regional soils with commercially available software package of PLAXIS 2D. The results of this study indicate that geotechnical properties across the Dubai city vary and affect the deformation characteristics of the ground due to tunnel excavation. The deformations around the tunnel and at the ground surface are significantly affected by the depth of the tunnel and diameter of the tunnel. The largest effect was created by the combination of 8 m tunnel at a depth of 10 m from the ground surface. To control the deformations to within acceptable limits, tunnel shall be located within the Calcareous Limestone at depths exceeding 20 m. Limiting deformations to within acceptable limits; however, imposes larger support pressures which can result in excessive investment in support design. Maximum deformations with in the tunnel are noted in the crown. This happens due to the arching effect of the soil above the crown which tends to share the stresses if some deformations are allowed. The deformations at the surface diminish laterally from the tunnel axis. The effect of tunneling on surface settlements is negligible after a lateral distance of 6 times the diameter of the tunnel from the tunnel alignment. Settlement monitoring guidelines are also developed as the result of this study. It is recommended to monitor the ground surface for settlement at least 3 times the tunnel diameter in both lateral directions. The settlement monitoring line should be installed in advance leading the face of the tunnel by 30 m. Three alert levels have been proposed.

Search Terms: Tunnels; Finite Elements; Deformations; TBM; UAE

Table of Contents

	Abstract.....	6
	Table of Contents.....	7
	List of Figures.....	9
	List of Tables.....	11
	CHAPTER 1: Introduction	12
1.1	General Introduction.....	12
1.2	Objective of Study.....	13
1.3	Organization of the Thesis.....	14
	CHAPTER 2: Background	16
2.1	Tunnelling Methods.....	16
2.1.1	Classical Methods.....	17
2.1.2	Open Face Tunnelling.....	19
2.1.3	Rock Mass Rating.....	25
2.2	Methods of Analysis.....	25
2.2.1	Lining Forces.....	28
2.2.2	Assessment of Settlements.....	29
2.2.3	Ground Pressure.....	37
2.2.4	Extension of Assessments.....	42
2.3	Numerical Modelling and Finite Elements.....	46
2.3.1	Historical Remarks.....	47
2.3.2	Finite Element Method and Basic Terms.....	48
2.4	PLAXIS 2D.....	54
2.4.1	Short Review of Features.....	55
	CHAPTER 3: Development of Models	58
3.1	Study Area.....	58
3.2	Geology.....	58
3.2.1	Physiography of Dubai.....	61
3.2.2	Geology of Dubai.....	62
3.3	Sites Considered for Modelling.....	63
3.4	Numerical Modelling of Sites.....	71
3.4.1	Component, Analysis, and Procedures.....	72

3.4.2	The Mohr-Coulomb Model.....	75
3.5	Verification Examples.....	77
3.5.1	Elastic Problems with Known Solutions.....	78
3.6	Combinations of Models.....	83
	CHAPTER 4: Results and Discussion	90
4.1	Typical Simulation Results.....	90
4.2	Effect of Soil Properties on Output.....	92
4.3	Deformation.....	96
4.3.1	Comparison of deformations at different sites.....	100
4.3.2	Forces on Tunnel Lining.....	103
4.4	Settlement Monitoring Program.....	105
	CHAPTER 5: Conclusions and Recommendations	110
5.1	Conclusions.....	110
5.2	Recommendations.....	112
	REFERENCES.....	114
	Appendix A – Borehole Logs.....	118
	Appendix B – Deformation Plots.....	147
	Appendix C – Deformations for All Combinations.....	176
	Vita.....	184

List of Figures

Figure 2.1	Tunnelling Classical Methods (Crown-Bar Method).....	18
Figure 2.2	Tunnelling Classical Methods (Cross-Bar Method)).....	19
Figure 2.3	Principals of conventional tunnelling to control ground stability	20
Figure 2.4	Shield tail with grouting of the ground-lining gap.....	21
Figure 2.5	Typical Layout of a TBM).....	24
Figure 2.6	Classification of tunnel Excavation Machines.....	24
Figure 2.7	Tunnel induced settlement trough.....	27
Figure 2.8	Principal components of ground deformation.....	27
Figure 2.9	Gaussian curve for transverse settlement trough and ground loss..	30
Figure 2.10	Relation between settlement trough width and tunnel depth.....	31
Figure 2.11	Observed width of surface settlement trough.....	32
Figure 2.12	GLR versus load factor LF in over consolidated clay.....	34
Figure 2.13	Longitudinal settlement trough above tunnel centre line.....	36
Figure 2.14	Illustration of development of ground pressures.....	37
Figure 2.15	Different distributions of ground loads on tunnel linings.....	38
Figure 2.16	Plane-strain design models for different depths and ground stiffnesses.....	39
Figure 2.17	Earth pressure changes due to the shield machine advancement...	43
Figure 2.18	Brief Flow Chart of Any Finite Elements Program.....	53
Figure 3.1	Plan of Dubai with location of Projects.....	60
Figure 3.2	Physiography Divisions of Dubai.....	62
Figure 3.3	Soil Formation representing Dubai Stratifications-Plate 1.....	65
Figure 3.4	Soil Formation representing Dubai Stratifications-Plate 2.....	66
Figure 3.5	Soil Formation representing Dubai Stratifications-Plate 3.....	67
Figure 3.6	Soil Formation representing Dubai Stratifications-Plate 4.....	68
Figure 3.7	Soil Formation representing Dubai Stratifications-Plate 5.....	69
Figure 3.8	Soil Formation representing Dubai Stratifications-Plate 6.....	70
Figure 3.9	Nodes and stress points.....	72
Figure 3.10	The Mohr Coulomb yield surface in principal stress space.....	76
Figure 3.11	Geometry of Smooth Rigid Strip Footing on Elastic So.....	78
Figure 3.12	Pressure Distribution at Smooth Rigid Strip Footing on Elastic Soil.....	79

Figure 3.13	Calculated deflections compared with analytical solutions for Ring Beam.....	80
Figure 3.14	Cylindrical cavity expansion.....	81
Figure 3.15	Mesh for cavity expansion.....	82
Figure 3.16	Relationships between radial displacement and cavity pressure....	82
Figure 3.17	Definition of E0 and E50 for standard drained triaxial test results.....	87
Figure 3.18	Stress circles at yield; one touches Coulomb's envelope.....	87
Figure 4.1	Deformation for site PJA with tunnel diameter 5.00 m at depth of 10.0 m.....	91
Figure 4.2	Contours of relative shear stress for site PJA with tunnel diameter 8.00 m at depth of 10.0 m.	92
Figure 4.3	Deformation plots for site AB with tunnel diameter 5.00 m at depth of 10.0 m.....	97
Figure 4.4	Deformation plots for site AB with tunnel diameter 5.00 m at depth of 20.0 m.	98
Figure 4.5	Deformation plots for site ABd with tunnel diameter 5.00 m at depth of 10.0 m.	99
Figure 4.6	Distribution of total displacements in the tunnel periphery.....	104
Figure 4.7	Distribution of axial force on the tunnel lining.....	104
Figure 4.8	Distribution of a) shear force and b) bending moment in the tunnel lining.....	105
Figure 4.9	Typical configuration of surface settlement monitoring points across the tunnel alignment.....	107

List of Tables

Table 2.1	Major Components of TBM.....	23
Table 2.2	RMR conditions and ratings.....	26
Table 2.3	Development of settlement profile.....	36
Table 3.1	The Litho-Stratigraphic Units of Dubai Area.....	63
Table 3.2	List of Projects Considered for the Soil Models.....	64
Table 3.3	Material properties of the tunnel lining (beam)	75
Table 3.4	Details of each Run.....	86
Table 3.5	Range of material properties at sites.....	88
Table 4.1	Maximum values of Deformations at Site AB (in mm)	98
Table 4.2	Maximum values of Deformations at Site ABd (in mm)	99
Table 4.3	Maximum values of Deformations (mm) for 5 m dia and 10 m depth.....	100
Table 4.4	Maximum values of Deformations (mm) for 5 m dia and 20 m depth.....	101
Table 4.5	Maximum values of Deformations (mm) for 8 m dia and 10 m depth.....	102
Table 4.6	Maximum values of Deformations (mm) for 8 m dia and 20 m depth.....	103

Chapter 1: INTRODUCTION

1.1. General Introduction

Expansion of transportation infrastructure in cities often involves the construction of tunnels. In cities it is difficult to avoid the effects of tunneling on the existing structures. Major cities in UAE are facing significant congestion in traffic flow and construction of new tunnels in near future may become unavoidable. Moreover, the connections of cities to each other will also require tunnels to meet the traffic demands. Many of these urban areas are in close proximity to sea and groundwater resources where soils are generally weak. The construction of major tunneling projects in UAE is foreseeable in near future; however, the behavior of regional soils to underground excavation is least understood.

Tunnel construction by means of TBM (Tunnel Boring Machine) has become a preferred method of construction nowadays. Moreover, this is well accepted by the environmentalist and the groups advocating green technology. This state-of-art technology limits all works underground in building the tunnel to keep the disturbance to land, wildlife and mankind activities at ground level to a minimum throughout the period of construction. Tunnel construction by TBM is quite different from the traditional Drill and Blast Method. The tunnel is excavated by means of a machine instead of blasting with explosives. The tunnel lining is constructed at the back of the machine immediately behind the TBM shield (Lee and Rowe, 2008). The soil behavior discussed in this study is assumed to be governed by an elastic perfectly plastic constitutive relation based on the widely adopted Mohr–Coulomb criterion with a non-associative flow rule.

Tunnel engineers traditionally use a number of elementary methods of analysis, which comprise a large variety of empirical, simple (mostly elastic or elastoplastic) analytical or bedded beam models for the assessment of surface settlements and lining forces. On reviewing the literature on the aspects of elementary design methods with respect to installation procedures, one gets the impression that peculiarities of support and excavation of different tunneling methods are hardly accounted for. Nevertheless, elementary methods of analysis are still frequently used

in engineering practice and they cannot be omitted as they reflect both tunneling tradition and design experience. However, with the rise of computer capacity, complex numerical methods came into the realm of design practice and tunneling can thus be simulated more realistically. Both non-linear ground behavior and complex geometries, such as ground layering or noncircular tunnel cross sections can easily be accounted for. Moreover, the effects of tunnel support installation may be incorporated, in order to arrive at appropriate loads on the lining and realistically estimate associated surface settlements.

The transition from elementary methods of analysis to advanced numerical analysis should not be abrupt and a sufficient validation in terms of measurements and engineering experience should be gained before bidding farewell to a well proven approach. The present thesis is intended to contribute to the effective application of numerical analysis of tunneling settlements and lining forces.

The construction of tunnels at shallow depths requires determination and continuous monitoring of soil settlement at the ground surface. The settlement and stability of the tunnel depends on many variables such as properties of soil, thickness of overburden, tunnel diameter, and most importantly excavation techniques that are governed by guidelines to the contractor. Consequently, settlement monitoring program must be implemented during the construction of tunnels. Such settlements may create unfavorable effects on buildings which were constructed at ground surface and are closer to the center of tunnel. Tunnel-induced settlements must be carefully predicted and monitored to avoid damage to nearby structures.

1.2. Objectives of Study

The objectives of this study are based on the review of available and published case studies involving predicted and observed behavior of tunnels. The observations recorded inside and outside (at the surface) of the tunnel along with other parameters such as tunneling techniques and support installation procedure will be reviewed to form the basis of simulation methodology for this study.

The purpose of the research is to develop numerical models, able to provide realistic modeling of the interaction between tunneling processes and the surrounding

soil applicable to the regional soils. In the long term such a model should become a useful predictive tool for development of construction specifications, guidelines, and development of settlement monitoring programs. Central to the analysis is the recognition that the tunnel, the soil and any adjacent buildings are inextricably linked by the ground surface settlement.

Moreover, this research is an attempt to evaluate the effect of geotechnical properties of soil, elasto-plastic behavior, tunnel diameter, and overburden on the analysis. The effect of soil arching effect on the stress acting on the tunnel as well as both axial forces and bending moment in the lining will be studied. Moreover, the critical case of construction which results in maximum lining internal forces and / or the maximum surface ground settlement will be determined.

The main outcomes of this research are summarized below:

1. Evaluation of the deformation behavior of regional soils due to the construction of tunnels.
2. Evaluation of the effect of tunnel diameter and overburden depth on the deformations in the soil mass.
3. Evaluation of the effect of properties of regional soils on the behavior of tunnel and ground surface.
4. Development of guidelines for the settlement monitoring program during tunneling.
5. Development of recommendations for the future studies on the numerical simulations of tunneling in the region.

1.3. Organization of The Thesis

The manuscript is organized in the following chapters:

Chapter 1: INTRODUCTION

Chapter 2: BACKGROUND. A discussion of different methods of tunnel construction, methods of analysis, and literature review are presented. This chapter also presents the general background of finite element analysis and PLAXIS 2D.

Chapter 3: DEVELOPMENT OF MODELS. In this chapter, the selected subsurface models and their development in the PLAXIS 2D are presented. Validation procedures and results are also presented.

Chapter 4: RESULTS AND DISCUSSION. This chapter presents the results of the modeling. The results present the effect of changing different parameters on the deformation characteristics of soils around the tunnel and ground surface. Guidelines for the settlement monitoring program are also developed on the basis of discussions and presented.

Chapter 5: CONCLUSION AND RECOMMENDATIONS. The main conclusions are drawn from this study and general recommendations for future studies are suggested.

Chapter 2: BACKGROUND

There is a difference between cut-and-cover construction methods for shallow tunnels, where a trench is excavated and roofed over, and underground construction methods, which are tunneling methods to undermine without removing the overburden ground. The first category of tunnels is reduced more or less to a general type of excavation problem; the second category is related to what is usually understood as tunneling in the sense of classical mining techniques (trenchless tunneling methods). In this thesis the focus is on shallow tunnels in soil, where depending on the method of construction it will be generally distinguished as open face tunneling.

2.1. Tunneling Methods

Methods of tunneling vary with the nature of the material to be cut through. When soft earth is encountered, the excavation is timbered for support as the work advances; the timbers are sometimes left as a permanent lining for the tunnel. Another method is to cut two parallel excavations in which the side walls are constructed first. Arches connecting them are then built as the material between them is extracted. Portions of the unexcavated center, left temporarily for support, may be removed later. A tunnel cut through rock frequently requires no lining. Hard rock is removed by blasting.

The choice of tunneling method may be dictated by:

- Geological and hydrological conditions,
- Cross-section and length of continuous tunnel,
- Local experience and time/cost considerations (what is the value of time in the project),
- Limits of surface disturbance and many others factors.

Tunnel construction methods:

- Classical methods
- Cut-and-cover
- Drill and blast
- Shields and tunnel boring machines (TBMs)
- Immersed tunnels
- Special methods (Tunnel jacking, etc.)

The process for bored tunneling involves all or some of the following operations:

- Probe drilling (when needed)
- Grouting (when needed)
- Excavation (or blasting)
- Supporting
- Transportation of muck
- Lining or coating/sealing
- Draining
- Ventilation

2.1.1. Classical Methods

Among the classical methods are the Belgian, English, German, Austrian, Italian and American systems. These methods had much in common with early mining methods and were used until last half of the 19th century. Excavation was done by hand or simple drilling equipment. Supports were predominantly timber, and transportation of muck was done on cars on narrow gauge tracks and powered by steam. Progress was typically in multiple stages i.e. progress in one drift, then support, then drifts in another drift, and so on. The lining would be of brickwork. These craft-based methods are no longer applicable, although some of their principles have been used in combination up to present day. Nevertheless some of the world's great tunnels were built with these methods.

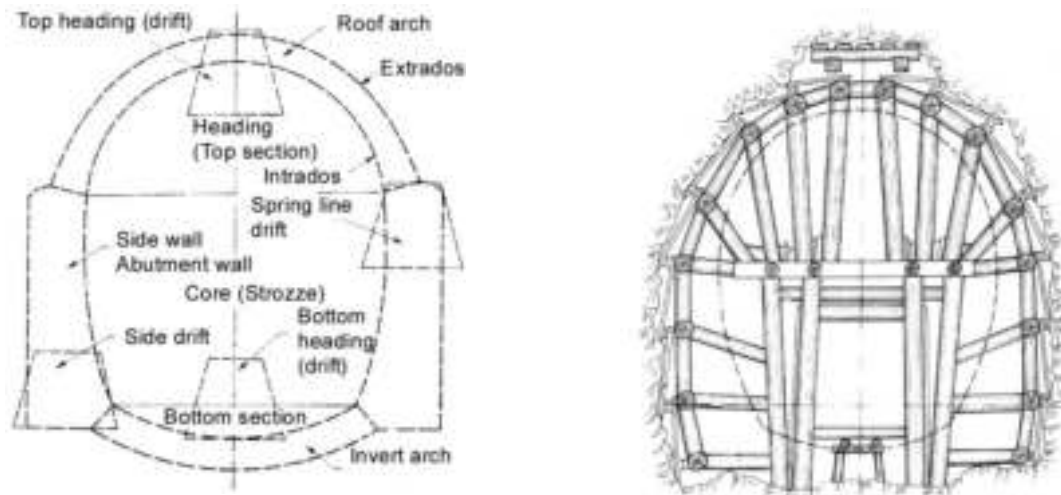


Figure 2.1: Tunneling Classical Methods (Crown-Bar Method) (U.S. Department of Transportation-Federal Highway Administration, 2009)

The English method (crown-bar method, Figure 2.1) started from a central top heading which allowed two timber crown bars to be hoisted into place, the rear ends supported on a completed length of lining, the forward ends propped within the central heading. Development of the heading then allowed additional bars to be erected around the perimeter of the face with boards between each pair to exclude the ground. The system is economical in timber, permits construction of the arch of the tunnel in full-face excavation, and is tolerant of a wide variety of ground conditions, but depends on relatively low ground pressures.

The Austrian method (cross-bar, Figure 2.2) required a strongly constructed central bottom heading upon which a crown heading was constructed. The timbering for full-face excavation was then heavily braced against the central headings, with longitudinal poling boards built on timber bars carried on each frame of timbering. As the lining advanced, so was the timbering propped against each length to maintain stability. The method was capable of withstanding high ground pressures but had high demand for timber.

The German method (core-leaving method) provided a series of box headings within which the successive sections of the side walls of the tunnel were built from the footing upwards, thus a forerunner of the system of multiple drifts. The method depends on the central dumping being able to resist without excessive movement pressure transmitted from the side walls, in providing support to the top 'key' heading

prior to completion of the arch and to ensuring stability while the invert arch is extended in sections.

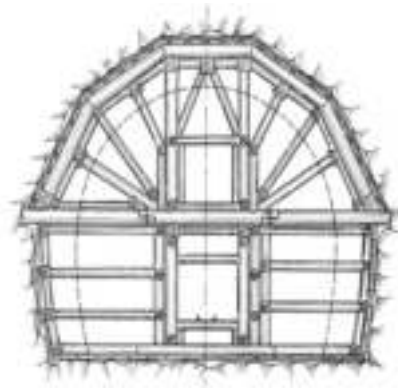


Figure 2.2: Tunneling Classical Methods (Cross-Bar Method) (U.S. Department of Transportation-Federal Highway Administration, 2009)

The Belgian system (underpinning or flying arch method) started from the construction of a top heading, propped approximately to the level of the springing of the arch for a horseshoe tunnel. This heading was then extended to each side to permit construction of the upper part of the arch, which was extended by underpinning, working from side headings. The system was only practicable where rock loads were not heavy.

The first sizeable tunnel in soft ground was the Tronquoy tunnel on the St Quentin canal in France in 1803, where the method of construction, based on the use of successive headings to construct sections of the arch starting from the footing, was a forerunner to the German system described above. The Rove Tunnel near Marseille measured 22 x 15.40 m, and was excavated with multiple drifts in which face of the tunnel is excavated in sections.

2.1.2. Open Face Tunneling

The discontinuous excavation and support sequence of conventionally driven tunnels involves the use of shotcrete (sprayed concrete) and the systematic installation of anchors (or a number of further supporting means) to support the ground. Whereas in the beginnings of conventional tunneling the method was specific to strong and

stable grounds, nowadays it is also applied to soft grounds. The flexibility of the method to account for the smaller stability and higher deformability of such grounds has been further and further developed. The use of versatile supporting means to increase the stability of softer grounds is also associated with a reduction of ground deformations. This is of utmost importance for the control of tunnel induced deformations to nearby existing structures. Last but not least the efficient interplay of the observational method and the controllability of tunnel induced deformations have made the method suitable also for urban tunneling.

Figure 2.3 illustrates an important means to increase the stability of tunnels by applying face and radial anchors. Besides the systematic use of shotcrete and anchors, the fast ring closure of the shotcrete lining at the excavation bottom is important to stop ongoing ground deformation. When approaching softer grounds or larger tunnel diameters, the face can be stabilized by an inclination of approximately $60\pm-70\pm$. The round length displayed in Figure 2.3 is usually in the order of 0.5m-1.5m (Kolymbas, 1998). Reducing the round length significantly contributes to the reduction of surface settlements.

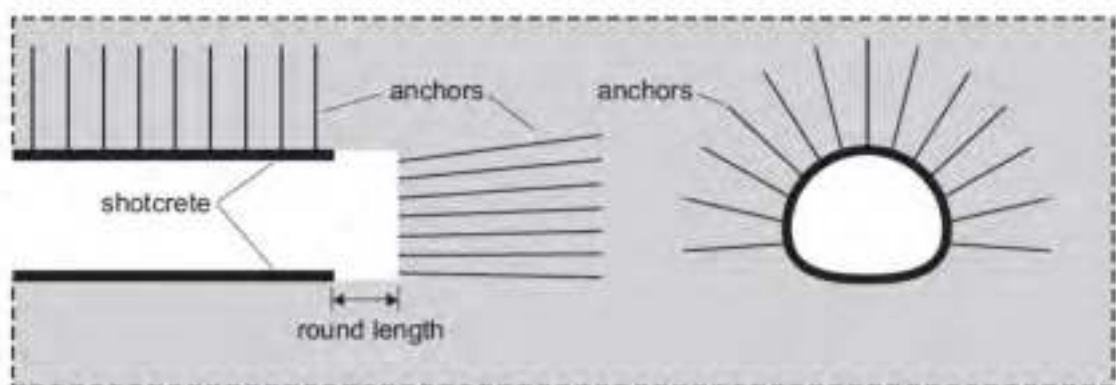


Figure 2.3: Principals of conventional tunneling to control ground stability and ground deformation: Systematic use of shotcrete and anchors.

Depending on ground quality, the excavation of the ground mass can be carried out by a variety of different excavation means. In softer grounds the material may be removed using special designed tunnel excavators. In jointed rock road-header machines can be used and for weak to strong rock the drill and blast method applies.

When approaching changing ground conditions the excavation means may be easily exchanged. This makes conventional tunneling a very flexible method when compared to mechanized tunneling methods (e.g. earth pressure balance machine, slurry machine or tunnel boring machine).

Until a final lining is placed, the primary shotcrete lining has to guarantee the stability of the ground alone. The sealing of the ground with shotcrete after each excavation is a stepwise procedure. In a first immediate action the ground is covered with a thin shotcrete layer to protect against rock fall. In a following step a lattice girder is applied and finally the full shotcrete lining is sprayed. Accompanied by deformation measurements the shotcrete lining will be thickened and if necessary supplemented with steel arches.

Shield tunneling was first introduced by the famous engineer Brunel, who underpassed the river Thames in London in the years 1825-1841 using a rectangular shield construction. The tunnel was hand-excavated and the tunnel lining was a bricklayer construction. A later tunnel underneath the Thames in 1869 used a circular shield and the tunnel lining consisted of cast iron segments. Because of the statically favorable shape of a circular tunnel, the rectangular shield was not further developed and the circular shield with the installation of a lining built up from tubing segments became the archetype of modern shield tunneling.

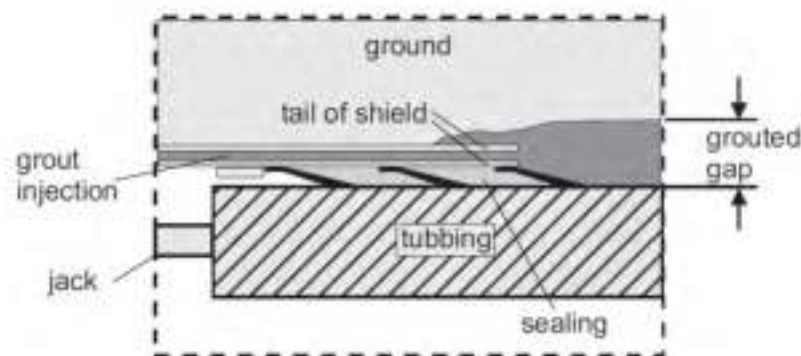


Figure 2.4: Shield tail with grouting of the ground-lining gap

Tunneling with a shield in particular is well suited for softer grounds which need continuous radial support. The shield is mostly a cylindrical construction out of steel. The shield has to be designed to be able to take all ground and working loads

with relatively small deformations. It is usually made of thicker steel plates at its front, to transfer the relatively high axial working forces of the jacks from the lining to the ground. At the shield tail, the steel is not as thick as at the shield front because only radial ground loading has to be accounted for. The inner shield diameter is somewhat larger than the outer diameter of the lining, enabling the installation of tubings (precast concrete lining segments) in cases where tunnels have to undergo curvatures. Depending on the length of the tubing segments, the equal length of one sequence of tunnel advance is usually in between 0:8m-2:0m.

After each sequential tunnel advance of one segment length, the jacks are released, giving space for a new tubing ring to be built. Tubings are installed inside the tail of the shield, which keeps the ground from deforming or falling into the excavated tunnel. Figure 2.4 shows a detailed view of the shield tail. Inside the shield tail, grout is pumped into the gap between ground and tunnel lining, to limit further radial ground deformation. To prevent the continuous grouting to flow into the shield, between shield tail and tubing ring a sealing is installed. The sealing consists of steel brushes filled with grease. During tunnel advance this sealing is sliding over the tubings.

An unstable tunnel face can be improved e.g. by applying steel plates which are connected to hydraulic jacks, giving a certain face pressure. Alternatively the soil at the face may be given its natural inclination, letting it roll into the shield, but ground deformation will be significantly larger. Underneath the ground water table open face tunneling is problematic and therefore the ground water table should be lowered. When tunneling underneath the ground water table or with larger tunnel diameters it is more efficient to apply closed face tunneling methods, where a shield is combined with a cutting wheel.

Tunnel construction by means of TBM (Tunnel Boring Machine) also known as a "mole", has become a preferred method of construction nowadays tunnels with a circular cross section. In addition, this is well accepted by the environmentalist and the green groups. This state-of-art technology limits all works underground in building the tunnel to keep the disturbance to land, wildlife and mankind activities at ground level to a minimum throughout the period of construction.

Table 2.1: Major Components of TBM (Andrew Hung Shing Lee, Engineering Survey System for TBM, 2007)

	Component	Function
1	Cutter Disc	To excavate rock or soft ground by the rotation of an assembly of teeth or cutting wheels under pressure against rock face.
2	Shield Skin	To keep the soil from getting into the machine and to provide a safe space for the workers.
3	Pushing Jack	To be in full contact with the erected segment and extend by hydraulic as the cutter disc turns and thrusts forward.
4	Main Drive	To provide a force in rotating the cutter disc and is powered by electricity.
5	Screw Conveyor	To move the spoil at the cutter disc and feed onto a conveyor system.
6	Erector	To erect the segments to form a complete ring after shoving at the tail of the TBM.
7	Back Up Facilities	To travel with the TBM and to service the operation of annular grouting, welding, extension of ventilation, power and track etc.

The TBM moved forward as it excavated the tunnel by extending the pushing jacks at the back. When the advancement of the machine reached distance of the length of a ring, the excavation stopped and the pushing jacks were retrieved, a concert circular ring in form of a numbers of segments were then put together at the tail of the shield. The pushing arms were once again extended in full contact with the concert ring just erected and excavation resumed. The cycle of excavation and ring erection repeated as the TBM advanced to form the lining of the tunnel. Tunnel diameters can range from a meter (done with micro-TBMs) to almost 16 meters to date.

Tunnel Boring Machines (TBMs) nowadays are full-face, rotational (with cutter heads) excavation machines that can be generally classified into two general categories: Gripper and Segment as shown in Figure 2.5. Based on Figure 2.5, there are three general types of TBMs suitable for rock tunneling including Open Gripper/Main Beam, Closed Gripper/Shield, and Closed Segment Shield, as shown within the dashed box on the Figure. (Andrew Hung Shing Lee, Engineering Survey System for TBM, 2007).

The open gripper/beam types of TBMs are best suited for stable to friable rock with occasional fractured zones and controllable groundwater inflows. Three common types of TBMs belong to this category including Main Beam (Figure 2.6), Kelly Drive, and Open Gripper (without a beam or Kelly).

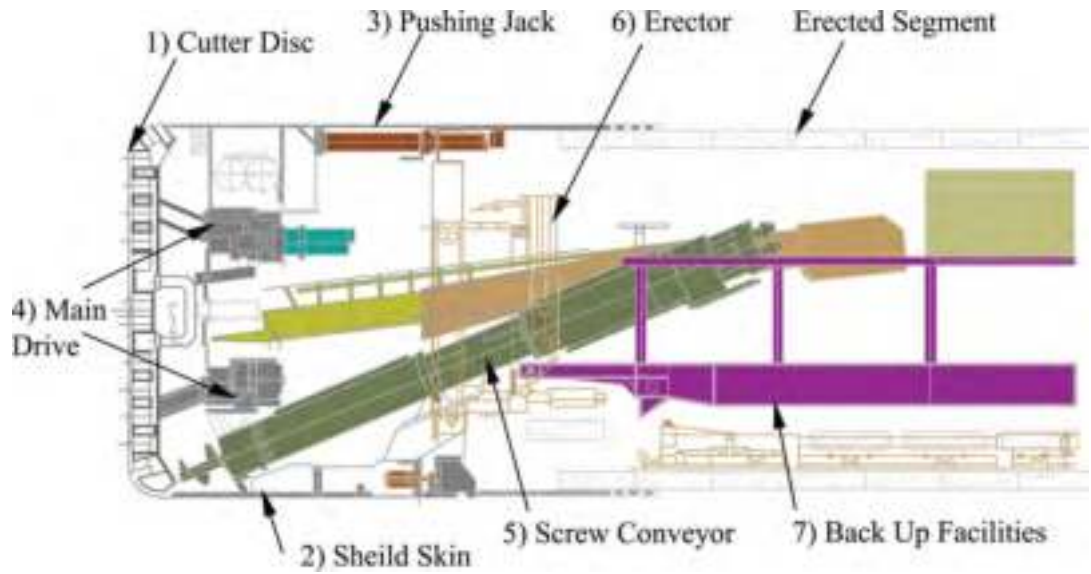


Figure 2.5: Typical Layout of a TBM (Andrew Hung Shing Lee, Engineering Survey System for TBM, 2007)

The closed shield type of TBMs for most rock tunneling applications are suitable for friable to unstable rocks which cannot provide consistent support to the gripper pressure. The closed shield type of TBMs can either be advanced by pushing against segment, or gripper. Note that although these machines are classified as a closed type of machine, they are not pressurized at the face of the machine thus cannot handle high external groundwater pressure or water inflows. Shielded TBMs for rock tunneling include: Single Shield, Double Shield, and Gripper Shield.

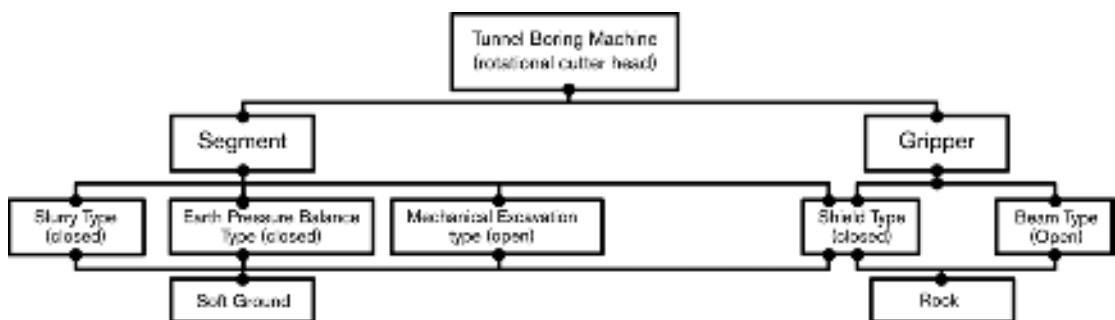


Figure 2.6: Classification of tunnel Excavation Machines (U.S. Department of Transportation-Federal Highway Administration, 2009)

2.1.3. Rock Mass Rating

Rock Mass Rating (RMR) is a scale that was developed by Norwegian Geotechnical Institute. This rating incorporates 5 different rock conditions and assigns rating on the basis of observed conditions. The final number is then adjusted for the orientation of tunnel with respect to dip and strike of the discontinuities. RMR is mostly suited for drill and blast tunneling according to New Austrian Tunneling Method (NATM). Table 2.2 presents the conditions and corresponding rating according to RMR method.

2.2.Methods of Analysis

When the tunneling engineer designs a tunnel structure, he guarantees that the structure is safe with respect to structural collapse and ground deformations during its projected lifetime. Depending on ground conditions and tunneling method he must choose an appropriate method of analysis and derive, or even invent, a structural model, i.e. a structural idealization. By applying equilibrium and compatibility conditions to the model, the engineer has to arrive at those criteria that are factors in deciding whether or not the design is safe. Different structural design methods and design models have been developed and they are used for different excavation and support sequences, for the preliminary and the final tunnel lining, or for different ground behavior, e.g. in discontinuous rock or homogeneous soil.

There is no other section of geomechanics where structural design methods have proven so controversial and debated as it is the case for tunnel constructions. Therefore a condensed overview of relevant computational methods for settlements and lining forces will be given in the following. Papers that applied a broader approach to all the complex aspects of tunneling, including different structural design methods, have been published e.g. by Craig and Muir wood (1978) or Einstein (1979-1980).

In the present thesis the focus is on tunneling in soil and soft rock rather than on tunneling in hard rock, although some of the structural design approaches may be generally applicable. In order to address geomaterials uniformly, regardless of whether it concerns soil or rock, in the present thesis the word ground will be used.

Table 2.2: RMR conditions and ratings

Strength of Intact Rock Material							
UCS	> 250 MPa	100 - 250 MPa	50 - 100 MPa	25 - 50 MPa	5 - 25 MPa	1 - 5 MPa	< 1 MPa
Rating J _{A1}	15	12	7	4	2	1	0
RQD	90% - 100%	75% - 90%	50% - 75%	25% - 50%	< 25%		
Rating J _{A2}	20	17	13	8	3		
Spacing of Discontinuities	> 2 m	0.6 - 2m	200 - 600 mm	60 - 200mm	< 60 mm		
Rating J _{A3}	20	15	10	8	5		
Condition of Discontinuities	Very rough surfaces	Slightly rough	Slightly rough Highly weathered	Slickensided surfaces	Soft gouge > 5 mm thick or Separation > 5 mm Continuous		
Rating J _{A4}	30	25	20	10	0		
Groundwater							
Inflow per 10 m (L/min)	None	< 10	10 - 25	25 - 125	> 125		
Rating J _{A5}	15	10	7	4	0		

When a tunnel in soil is planned, ground movements are an important topic to be considered for tunnel design. Depending on the method of tunnel construction different support measures are taken to guarantee stability and to limit deformation. Urban tunneling is aimed at reducing ground deformations to a minimum, but in deep tunneling tolerable deformations may be significantly larger. No matter what tunneling method the ground will be loaded or unloaded and deformations will inevitably take place, leading to a settlement trough as shown in Figure 2.7. This thesis focuses on deformations due to open face conventional tunneling and closed face shield tunneling, as indicated in Figure 2.8.

Mair and Taylor (1997) summarized the following primary components of ground deformation associated with closed shield tunneling:

1. Movement of the ground towards the face, due to stress relief.
2. Radial ground movement towards the shield, due to over-cutting and ploughing.
3. Radial ground movement into the tail void, due to a gap between shield and lining.
4. Radial ground movement towards the lining, due to deformation of the lining.
5. Radial ground movement towards the lining due to consolidation.

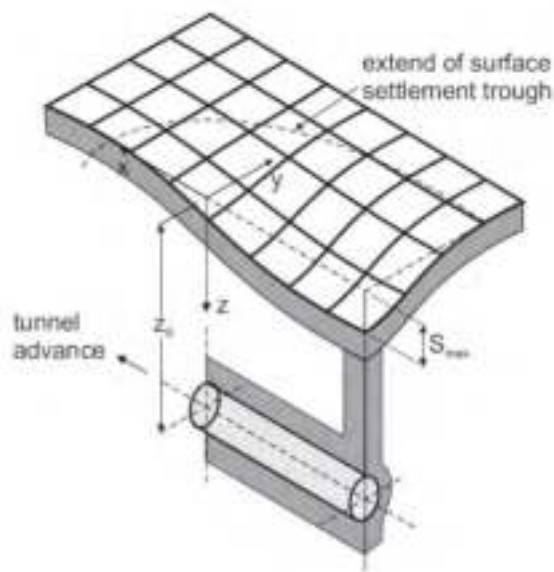


Figure 2.7: Tunnel induced settlement trough after Attewell et al. (1986)

For shield tunneling with adequate face support (Fig. 2.8a), the first component of ground deformation will be relatively small, but the second component may be appreciable; in particular for a somewhat conical shield or in case of over-cutting, as well if there are steering problems in maintaining the alignment of the shield. The third component of ground deformation can be minimized by grouting, but this component is strongly influenced by the experience of the crew and the ground pressure control being implemented. This third component is usually the major cause of settlements. Component four tends to be of minor importance in relation to conventional tunneling. Component five can be of importance for tunneling in soft soils with low permeabilities. In case of insufficient face pressure the pore water pressure dissipation/consolidation phenomenon may take place in front of the tunnel.

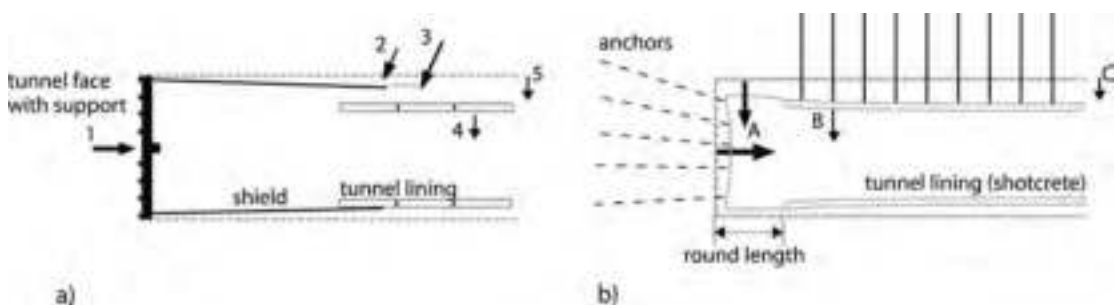


Figure 2.8: Principal components of ground deformation: a) Closed shield tunneling (after Mair and Taylor (1997)), b) open face tunneling

For open face tunnels (Figure 2.8b) the following main causes of settlements can be specified:

- A. Movement of the ground towards the non-supported tunnel heading.
- B. Radial ground movement towards the deforming lining.
- C. Radial ground movement towards the lining due to consolidation.

Ground movement (A) towards an unsupported tunnel heading is obvious. No doubt, this component of settlements can be reduced by, e.g., reducing the unsupported round length, or by the use of face anchors, but heading deformations remains significant. The radial ground movement (B) towards the lining is relatively large, as an initially ductile shotcrete lining is used for temporary support. Various different additives are often used to accelerate the hardening of the concrete and thus its stiffening, to allow for an increase of the tunnel excavation rate. When tunneling in grounds with low permeabilities some consolidation after tunnel construction may take place. In cases where the finished tunnel will act as a drain, or where other reasons impose consolidation to the surrounding ground, delayed radial movements of type (C) may occur. In grounds with high permeabilities, the pore water pressure dissipation/consolidation phenomenon also tends to take place in front of the tunnel face and ground movements may occur quickly during construction.

For tunneling in the urban environment, deformations are a major design topic, as existing structures might be damaged by differential settlements. When interaction problems of tunnels with existing structures need to be accounted for, a green field settlement trough (Figure 2.7) is often assumed as it implies a conservative approach. Independent of the tunneling method the shape of the green field settlements is well matched by a Gaussian function as discussed in the following sections.

2.2.1. Lining Forces

The lining, whether it be temporary or permanent, must withstand ground pressures with a sufficient margin of safety. The assessment of the water pressure is straight forward, but effective stresses on the lining depend again significantly on installation procedures. Mair and Taylor (1997) report that this stress may amount up to 50% of the overburden stress.

In urban shield tunneling ground deformation is minimized by face support and grouting, but this increases loads on linings so that effective stresses may get more close to the overburden stress. Craig and Muirwood (1978) stated that monitoring of stresses in shield tunnel linings has shown that the average stresses generally increase during the first few months up to 50% - 70% of the equivalent overburden stress. Higher stress concentrations have been recorded in the early measurements, but these may be partly associated with moment stress, as reported by Craig and Muirwood (1978).

In the period of planning a tunnel structure the engineer has to rely on a method of analysis, from which he may derive criteria whether the design is suitable, safe and economical. Relevant methods for the assessment of bending moments and normal forces are to be considered.

2.2.2. Assessments of Settlements

The most common empirical method to predict ground movements is based on a Gaussian distribution, which is often referred to as the empirical method. Schmidt (1969) and Peck (1969) were the first to show that the transverse settlement trough, taking place after construction of a tunnel, in many cases can be well described by the Gaussian function:

$$S_v(y) = S_{vmax} \cdot e^{-\frac{y^2}{2i^2}} \quad [2.1]$$

where S_{vmax} is the settlement above the tunnel axis, y is the horizontal distance from the tunnel axis and i is the horizontal distance from the tunnel axis to the point of inflection of the settlement trough, as shown in Figure 2.9. The volume of the settlement trough (per unit length of tunnel) V_i is obtained by integrating. These yields

$$V_i = \int S_v(y) \cdot dx = \sqrt{2\pi} \cdot i \cdot S_{vmax} \quad [2.2]$$

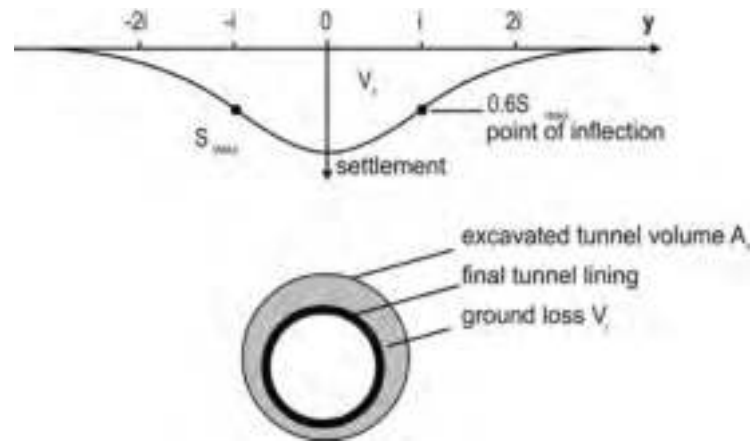


Figure 2.9: Gaussian curve for transverse settlement trough and ground loss V_t

In addition to the settlement volume V_s one has to consider the ground loss V_t . This is the volume of the ground that has deformed into the tunnel after the tunnel has been constructed, as illustrated in Figure 2.9. For tunneling in undrained ground, the settlement volume is almost equal to the ground loss, but the settlement volume is smaller for drained excavations. Dilation and swelling due to unloading may result in soil expansion, such that $V_s < V_t$ (Cording and Hansmire, 1975). However, differences remains small and $V_s = \frac{1}{4} V_t$. As the ground loss depends more or less linearly on the tunnel volume, it is convenient to consider the ground loss ratio.

$$GLR = \frac{V_t}{A_t} = \frac{V_g}{A_t} \quad [2.3]$$

where A_t is the tunnel volume per unit of length. It follows from Equations 2.1 – 2.3 that $S_{vmax} \approx \frac{1}{4} V_t$

$$S_{vmax} \approx \frac{A_t}{i \cdot \sqrt{2\pi}} \cdot GLR \quad [2.4]$$

$$S_v(y) \approx \frac{A_t}{i \cdot \sqrt{2\pi}} \cdot GLR \cdot e^{-\frac{y^2}{2i^2}} \quad [2.5]$$

Assuming the Gaussian curve to assess the distribution of transverse surface settlements, one needs information on two input parameters, namely the distance to

the point of inflection i for the width of the settlement trough and the ground loss ratio GLR for the depth of the settlement trough.

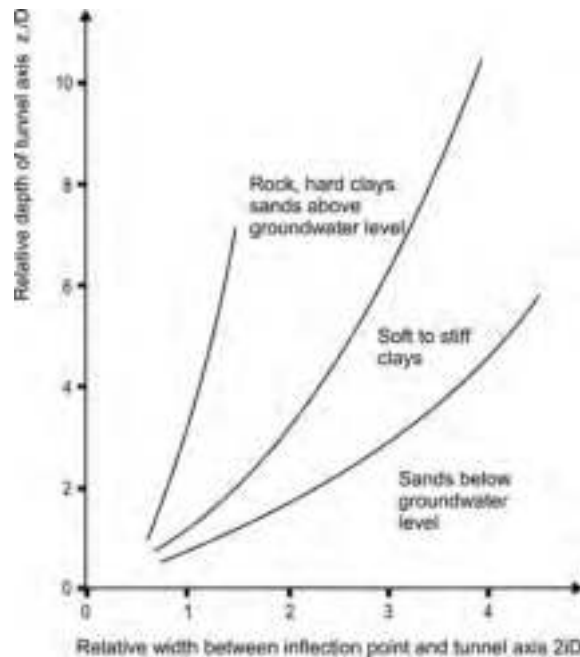


Figure 2.10: Relation between settlement trough width and tunnel depth for different grounds (Peck, 1969)

The distance from the tunnel axis to the inflection point i , which is determining the width of the settlement trough, has been subject to many investigations. PECK (1969) suggested a relationship to tunnel depth z_0 and tunnel diameter D , depending on ground conditions, as shown in Figure 2.10. After the suggestion by PECK many other authors have come up with similar relationships, e.g. Cording and Hansmire (1975) or Clough and Schmidt (1981). O'reilly and New (1982) presented results from multiple linear regression analyses performed on field data, confirming the strong correlation of i with tunnel depth, but showing no significant correlation of i with tunnel diameter (except for very shallow tunnels, with a cover to diameter ratio less than one) or method of construction. They stated, that for most practical purposes the regression lines may be simplified to the form

$$i = K \cdot z_0 \quad [2.6]$$

where K is a trough width parameter, with $K \approx 0.5$ for clayey grounds and $K \approx 0.25$ for sandy grounds.

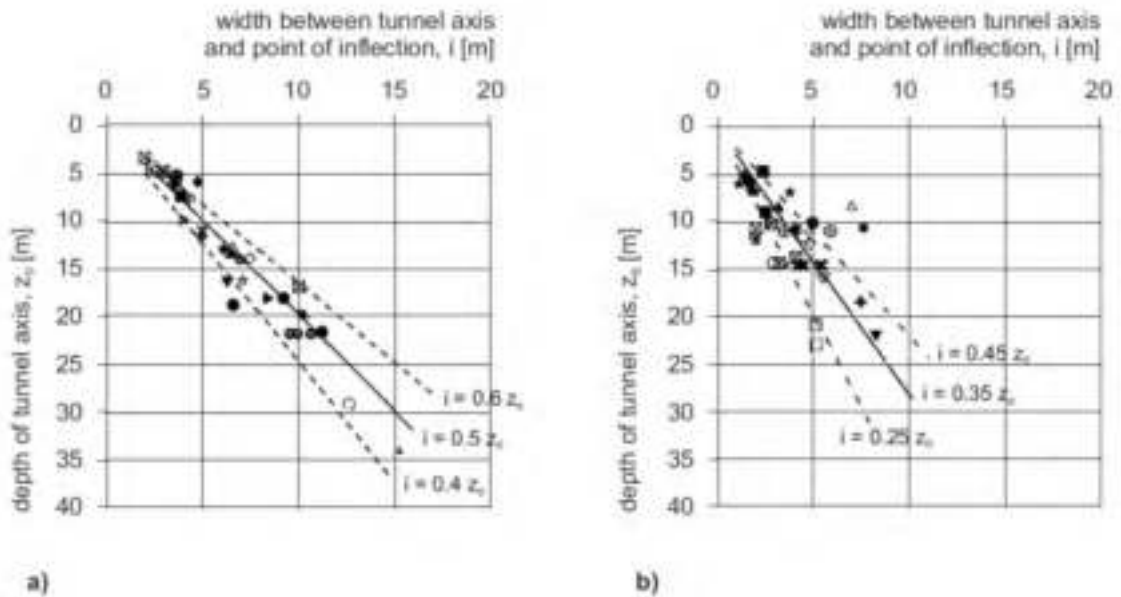


Figure 2.11: Observed width of surface settlement trough as a function of tunnel depth: a) In clays, b) in sands and gravels (Mair and Taylor, 1997)

The approach of Eq. 2.6 has been generally confirmed by Rankin (1988), who presented a variety of tunnel case histories in clayey, sandy, residual and in mixed grounds. Mair and Taylor (1997) presented a large number of tunneling data with different linear regressions for tunnels in clays and tunnels in sands and gravels. As shown in Figure 2.11, the regressions confirm the findings of O’reilly and New (1982) for clayey soils, with a trough width parameter ranging in between 0.4 and 0.6, with a mean value of $K = 0.5$. However, for sandy soils they obtain a K ranging in between 0.25 and 0.45, with a mean value of 0.35, indicating somewhat wider settlement troughs.

According to Craig and Muir Wood (1978) it is generally found that the volume of the settlement trough at the surface is approximately equivalent to the volume of the ground lost in the tunnel. The ground loss ratio GLR in Equation 2.3 is used for an initial estimate of S_{vmax} . The method of construction of the tunnel will have a considerable effect on the ground loss ratio. In shield tunneling the ground loss is predominantly a result of tail void grouting and face pressure. If the ground is stable

enough and the lining can be erected and grouted without the ground falling onto the lining, very little settlement will occur.

If the ground falls onto the lining and fills the grouting space, the whole of this movement will be reproduced at the surface. Depending on equipment, control procedures and experience of the crew, GLR-values between 0.5% and 2% are realistic in homogeneous ground. In sands a loss of only 0.5% can be achieved, whereas soft clays involve the range from 1% to 2%, as reported by Mair (1996). Considering data for mixed ground profiles with sands or fills overlaying tertiary clays, Mair and Taylor (1997) reported values between 2% and 4%. In conventional driven tunnels the GLR is largely controlled by the round length and the size of the (partial) excavations, whilst ground stiffness and initial stresses also have a significant influence. Mair (1996) concluded that ground loss ratios in stiff clays are between 1% and 2%, whilst conventional tunneling in London clay has resulted in even smaller losses varying between 0.5% to 1.5%.

Many authors have proposed various different relationships for ground loss ratios. Several proposals are related to the stability number N , defined by Broms and Bennermark (1967) as

$$N = \frac{p_v - p_t}{c_u} \quad [2.7]$$

for tunneling under undrained conditions, where p_v is the total overburden pressure at tunnel axis level, p_t is the tunnel face support pressure (if present) and c_u is the undrained shear strength of the ground. Here it should be noted that Ruse (2004) defined the stability number by the equation

$$P_f = P_v - C_u \cdot N_f \quad [2.8]$$

where p_f is the minimum face support pressure at failure and N_f a given function of the tunnel cover over tunnel diameter ratio $H=D$. In fact it would be better to refer to N as the mobilized stability number and it should be obvious that $N = N_f$.

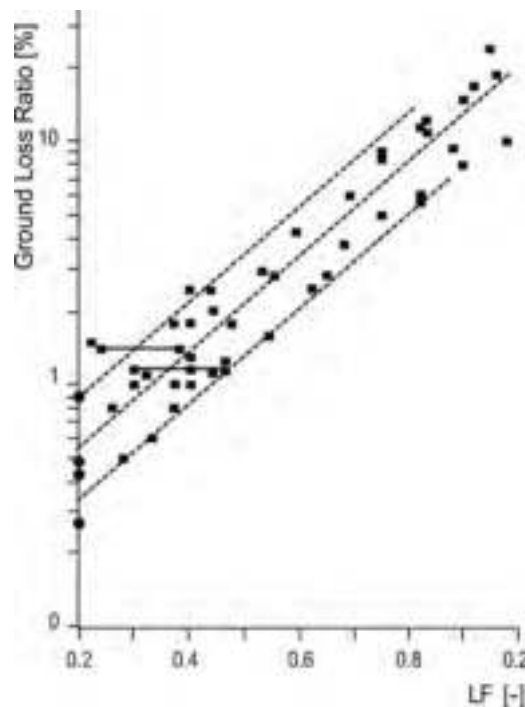


Figure 2.12: GLR versus load factor LF in over consolidated clay (Macklin, 1999)

For tunnels in undrained clays, Clough and Schmidt (1981) proposed a relationship between mobilized stability number N and ground loss ratio based on the closed form solution for the unloading of a circular cavity in a linear elastic-perfectly plastic continuum under axisymmetric conditions. According to Clough and Schmidt for N less than 2 the response is elastic with small ground movements and the tunnel face being stable. For N between 2 and 4 loads increase and limited plastic yielding occurs, while for N between 4 and 6 the yielding zone is spreading leading to larger movements. For N greater than 6 the yielding zone is significant, leading to tunnel face instability with large ground movements. From a mechanical point of view such findings should be generalized by considering the ratio of $N=N_f$ rather than simply N , as N_f is not a constant but is heavily dependent on tunnel depth.

Attewell et al. (1986) and Uriel and Sagaseta (1989) presented field data of ground loss ratios related to the mobilized stability number, based on CLOUGH and SCHMIDT's proposal. The results show a very wide scatter, which is probably associated with the use of N rather than $N=N_f$.

Recent work of Macklin (1999) on the assessment of Ground Loss Ratio (GLR) is shown in Figure 2.12. He related measured GLR-data from different tunneling projects in overconsolidated clay to the load factor $LF = N=N_f$, which is the inverse of the factor of safety. For $LF > 0.2$ he proposed the linear regression

$$GLR = 0.23 \cdot e^{4.4(LF)} \quad [2.9]$$

Considering the fact that measured GLR data in Figure 2.12 show a considerable scatter, MACKLIN emphasizes that for design purposes the range of values Figure 2.12 should be considered, rather than just Eq. 2.9. However, ground movements are affected by a large number of different factors and thus such relations on the assessment of GLR can be indicative only. It would seem that Figure 2.12 ideas has not yet found its way into engineering practice, but the idea of estimating settlements in relation to a factor of safety or load factor would seem to be sound.

Longitudinal Surface Settlement. Besides the consideration of the transverse settlement profile, the longitudinal profile also is important. In cases where information on the three-dimensional influence of settlements is required, where buildings might be subjected to twisting and respective torsion forces, longitudinal settlements need to be analyzed. Attewell and Woodman (1982) showed that the longitudinal settlement profile can be derived, by considering a tunnel as a number of point sources in the longitudinal direction and by superimposing the settlement craters caused by each point source. The assumption that the incremental longitudinal settlement trough is a Gaussian curve, leads to the logical extension that the longitudinal settlement trough should follow the shape of a cumulative probability curve. The settlement above the tunnel center line at location x can be obtained from the equation

$$S_v(x) = S_{vmax} \cdot \frac{1}{i \cdot \sqrt{2\pi}} \cdot \int_{-\infty}^{\frac{x}{i}} e^{-\frac{t^2}{2i^2}} \quad [2.10]$$

where x is the distance from the tunnel face in the longitudinal direction of the settlement trough, as shown in Figure 2.7. Attewell and Woodman (1982) have

validated the assumption of a cumulative probability function reasonably well by an examination of several field study reports.

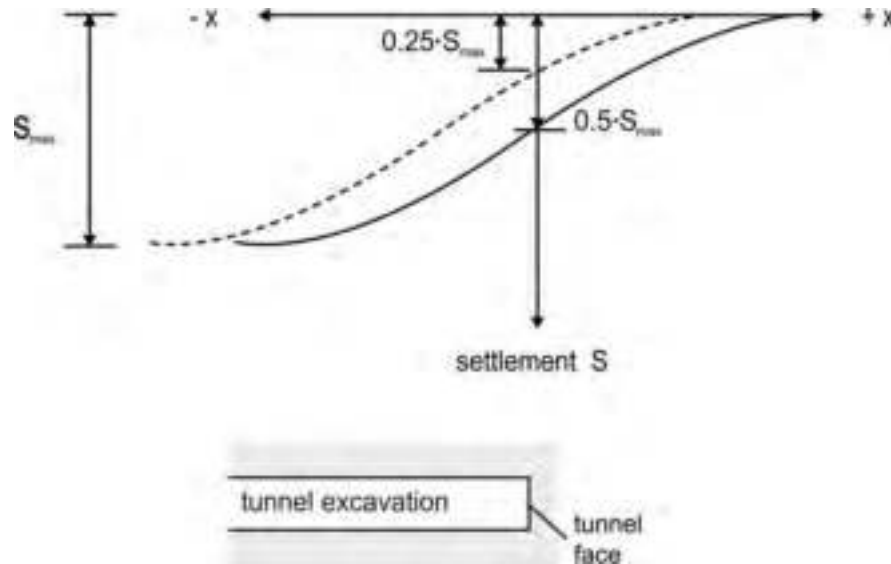


Figure 2.13: Longitudinal settlement trough above tunnel center line after Attewell et al. (1986)

Attewell et al. (1986) assumed that the settlement directly above the tunnel face ($x = 0$) coincides with 50% of the maximum settlement S_{max} , as indicated in Figure 2.13. This may be appropriate in case of open face tunneling. However, for closed face tunneling settlements ahead of the tunnel face will reduce significantly. Mair and Taylor (1997) concluded that for closed face tunneling much lower values of only 25% - 30% are to be obtained, which leads to a translation of the longitudinal settlement profile as indicated by the dashed line in Figure 2.13.

Table 2.3: Development of settlement profile (Craig and Muir Wood, 1978)

Type of ground	Percentage of total settlement completed	
	At face of shield [%]	At passage of tail of shield [%]
Sand above water table	30-60	60-80
Stiff clays	30-60	50-75
Sand below water table	0-25	50-75
Silts and soft clays	0-25	30-50

Craig and Muir Wood (1978) have reviewed shield tunnels and stated that the percentage of the maximum settlement that occurs ahead of the shield, over the shield and behind the shield varies for different grounds. In general the percentages fall into the ranges given in Table 2.3. They stated that 80% - 90% of the maximum settlement will be complete when the face of the tunnel has travelled a distance equivalent to one to two times the depth of the tunnel.

2.2.3. Ground Pressures

The deformations resulting from tunnel installation procedures reduce the primary ground pressures and create loads on the lining. The loads correspond to that fractional part of the primary ground pressures which acts on the sustaining lining. The distribution and magnitude of ground pressures on tunnel linings, which will develop during and after the construction of a tunnel, is influenced by a large number of different factors, such as ground and lining stiffnesses, geometry of the tunnel cross-section and installation procedures.

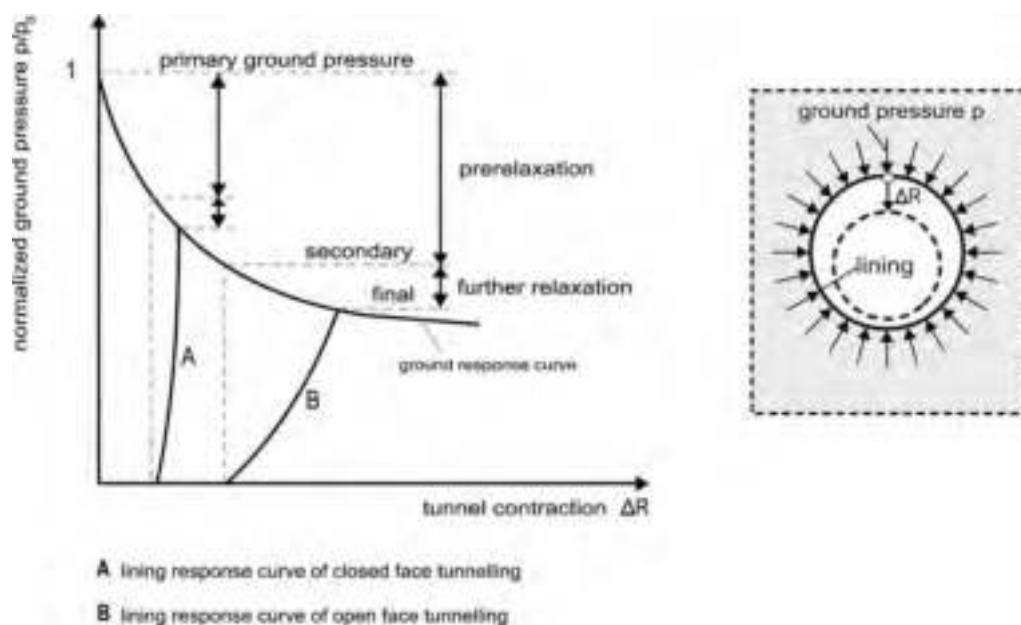


Figure 2.14: Illustration of development of ground pressures on tunnel linings adopting ground response curve

In order to arrive at an appropriate estimate of both distributions and magnitudes of ground pressures, the design of a tunnel should take these factors of interaction into account.

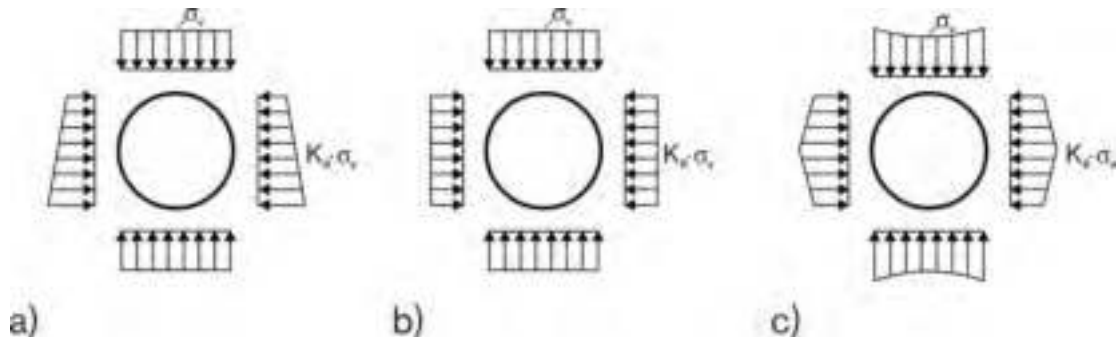


Figure 2.15: Different distributions of ground loads on tunnel linings.

Figure 2.14 illustrates the development of ground pressures on tunnel linings adopting the ground response curve. As shown by this figure, the amount of the ground pressure on the tunnel lining is influenced by a reduction of primary ground pressures before the tunnel lining is installed. Starting from primary ground pressures tunnel excavation induces stress prerelaxation to the ground, reducing primary ground pressures down to a secondary state of stress.

Figure 2.14 shows that the amount of stress prerelaxation is governed by the tunneling method, i.e. tunnel installation procedures. In the case of closed face tunneling ground deformations are minimized and therefore the amount of stress prerelaxation is generally relatively small. In open face tunneling on the contrary, the excavation of an unsupported cut stretch leads to a relatively high ground mobilization and the associated stress prerelaxation is thus relatively large.

In order to guarantee ground stability after tunnel excavation a lining is installed. As demonstrated by Figure 2.14, lining deformation imposes some further stress relaxation to the surrounding ground and the secondary ground pressures are reduced down to final pressures on the tunnel lining. For shield tunneling the use of relatively stiff precast segmental linings (accounting for some stiffness reduction of joints between lining segments) will generally show relatively small lining deformation but in conventional tunneling lining deformation may become relatively

large. Figure 2.14 shows that the amount of the further stress relaxation resulting from tunnel lining deformation is relatively small compared to the amount of the stress prerelaxation.

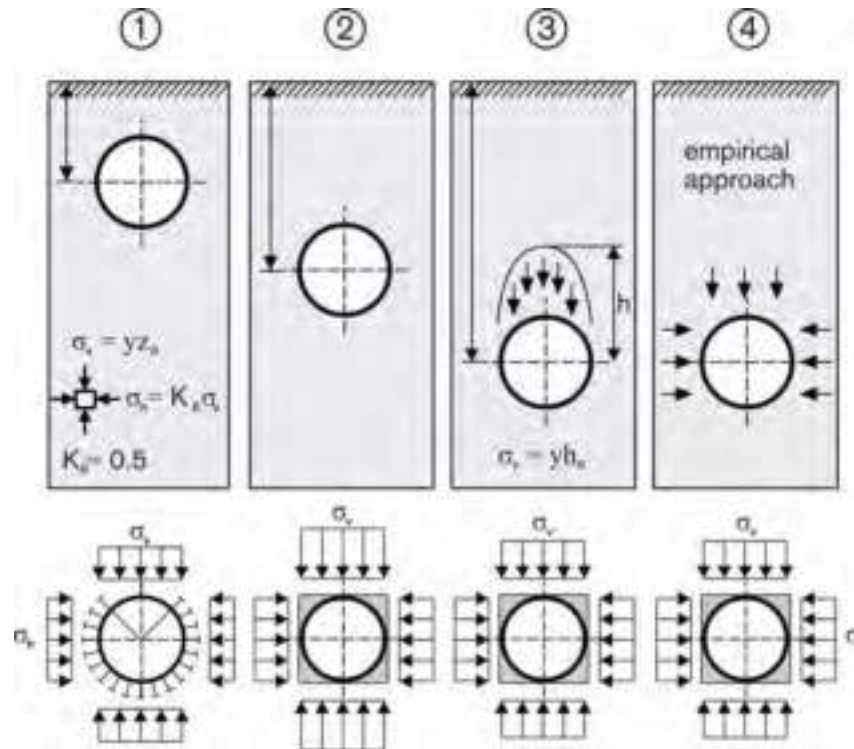


Figure 2.16: Plane-strain design models for different depths and ground stiffnesses (ITA, 1988)

In order to assess structural forces in tunnel linings using a suitable structural model, both the amount of stress prerelaxation and the amount of further stress relaxation have to be accounted for. Analytical solutions of continuum models or bedded beam calculations incorporate lining deformations resulting from ground loading and hence the associated further stress relaxation of the ground is automatically accounted for. In contrast the effects of stress prerelaxation, i.e. tunnel installation procedures, are not automatically accounted for and assumptions about its magnitude have to be made.

Besides stress prerelaxation the distribution of primary ground pressures is important to be considered in tunnel analysis. In the following approaches for the distribution of primary ground pressures and the amount of secondary ground pressures resulting from stress prerelaxation will be briefly reviewed.

Distribution of primary ground pressures Figure 2.15 shows a variety of different structural models with different distributions of primary ground pressures on the tunnel lining. The distribution of increasing primary horizontal pressures with depth as indicated by Figure 2.15a) is used for analyzing shallow tunnels, whereas constant horizontal pressures as shown by Figure 2.15b) are used for deep tunnels. The reason for reducing horizontal stresses with depth as indicated in Figure 2.15c) is not made clear in most of the literature.

Amount of secondary ground pressures The amount of the secondary ground pressure is influenced by the sum of all stress redistributions which have been caused during tunnel excavation. Before the tunnel lining is installed, ahead of the tunnel face and around the shield machine (or around the unsupported cut-stretch in conventional tunneling) some stress redistribution inevitably takes place resulting in stress preredelaxation. Depending on tunnel installation procedures, tunnel depth and ground properties, stress preredelaxation may become relatively large and secondary ground pressures may reduce significantly.

Duddeck and Erdmann (1982) distinguish between shallow tunnels with $z_0 \geq 2D$, moderately deep tunnels with $2D \leq z_0 \leq 3D$ and deep tunnels with $z_0 \geq 3D$. For shallow and moderately deep tunnels they propose that no stress preredelaxation takes place at the crown of the tunnel, applying full primary stresses on top of the tunnel. Hence, it is assumed that in the final state (some years after the construction of the tunnel), the ground eventually will return to nearly the same condition as before the tunneling. Changes in ground water levels, traffic vibrations, etc., may provoke this readjustment. Indeed, Craig and Muir Wood (1978) report that the instrumentation of existing shallow tunnels is 50 to 75 years old, which have been required to be dismantled during the construction of new works, has shown combined hoop and bending stresses in the lining equivalent to the overburden pressure. For tunnels in sands below the water table they state that measurements have shown combined stresses between 80% and 100% of the equivalent overburden stress, which may develop within the first few months.

For deep tunnels it is obvious that some stress preredelaxation needs to be accounted for to reduce the loads on the lining. Duddeck and Erdmann (1982) argue that no matter what tunnel depth, allowance should be made for a tendency towards

larger or lower ground stresses, acting on the lining in regard to, at least, cohesion, stiffness of the ground, time to closure of the tunnel ring, excavation procedure, erection method for the lining, time-dependent behavior of the ground and the lining and effects of groundwater. Thus the transition from shallow to deep tunnels is not sharp and the three cases overlap.

To account for installation of closed face tunneling, Muir Wood (1975) proposed to take only 50% of the initial ground stresses into consideration. Indeed, in present two-dimensional numerical analyses of open face tunneling, a stress reduction factor, being referred to as unloading or beta factor, of around 50% is commonly used, but this value would seem to be rather low for modern closed face tunneling. Because of the relatively high mobilization of the grounds shear strength in open face tunneling, this method requires a ground with a pronounced cohesion and therefore a significant stress preresolution may generally be justified.

The topic of ground pressures on tunnel linings with regard to different structural design models, tunnel depths and ground stiffnesses has also been reviewed by the ITA (1988)-working group on General Approaches to the Design of Tunnels. Figure 2.16 categorizes four different approaches of structural design models:

1. bedded-beam model for very shallow tunnels in soft ground
2. continuum model for tunnels at shallow depth and moderately stiff ground,
3. continuum model for deep tunnels in stiff ground,
4. continuum model for deep tunnels, empirical approach for ground pressures

For tunnels at shallow depth in soil, immediate support must be provided by a relatively stiff lining. Here it is agreed that the three-dimensional stress release at the face of the tunnel during excavation may be neglected. Therefore in cases (1) and (2) of Figure 2.16 no stress preresolution is taken into account incorporating full primary ground pressures.

Case (3) assumes that some stress preresolution is caused by deformations that occur before the lining participates. In rock or in highly cohesive soil, the ground may be strong enough to allow a certain unsupported section at the tunnel face. Stress preresolution is also assumed for tunnels having a high overburden, and a reduction of the acting crown pressure (as represented in Figure 2.16 by $h < z_0$) is taken into

account. Confirming these recommendations, Craig and Muir Wood (1978) discuss measurements of tunnels in rock, where readings have been taken of the stresses in the arch ribs prior to the casting of a cast in-situ lining. Their presented results generally show relatively low stresses.

In case (4), the ground stresses acting on the lining are determined by an empirical approach, which may be based on previous experiences with the same ground and the same tunneling method, on in-situ observations and monitoring of initial tunnel sections, on interpretation of the observed data and on continuous improvements of the design model. Here, some reduction of stresses may generally be incorporated.

2.2.4. Extension of Assessments

During shield tunneling operations, the magnitude and distribution of ground deformation are largely controlled by construction process. The factors that affect the ground deformation are:

- I. Changes in earth pressure at the cutting face,
- II. Variation of external forces applied to the machine such as jacking forces,
- III. Shearing of soil at the shield-soil interface due to friction,
- IV. Introduction of the tail void and injection of backfill between the tunnel lining and excavated tunnel cavity,
- V. Over excavation due to steering of the machine, and
- VI. Long term consolidation due to excess pore pressure dissipation and changes in groundwater hydraulic conditions.

Many of the above factors are closely linked to the interaction between the soil and shield machine, which cause the stress state of the soil to change. The possible earth pressure changes due to the shield machine advancement are illustrated in Figure 2.17. The figure is based on extensive earth pressure and deformation measurements.

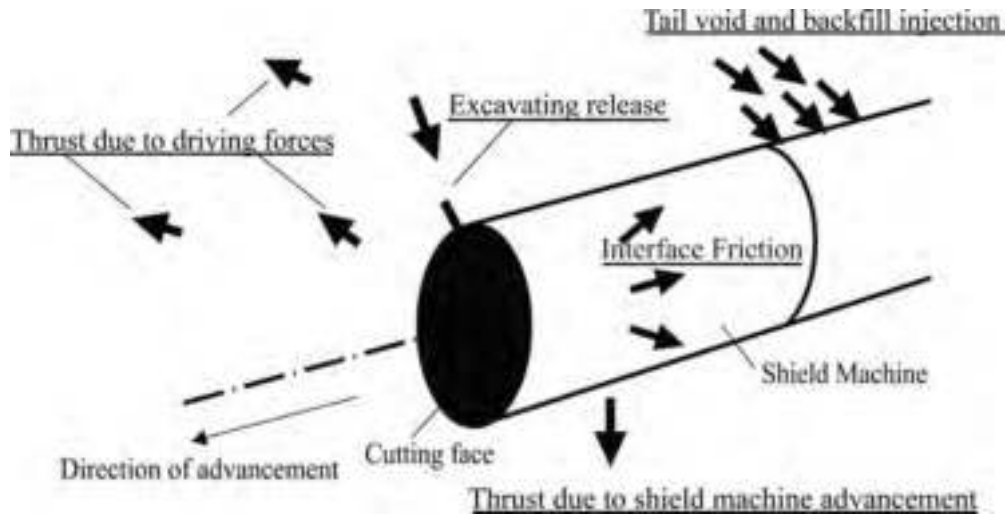


Figure 2.17: Earth pressure changes due to the shield machine advancement

The figure implies that the nature of the problem is three-dimensional and that the magnitude of earth pressure change is related to the machine characteristics, construction procedure, operator's control, etc. Therefore, when estimating the ground deformation caused by shield tunnel construction, care should be taken of how to model the characteristics of the machine and the construction process.

Because of the complex boundary conditions of a shield tunneling problem, the use of the finite element method is one of the popular methods to investigate the ground deformation behavior. In general, the finite element analysis results reported in the literature have contributed greatly in understanding various deformation mechanisms associated with shield tunneling. However, these past studies are often made to examine the above-mentioned factors individually. Also, many of the reported analyses use the in-situ stress condition as the initial condition of the problem without any in-depth consideration of other factors affecting the change in the stress state of the soil. For example, both the steering problem and interface friction problems are expected to influence the soil conditions around the shield machine at the same time during its advancement and their effects cannot possibly be analyzed separately. Therefore, there is a need to examine the combined effect of various aspects of shield tunneling operations on ground deformation within one analysis. The construction process of a shield operation is often modeled by applying

external forces, introducing traction, or forcing displacements at the boundary nodes of a finite element mesh under a spatially fixed tunnel configuration.

This literature contains eight papers presented at conferences between 1994 and 1999. These papers present many of the findings of an ongoing project on the understanding of the interaction between tunneling processes, the associated ground movements and possible damage to adjacent buildings. The research at Oxford is recorded in three theses (Augarde et al. 1995), and two further research students (Bloodworth 1999) are currently working in this area.

The program has been divided into three broad phases:

- Preliminary work (Chow) using two-dimensional analysis.
- Development of 3-D analyses of tunnels (including lining), the surrounding ground and masonry buildings
- Calibration of the methods against case records, and development of tunnel installation procedures and analysis of compensation grouting.

The first paper (Burd et al. 1994) sets out the general approach that was planned for the subsequent research, drawing on the preliminary study. The conclusion was that in order to capture correctly the pattern of deformation, it is necessary to take great care in the choice of soil model.

The second (Augarde et al. 1995) provides more details on the numerical procedures adopted in the research. The conclusion was that a simple elastic soil model has been used to demonstrate the finite element analysis of an unlined tunnel excavation and shows reasonable agreement with the methods currently used to predict settlement trough shape. Further enhancements to improve the constitutive model of the soil mass and the addition of a lining should improve the result! Although the adoption of the former will lead to considerable solution time.

The third (Augarde et al. 1998) reports the experience in using these methods to analyze typical tunneling problems. The conclusion was that further work is underway to increase the scope of the model and to improve its efficiency. In particular, the modeling of compensation grouting, using interface finite elements, is under development. It is also intended to develop an effective stress model for soil in order to study the effect of consolidation settlements. The behavior of the shell

elements in the model has prompted an investigation of other methods of modeling volume loss. It appears possible to use thin continuum elements with high stiffness for the lining, which should remove any difficulties associated with element non-compatibility.

The fourth paper (Houlsby et al. 1999) is a general report on the results of the second phase of research. The conclusion was that advanced numerical techniques are capable of modeling complex problems of soil-structure interaction involving the influence of tunneling operations on the surface settlement.

Bloodworth and Houlsby (1999) report one comparison of the analyses with a case history (of a shaft construction rather than a tunnel). The conclusion was that the importance of the building weight in increasing the settlements compared to the "greenfield case was seen, as was noted by Liu (1997) in 2-D analyses.

Augarde et al. (1999) present more detail on the numerical aspects of the calculations, particularly developments in tunnel installation modeling. The conclusion was that the processes that occur during the construction of a real tunnel are highly complex, and a simplified approach is adapted to model liner installation, ground loss and the application of face support.

Houlsby et al. (1999) presents the details of the non-linear model used for undrained clay in the analyses: this was developed primarily for this project, and the nonlinearity is important for the pattern of settlements predicted. The conclusion was that Expressions have been presented for the stiffness and compliance matrices for model for the undrained behavior of clay using multiple yield surfaces. The model allows realistic fitting of observed features of soil behavior such as small strain non-linearity; hysteresis, and the dependence of stiffness on past stress history.

Finally Bloodworth and Houlsby (1999) report some of the experience of the transfer of the FE code to the Oxford Supercomputer OSCAR for the later analyses. The conclusion that was using Mohr Coulomb soil constitutive model will give acceptable results on condition that the correct construction stages to be modeled.

2.3. Numerical Modeling and Finite Element

The main purpose of modeling the soil stress-strain relationship is to predict the soil behavior due to external loading, excavation, and variation of ground water table. The engineer has to employ the prediction in the design and the analysis of geotechnical structures. He must also select the appropriate engineering modifications based on comparisons of the actual situations and the predictions, as (Terzaghi, 1936) has stated: “our theories will be superseded by better ones, but the results of observations in the field will remain as a permanent asset of inestimable value to our profession”.

For a long time, soil mechanics has been based on Hooke’s law of linear elasticity for stress and deformation analysis of a soil mass under a footing, or behind a retaining wall, where no failure of the soil is involved. This is known as elasticity problems in soil mechanics. On the other extreme, the theory of perfect plasticity is used to deal with the conditions of ultimate failure of a soil mass. Problems of earth pressure, retaining walls, bearing capacity of foundations, stability of slopes are all considered in the realm of perfect plasticity. These are called the stability problems. The progressive failure problems deal with the elastic-plastic transition from the initial linear elastic state to the ultimate state of the soil by plastic flow, and they are used to deal with tunnel analysis, for instance. The essential set of equations for the solution of progressive failure problems is the constitutive equations of soils. Long-term settlement problems and consolidation problems, however, are treated in soil mechanics as essentially visco-elastic problems.

The first part of the review deals with the fundamentals of the theory of elasticity. Then the classification of the models are studied, followed by brief details of elastic models, plastic models for uniaxial behavior, models applying the incremental theory of plasticity, models applying the deformation theory of plasticity, and models applying the flow theory of plasticity. The nonlinear elastic-perfectly plastic models will be studied in details specially Mohr-Coulomb model which is proposed to be used in this research. Hardening plasticity models including nested and bounding surface models are then discussed. Finally, the continuum modeling applying the critical state concept is explored. The details of some of the models presented above are supplied in the appendix.

2.3.1. Historical Remarks

For a long time, elasticity was developed based on Hooke's law of linear elasticity for stress and deformation analysis. Cauchy developed a model, which is both reversible and path-independent, which is non-linear perfectly elastic model. The Hyperelastic model can be regarded as a special case of Cauchy elastic model where secant modulus relating stresses to strains to ensure that no energy is generated in any loading-unloading cycle. The hyperelasticity has been formulated by Evan, and Pister, 1966; Saleeb, and Chen, 1981, and among others in soil mechanics. The Hyperelastic model may introduce a further improvement where the rate of stress is a function in the rate of strain and the current state of stress. Duncan, 1980, proposed a nonlinear hyperbolic model. This model used the tangential modulus, E_t as a function of the stress and strain levels.

Perhaps the first reference in the history of plasticity can be attributed to Coulomb essay in 1773, who proposed a yield criterion for solids such as soils. Subsequently, Rankine in 1853 applied Coulomb's concept to problems of the calculation of earth pressure on retaining walls. However, it is generally believed that the origin of plasticity, as a branch of mechanics of continua, dates back to a series of papers by Tresca from 1864 to 1872, who is regarded as the first one to perform a scientific study of the plasticity of metals. In these papers, he regarded the extrusion of metals, he proposed the first yield condition: metal yields plastically when the maximum shear stress attains a critical value. The actual formulation of the theory was done by Venant, St, 1870, who introduced the basic constitutive relation for what can be termed today perfectly plastic materials in plane stress. The salient feature of this formulation was the suggestion of a flow rule stating that the principal axes of the strain increment coincide with the principal axes of the stress. It remained later for Levy, 1870, to obtain the general equation in three dimensions. A generalization similar to the results of Levy was arrived independently by Von-Mises, 1913, in a landmark paper, accompanied by his well-known pressure intensive yield criterion (J_2 -theory, or octahedral shear stress yield condition). Prandtl, 1924 extended the Venant, St., Venant, Levy, and Von-Mises equations for the plane continuum problem, to include the elastic component of the strain, and Reuss, 1930 further expanded their extension to three dimensions. Von-Mises, 1928, generalized his previous work for perfectly plastic solids, to include a general yield function and

discussed the relation between the direction of plastic strain rate and regular or smooth yield surface; thus introducing formally the concept of using the yield function as a plastic potential in the incremental stress-strain relations of flow theory. Being currently well known, the Von-Mises yield function may be regarded as a plastic potential for the Venant, St., Levy, Von-Mises, Prandtl, and Reuss stress-strain relations. The appropriate flow rule associated with the Tresca yield condition, which contains singular regimes (discontinuities in derivatives with respect to stress), was discussed by Reuss, 1932 and 1933. Since great emphasis was placed on problems involving flow of perfect plasticity in the years before 1940, the development of the incremental constitutive relationships for hardening materials proceeded more slowly. For example Prandtl, 1928, attempted to formulate general relations for hardening behavior, and Melan, 1938 generalized the foregoing concepts of perfect plasticity and gave incremental relations for hardening solids with smooth yield surface. Also uniqueness theorem for elastic-plastic incremental problems was discussed by Melan, 1938, for both perfectly plastic and hardening materials based on some limiting assumptions (Calladine, C. R. "Engineering Plasticity", Pergamon Press, London, 1981).

2.3.2. Finite Element Method and Basic Terms

The finite elements method is a powerful numerical technique for analyzing different types of geotechnical problems to obtain an approximate solution to a wide range of engineering problems. It is used for continuum problems such as soil-structure interaction problems, underground excavations, stress analysis, vibration analysis, fluid mechanics, and heat transfer. An exact analytical solution is not always available. For such cases, the finite elements method provides a very good tool.

In 1906, researches suggested a coherent analogy for stress analysis. The continuum was replaced by a regular pattern of elastic bars. Properties of the bars were chosen in such a way that caused displacement of the joints to approximate displacements of points in the continuum. The method sought to capitalize on well-known methods of structural analysis.

Courant appears to have been the first to propose the finite elements method in its current known form. In 1941, within a mathematics lecture, published in 1943, he

used the principle of stationary potential energy and piecewise polynomial interpolation over triangular sub regions to study the Saint-Venant torsion problem. Courant's work was ignored until engineers had independently developed it.

None of the foregoing work was of much practical value at the time because there were no computers available to generate and solve large sets of simultaneous algebraic equations. It is no accident that the development of finite elements coincided with the major advances in digital computers and programming languages.

By the year 1953, engineers had written stiffness equations in matrix format and solved the equations with digital computers. Most of this work took place in the aerospace industry. At this time (1953), a large problem was one with 100 degrees of freedom (d.o.f.) at the Boeing Airplane Company. Tuner suggested that triangular plane stress elements be used to model the skin of delta wing. This work, published almost simultaneously with similar work done in England, marks the beginning of widespread use of finite elements. Much of this early work went unrecognized because of the company's policies against publication.

Starting with the 1960ies the last forty years have led to a significant development and advance in the application of numerical methods to tunneling. Whereas in the beginning of its development, numerical analysis as a design tool was often criticized, nowadays the increase of computer capacity has caused a revolution within the field of tunneling. There are no significant tunneling projects any more, which are carried out without the support of full numerical analyses. No doubt, simplified methods as discussed in the previous section still play an important role and they cannot be omitted, as they reflect both tunneling tradition and experience. But the days are gone in which tunnel design was based on experience, intuition and analytical solutions of simple continuum models alone. Today tunneling engineers are provided with a wide range of various modern numerical tools: Finite Element Method, Finite Difference Method, Boundary Element Method, Discrete Element Method, etc. Cumbersome data input and viewing of calculation results may soon be remembered as a thing of the past, as modern user-friendly data pre-and post-processing tools are being developed. Automatic mesh generation and colored output graphs make such calculations even more attractive to the engineer. Thanks to powerful computer capacity and user friendly software, numerical analyses that once

took weeks are being performed within a few days and in future within a few hours. The advantages of numerical analysis are obvious. Both complex material behavior and boundary conditions can be taken into account, whilst parametric studies to improve the design can be easily carried out.

The name (Finite Elements Method) was introduced by Clough, 1960. The practical value of the method was soon obvious. New elements for stress analysis applications were developed, largely by intuition and physical argument. In 1963, the finite elements method gained respectability when it was recognized as having a sound mathematical function: it can be regarded as the solution of a variation problem by minimization of a function. Thus the method was seen as applicable to all field problems that can be cast in a variation form. Papers about the applications of finite elements to problems of heat conduction and seepage flow appeared in 1965.

Large general-purpose finite elements computer programs emerged during the late 1960's and early 1970's. Examples include ANSYS, ASKA, NASTRAN, and COSMOS. Each of these programs included several kinds of elements and could perform static, dynamic, and heat transfer analysis. Additional capabilities were soon added. Also added were preprocessors (for data input) and postprocessors (for results evaluation). These processors rely on graphics and make it easier, faster, and cheaper to do finite elements analysis. Graphics development became intensive in the early 1980s as hardware and software for interactive graphics became available and affordable.

A general-purpose finite elements program typically contains over 100,000 lines of code and usually resides on a mainframe or a superminicomputer. However, in the mid-1980s, adaptation of general-purpose programs began to appear on personal computers. Hundreds of analysis and analysis-related programs are now available, large and small, general and narrow, cheap and expensive, for lease or purchase.

Ten papers about finite elements were published in 1961, 1934 in 1966, and 844 in 1971. By 1976, two decades after engineering applications began, the cumulative total publications about finite elements exceeded 7000. By 1986, the total was about 20,000 (Finite Elements in Geotechnical Engineering", Pineridge Press, Swansea, U. K., 1981.)

For a condensed overview of numerical methods applicable to geotechnical problems the reader is referred to Schweiger (1995). The most relevant numerical method for tunneling applications is the Finite Element Method (FEM). The method has been presented throughout the literature and detailed descriptions are available e.g. by Zienkiewicz and Taylor (1991) or Bathe (1982). In the following a contribution will be given to the modeling of tunnels with the help of the FEM. The present thesis is intended to discuss some of the points which are of major importance for FE-analysis of tunneling settlements and lining forces. Besides the consideration of different constitutive models for use in FEM, the influence of the tolerated equilibrium error in numerical analysis, the influence of FE-mesh dimensions and the mesh coarseness as well as the modeling of initial ground stresses will be discussed in this section. Here-after the focus will be on both three- and two-dimensional FE-installation procedures for conventional driven tunnels and shield tunneling. All results presented have been obtained by using the two-dimensional versions of the FE-code PLAXIS.

The method of finite elements is widely used in the field of civil engineering to solve, numerically, the problems that are too complicated to be analytically solved. It is well known that the procedure through which the solution is achieved Naylor, and Pand, 1981, can be described in six steps as follows:

Step 1: Discretization of the continuum by dividing the region into discrete elements using appropriate variety of elements (type, shape, size, ...etc.). The number and the type of these elements depend on the type of the problem and the required degree of accuracy.

Step 2: Selection of the interpolation functions. Express the unknown field variables (e.g. displacement, and rotation) at any point within the element in terms of values at the nodal points only through a set of approximate functions called (Interpolation Functions). The interpolation functions are taken as polynomials for simplicity of integration and differentiation. The degree of the polynomial depends on the number of nodes assigned to the element, continuity requirement at each node, continuity required along the interelement boundaries.

Step 3: Calculating the stiffness matrix, $[K]$, and the load vector $\{P\}$ for each element. Element equations are usually stored in an element library.

Step 4: Assembling the element equations (lumping) into the system equations which assures point wise satisfaction of compatibility of deformation requirements. Boundary conditions are only available at the node points not on the element's boundary line.

Step 5: Solving the system equations, (linear or nonlinear) for the field variables at the nodes.

2D Mesh Dimensions. For the two-dimensional parametric studies different diameters D and cover to diameter ratios H/D have been considered in order to arrive at the appropriate dimensions of the mesh height h between the tunnel invert and the bottom boundary and the minimum mesh width w between the vertical boundaries. Analyses were carried out for a total of 16 variations. First of all the appropriate dimensions for the bottom boundary have been evaluated. Hereafter the bottom boundary was fixed and the minimum dimensions for the width of the vertical boundaries have been considered.

Bottom boundary. The results obtained for the bottom boundary h can be summarized as:

$$h = (1.3-2.2) \times D \quad \text{for } D = 4m-12m \quad [2.11]$$

comparing well to the recommendations of $(2 - 3) \times D$ from the tunnel center point to the bottom boundary, i.e. $h = (1.5 - 2.5) \times D$, as given by Meissner (1996).

Mesh width. After the evaluation of the bottom mesh dimension these results were incorporated into the mesh variations for the evaluation of sufficient mesh widths w . The results obtained for the mesh width w can be well approximated by the equation

$$w = 2D \left(1 + \frac{H}{D} \right) \quad [2.12]$$

The strong correlation with the ratio H/D is logical: the deeper the tunnel the wider the surface settlement trough and vice versa. Compared to the recommendations

of $w = (4-5) \times D$ by Meissner (1996), the present criterion leads to considerably wider FE-meshes for ratios $H/D \geq 1.5$. The indication of Eq. 2.12 that surface settlement troughs will become very wide for very deep tunnels may need a further consideration. The criterion that the boundary settlement should not exceed 1% of the maximum center line settlement may not be required for relatively wide settlement troughs of relatively deep tunnels, as here the magnitudes of resulting surface settlements will generally be relatively small. Therefore an upper bound of the mesh width w when approaching relatively deep tunnels might be considered.

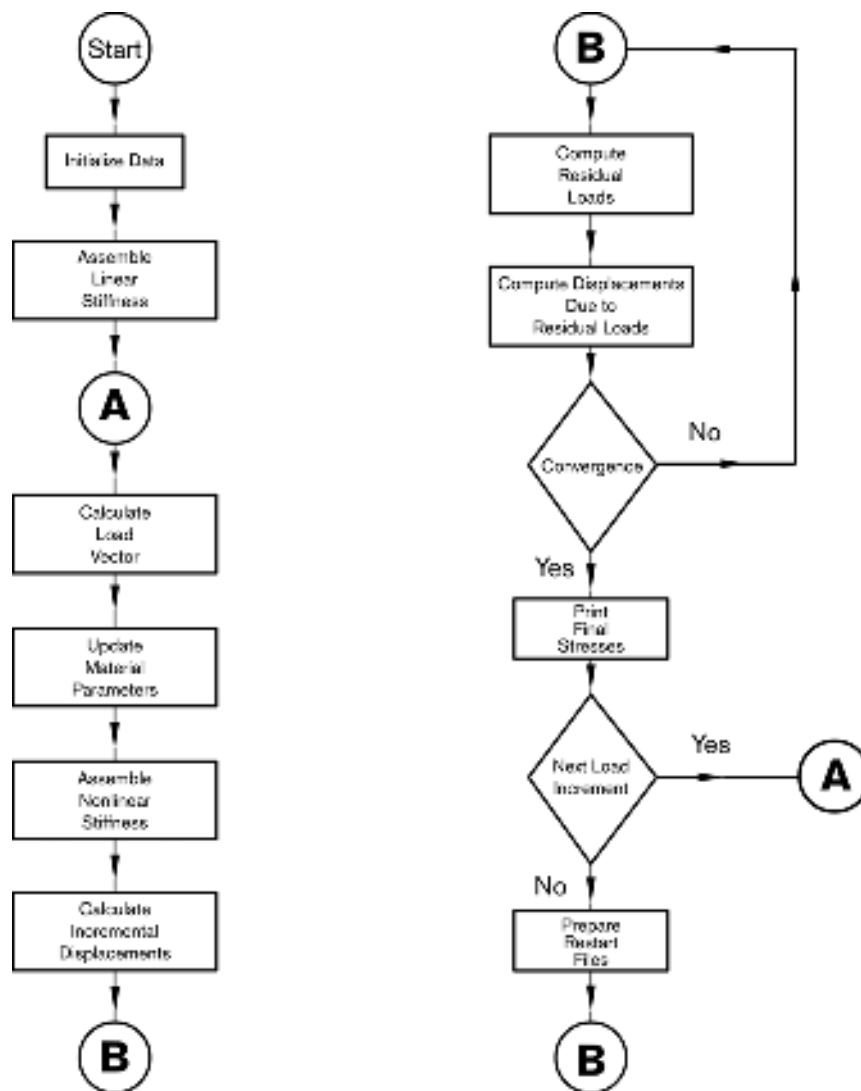


Figure 2.18: Brief Flow Chart of Any Finite Elements Program. (Finite Elements in Geotechnical Engineering”, Pineridge Press, Swansea, U. K., 1981.)

The Influence of Mesh Coarseness. If properly formulated and implemented, the FE-solution converges to the true solution when the number of degrees of freedom is increased. In such 3D analyses the consume of computer resources can increase rapidly and one would thus like to reduce the number of nodes to a minimum keeping computational results within a certain margin of accuracy. Therefore parametric studies of the mesh coarseness are required.

For 2D surface settlements it was observed Moller (2006) that they require a relatively fine local mesh coarseness, whereas 2D structural forces are little affected, requiring only a relatively coarse local mesh. On the contrary it will be shown that 3D structural forces are most sensitive to a variation of the number of nodes per round length, requiring relatively fine 3D meshes with a high number of elements.

In the following some results of the parametric studies on the 3D mesh coarseness will be highlighted. For a more detailed description of results from 2D and 3D mesh coarseness studies of surface settlements and structural forces the reader is referred to Moller (2006).

2.4. PLAXIS 2D

The PLAXIS 2D is a Finite Element Code for Soil and Rock Analyses that is capable of performing a practical analysis tool for use by geotechnical engineers considering linear and nonlinear structural analysis and anisotropic behavior of soils and/or rock. Plaxis is a finite element package that has been developed specifically for the analysis of deformation and stability in geotechnical engineering projects. The simple graphical input procedures enable a quick generation of complex finite element models, and the enhanced output facilities provide a detailed presentation of computational results. The calculation itself is fully automated and based on robust numerical procedures. This program is supporting two-dimensional analysis as well as ax- symmetric analysis.

It is worth mentioning here that, though the used program is very powerful and is capable of performing many types of analysis, this is an advantage in this work, as the author had to go through few numbers of manuals before discovering what is

relevant to structural analysis and what is not. A program that is mainly dedicated to structural or geotechnical analysis is saving a lot of time and effort.

Also, there were some numerical problems associated with using two elasto-plastic materials in the same model with extend values of material properties. These problems were discovered when some of the computer runs failed to reach convergence. The author asserted these numerical problems by changing the type of iteration, method of integration, time curve,...etc.

To avoid any problems with further users of this program in analyzing tunnels, procedures are developed that can be initiated just after starting the program, as shown lately. These procedures are very powerful feature of the program (parametric study), which the use of variables is to analyses the tunnel with exact modeling of the construction stages using TBM. The user can use these procedures and changing the values of parameters to suit his model before running the program. Later, the file can be initiated and it will not take more than 3 minutes before the results are printed on the screen.

2.4.1. Short Review of Features

Geotechnical applications require advanced constitutive models for the simulation of the non-linear behavior of soils. In addition, since soil is multi-phase material, special procedures are required to deal with hydrostatic and non-hydrostatic pore pressures in the soil. Although the modeling of the soil itself is an important issue, many geotechnical engineering projects involve the modeling of structures and the interaction between the structures and the soil. Plaxis is equipped with special features to deal with the numerous aspects of complex geotechnical structures. A brief summary of the important features of the program is given below.

Graphical Input of Geometry Models. The input of soil layers, structures, construction stages, loads and boundary conditions is based on convenient drawing procedures (CAD), which allows a detailed and accurate modeling of real situations to be achieved. From this geometry model a finite element mesh is automatically

generated. Plaxis allows for fully automatic generation of unstructured finite element meshes with options for global and local mesh refinement. High order elements are available to enable a smooth distribution of stresses in the soil and an accurate prediction of failure loads. Special beam elements are used to model the bending of tunnel linings. The behavior of these elements is defined using a flexural rigidity, a normal stiffness and an ultimate bending moment. Beams may be used together with interfaces to perform highly realistic analyses of a large range of geotechnical structures.

These joint elements are needed for calculations involving soil-structure interaction. They may be used to simulate the thin zone of intensely shearing material at the contact of tunnel lining and the surrounding soil. Values of interface friction angle and adhesion that are not necessarily the same as the friction angle and cohesion of the surrounding soil may be assigned to these elements.

Plaxis offers a convenient option to create circular tunnels composed of arcs. Beams and interfaces may be added to model the tunnel lining and the interaction with the surrounding soil. Fully isoparametric elements are used to model the curved boundaries within the mesh.

Fixities are prescribed displacements equal to zero. These conditions can be applied to geometry lines as well as to geometry points in x and y directions. A convenient option exists to use standard boundary conditions that apply in most cases.

Material properties for soil, as well as for structural elements are entered in a project database. Material data sets from the projects database may be copied to the global database, for use in other runs. Multi-linear pore pressure distributions can be directly generated on the basis of phreatic lines.

Plaxis distinguishes between drained and undrained soils to model permeable sands as well as most impermeable rocks. Excess pore pressures are computed during plastic calculations when undrained soil layers are subjected to loads. Undrained loading situations are often decisive for the stability of geotechnical structures.

Plaxis can be run in an automatic step-size and automatic time step selection mode. This avoids the need for users to select suitable load increments for plastic

calculations by themselves and it guarantees an efficient and robust calculation process.

This feature enables accurate computations of collapse loads and failure mechanisms to be carried out. In conventional load-controlled calculations the iterative procedure breaks down as soon as the load is increased beyond the peak load. With arc-length control, however, the applied load is scaled down to capture the peak load and any residual loads.

Using this option the finite element mesh is continuously updated during the calculation. For some situations, a conventional small strain analysis may show a significant change of geometry. In these situations it is advisable to perform a more accurate Updated Lagrangian calculation.

The Plaxis postprocessor has enhanced graphical features for displaying computational results. Exact values of displacements, stresses and structural forces can be obtained from the output tables or graphs.

Chapter 3: DEVELOPMENT MODELS

3.1. Study Area

The scope of the study addresses regional geology of UAE in general and Dubai in particular with unique depositions. Mostly sandy soils and weak rock of calcite origin predominates the superficial geology. The ground water table is generally high. Interpretation of the geotechnical properties are performed information from borehole logs and reports. In this chapter, the selection of subsurface soil models for emirate of Dubai and their development in the PLAXIS 2D will be presented. Around 14 subsurface models are envisioned to represent adequately the study area. Validation procedures and results are also presented. Liquefaction is a problem in the reclaimed and very loose soils to dynamic loads and is not considered.

The tunnel lining will be assumed to behave as linear elastic material, with appropriate elastic modulus and Poisson's ratio. The soil will be assumed to have non-linear characteristics following the Mohr-coulomb criterion.

Finite element development is based on plane strain idealized 15 noded isoparametric element to model the soil, and two node curved bar element are used to simulate lining of the tunnel. Since the model is symmetric, only one symmetric half (the right half) is considered. The plane of symmetry is a smooth boundary and fixed vertical ends will be used to restrict the movement of the ends of the model. The problem is a two – dimensional continuum finite element which is a plan strain case. Only in-plane displacements, strains and stresses are generated. The normal and shear stress components in the horizontal (longitudinal) direction are zero or negligible.

The performance and accuracy of the software is validated by carrying out analyses of problems with known analytical solutions (Elastic & Plastic).

3.2. Geology

Dubai with an area of 3885 sq.km, is the second largest emirate in the UAE. It has a population of about 1.47 million and a GDP per capita standing as 3rd in the

Middle East and 14th in the world. The Rulers of Dubai have an advance thinking of a developed society and are constantly devolving all buildings and infrastructure facilities- transport, schools hospitals, tourism developments and other amenities of an advanced society.

The deposits of the United Arab Emirates Coastline and the floor of the Arabian Gulf are mostly Pleistocene or recent in age. The Arabian Gulf is an area of extensive carbonate sedimentation, and the nature and distribution of the sediments is governed by the recent geological history and the structural setting of the Gulf, the orientation of the coastline and the prevailing winds.

A full geological summary can be founded in “Geotechnical Practice and ground conditions in the coastal regions of the United Arab Emirates”, R.J. Epps, 1980. The coastline around Dubai and Sharjah is essentially a linear feature and is largely formed from lateral accretion offshore of beach and dune sand overlying Miliolite sandstone. At Dubai and Sharjah, the coastline is dissected by channels or creeks and consists of a beach / dune complex with development of sabkha plains in the hinterland at the head of the creeks. Furthermore, erosion capillary rise phenomena as well as evaporations have led to extensive silt deposit in some areas especially near to the creeks. Recent sediments overlying Aeolian carbonate sandstone are therefore general encountered with occasional development of bioclastic limestone. However, the Miliolite Sandstone represents a former Aeolian deposit and tends to reflect the morphology of the dunes in which it was formed.

The surface level of the sandstone therefore varies appreciably over the area, being exposed at ground level in some localities in Dubai, and occurring at depths of up to 10 or 12 meters elsewhere. Towards Sharjah, the sandstone passes laterally into sand with cemented and sandstone layers, which is encountered to the depth of penetration of normal site investigation boreholes. In Sharjah, large thickness of recent carbonate sands are encountered, which tend to become cemented with depth to form bands of carbonated sandstone and strongly cemented sand, with un cemented and weakly cemented layers.

There is a long list of exciting structures that were unimaginable until they were executed in Dubai, including the world’s tallest tower- Burj Khalifa (Dubai), the largest indoor ski slope with its own ski lift, the largest man made islands in the world (Palm Jumeirah Palm Jebel Ali, Palm Deira, World), Dubai Metro Rail (Red, Green lines), the underwater hotel etc.

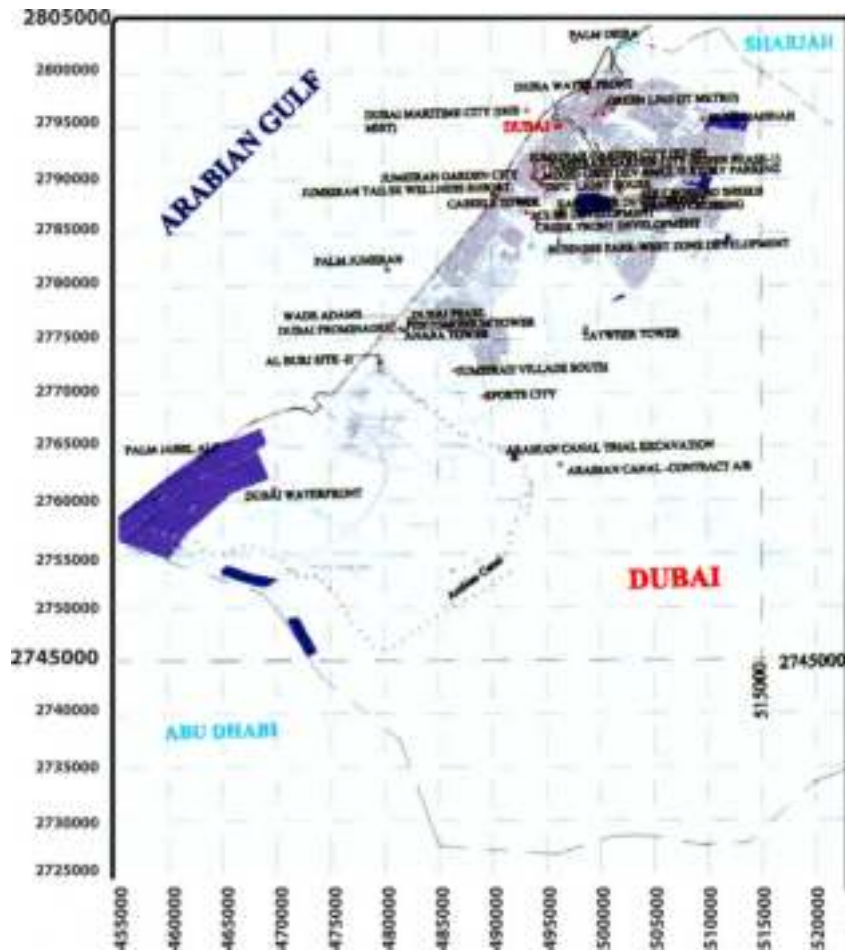


Figure 3.1: Plan of Dubai with location of Projects

Today, such engineering marvels have become an attraction for the tourists and visitors to Dubai. Projects worth billions are contemplated in Dubai. In the technicalities of all these developmental works, Geotechnique plays a sustainable role. Dubai is characterized by a mainland of desert/ sand dunes and a coast line of over 50 km along the Arabian Gulf. Occupying the northern part of UAE, the state of Dubai is bound by the states of Sharjah and Abu Dhabi to the East, West and SW, respectively, and the Arabian Gulf to the North1 North West (Figure 3.1). The state is thickly populated in about 55% of the total area closer to the NE-SW trending coastal belt, with active developmental works involving construction of tower structures, buildings, villas, roads, metro rail and power and desalination plants, etc.

3.2.1. Physiography of Dubai

Physiographically, the area of Dubai state (Figure 3.2) can broadly be divided as the main land and coastal belt in a ratio of 9: 1. The details of the physiographic units with their engineering geology, ground and geotechnical characteristics are discussed below:

The terrain is mostly occupied by the Aeolian / desert sand dunes (Figure 3.2). The inter-dunal areas / low land / depressions, covering vast areas of about 3500 sq m (80% of the area of Dubai), contain hard encrustations of local / in- land sabkah, in areas with near surface water table and thin sheets of aeolian sand overlying the local fans of gravels. The sand dunes closer to the coastal belt are: light colored - light yellowish-brown - due to enrichment of carbonate source material from the sea shells and the rocks. The inland dunes are of dark color – dark brown to brown - due to oxidation in arid environment.

The elevations vary from sub-sea levels to El. +100 m in the desert dunes, lying to the south. The intervening depressions between the long longitudinal dunes have hard encrustations of sabkah and locally coarse to very coarse alluvial fan deposits. The ground water level in these reaches is noticed at shallow depths (could be perched water).

The +50 km long coastal belt, covering about 10% of Dubai along the Arabian Gulf coast (Figure 8.2) is identified between sub-sea level to 4 m asl. The zone is marked by raised beach deposits of calcareous Oolitic sand, locally forming fringing sandpits, shoals and small islands. The coastal sabkah are noticed along the coast and inland up to El. 2 4 m asl. The gradient of the coastal zone towards the sea is around 1:1000. Some of the onshore islands are part of the extensively developed sabkah deposits. The creeks of Dubai are seen with sabkah deposits which are locally masked by thin cover of beach or desert sand. Recent sediments of 6-8 m thickness, deposited during the geologically recent eustatic sea level changes (late Pleistocene), consisting of silt, silty fine sand with shells and some gravels, are noticed in the main-land reaches close to the coastal belt. These sediments are loosely compacted.

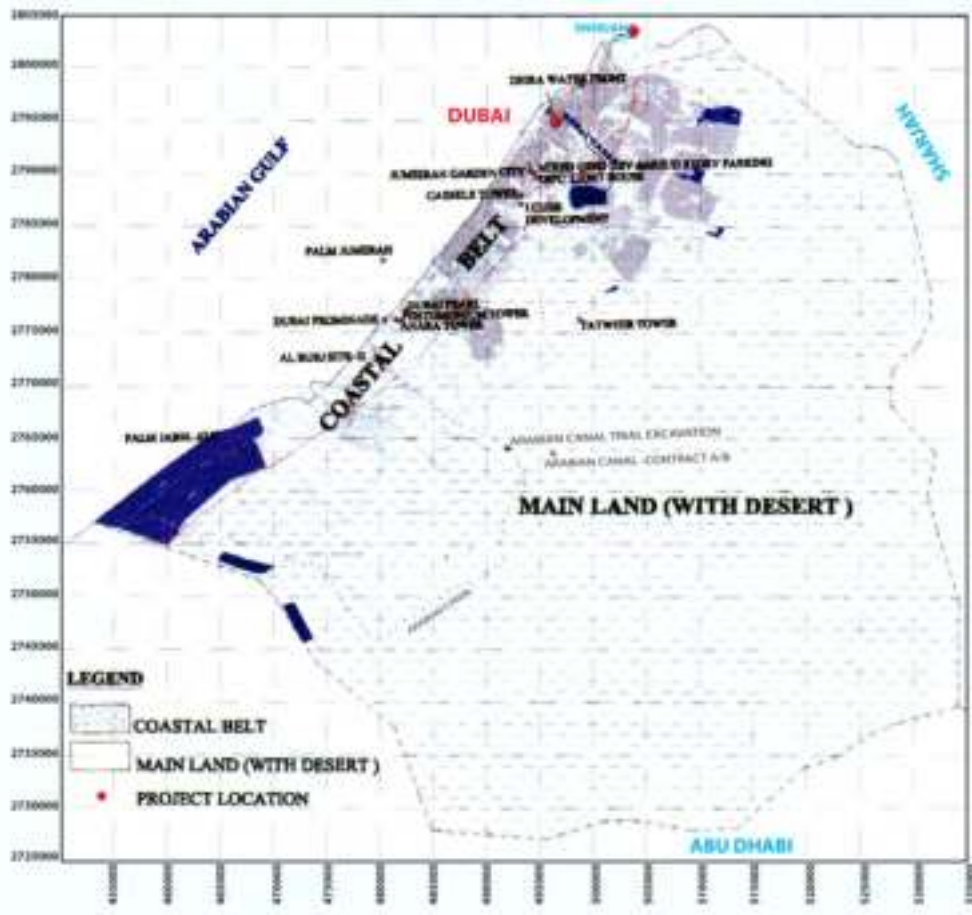


Figure 3.2: Physiography Divisions of Dubai

3.2.2. Geology of Dubai

Dubai area is covered with Middle to Upper Tertiary group of rocks underlying the recent soil/ desert sand or beach sand of varying thickness of 0.5 - 17 m. The rocks were deposited in a shallow sea continental shelf platform depositional environment, very similar to the present day depositional environment in the Gulf. The interpreted soil and rock units noticed in Dubai area (Table 3.1) are an interlayered sequence of silty to fine sandy soils with shells, which are underlain by an inter-bedded sequence of sandstones (Arenaceous unit), siltstone claystone (Argillaceous unit), conglomerates (Conglomeratic unit), and Gypsum (sabkah) beds. The inter-bedding indicates facies variations due to fluctuating energy conditions in the depositional basin. The sabkah (evaporites) deposits with interbeds of siltstone clay stones indicate a saline arid environment of depositions with restricted circulation. The rocks in general are sub-horizontally bedded with rolling dips of $<10^\circ$ and a

regional dip towards North Northwest. The generalized lithostratigraphy of Dubai area is given in (Table 8.1).

Table 3.1: The Litho-Stratigraphic Units of Dubai Area

Period	Unit	Lithologic Group	Thickness (m) (approx)	Elevation (m) (approx)	Description
Quaternaries	I	Over burden	<1 – 17	Varying	Includes all soils of following origins.
	Ia	Aeolian sand	1.0– 3.5		Brownish, Fine to very fine Dune sand in the desert
		Beach sands			Light grey, medium to fine sand on the beach/ coast.
(Pleistocene?)	Ib	Recent Sediments	6 – 10	Varying	Loose to Medium dense, brownish, silty-fine sand with sea shells (deposited during the sea level fluctuations, due to eustatic changes).
	Ic	<u>Recent Sabkah</u> Inland (desert) & Coastal sabkah	0.5– 2.5	<1 to +2.5	<i>Inland:</i> dark brownish coloured, poorly compacted. exposed in inter-dunal areas. <i>Coastal:</i> Light brownish coloured, friable/ poorly compacted.
Early to middle Tertiary	II	Rudite group of Rocks	0.5 – 5.0	Varying	Inter-beds of reddish brown Polymictic Conglomerates and calcirudite of varying thickness from 0.5 to 5.0 m. medium to fine gravels of basic/ igneous rock, sand stone, siltstone and cherts. Occur as interbeds only in Arenites and Argillites.
	III	Arenite group of Rocks (Sand stones)	5 – 35	Between +55 and -10	Grayish brown to light brown medium to fine grained sandstone with inter-beds of destructured (class 'D'; chemically weathered/ decomposed) sandstones. Pebbly / gravelly calcareous sandstone/ calcarenites, Conglomeratic calcareous Sand- stone. Gravels of gypsum also noticed locally.
	IV	Argillite/ Lutite group of Rocks (Siltstone/ claystone)	+75	-35 to -200	- Light grey to greenish grey calcareous siltstone with interbeds of conglomerate, gypsum and sandstone. - Conglomeratic siltstones with gravels of siltstone, sandstone, igneous/ ophiolite suit of rocks and crystalline gypsum. - Clay stone/ siltstone (MM - MH) between El. -85 to -100 m. inter-laminations and angular clasts of gypsum also noticed locally.
	V	Deep- seated / Paleo Sabkah deposits/ gypsum beds	+20	- 95	Light grey to colour less/ transparent, Crystalline Gypsum / Anhydrite beds, hard and Compact. With inter laminations of siltstone (ME)/ clay (CE).

3.3. Sites Considered for Modeling

The following engineering geology of Dubai has been brought out, with a view of disseminate the information on the typical ground characteristics of Dubai from

around 27 soil investigation reports as per (Table 3.2). 14 Soil Formation Models which represent Dubai Stratifications considered in the study are as per the descriptive logs in Appendix I.

Table 3.2: List of Projects Considered for the Soil Models

ACES Ref.	Name of Project (with abbreviation)	Location	Structure/ Height (m)	Max. depth of Bore Hole (m)	Av. GL/ EL, DMD (m)
*S/D07-195/ 222	Arabian Canal - Contract A/B * (AC)	Dubai, U.A.E.	Canal Development	61 – 150	55.18
S/D08-004	Arabian Canal- Trial Excavation (ACTe)	Dubai, U.A.E.	Canal Development	100.5	31.581
-	Al Burj site 2 (AB)	Dubai	Super Tower	201	2.65
S/D07-159	Cassels Tower (CT)	Business Bay,	Towers	90	2.963
*S/D08-019	Creek front Development – Business Park (BP)	Business Bay	Towers	50	3.57
S/D06-239	Dubai Metro Project – Greenline (JTM)	Salz Al din to Airport Road,	Elevated track	41 – 43	3.81
*S/D08-025	Dubai Promenade Link Bridge (P)	Marina	Bridge	40.00	4.02
S/D07-156	DIFC Lighthouse (LH)	Shk. Zayed Road	Towers	100	2.02
S/D07-206	Dubai Pearl (DP)	Al Safouh	Towers	80	2.28
*S/D08-024	Deira Water Front Dev't. (DWFD)	Deira Corniche	Towers	40	3.02
S/D08-149	Dubai Maritime City - IRIS MIST. (MC)	Maritime City	Towers	100.00	5.65
S/D06-055	Dubai Water Front (DWF)	Water Front	Towers	53.35	9.49
S/D08-018	Dubai Promenade- N027 (P1)	Mina Seyahi, Marina	Towers	100	2.685
*S/D08-091	East Gate - SouthEast Zone(EG)	Business Bay	Comm / Resd. Dev't	55	6.242
S/D08-048	Hard Rock Tower -Mixed Used Dev't. (HRT)	Shk. Zayed Road	Towers	100	2.536
S/D07-053	I-Cube Development	Business Bay	Towers	80	3.527
S/D08-050	Jumerah Garden City -EP-07. (JG7)	Al Satwa,	Towers, Villas and Canals	150	4.2964
S/D08-061	Jumerah Garden City -EP-09. (JG9)	Al Satwa,		80	3.47
S/D08-131	Jumerah Garden City -Super phase 1 (JGsp)	Al Satwa,		80	2.63
S/D07-149	Pentominium Tower (PT)	Marina	Towers	125	2.086
S/D08-046	Proposed Crescent - Plot PACA-69 (PJA)	Palm Jebel Ali	Towers	80	2.36
*S/D07-008	Prop. Palm Jumerah Hotel (PJH)	Palm Jumerah	Towers	50	4.14
S/D08-110	Proposed 2B+G+18 - Ruffi Twin Towers. (RTT)	Sports City	Towers	30.00	28.01
*S/D08-092	Sixth Crossing - Sheikh Rashid Crossing	Sheikh Rashid Crossing	Bridges	40.00	8.75
S/D08-011	Tatweer Tower (TT)	Emirates Road	Towers	120	24.355
S/D08-097	Tamoor Super High Rise Tower - Anara Tower (AT)	Al Sufouh Second	Towers	150	3.2678
*S/D08-037	West Zone Dev't. - Business Park (BP)	Business Bay	Towers	40	1.51

NB: *- In addition, data on bedrock and water table were taken from few more boreholes of 18 – 60 m depth

The sites considered for this study are shown in the following figures and series of plates inferred from the sections of two boreholes. Figures 3.3 to 3.8 includes

6 Plates showing 14 Soil Formation Models which represent Dubai Stratifications considered in the study.

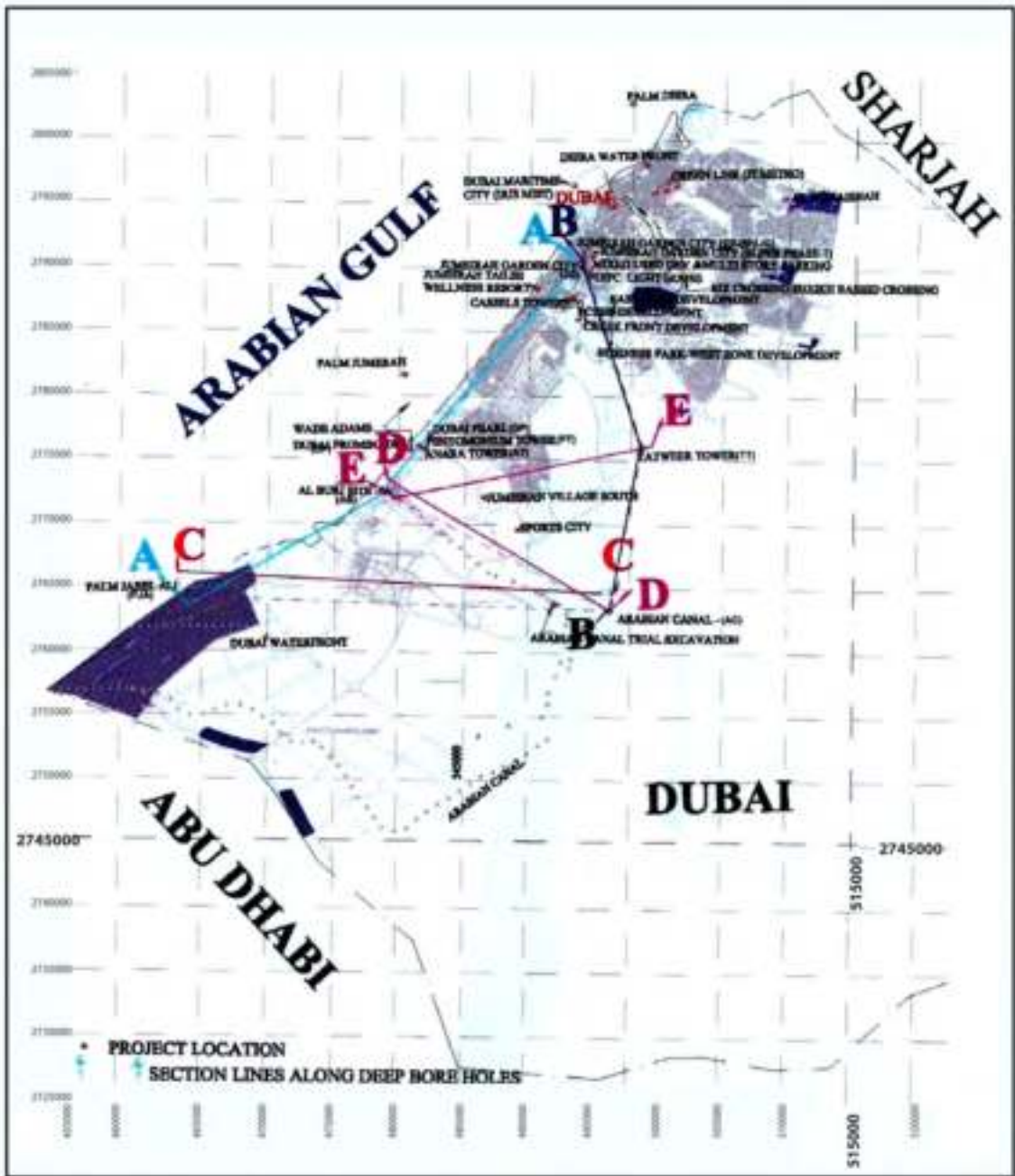


Plate I : plan of Dubai shwing cross section lines

Figure 3.3: Soil Formation representing Dubai Stratifications

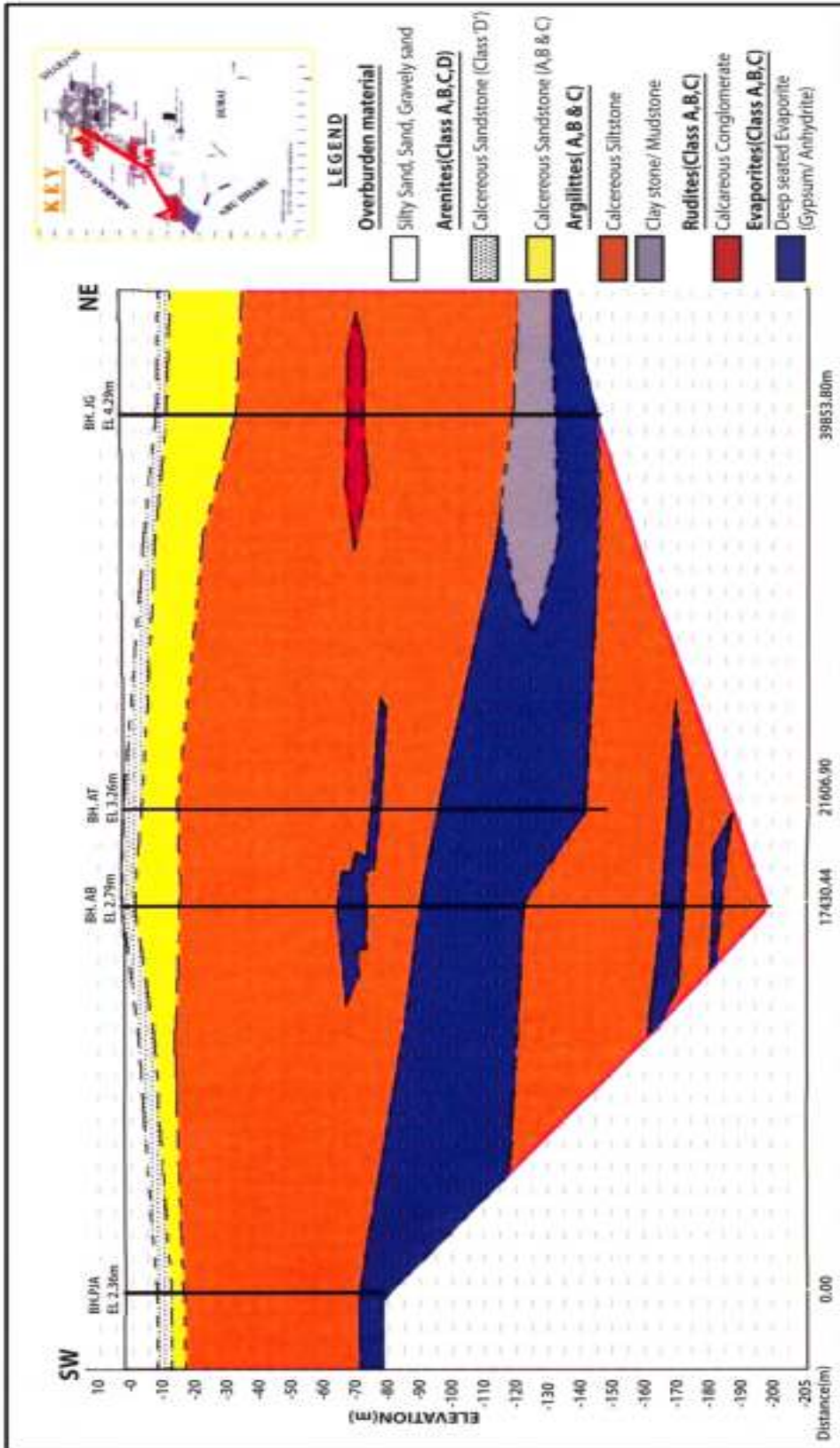


Plate II : Sction AA (Refer Plate I for section line and Appendix A for abbreviation)

Figure 3.4: Soil Formation representing Dubai Stratifications

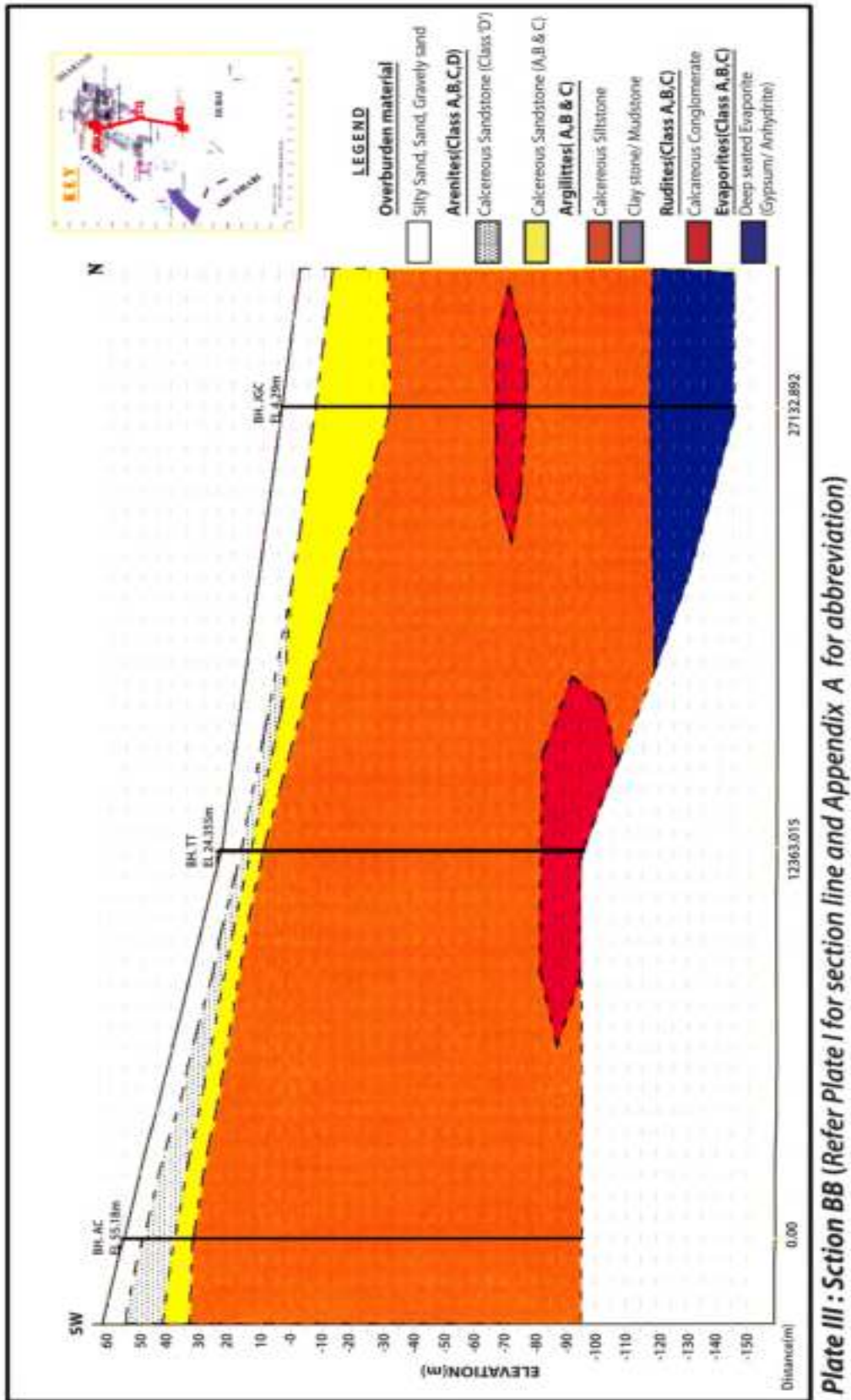


Figure 3.5: Soil Formation representing Dubai Stratifications

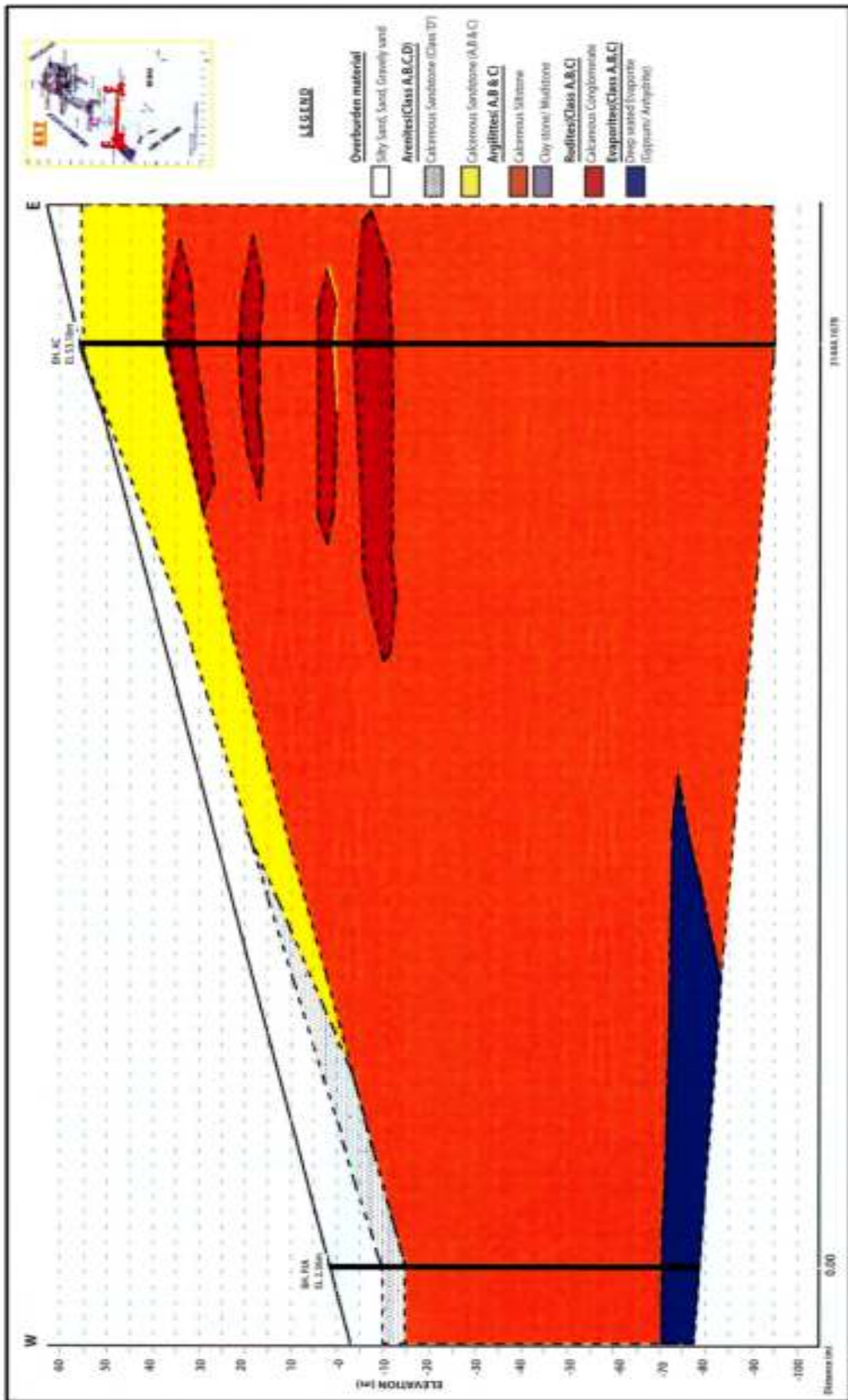


Figure 3.6: Soil Formation representing Dubai Stratifications

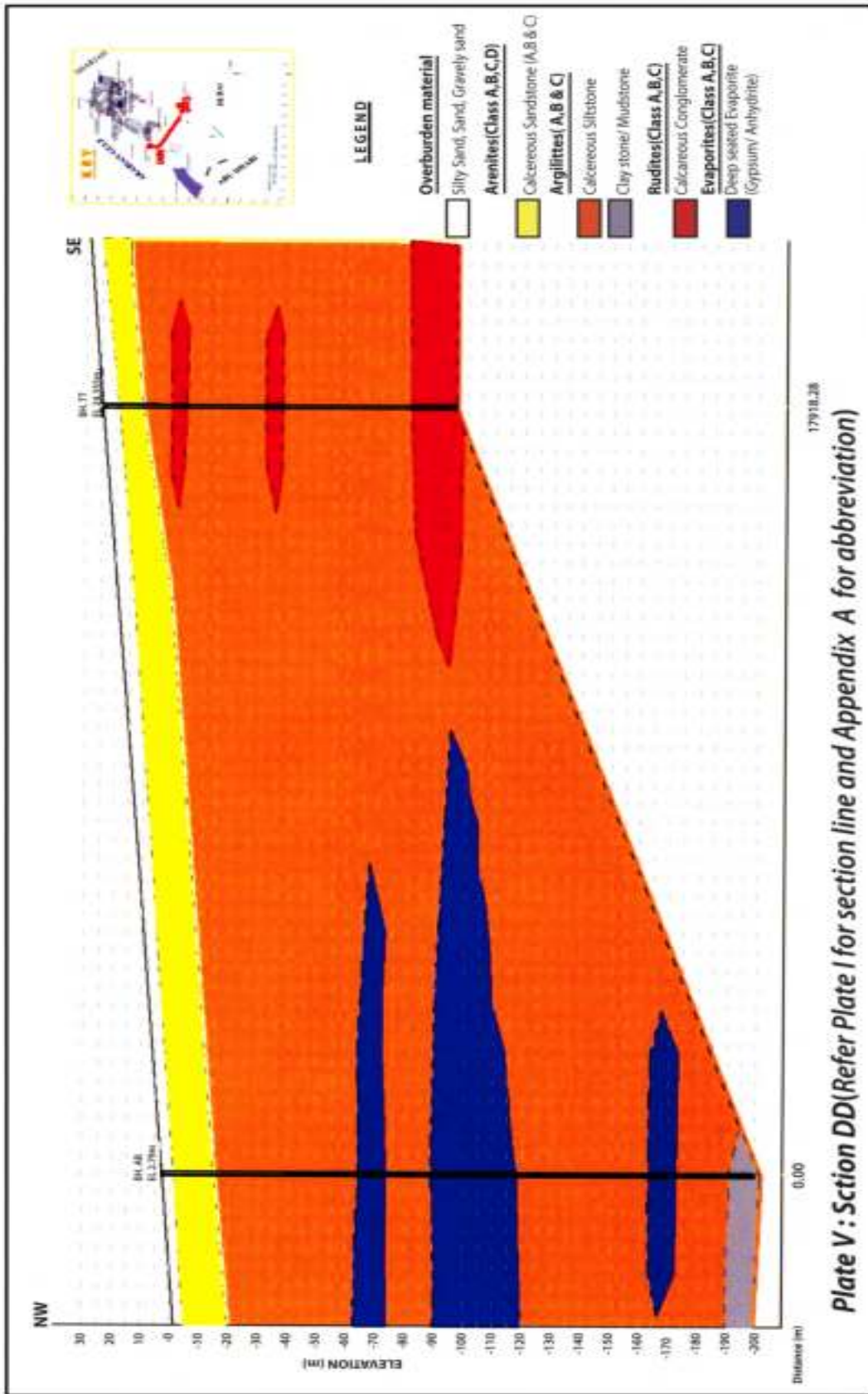


Figure 3.7: Soil Formation representing Dubai Stratifications

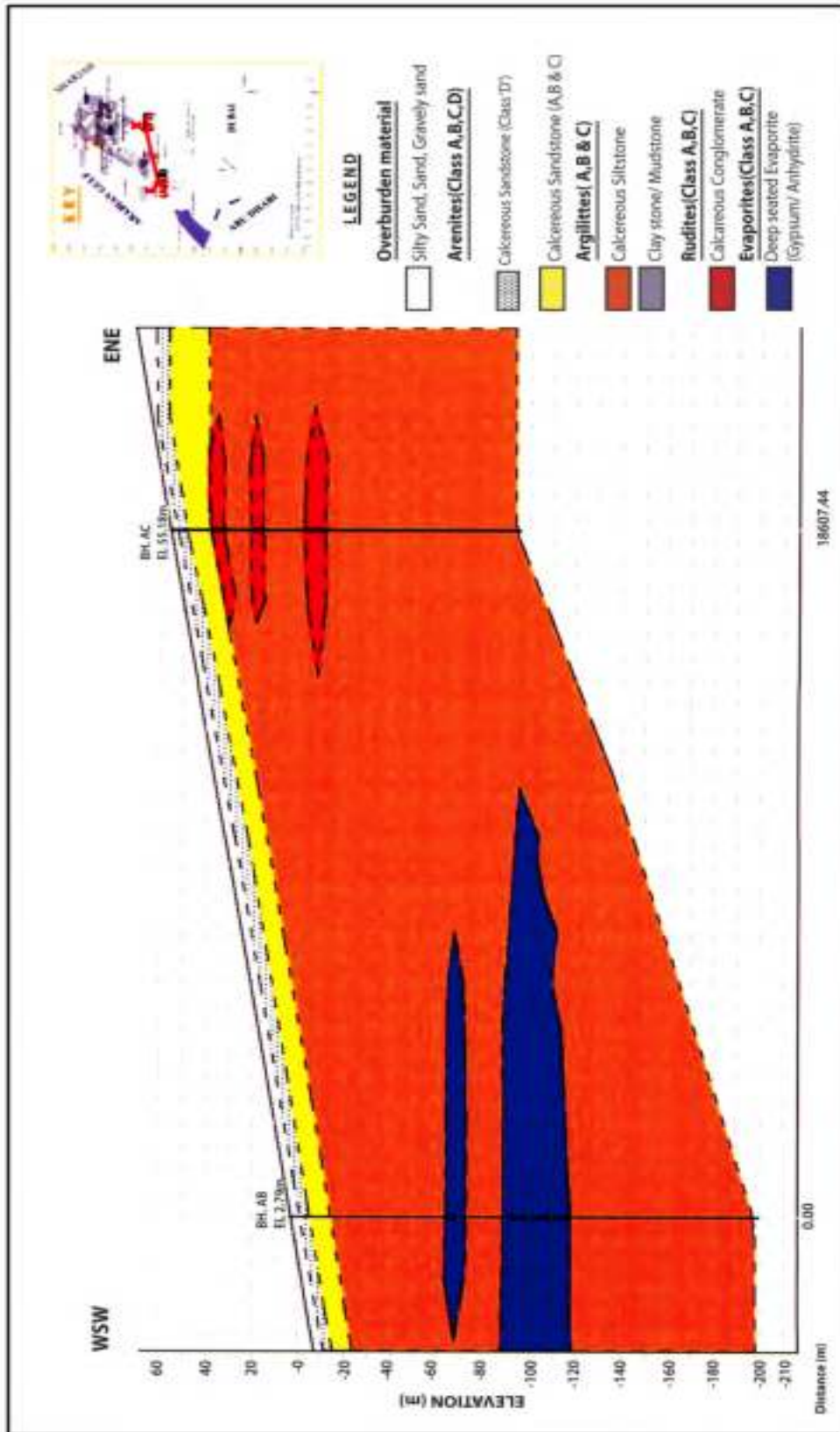


Figure 3.8: Soil Formation representing Dubai Stratifications

Rock Structure. Structural geology is the understanding of the joints and discontinuities in rock mass which plays a vital role in the design of engineering structures like shallow foundations, excavations, slopes and underground structures. In view of the thick deposits of aeolian sand dunes / soil cover, out-crops of rock are scanty, except a few of pliocene sandstones seen in the main land area in the southern parts of Dubai. Excavations for the construction of engineering structures in the main land area expose rock formations at depths ranging from 1 to 10 m. such exposures are seen around the sports city area and the Arabian canal.

For geotechnical engineering, the nature of formation of these discontinuities is important as similar categories of discontinuities (joint sets), showing similarities in their properties of dimensions and shears strength, are used in the review of the stability of a site.

Ground Water Table. The water table in the Dubai area varies between 8-12 m in the main land area and 1-7 m in the coastal belt. The general flow gradient is towards North West (NW), i.e. towards the Arabian Gulf. The flow pattern in the coastal belt zone indicates local flow concentrations which could be due to excessive pumping activity during constructions. In the main land area, the ground water conditions show a general gradient towards NW. Perched water tables are noticed in the southern parts of the main land at shallow depths of 2-5 m (Arabian Canal project) Fluctuations in the water table up to 11 m (Dubai Silicon Oasis developments) are noticed in the main land areas with the seasonal variation.

3.4. Numerical Modeling of Sites

In a finite element mesh three types of components can be distinguished, as described below.

During the generation of the mesh, clusters are divided into triangular elements. 15-node triangles are available for a more accurate calculation of stresses and failure loads. Meshes composed of 15-node elements are actually much finer and

much more flexible, but calculations with these meshes are also much more time consuming than calculations with 6-node elements.

A 15-node triangle consists of 15 nodes. The distribution of nodes over the elements is shown in Figure 3.9. During a finite element calculation, displacements are calculated at the nodes.

In contrast to displacements, stresses are calculated at individual Gaussian integration points (or stress points) rather than at the nodes. A 15-node triangular element contains 12 stress points as indicated in Figure 3.9a and a 6-node triangular element contains 3 stress points as indicated in Figure 3.9b.

15 node element was preferred over smaller node elements to accommodate non-linearity of the soil. Since the modeling of the soil is based on mohr-coulomb criterion which incorporates non-linear plastic behavior, the higher number of nodes are considered suitable for this reason.

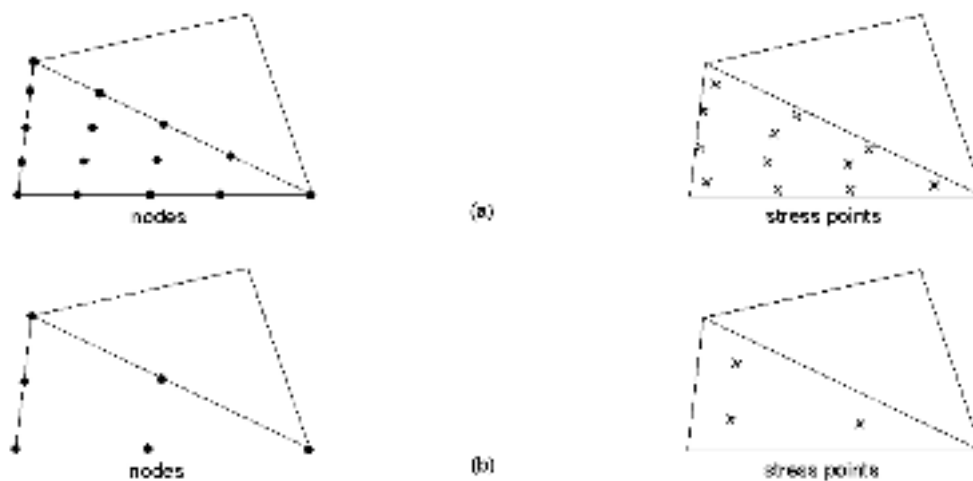


Figure 3.9: Nodes and stress points

3.4.1. Components, Analysis and Procedures

The three types of components in a geometry model are described below in detail. After the creation of a geometry model, a finite element model can

automatically be generated, based on the composition of clusters and lines in the geometry model. Points from the start and end of lines.

Lines are used to define the physical boundaries of the geometry, the model boundaries and discontinuities in the geometry. A line can have several functions or properties.

Clusters are areas that are fully enclosed by lines. Plaxis automatically recognizes clusters based on the input of geometry lines. Within a cluster the soil properties are homogeneous. Hence, clusters can be regarded as parts of soil layers. Actions related to clusters apply to all elements in the cluster.

A shield tunnel is constructed by excavating soil at the front of a tunnel boring machine (TBM) and installing a tunnel lining behind it. In this procedure the soil is generally over-excavated, which means that the cross sectional area occupied by the final tunnel lining is always less than the excavated soil area. Although measures are taken to fill up this gap, one cannot avoid stress re-distributions and deformations in the soil as a result of the tunnel construction process. In order to avoid damage to existing buildings or foundations on the soil above, it is necessary to predict these effects and to take proper measures.

It is possible to simulate construction and excavation processes by activating and deactivating clusters of elements. This procedure allows for a realistic assessment of stresses and displacements as caused.

Different practical methods are implemented to analyze the deformations that occur due to the construction of the tunnel. These procedures are developed that can be initiated just after starting the program, as shown below. These procedures are very powerful feature of the program, which the use of variables is to analyses the tunnel with exact modeling of the construction stages using TBM. The user can use these procedures and changing the values of parameters to suit his model before running the program. For each new project to be analyzed it is important to create a geometry model first.

A geometry model is a representation of a real problem and consists of points, lines and clusters. A geometry model should include a representative division of the subsoil into distinct soil layers, structural objects, construction stages and loadings. The model must be sufficiently large so that the boundaries do not influence the results of the problem to be studied. Since the situation is more or less symmetric, only one symmetric half (the right half) is taken into account in the plane strain model. From the center of the tunnel the model extends for 50 m in horizontal direction. This extends distance obtained after many preliminary trials until getting almost no stresses and displacement at these edges.

The basic geometry including the soil layers (but excluding the tunnel), can be created. For the generation of the tunnel we will use the tunnel designer, which is a special tool within Plaxis that enables the use of circle segments to model the geometry of a tunnel. The tunnel considered here is the right half of a circular tunnel and will be composed of four segments. A lining and interface can be assigned directly to all tunnel sections. A tunnel lining consists of curved beams. The lining properties can be specified in the material database for beams. Similarly, a tunnel interface is nothing more than a curved interface.

The Contraction parameter can be used to simulate the volume loss in the soil due to the construction of the tunnel. This procedure can be activated in plastic calculations. Activation of the contraction procedure during a plastic calculation results in a homogeneous 'shrinkage' of the tunnel lining, which reduces the cross section area of the tunnel. The Contraction parameter is defined as the reduction of the tunnel area as a percentage of the original tunnel area. A contraction can only be specified for circular tunnels with a homogeneous tunnel lining.

Boundary Conditions. Applying the appropriate boundary conditions as the plane of symmetry is a smooth boundary and fixed vertical ends will be used to restrict the movement of the ends of the model perpendicular to the plane of symmetry only. The upper plane of the mesh is left free. Other side boundaries and the bottom plane are fixed. The beam (tunnel lining) that extends to a geometry boundary that is fixed in at least one direction obtains fixed rotations.

Material Properties. The material properties for the different soil layers and interfaces are as per Appendix I. For all layers the material behavior is set to drained since we are interested in the long term deformations. A beam data set has to be created with the properties of the tunnel lining. These properties are listed in Table 3.3 which will be fixed for all the runs for the purpose of comparison.

Table 3.3: Material properties of the tunnel lining (beam)

Parameter	Name	Value	Unit
Type of behaviour	<i>Material type</i>	Elastic	
Normal stiffness	<i>EA</i>	$1.4 \cdot 10^7$	kN/m
Flexural rigidity	<i>EI</i>	$1.43 \cdot 10^5$	kNm ² /m
Equivalent thickness	<i>d</i>	0.35	m
Weight	<i>w</i>	8.4	kN/m/m
Poisson's ratio	<i>v</i>	0.15	-

3.4.2. The Mohr-Coulomb model

The Mohr-Coulomb yield condition is an extension of Coulomb's friction law to general states of stress. In fact, this condition ensures that Coulomb's friction law is obeyed in any plane within a material element.

The full Mohr-Coulomb yield condition can be defined by three yield functions when formulated in terms of principal stresses (see for instance Smith & Griffith, 1982):

$$f1 = \frac{1}{2} |\sigma_2' - \sigma_3'| + \frac{1}{2} (\sigma_2' + \sigma_3') \sin \varphi - c \cos \varphi \leq 0 \quad [3.1]$$

$$f2 = \frac{1}{2} |\sigma_3' - \sigma_1'| + \frac{1}{2} (\sigma_3' + \sigma_1') \sin \varphi - c \cos \varphi \leq 0 \quad [3.2]$$

$$f3 = \frac{1}{2} |\sigma_1' - \sigma_2'| + \frac{1}{2} (\sigma_1' + \sigma_2') \sin \varphi - c \cos \varphi \leq 0 \quad [3.3]$$

The two plastic model parameters appearing in the yield functions are the well-known friction angle ϕ and the cohesion c . These yield functions together represent a hexagonal cone in principal stress space as shown in Figure 3.10

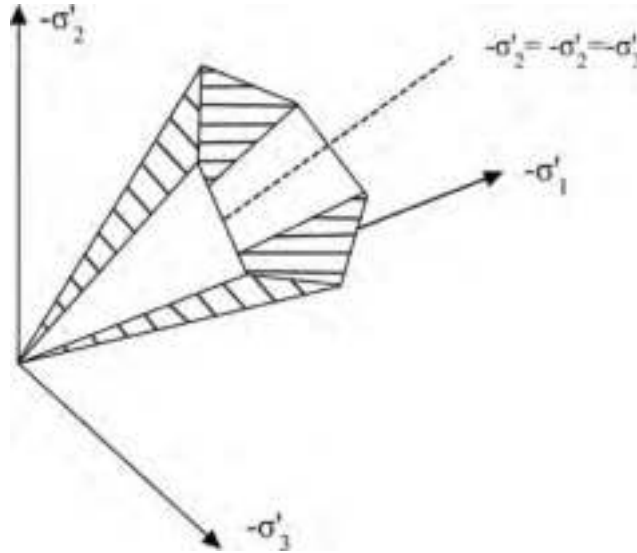


Figure 3.10: The Mohr-Coulomb yield surface in principal stress space ($c = 0$)

In addition to the yield functions, three plastic potential functions are defined for the Mohr-Coulomb model:

$$g1 = \frac{1}{2} |\sigma_2' - \sigma_3'| + \frac{1}{2} (\sigma_2' + \sigma_3') \sin \psi \quad [3.4]$$

$$g2 = \frac{1}{2} |\sigma_3' - \sigma_1'| + \frac{1}{2} (\sigma_3' + \sigma_1') \sin \psi \quad [3.5]$$

$$g3 = \frac{1}{2} |\sigma_1' - \sigma_2'| + \frac{1}{2} (\sigma_1' + \sigma_2') \sin \psi \quad [3.6]$$

The plastic potential functions contain a third plasticity parameter, the dilatancy angle ψ . This parameter is required to model positive plastic volumetric strain increments (dilatancy) as actually observed for dense soils. A discussion of the entire model parameters used in the Mohr-Coulomb model is given at the end of this section.

When implementing the Mohr-Coulomb model for general stress states, special treatment is required for the intersection of two yield surfaces. Some programs use a smooth transition from one yield surface to another, i.e. the rounding-off of the corners (see for example Smith & Griffith, 1982). In PLAXIS, however, the exact form of the full Mohr-Coulomb model is implemented, using a sharp transition from one yield surface to another. For a detailed description of the corner treatment the reader is referred to the literature (Van Langen & Vermeer, 1990).

For $c > 0$, the standard Mohr-Coulomb criterion allows for tension. In fact, allowable tensile stresses increase with cohesion. In reality, soil can sustain none or only very small tensile stresses. This behavior can be included in a PLAXIS analysis by specifying a tension cut-off. In this case, Mohr circles with negative principal stresses are not allowed. The tension cut-off introduces three additional yield functions, defined as:

$$f_4 = \sigma_1' - \sigma_t \leq 0 \quad [3.7]$$

$$f_5 = \sigma_2' - \sigma_t \leq 0 \quad [3.8]$$

$$f_6 = \sigma_3' - \sigma_t \leq 0 \quad [3.9]$$

When this tension cut-off procedure is used, the allowable tensile stress, σ_t , is, by default, taken equal to zero. For these three yield functions an associated flow rule is adopted. For stress states within the yield surface, the behavior is elastic and obeys Hooke's law for isotropic linear elasticity. Hence, besides the plasticity parameters c , ϕ , and ψ , input is required for elastic shear Young's modulus E and Poisson's ratio.

3.5. Verification Examples

The performance and accuracy of PLAXIS has been carefully tested by carrying out analyses of problems with known analytical solutions. A selection of these benchmark analyses is described.

Elastic benchmark problems. A large number of elasticity problems with known exact solutions are available for use as benchmark problems. A selection of

elastic calculations is described; these particular analyses have been selected because they resemble the calculations that PLAXIS might be used for in practice.

Plastic benchmark problems. A series of benchmark calculations involving plastic material behavior is described. This series includes the calculation of collapse loads and the analysis of slip at an interface. As for the elastic benchmarks only problems with known exact solutions are considered.

3.1.5. Elastic problems with known solutions

A series of elastic benchmark calculations is described in this section. In each case the analytical solutions may be found in many of the various textbooks on elasticity solutions, for example Giroud (1972) and Poulos & Davis (1974).

Smooth Rigid Strip Footing on Elastic Soil. The problem of a smooth strip footing on an elastic soil layer with depth H is shown in Figure 3.11. This figure also shows relevant soil data and the finite element mesh used in the calculation. A uniform vertical displacement of 10 mm is prescribed to the footing and the indentation force, F , is calculated from the results of the finite element calculation. Since the problem is symmetric it is possible to model only one half of the situation as shown in Figure 3.11.

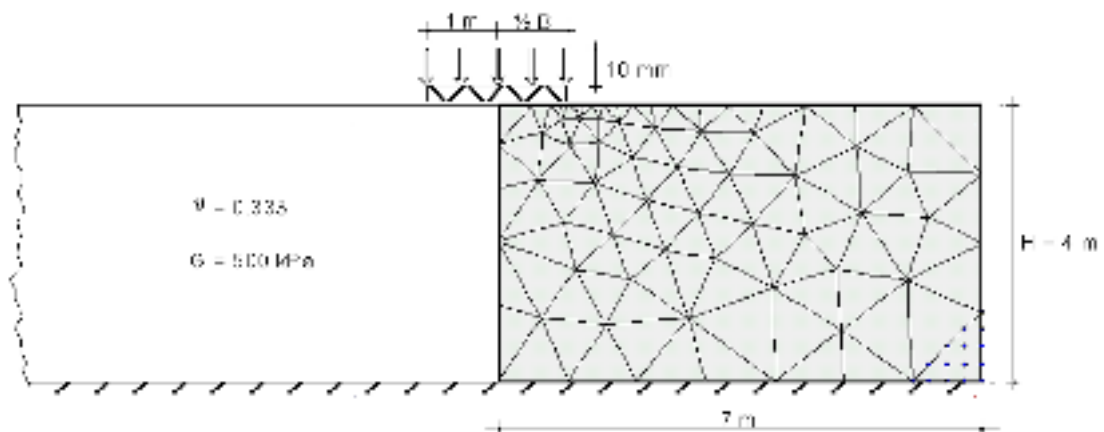


Figure 3.11: Geometry of Smooth Rigid Strip Footing on Elastic Soil

The footing force resulting from a rigid indentation of 10 mm is calculated to be $F=15.26$ kN. (Note that when only half of the elastic halfspace is modeled the force calculated by PLAXIS will be exactly one half of this value).

Giroud (1972) gives the analytical solution to this problem in the formula above, where H is the depth of the layer, B is the total width of the footing and k is a constant. For the dimensions and material properties used in the finite element analysis this solution gives a footing force of 15.15 kN. The error in the numerical solution is therefore about 0.7%.

Figure 3.12 gives both the analytical and numerical results for the pressure distribution underneath the footing. This figure shows that the numerical results agree very well with the analytical solution.

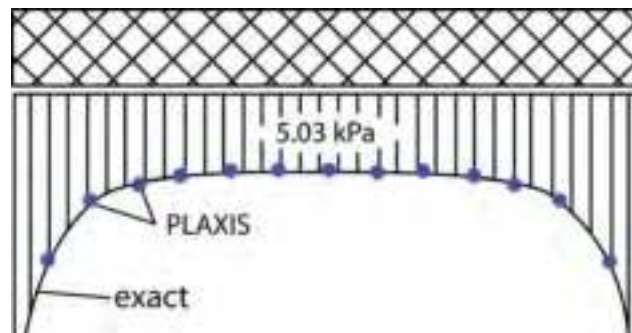


Figure 3.12: Pressure Distribution at Smooth Rigid Strip Footing on Elastic Soil

Performance of shell elements. A beam in PLAXIS can be applied as a tunnel lining. By using this element, 3 types of deformations are taken into account: shear deformation, compression due to normal forces and obviously bending.

A ring with a radius of $R=5$ m is considered. The Young's modulus and the Poisson's ratio of the material are taken respectively as $E=106$ kPa and $\nu=0$. For the thickness of the ring cross section, H , several different values are taken so that we have rings ranging from very thin to very thick. In order to model such a ring the bottom point of the ring is fixed with respect to translation and the top point is

allowed to move only in the vertical direction. Then the load $F=0.2$ kN/m is applied only at the top point. Geometric non-linearity is not taken into account.

The calculated vertical deflections at the top point are presented in Figure 8.22. The deformed shape of the ring is also shown in Figure 3.13. The calculated normal force at the belly of the ring is 0.50 for all different values of ring thickness. The calculated bending moment at the belly varying from 0.182 to 0.189 as the ring changes from thin to thick.

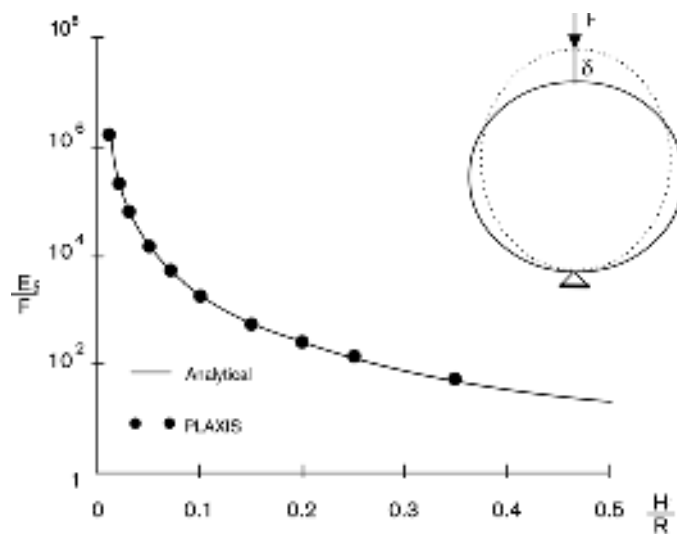


Figure 3.13: Calculated deflections compared with analytical solutions for Ring Beam

The analytical solution for the deflection of the ring is given by Blake (1959), and the analytical solution for the bending moment and the normal force can be found from Roark (1965). The vertical displacement at the top of the ring is given by the following formula (Eq. 3.10):

$$\delta = \frac{F \lambda}{E} \left[1.788 \lambda^2 + 3.091 \frac{0.637}{1+12 \lambda^2} \right] \text{ with } \lambda = R/H \quad [3.10]$$

The solid curve in Figure 3.13 is plotted according to this formula. It can be seen that the deflections calculated by PLAXIS fit the theoretical solutions very well. Only for a very thick ring some errors are observed, which is about 7 per cent for

$H/R=0.5$. But for thin rings the error is nearly zero. The analytical solution for the bending moment and normal force at the belly is 0.182 and 0.5 respectively. Thus even for very thick rings the error in the bending moment is just 4 per cent, and the error in the normal force is only 0.2 percent.

Cylindrical Cavity Expansion. For expansion of a cylindrical cavity (Figure 3.14) in an elastic perfectly-cohesive soil, theoretical solutions exist for both large and small displacement analysis Sagaseta (1984). A cylindrical cavity of initial radius a_0 is expanded to radius a by the application of an internal pressure p . The radius of the elastic-plastic boundary is represented by r . The soil is incompressible with an angle of friction of zero and cohesion c .

The axisymmetric mesh used in the calculations is shown in Figure 3.15. In these calculations the ratio G/c is taken to be 100 and Poisson's ratio is 0.495. Since the theoretical solutions are based on an infinite continuum a correcting material cluster is added to the perimeter of the mesh; this correcting cluster has a Poisson's ratio of 0.25 and a Young's modulus of $5E/12$ where E is the soil Young's modulus. The tension cut-off must be deactivated to get correct results. Calculation of the correcting layer properties is described in Burd & Houlsby (1990).

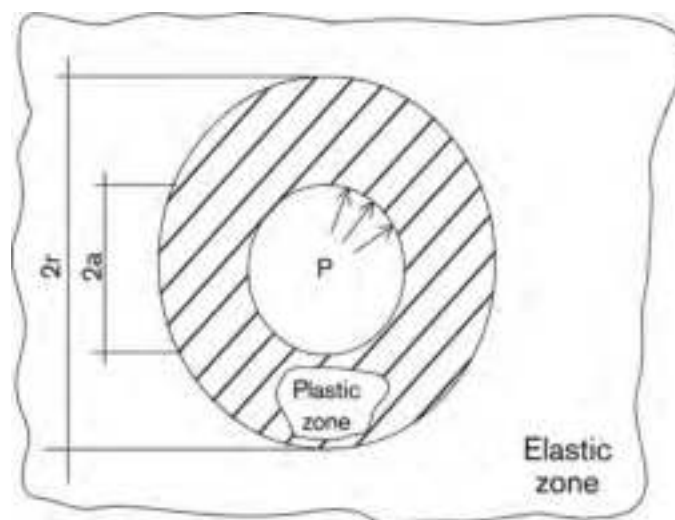


Figure 3.14: Cylindrical cavity expansion

The computed relationships between cavity pressure and radial displacement are given in Figure 3.16; computed results agree very well with the analytical solutions. In order to obtain the cavity pressure from the PLAXIS results it is necessary to divide the computed force per unit radian acting on the cavity surface by the thickness of the soil slice and the cavity radius. The large displacement solution was obtained with an update mesh analysis.

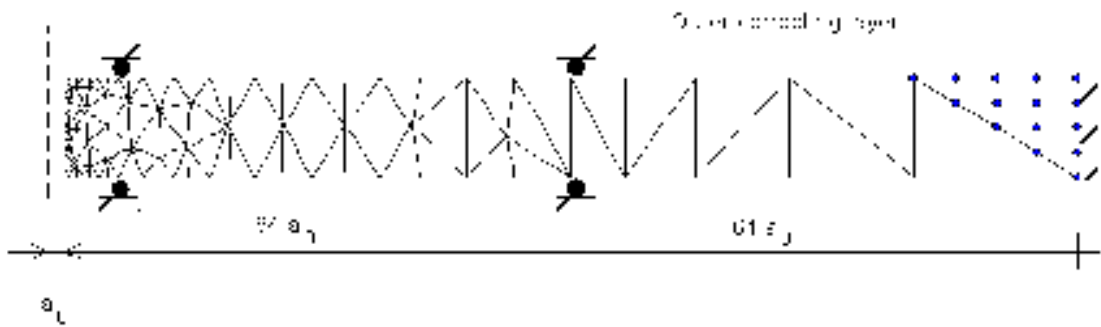


Figure 3.15: Mesh for cavity expansion

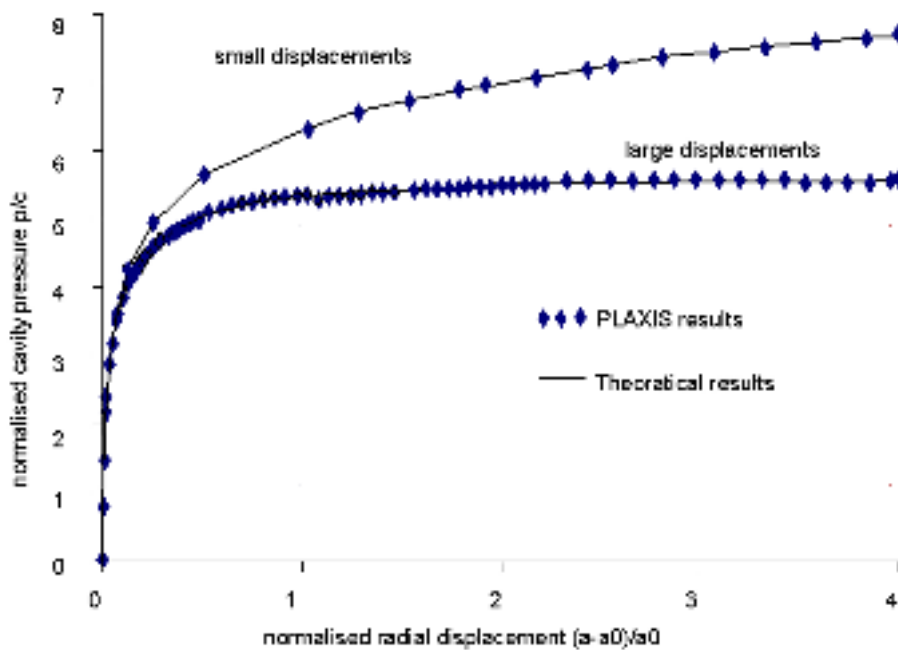


Figure 3.16: Relationships between radial displacement and cavity pressure

3.6. Combination of Models

The major parametric study for the tunnel geometry was the depth as well as the diameter for both one and two way tunnels so the 14 models was solved for two combinations of depth as well as two combinations of diameter. The number of problems was $(14 \times 2 \times 2 = 56)$ problems). Each problem has 3 steps (i.e. the 1st step was for the initial stress case, the 2nd step will be for the support installation and the third step will be for the full support installation after tunnel contraction). The total number of runs was $(56 \times 3 = 168)$ runs).

The followings are the prefixes used for the 14 soil models representing Dubai subsurface soil properties:

1. **PJA** : Palm Jebel Ali
2. **AB** : Al Burj
3. **AT** : Anara Tower
4. **JG** : Jumeirah Garden
5. **AC** : Arabian Canal
6. **TT** : Tatweer Tower
7. **JGc** : Jumeirah Garden – Section “c”
8. **PJAc** : Palm Jebel Ali – Section “c”
9. **ACc** : Arabian Canal – Section “c”
10. **ABd** : Al Burj – Section “d”
11. **TTd** : Tatweer Tower – Section “d”
12. **ABe** : Al Burj – Section “e”
13. **ACe** : Arabian Canal – Section “e”
14. **Creek** : Creek

The locations of the exploration points are as per Figure 3.1. The stratifications as well as the soil properties used in the analysis are mentioned in the descriptive boreholes as per Appendix I.

Each tunnel was studied for the shallow and the deep depths of 10.00 m and 20.00 m respectively. Each tunnel was studied for two diameters of 5.00 m and 8.00 m for one way and two way tunnels respectively. The properties of the tunnel were kept fixed for all the runs as per Table 7.5 for the proposed of comparison. Details of each run are mentioned in Table 3.4.

Each problem has 3 steps (i.e. the 1st step was for the initial stress case, the 2nd step will be for the support installation and the third step will be for the full support installation after tunnel contraction).

Initial Conditions (Step 1). The water weight was taken 10 kN/m³. The water pressures were generated on the basis of a general phreatic line at a level of the ground water table as per the descriptive boreholes in Appendix I. In addition, the K₀-procedure was used to generate the initial effective stresses with the appropriate values of K₀.

K₀ Procedures are used when the initial stresses are generated. It is possible to enter values for the coefficient of lateral earth pressure for each individual soil cluster. The coefficient, K₀, represents the ratio of the horizontal and vertical effective stresses. In practice, the value of K₀ for a normally consolidated soil is often assumed to be related to the friction angle by the empirical expression:

$$K_0 = 1 - \sin \varphi \quad [3.11]$$

In rock soils, K₀ would be expected to be larger than the value given by this expression. Using very low or very high K₀-values in the K₀ -procedure may lead to stresses that violate the Coulomb failure condition. In this case Plaxis automatically reduces the lateral stresses such that the failure condition is obeyed. Hence, these stress points are in a plastic state and are thus indicated as plastic points. Although the corrected stress state obeys the failure condition, it may result in a stress field which is not in equilibrium. It is generally preferable to generate an initial stress field that does not contain plastic points. For a cohesionless material it can easily be shown that to avoid soil plasticity the value of K₀ is bounded by:

$$\frac{1 - \sin \varphi}{1 + \sin \varphi} < K_0 < \frac{1 + \sin \varphi}{1 - \sin \varphi} \quad [3.12]$$

When the K₀ -procedure is adopted, Plaxis will generate vertical stresses that are in equilibrium with the self-weight of the soil. Horizontal stresses, however, are calculated from the specified value of K₀. Even if K₀ is chosen such that plasticity does not occur, the K₀ -procedure does not ensure that the complete stress field is in

equilibrium. Full equilibrium is only obtained for a horizontal soil surface with any soil layers parallel to this surface and a horizontal phreatic line.

Construction of the Tunnel (Step 2). In order to simulate the construction of the tunnel it is clear that a staged construction calculation is needed in which the tunnel lining was activated and the soil clusters inside the tunnel were deactivated. Deactivating the soil inside the tunnel only affects the soil stiffness and strength and the effective stresses. Without additional input the water pressures remain. In order to remove the water pressure inside the tunnel a low user-defined phreatic line should be introduced for the soil clusters in the tunnels and the water pressures should be regenerated. This Second calculation phase after the initial stresses is a plastic calculation and load advancement ultimate level.

Installation of the Tunnel Lining (Step 3). In addition to the installation of the tunnel lining, the excavation of the soil and the de-watering of the tunnel, the volume loss was simulated by applying a contraction to the tunnel lining. This contraction was defined during the creation of the tunnel in the input program. The contraction of the tunnel lining by itself does not introduce forces in the tunnel lining. Eventual changes in lining forces as a result of the contraction procedure are due to stress redistributions in the surrounding soil or to changing external forces.

The tunnel lining will be assumed to behave as linear elastic material, with appropriate elastic modulus and Poisson's ratio. The soil will be assumed to have non-linear characteristics following the Mohr-coulomb criterion. The Mohr-Coulomb model requires a total of five parameters (i.e. Young's modulus, Poisson's ratio, Friction angle, Cohesion and Dilatancy angle), which are generally familiar to most geotechnical engineers and which can be obtained from basic tests on soil samples.

The values of the stiffness parameter adopted in a calculation require special attention as many geomaterials show a non-linear behavior from the very beginning of loading. In soil mechanics the initial slope is usually indicated as E_0 and the secant modulus at 50% strength is denoted as E_{50} (see Figure 3.17). For materials with a large linear elastic range it is realistic to use E_0 , but for loading of soils one generally

uses E50. Considering unloading problems, as in the case of tunneling and excavations, one needs Eur instead of E50.

Table 3.4: Combinations of diameters and depths for each site

Soil Model	Exploration Point	Tunnel Diameter	Tunnel Depth [m]
1	PJA	5.00 m	10/20
		10.00 m	10/20
2	AB	5.00 m	10/20
		10.00 m	10/20
3	AT	5.00 m	10/20
		10.00 m	10/20
4	JG	5.00 m	10/20
		10.00 m	10/20
5	AC	5.00 m	10/20
		10.00 m	10/20
6	TT	5.00 m	10/20
		10.00 m	10/20
7	JGc	5.00 m	10/20
		10.00 m	10/20
8	PJA _c	5.00 m	10/20
		10.00 m	10/20
9	AC _c	5.00 m	10/20
		10.00 m	10/20
10	AB _d	5.00 m	10/20
		10.00 m	10/20
11	TT _d	5.00 m	10/20
		10.00 m	10/20
12	AB _e	5.00 m	10/20
		10.00 m	10/20
13	AC _e	5.00 m	10/20
		10.00 m	10/20
14	Creek	5.00 m	10/20
		10.00 m	10/20

For soils, both the unloading modulus, Eur, and the first loading modulus, E50, tend to increase with the confining pressure. Hence, deep soil layers tend to have greater stiffness than shallow layers. Moreover, the observed stiffness depends on the stress path that is followed. The stiffness is much higher for unloading and reloading than for primary loading. Also, the observed soil stiffness in terms of a Young's modulus may be lower for (drained) compression than for shearing. Hence, when

using a constant stiffness modulus to represent soil behavior one should choose a value that is consistent with the stress level and the stress path development.

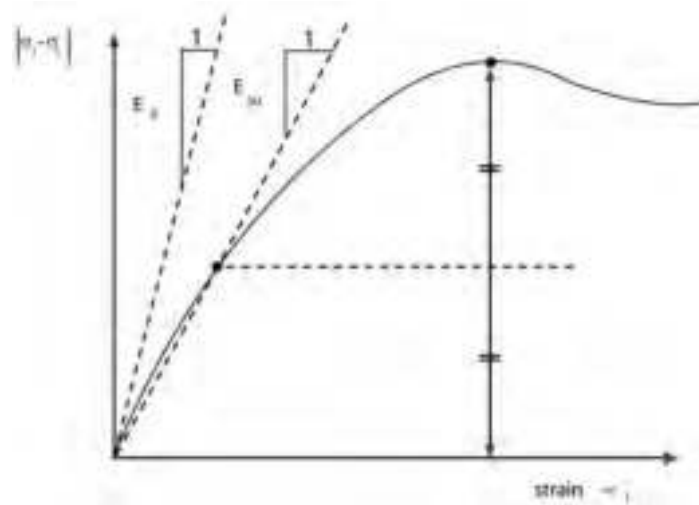


Figure 3.17: Definition of E_0 and E_{50} for standard drained tri-axial test results

In many cases one will obtain ν values in the range between 0.3 and 0.4. In general, such values can also be used for loading conditions other than one-dimensional compression.

The cohesive strength has the dimension of stress. Cohesionless sands ($c = 0$), Cohesion for rock materials was evaluated from the collected soil investigation reports for the regional soil for Dubai.

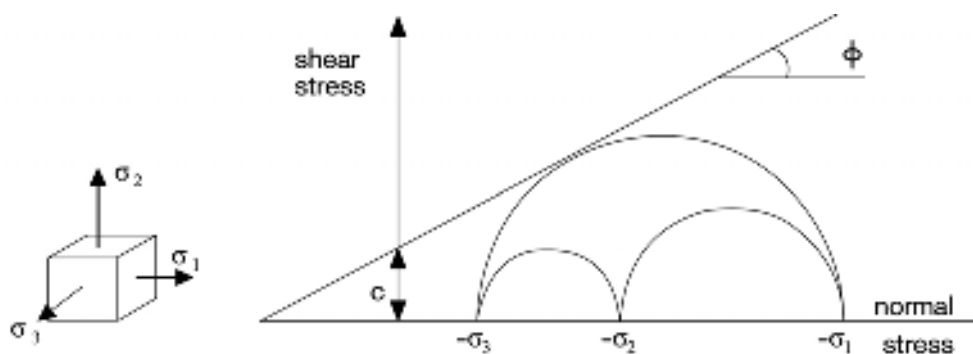


Figure 3.18: Stress circles at yield; one touches Coulomb's envelope

The friction angle, ϕ (phi), is entered in degrees. High friction angles, as sometimes obtained for dense sands, will substantially increase plastic computational effort. The computing time increases more or less exponentially with the friction angle. Hence, high friction angles should be avoided when performing preliminary computations for a particular project.

Table 3.5: Range of material properties at different sites

Site	Wet weight kN/m ³	E kN/m ²	Poisson's ratio	c kN/m ²	Friction angle	Dilatancy angle
AB	18.5-24	23520- 14300000	0.2-0.35	0-57	24-34	0-4
ABd	18.5-24	23520- 14300000	0.2-0.35	0-57	24-34	0-4
Abe	18.5-24	23520- 14300000	0.2-0.35	0-57	24-34	0-4
AC	17-23	23000- 9500000	0.25-0.35	0-54	25-35	0-5
Acc	22-24	5000000- 15700000	0.2-0.3	50-59	25-30	0
ACe	17-24	23000- 15700000	0.2-0.35	0-59	25-35	0-5
AT	18.5-24	23520- 14300000	0.2-0.35	0-57	24-34	0-4
Creek	17-23	23000- 9500000	0.25-0.35	0-54	25-35	0-5
JG	17-24	23000- 14300000	0.2-0.35	0-57	25-35	0-5
JGC	17-24	23000- 14300000	0.2-0.35	0-57	25-35	0-5
PJA	17-23.5	23000- 14300000	0.2-0.35	0-57	25-35	0-5
PJAc	17-23.5	23000- 14300000	0.2-0.35	0-57	25-35	0-5
TT	17-23	23000- 9500000	0.25-0.35	0-54	25-35	0-5
TTd	17-24	23000- 14300000	0.2-0.35	0-57	25-35	0-5

The friction angle largely determines the shear strength by means of Mohr's stress circles. A more general representation of the yield criterion is shown in Figure 3.18. The considered values of the internal shearing resistance angle were adapted from the tri-axial tests illustrated in the soil investigation reports.

The dilatancy angle, ψ (psi), is specified in degrees. The dilatancy of sand depends on both the density and on the friction angle. For quartz sands the order of magnitude is $\psi \approx \phi - 30^\circ$. For ϕ -values of less than 30° , however, the angle of dilatancy is mostly zero. A small negative value for ψ is only realistic for extremely loose sands and rocks. (Bolton, 1986). Table 3.5 presents the range of physical properties of different soils/rocks used in the numerical models at different sites.

Chapter 4: RESULTS AND DISCUSSIONS

Numerical analysis techniques, such as the finite element method, have permitted the incorporation of some effective factors, which could not be easily included in the previous analysis procedures, used to solve geotechnical-engineering problems. In some cases, as that of the tunnel analysis, the basic problem is to handle a two dimensional half-space elasto-plastic analysis, implement an interface friction element between the tunnel and the soil and to model exactly the stages of construction. In the last decades, considerable attention has been directed towards the application of the elasto-plastic constitutive models into finite element computer codes in order to solve the existing problems numerically (Naylor et. al, 1981). However, many researchers have used various simplifications to avoid sophisticated calculations, including elasto-plastic analysis.

The construction of tunnels at shallow depths requires determination and continuous monitoring of soil settlement at the ground surface. The settlement and stability of the tunnel depends on many variables such as properties of soil, thickness of overburden, tunnel diameter, and most importantly excavation techniques. Consequently, settlement monitoring program must be implemented during the construction of tunnels. Such settlements may create unfavorable effects on buildings which were constructed at ground surface and are closer to the center of tunnel. Tunnel-induced settlements must be carefully predicted and monitored to avoid damage to nearby structures. This chapter presents the results and discussion on the numerical modeling of different sites for tunneling.

4.1. Typical Simulation Results

The typical output of PLAXIS is presented the following section. The deformations in the deformed model are measured at the following locations which will be discussed in later sections.

- 1) Deformations at the surface as a function of lateral distance from the tunnel axis for all cases. The lateral distance was three times the depth of the crown of the tunnel.
- 2) Deformations at the half way between the crown of the tunnel and ground surface as a function of lateral distance from the tunnel axis. The lateral distance was three times the depth of the crown of the tunnel.
- 3) Deformations at the crown of the tunnel for all cases
- 4) Deformations at 45° from the center (shoulder) of the tunnel for all.

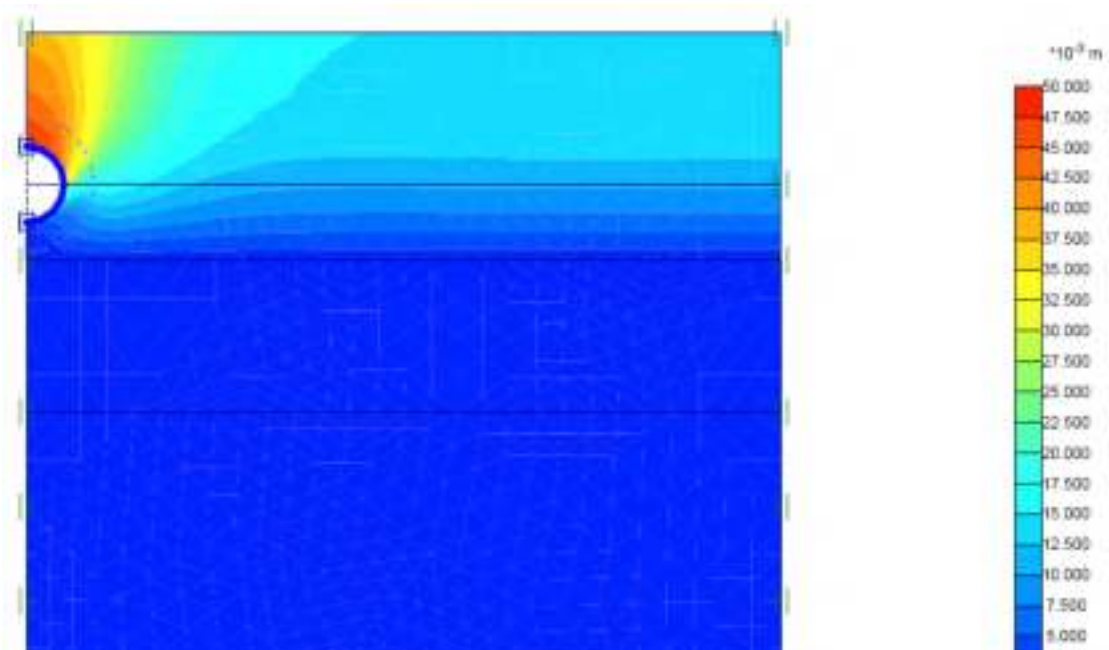


Figure 4.1: Deformation for site PJA with tunnel diameter 5.00 m at depth of 10.0 m.

Detailed account of numerical models pertaining to different sites and figures are presented in Appendices. Figure 4.1 presents the typical deformed model with deformation contours for site PJA with tunnel diameter 5.00 m at depth of 10.0 m.

Similarly a typical plot of relative shear is presented in Figure 4.2. Other plots of total stresses, effective stresses, horizontal displacements, and plastic points are presented in the appendix.

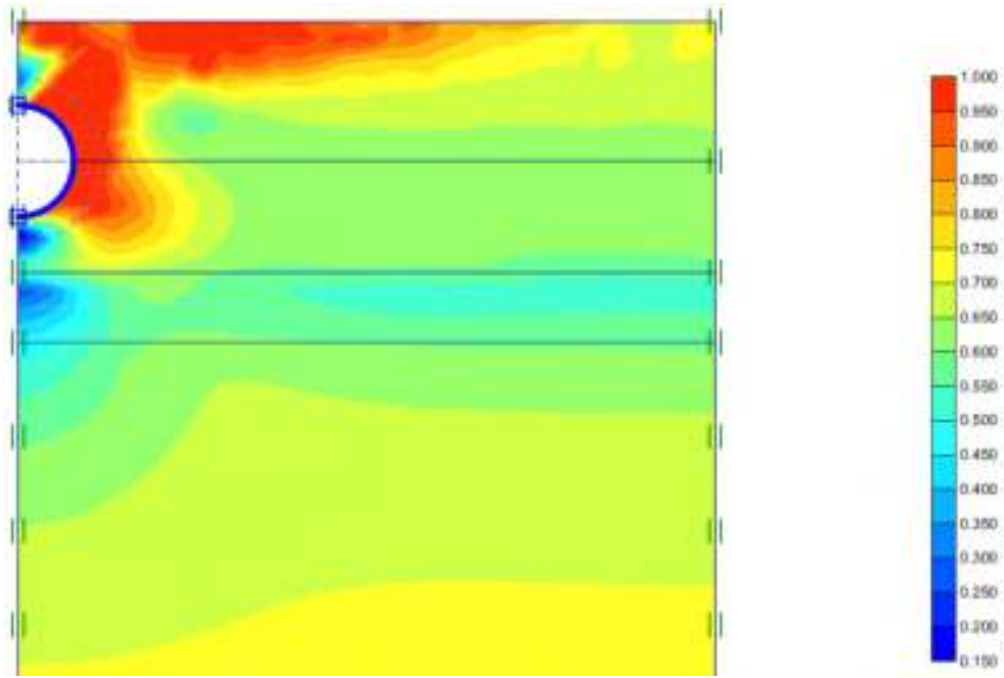


Figure 4.2: Contours of relative shear stress for site PJA with tunnel diameter 8.00 m at depth of 10.0 m.

4.2. Effect of different soil properties on the output

Soil properties such as Young's Modulus, Poisson's ratio, and other soil parameters can have significant effect on the outcome of the numerical modeling. The effect of some of the soil properties are discussed in the following.

Effect of Model Choice. In all cases of assumed soil models, the deformations are greatly affected. If the purpose of the study is to get the deformations, a proper choice of the model should be made. This conclusion was reached by Griffiths, 1982, and De Brost, and Vermeer, 1984. Models are required to match previously obtained field or laboratory test results. This is not what engineers really require from a soil model, as material parameters usually obtained from soil tests depend on slightly scattered data that gives a small range of tolerance for calculating them. So, unless justified, any values other than the mean value should not be adopted to match the obtained results.

Effect of Young's Modulus. To study the effect of the Young's modulus of soil / rock on the deformation of the tunnel, a parametric study was performed. In all the subsequent runs, each soil / rock type has been given a fixed angle of shearing resistance, ϕ while the Young's modulus, E_s has been altered within the range of possible values for each soil / rock type. The value of soil Young's modulus, E_s is the most important parameter in the behavior of the tunnel prior to plasticity when the elastic deformation is studied. In case of loose and very loose sands, the elastic analysis is very safe; i.e. the elastic behavior is close to the actual behavior since the permissible deformation is limited. Thus, in case of loose and very loose sands, the Young's modulus must be determined accurately.

In general, increasing the value of Young's modulus, E_s decreases the value of the tunnel deformations and accordingly the tunnel internal forces. Though in practice, both values of E_s and (ϕ) apply to one kind of soil / rock, and the degree of accuracy of the compatibility between the laboratory testing and real soil would not allow for a decisive recommendation concerning which value to use. This parameter E_s is the most influencing parameter in the analysis, and its value obtained from laboratory testing should be determined precisely as it affects the accuracy of any analysis.

Effect of Poisson's Ratio. To study the effect of the Poisson's ratio of sand / rock on the deformation of the tunnel, a parametric study is performed. In the analysis, each sand / rock type has a fixed values of angle of shearing resistance (ϕ) and Young's modulus E_s , while the Poisson's ratio of sand (ν) has been changed in the range of 0.27 to 0.49. It is clear that the effect of the Poisson's ratio of sand (ν) is insignificant.

It is important to mention here that the only effect of Poisson's ratio is in the initial stresses calculation, the weighting is considered by activating the acceleration option in the input file. Activation of the acceleration option permits the initial stresses to be generated. The earth pressure is then generated where ($\sigma_x = k_0 \sigma_y$), where k_0 is the coefficient of earth pressure which is calculated according to the theory of elasticity ($k_0 = \nu / (1 - \nu)$). Again, this has a minor effect specially in case of

sands in which k_0 ranges from 0.30 to 0.60, while k_0 may be calculated from ($k_0=1-\sin \phi$).

Effect of Angle of Shearing Resistance. To study the effect of the angle of shearing resistance of sand, (ϕ) on the deformation of the tunnel, a parametric study has been performed. In the analysis each sand / rock type, for the value of Young's modulus, E_s has been kept constant while the angle of shearing resistance, (ϕ) has been altered within the range of possible values for each sand / rock type.

Increasing the value of the angle of shearing resistance, (ϕ) decreases the values of tunnel deformations and accordingly the tunnel internal forces. This can be attributed to the fact that the slope of Mohr-Coulomb failure surface increases with the increase of the value of (ϕ). Thus, slightly increasing the elastic zone and decreasing the possibility of elements to reach plasticity stage. On the other hand, since the angle of shearing resistance, (ϕ) for soil is limited, its effect is also limited.

Effect of Coefficient of Friction. The incremental-iterative algorithm for the interface gap friction element starts for each load step by assuming that the interface state remains as in the previous, just completed step. For the initial load step, the node pairs are assumed fixed and reside in the same geometric location. In general, the solution must be determined iteratively wherein a particular state is assumed and solved to obtain a trial solution. The trial solution is used to determine whether the assumed state is correct or not, and to determine which state is more likely to be correct. At the same time, the trial solution is used to estimate new load vector parameters depending on whether the new state is assumed.

The friction angle of the tunnel-soil interface ranges ($\delta=0.50$ to 0.75ϕ). In the present study the value of (δ) was chosen to be $=0.65\phi$, where (ϕ) is the angle of the internal friction implemented in the input file. The friction coefficient between tunnel and sand (μ) used in defining the gap-friction elements, is ($\mu=\tan\delta$). The dilatancy angle of the interface was taken to be equal to zero. In the current analyses, the

tension analysis (Zienkiewicz et al., 1968) was applied, in which the minimum principal stresses was not kept positive for each element.

In this section, the effect of altering the coefficient of friction is investigated. First, the problem is solved assuming full bond ($\mu=\infty$) between the tunnel and the surrounding soil (no interface elements were used). Then, interface elements were introduced with different values of the coefficient of friction (μ), including the theoretical case of ($\mu=0$). Using interface element with $\mu= 0.3$ decreases the tunnel deformation to about 63% of its value assuming full bond, which is a theoretical case. This means that using interface elements has a great effect on the resulting deformations and accordingly the tunnel internal forces.

Effect of Tunnel Diameter. The effect of the tunnel diameter is investigated by using different two values of the tunnel diameter (i.e. 5.00 m & 8.00 m). As the tunnel diameter increases at same depths, the axial forces and bending moment values increases but the shearing values decreases. The effect of the tunnel diameter on the maximum ground settlement has been investigated. As the tunnel diameter increases at same depths, the maximum ground settlement increases.

Effect of Tunnel Depth. The effect of the tunnel depth is investigated by using different two values of the tunnel depth (i.e. 10.00 m & 20.00 m). As the tunnel depth increases with the same diameter, the shearing forces and bending moment values decreases but the shearing values increases.

The effect of the tunnel depth on the maximum ground settlement has been investigated. As the tunnel depth increases with the same diameter, the maximum ground settlement decreases.

Effect of Elasto-Plastic Behavior. Trial run is performed using the elastic behavior, linear elastic, nonlinear elastic, and then nonlinear elastic-no tension analysis, in which the soil is not allowed to carry any tensile stresses. The run is then

performed using the elasto-plastic Mohr-Coulomb model for soil / rock. Finally, the interface gap friction element was inserted between the tunnel and soil / rock elements in the elasto-plastic analysis.

If the elasto-plastic behavior is considered to be the most rational behavior, then linear elastic behavior is completely rejected as it gives about 58% of the maximum ground settlement in the plastic stage using elasto-plastic behavior. The elastic no-tension analysis is still rejected as it gives about 68% of the maximum ground settlement using elasto-plastic behavior. The nonlinear model can be considered simpler and better than the elasto-plastic model in our case, at which elasto-plastic models are very sophisticated specially that results of the two behaviors are almost identical in step 1 & 2. The remaining problem will be the determination of the plastic stage. The elasto-plastic model using interface gap friction elements is the most convenient approach to use in this study.

For tunnel analysis, serviceability criteria govern the design; only one small zone is expected to fail, as the tunneling process mainly affects the topmost elements above the center of the tunnel at and near the ground surface. Elasto-plastic elements are a must to be modeled for these elements at least. The confining pressure at the rest of the elements far from the ground level is very much higher than that at near the ground surface.

Obviously, it all depends on the user. Nothing is called the best soil model. Every model has its own limitations. The user should be aware of them to get the best out of his model, and to know the range of application of his work. Generally, linear elastic analysis may be the worst in case of tunneling analysis. Yet, the use of interface gap friction element that describes the interaction between the tunnel and the soil / rock is a must as it can model the contraction process of the tunnel lining.

4.3. Deformations

Deformations were recorded at four different locations on the model and plotted separately to evaluate and discuss the effect of different combinations. The deformations were measured at the ground surface (above the centerline of tunnel),

half way between the surface and the crown, at the crown and at the shoulders of the tunnel which are located at 45° from the center of the tunnel upwards.

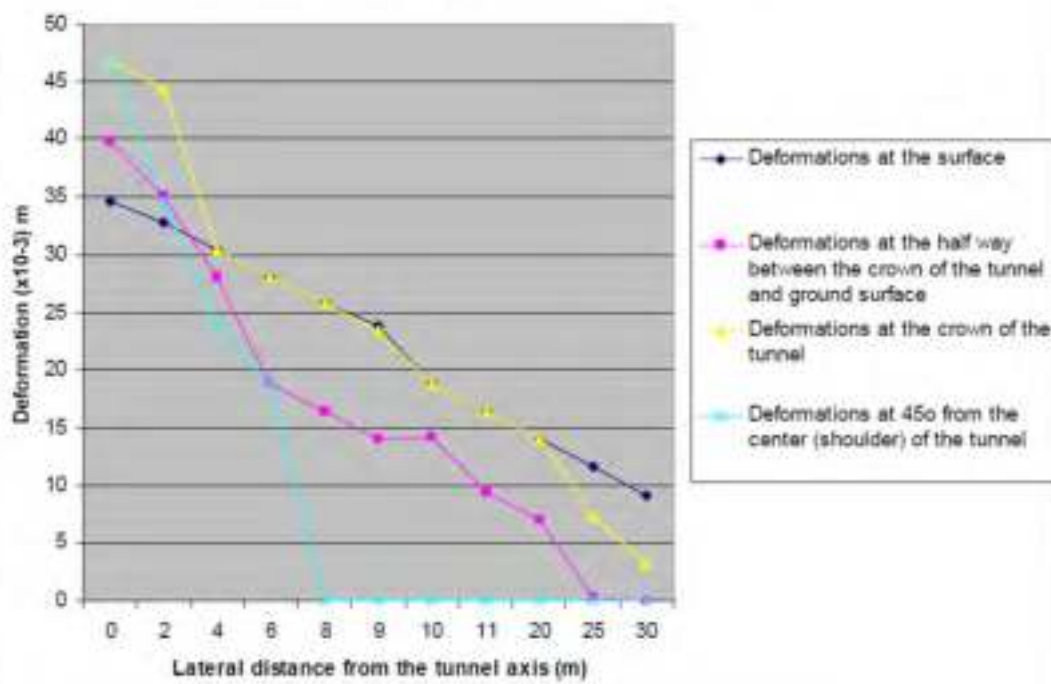


Figure 4.3: Deformation plots for site AB with tunnel diameter 5.00 m at depth of 10.0 m.

Site AB. The deformations at different locations of the soil model for Site AB are presented in Figure 4.3. As expected the largest deformation occurs at the crown with decreasing deformations as one move towards the surface. The deformation at the surface is recorded as close to 35 mm which is significant deformation considering the open face tunneling in the site.

Similarly the deformations for the 5 m tunnel at depth of 20 m are presented in Figure 4.4. This figure indicates decrease in deformations at all points due to increased depth of the tunnel. The increase in the depth of the tunnel results in geomaterials supporting itself in the form of arching action. The deformation at the surface reduces to approximately 21 mm.

Figures 4.3 and 4.4 also indicate that the critical position for the measurement of deformations with in the soil is directly above the crown. Hence the following results and discussions pertain to the deformations on or directly above the crown.

The deformations also decrease with increase in lateral distance from the tunnel axis. At about 6 times the diameter of the tunnel the magnitude of deformations becomes negligible.

The deformation increases as the tunnel diameter increase and the comparison of deformations for different combinations for site AB is presented in the Table 4.1.

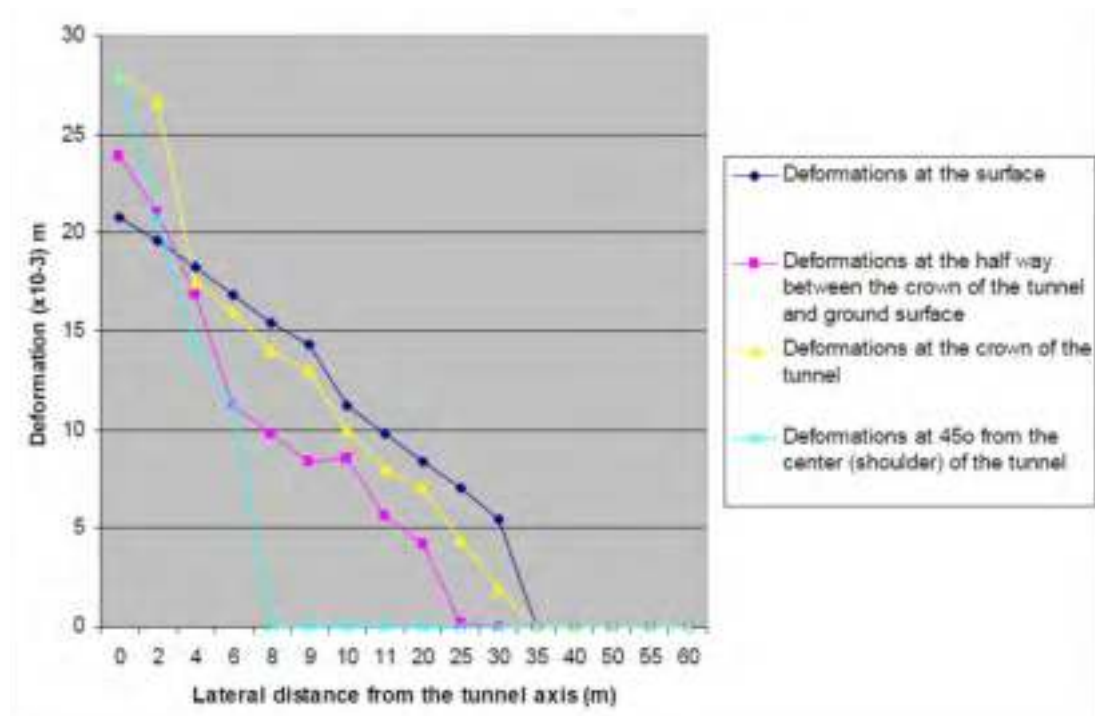


Figure 4.4: Deformation plots for site AB with tunnel diameter 5.00 m at depth of 20.0 m.

The maximum deformations at site AB is calculated for the 8 m tunnel excavated at 10 m diameter. The deformation is recorded as 70 mm which is almost 80 % more than calculated for a 5m tunnel excavated at 10 m depth.

Table 4.1: Maximum values of Deformations at Site AB (in mm)

Location	Dia. 5 m & Depth 10m	Dia. 5 m & Depth 20m	Dia. 8 m & Depth 10m	Dia. 8 m & Depth 20m
At Surface	35	21	52	31
At Half way	40	24	60	36
Crown	47	28	70	42
Shoulder	47	28	70	42

Site ABd. The deformations at different locations of the soil model for Site ABd are presented in Figure 4.5 and Table 4.2. As expected the largest deformation occurs at the crown with decreasing deformations as one move towards the surface. The deformation at the surface is recorded as close to 43 mm which is greater than Site AB.

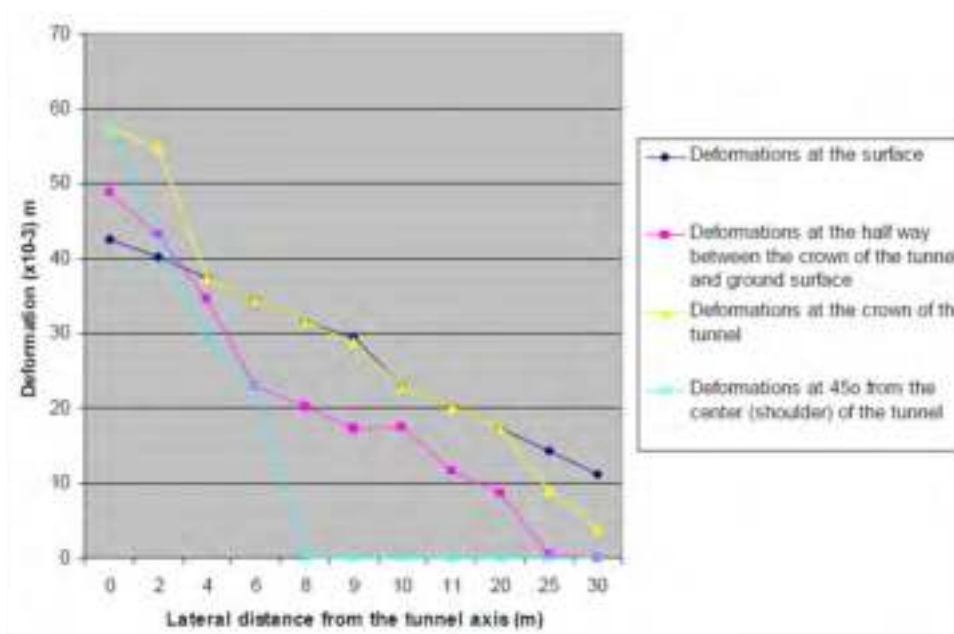


Figure 4.5: Deformation plots for site ABd with tunnel diameter 5.00 m at depth of 10.0 m.

Table 4.2: Maximum values of Deformations at Site ABd (in mm)

Location	Dia. 5 m & Depth 10m	Dia. 5 m & Depth 20m	Dia. 8 m & Depth 10m	Dia. 8 m & Depth 20m
At Surface	43	26	64	39
At Half way	49	29	73	44
Crown	58	35	87	52
Shoulder	58	35	86	52

The deformation plots for other sites and combinations can be found in the appendices. The comparison of deformations at different sites at different locations with soil mass and different combinations of diameters and depths are presented in the following section.

4.3.1. Comparison of Maximum Deformations at Different Sites

The comparison of maximum deformations within the soil mass for different sites and different combinations of tunnel diameters and depths are presented in the following sections. The deformations are compared at four locations within the soil mass as discussed earlier.

The discussions are mostly based on deformations recorded at surface which are important in tunneling operations. The convergencies recorded within the tunnel are directly related to deformations at the surface but the contingencies at the surface are more important as it can affect the existing structures and life lines.

Diameter = 5m and Depth = 10 m. Table 4.3 presents the comparison of maximum deformations at different sites for a tunnel of 5 m in diameter and a crown depth of 10 m. The table indicates that the variation in the deformations at different locations within the soil mass for different sites is substantial.

Table 4.3: Maximum values of Deformations (mm) for 5 m dia and 10 m depth

Site	Surface	Halfway Crown	Shoulder
AB	35	40	47
ABd	43	49	58
Abe	38	40	47
AC	36	42	49
ACc	41	47	55
ACe	37	42	50
AT	32	37	44
Creek	37	43	50
JG	36	42	49
JGC	35	40	48
PJA	37	43	50
PJAe	36	41	49
TT	37	42	50
TTd	39	45	53

The minimum deformation at the surface of 32 mm occurs at site AT which is about 12 mm smaller than the deformations at surface at site ABd. The increase of 36 % in deformation is significant considering not much variation in soil properties

among the sites. These values suggest that tunneling in Dubai area can be challenging in terms of settlement control at the surface. The tunneling method should be adjusted to comply with strict monitoring and full face supported excavation. The surface settlement could be of significant importance if larger tunnels are to be excavated by use of TBM.

Diameter = 5m and Depth = 20 m. The comparison of deformations for a 5 m tunnel excavated at 20 m depth is presented in Table 4.4. Although the deformations has reduced due to the depth of the same diameter tunnel, the total settlements recorded at surface are still significant and can lead to obvious distress at the surface. The minimum settlement recorded at site is 19 mm compared to maximum settlement at ABd site of 25 mm which is 32 % more than the deformation recorded at the surface of AT site.

Table 4.4: Maximum values of Deformations (mm) for 5 m dia and 20 m depth

Site	Surface	Halfway Crown	Shoulder
AB	21	24	28
ABd	26	29	35
Abe	21	24	28
AC	22	25	29
ACc	24	28	33
ACe	22	25	30
AT	19	22	26
Creek	22	26	30
JG	22	25	30
JGC	21	24	29
PJA	22	26	30
PJAc	21	25	29
TT	22	25	30
TTd	23	27	32

Diameter = 8m and Depth = 10 m. The deformations at different sites for a 8 m diameter tunnel is expected to increase significantly compared to a 5 m tunnel at the same depth. Table 4.5 presents the deformations for a 8 m diameter tunnel excavated at 10 m depth at different sites in Dubai.

The maximum deformation is again recorded at ABd site which is 20 mm more than 5 m tunnel at the same site and depth. This increase amounts to almost 50 percent. This amount of deformations can be unacceptable in any form of tunneling operations and can lead to development of significant surface trough.

The relationship of increase in surface settlement with tunnel diameter can also be explained with the additional loss of volume that occurs due to a larger excavated volume (Chapter 3). The larger loss of volume directly influences not only the depth of settlement trough but also the width and length of the settlement trough.

Table 4.5: Maximum values of Deformations (mm) for 8 m dia and 10 m depth

Site	Surface	Halfway Crown	Shoulder
AB	52	59	70
ABd	64	73	86
Abe	52	60	71
AC	55	63	74
ACc	61	70	82
ACe	55	63	74
AT	48	55	65
Creek	56	64	75
JG	54	62	73
JGC	53	61	71
PJA	56	64	75
PJA _c	54	62	72
TT	55	63	74
TTd	58	67	79

Diameter = 8m and Depth = 20 m. Table 4.6 presents the deformations recorded at different sites with in soil mass for a tunnel of 8 m excavated at depth of 20 m. As noted for the tunnel of 5 m diameter the deformations reduced with the increase in tunnel depth. Interestingly the maximum deformation at the surface occurring at site ABd is larger than the minimum deformation occurring at site AT by the same percentage of 31 %.

Table 4.6: Maximum values of Deformations (mm) for 8 m dia and 20 m depth

Site	Surface	Halfway Crown	Shoulder
AB	31	36	42
ABd	38	44	52
Abe	31	36	42
AC	33	38	44
ACc	37	42	50
ACe	33	38	45
AT	29	33	39
Creek	33	38	45
JG	33	37	44
JGC	32	36	43
PJA	33	38	45
PJAc	32	37	43
TT	33	38	45
TTd	35	40	47

4.3.2. Forces on the tunnel lining

Along with deformations, the forces on the tunnel lining were also studied. Although the main objective of the study was to evaluate the deformations in the soil mass due to tunneling activity, the analysis of forces in tunnel lining was also of interest. The bending of tunnel lining and subsequent design involves detailed analysis of the forces in the tunnel lining.

The detailed analysis of the tunnel lining is recommended as one of the future study that should be carried out for Dubai area. This section presents some typical outcomes of forces in tunnel lining and its locations. Figure 4.6 presents the distribution of displacements within the tunnel lining. This figure indicates that maximum displacement occurs at the crown of the tunnel which is supported by the results presented in the earlier sections.

The minimum deformation occurs in the invert of the tunnel. The deformation in the tunnel invert is related to the squeezing pressure of the soil mass surrounding the tunnel. The anisotropic nature of the stresses in the soil mass can lead to larger displacements in the tunnel at locations other than the crown. Since the soil mass modeled in this study does not incorporate any residual stresses in the horizontal direction or uplift pressures due to tectonic activity, the maximum displacements are expected to happen at the crown of the tunnel.

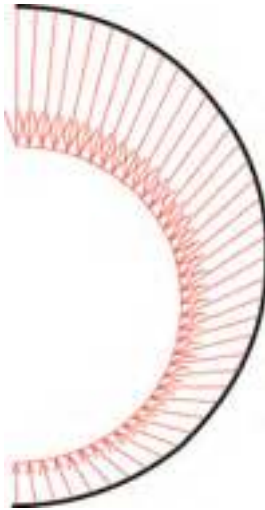


Figure 4.6: Distribution of total displacements in the tunnel periphery.

Figure 4.7 presents the distribution of axial force on the tunnel lining. The axial force increases towards the invert. This behavior can be explained by the tunnel arching effect where some of the stress in vertical direction over the crown is supported by the soil itself. This arching condition allows for the reduction in the axial force on the crown relative to the sides and invert. It should be noted here that arching effect will only be observed if significant deformations are allowed.



Figure 4.7: Distribution of axial force on the tunnel lining.

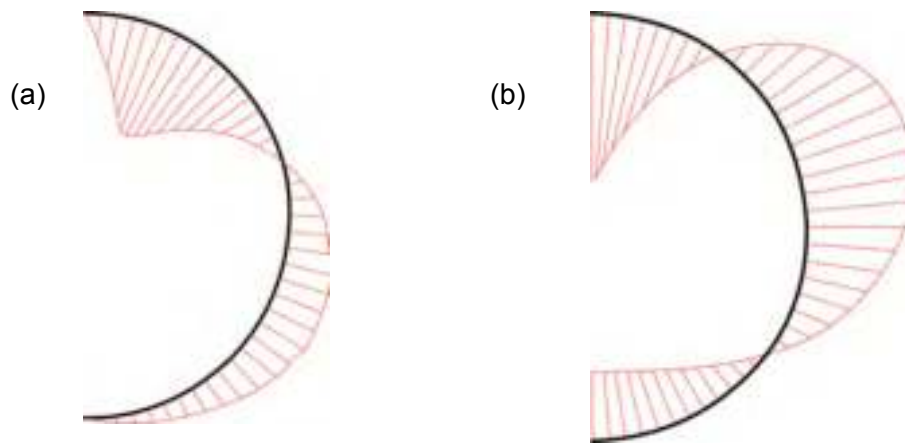


Figure 4.8: Distribution of a) shear force and b) bending moment in the tunnel lining.

Similarly Figure 4.8 presents the distribution of shear force and bending moments in the tunnel lining. Figure 4.8 indicates that the maximum shear force occurs at the approximate location of shoulders whereas the maximum bending moment correlates with the locations of crown and side walls of the tunnel. Significant bending moments are also indicated in the invert of the tunnel.

The above noted results and figures indicate that settlement with in the soil mass due to tunneling in Dubai area depends on soil properties, tunnel diameter, and tunnel depth. The results indicate that tunnels located within the weak calcareous sandstone found at around 15 m depth from the surface can provide better protection against the surface settlement. The depth of tunnel shall be at least 20 m from the surface to successfully control the settlements and make changes in the construction operation and sequences.

The AT area of Dubai which is in Jumeirah offers the best subsurface conditions for tunneling in terms of deformations. The area of ABd which is located near Dubai waterfront can yield significant settlements due to tunneling at the surface.

4.4. Settlement Monitoring Program

The results of this study are used to develop some guidelines on the monitoring of deformations resulting from the tunnel operations. These guidelines are

incorporated in the proposed settlement monitoring program presented in the following sections. The settlement monitoring program can be used to observe the deformations at the surface and initiate actions to control and mitigate the deformations. The clauses provided in these guidelines can be used with appropriate amendments to form the basis of contract package.

The purpose of settlement monitoring is to prevent damage to existing utilities and highway structures along the tunnel alignment. Ground settlement includes settlement due to lost ground and dewatering/drainage.

Guidelines. All measurement points shall be installed and surveyed before the start of excavation to establish benchmarks/baseline.

Surface monitoring points will be installed to cover the length of across the tunnel equal to at least 6 times the diameter of the tunnel (Figure 4.9). The settlement monitoring array should be in place at least 30 m before the tunnel face reaches the array. The spacing between the arrays should therefore be at least 30 m. Two types of surface monitoring points shall be installed. One type of points will be located on the surface with ends fixed below the frost penetration depths whereas one additional point on the surface shall be located top of the crown. This additional point should be anchored deep at a point half way between the surface and the crown to monitor the deformation before they propagate to the surface.

Surface monitoring points will be located at not greater than 3m intervals across the tunnel alignment. The surface monitoring will be identified using paint marks. Surface monitoring points shall be founded below frost penetration depths. The interval and/or marking of the points should be changed with client's approval. The final instrumentation plan should be finalized when Contractor's proposed construction method is available.

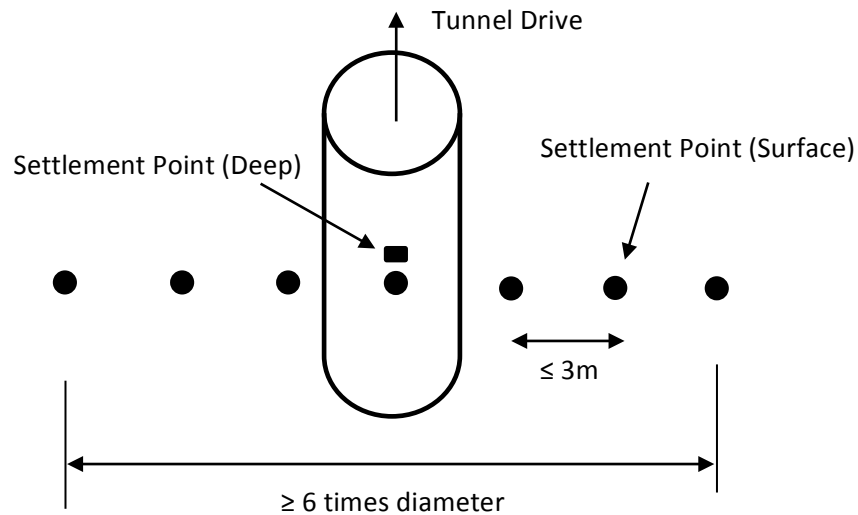


Figure 4.9: Typical configuration of surface settlement monitoring points across the tunnel alignment.

A condition survey for tunnel alignment will be carried out prior to commencement of construction and documented for the purpose of requirement of restoration. The condition survey shall document visible flaws such as cracks, distortions and deviations, heaves, and depressions. This surface survey will be completed during the installation of the monitors and again once the tunnel has been completed.

An average of at least two readings shall be taken to establish the initial conditions. The reading and collection of data from the surface monitoring points shall be read and recorded by the Contractor during the construction period and after construction for period of at least 2 weeks provided that further settlement has stopped.

A minimum of three (3) sets of reading be taken daily, provided that movements are within anticipated limits. Otherwise, the frequencies should increase according to a pre-planned interval.

Monitoring of movements is required during work stoppages, such as during non-operation period (off-shifts) or weekends. A minimum of three (3) sets of readings should be taken daily. Measurements of the monitoring points shall be reported promptly to client for review.

A procedure is required to be established in consultation with client so that the monitoring data and the interpreted data will reach all parties as soon as necessary. The contract administrator/consultant and the Contractor should interpret monitoring data as needed for the purpose of on-going construction. The Engineer should be contacted for technical support to the prime Consultant in the interpretation of ground movements and review of the Contractor's response when Review and Alert Levels are reached.

The acceptable surface settlement (or heave) will be according to criteria as specified below.

Baseline Reading – A baseline reading of the instrumentation shall be taken prior to commencement of the work. An average of at least two initial readings shall be recorded as baseline reading.

Review Level – A maximum value of 10 mm relative to the baseline readings is suggested for this project. If this level is reached, the method, rate or sequence of construction, or ground stabilization measures should be reviewed or modified to mitigate further ground displacements.

Alert Level – A maximum value of 15mm relative to the baseline readings is suggested for projects. If this level is reached, the Contractor shall cease construction operations and to execute pre-planned measures to secure the site, to mitigate further movements and to assure safety of public and property.

The client, the prime consultant and Engineer should review the Contractor's proposed method of construction. The proposed method should include a description of the potential loss of ground, and calculation of the maximum settlement in relation to the Contractor's procedure and equipment, alternative/remedial measures when review level of measurement is reached; and contingency/remedial measures when alert level of measurement is reached.

In addition to the monitoring program to assess the adequacy of the construction method to control potential ground movements and groundwater, the Contractor is responsible for reinstatement (such as surface paving) should

movements or other surface distress occur, and provide a reasonable warranty period acceptable to client. Remedial measures shall be approved by client.

The contractor shall retain a qualified Geotechnical Consultant to supervise the installation of surface settlement points on site and to provide direction, technical input and field inspection on projects.

Chapter 5: CONCLUSIONS AND RECOMMENDATIONS

The analysis of tunnels has been studied with a very good degree of accuracy by lots of researchers in the past. Early attempts for the analysis of tunnels used the analytical methods. Later, many attempts have been made to make finite element analysis of tunnels in the elastic stage. Two-dimensional analysis for tunnels using elastic perfectly plastic Mohr – Coulomb model for sand / rock is presented in this work. This study was performed on small and large diameter tunnels (5 m and 10 m), shallow or deep tunnels (10 m and 20 m) for 14 subsurface soil models for locations with in Dubai metropolitan area.

Tests were done to check the validity of using the available readymade package of PLAXIS 2D. The performance and accuracy of the software were validated by carrying out analyses of problems with known analytical solutions (Elastic & Plastic). A series of elastic benchmark calculations such as the analytical solution of a smooth strip footing on an elastic soil layer, strip loading on elastic Gibson soil, bending of beams, bending of plates, updated mesh analysis of a large deflected cantilever and performance of tunnel lining shell elements were used.

A series of plastic benchmark calculations such as bearing capacity of circular footing, bearing capacity of strip footing or contraction of a cylindrical cavity (tunnel) in soil was used. Parametric study using the proposed approach for different soil parameters, tunnel diameter, and tunnel depth, was performed to evaluate the effect of different combinations of tunnel diameters and depths on overall behavior of the model including the deformations. Results of the two-dimensional analysis are summarized in the next section.

5.1. Conclusions

The value of soil Young's modulus, E_s is the most important parameter in the behavior of the tunnel prior to reaching the soil's plastic stage when the elastic deformation of the tunnel is studied. In case of loose and very loose sands, the elastic analysis is very safe; i.e. the elastic behavior is close to the actual behavior since the

permissible deformation is limited. Thus, in case of loose and very loose sands, Young's modulus must be determined accurately. In general, increasing the value of Young's modulus, E_s decreases the value of the tunnel deformation and accordingly decreasing the tunnel internal forces.

The effect of Poisson's ratio (ν) is insignificant. But it is important to mention here that the only effect of Poisson's ratio is in the initial stress calculation. The earth pressure is generated depending on the value of the sand / rock Poisson's ratio. Again, this has a minor effect especially in case of sands in which k_0 ranges from 0.30 to 0.60.

Increasing the value of the angle of shearing resistance, ϕ , decreases the values of tunnel deformation and accordingly decreasing the tunnel internal forces. This can be attributed to the fact that the slope of Mohr-Coulomb failure surface increases with the increase of the value of ϕ .

Using interface element with $\mu = 0.3$ decreases the head deformation of the tunnel to about 63% of its value assuming full bond, which is a theoretical case. This means that using interface elements has a great effect on the resulting settlements. The value of coefficient of friction which proven to be most suitable was, $m = \tan(0.65\phi)$, at which ($\delta \approx 0.65\phi$).

As the tunnel diameter increases at same depths, the maximum ground settlement increases. As the tunnel depth increases with the same diameter, the maximum ground settlement decreases. The tunnels should be constructed at least 20m below the ground surface in Dubai area with in the Calcareous Limestones to successfully limit the deformations with in the soil mass which can reflect as significant surface settlements. The tunnel should be constructed as full closed face tunnel operations if shallower depths are desired.

The maximum vertical displacement is at the tunnel crown or shoulder and it is less at the half way between the crown of the tunnel and ground surface and accordingly the vertical displacement is also lower at the ground surface. This can be explained with respect to the soil arching around the tunnel as it is very clear from the stress distribution around the tunnel body. It is also noted that at a lateral distance of

more than two times the tunnel depth or 6 times the tunnel diameter, the vertical deformation tends to become insignificant.

The results due to the simulation of the volume loss indicate that the axial force becomes smaller with each calculation phase and progression of deformation. The bending moments, however, remains larger. This phenomenon is explained by soil arching around the tunnel body. The deformed mesh indicates a settlement trough at the ground surface. The plot of effective stresses shows and confirms that arching occurs around the tunnel. This arching reduces the stresses acting on the tunnel lining. As a result, the axial force is lower in the crown compared to the invert of the tunnel.

If the elasto-plastic behavior is considered to be the most rational behavior, then linear elastic behavior is not suitable as 58% of the maximum ground settlement occurs in the plastic stage when using elasto-plastic behavior. The nonlinear model can be considered as the results of the two behaviors are almost identical. The elasto-plastic model using interface gap friction elements is the most convenient approach.

5.2. Recommendations

Simulation of the construction of shield tunnels using the contraction method using Plaxis is an attempt to simulate the construction process of tunnels with a concrete lining. The major point in such an analysis is to account for the three-dimensional arching effect that occurs within the soil and the deformations that occur around the unsupported front of the tunnel. Future study should look at the 3 dimensional analysis of this settlement trough and also the effect of tunneling in front of the tunnel face.

This study did not look at the effect of tunneling on adjacent structures or the effect of adjacent structures on deformations and stresses. A future study involving the surcharge loadings and tunnel elements in the numerical modeling will be very valuable in developing guidelines for tunneling operations and monitoring programs in future.

Future studies could also look into the effect of sequence of support installation on the behavior of deformations and stress distributions around the tunnel in soil mass.

More areas within Dubai metropolitan can be modeled to evaluate the behavior of regional soils in greater detail. This can involve more combinations of depth and diameters. The areas can be extended into the emirate of Dubai to explore more subsurface conditions because the future of tunnels can extend beyond the urban areas.

REFERENCES

- H.S. Andrew, "Engineering Survey System for TBM (Tunnel Boring Machine) Tunnel Construction", *Hong Kong SAR, China* 13-17, May 2007.
- P. B. Attewell, and J. P. Woodman, 'Predicting the dynamics of ground settlement and its derivatives caused by tunneling in soil'. *Ground Engineering*, 15(8):13–22, 1982.
- P. B. Attewell, , J. Yeates, and A. R. Selby, 'Soil Movements Induced by Tunneling and their Effects on Pipelines and Structures'. *Blackie*, Glasgow, 1986.
- C.E Augarde, H.J. Burd, and G.T. Houlsby, "A Three-Dimensional Finite Element Model of Tunneling", *Proc. 4th Int. Symp. on Numerical Models in Geomechanics - NUMOG V*, Davos, Switzerland, 6-8 September, 1995. Rotterdam: Balkema. pp. 457- 462.
- C.E. Augarde, , C. Wisser, and H.J Burd,, "Numerical modeling of tunnel installation procedures". *Proc. 7th International Symposium on Numerical Methods in Geomechanics – NUMOG VII*, Graz, 1-3 September, 1999.
- K. J. Bathe, *Finite Element Procedures in Engineering Analysis*. Prentice Hall, Englewood Cliffs, 1982.
- A.G. Bloodworth, and G.T. Houlsby, "Three Dimensional Analysis of Building Settlement Caused by Shaft Construction", *Proc. International Symposium on Geotechnical Aspects of Underground Construction in Soft Ground*, Tokyo, 21 -23 July, 1999.
- M. D. Bolton, The strength and dilatancy of sands. *Geotechnique* 36, No. 1, 65-78, 1986
- B. B. Broms, and H. Bennermark, Stability of clay at vertical openings. *ASCE Soil Mechanics and Foundations Division*, 93(SM1), 1967.
- G. W. Clough, and B. Schmidt, Soft Clay Engineering, chapter *Design and performance of excavations and tunnels in soft clay*, pages 569–634. Elsevier, 1981.
- E. J. Cording, and W. H. Hansmire, Displacements around soft ground tunnels - general report. *In 5th Pan American Conference on Soil Mechanics and Foundation Engineering, Session IV*, pages 571–632, Buenos Aires, 1975.
- R. N. Craig, and A. M. Muir Wood, A review of tunnel lining practice in the united kingdom. Supplem. 335, *Transport and Road Research Laboratory*, 1978.

- J. M. Duncan, P. Byrne, , K. S. Wong, and P. Mabry, , "Strength, stress-strain and bulk modulus parameters for finite element analysis of stresses and movements in soil masses", *Report No. UCB/GT/80-01*, Dept. Civil Engineering, U.C. Berkeley, 1980.
- H. Duddeck, and J. Erdmann, Structural design models for tunnels. *Tunneling* 82, pages 83–91, 1982.
- H. H. Einstein, Improved design of tunnel supports. Cambridge, Massachusetts Institute of Technology, Department of Civil Engineering, 1 to 6, 1979-1980.
- R.J. Epps “Geotechnical Practice and ground conditions in the coastal regions of the United Arab Emirates”, 1980
- R.J. Evans, & K.S. Pister, 1966. Constitutive equations for a class of nonlinear elastic solids, *Int. J. Solids Struct.*, Vol 2, 427-455
- J.P Giroud, “Settlement of rectangular foundation on soil layer”, *Journal of the Soil Mechanics and Foundations Division*, ASCE, 98, SM 1, pp. 149-154, 1972,
- G.T. Houlsby, , H.J. Burd, and C.E. Augarde, "Analysis of Tunnel-Induced Settlement Damage to Surface Structures", *Proc. XII European Conference on Soil Mechanics and Geotechnical Engineering*, Amsterdam, 7-10 June, 1999.
- ITA. Views on structural design models for tunneling. *Advances in tunneling technology and subsurface use*, 2(3):153–229, 1982.
- D. Kolymbas, Geotechnical-Tunneling und Tunnel mechanics. Springer-Verlag, 1998.
- K.M. Lee, and R. K. Rowe “An analysis of three-dimensional ground movements: the Thunder Bay Tunnel”, *Canadian Geotechnical Journal*, 2008.
- R. J. Mair, Settlement effects of bored tunnels. *In International Symposium on Geotechnical Aspects of Underground Construction in Soft Ground*, pages 43–53, London, 1996.
- R. J. Mair, and R. N. TAYLOR, Bored tunneling in the urban environment. *In 14th international Conference on Soil Mechanics and Foundation Engineering*, pages 2353–2385, Hamburg, 1997.
- S. R. Macklin, The prediction of volume loss due to tunneling in overconsolidated clay based on heading geometry and stability number. *Ground Engineering*, 32(4):30– 33, 1999.
- H. Meissner, Tunnel under Tage –Numerical modeling in Geotechnical Engineering, *Geotechnique*, 19(2):99–108, 1996.
- S. M. Moller, Finite Element Dimensions, PhD Thesis. Institute of Geotechnical Engineering, University of Stuttgart, Stuttgart, 2006.

- A. M. Muir Wood, The circular tunnel in elastic ground. *Geotechnique*, 25(1):115–127, 1975.
- M. P. O’ Reilly, and B. M. New, Settlements above tunnels in the united kingdom - their magnitude and prediction. *Tunneling 82*, pages 173–181, 1982.
- R. B. Peck, Deep excavations and tunneling in soft ground. *In 7th int. Conference on Soil Mechanics and Foundation Engineering*, pages 225–290. Sociedad Mexican de Mecanica de Suelos, A. C., 1969.
- PLAXIS User Manual, Version 7, 1998.
- H.G. Poulos, and E.H Davis,. Elastic solutions for soil and rock mechanics. 1974
- W. J. Rankin, Ground movements resulting from urban tunneling: prediction and effects. *In Conference on Engineering Geology of Underground Movements*, pages 79–92, Nottingham BGS, 1988.
- N. M. Ruse, Raumliche Betrachtung der Standsicherheit der Ortsbrust beim Tunnelvortrieb. PhD thesis, Institute of Geotechnical Engineering, University of Stuttgart, Stuttgart, 2004
- A.F. Saleeb, and W.F. Chen, ‘Elastic-Plastic Large Displacement Analysis of Pipes’, *Journal of the Structural Division, ASCE*, Vol. 107, No. ST4, pp. 605-626, 1981.
- C. Sagaseta, Quasi-Static Undrained Expansion of A Cylindrical Cavity in Clay in The Presence of Shaft Friction and Anisotropic Initial Stresses, *Research report, Oxford University*. 1984
- B. F. Schmidt, Settlements and ground movements associated with tunneling in soils. Phd thesis, University of Illinois, Urbana, 1969.
- H. F. Schwinger, Finite-Element Method in Geotechnical Engineering, Technical Report to University at Graz, 1995.
- I.M. Smith, , and D.V. Griffith, “Programming the Finite Element Method”, Second Edition. John Wiley & Sons, Chisester, U.K., 1982
- Technical Manual for Design and Construction of Road Elements, U.S. Department of Transportation, Federal Highway Administration, 2009
- K. Terzaghi , R. B. Peck and G. Mesri, “Soil Mechanics in Engineering Practice” , John Wiley & Sons Inc., Third Edition, 1996
- A. O. Uriel, and C. Sagaseta, General report: Discussion session 9: Selection of design parameters for underground construction. *In 12th International Conference on Soil Mechanics and Foundation Engineering*, volume 4, pages 2521–2551, Rio de Janeiro, 1989.

- H. Van Langen & P.A. Vermeer, Automatic Step size correction for non-associated plasticity problems. *Int. Journal of Numerical Methods in Engineering*, 29: 579-598, 1990
- O. C. Zienkiewicz, and R. L. Taylor, *The Finite Element Method*. McGraw Hill, London, 4 edition, 1991.

Appendix A
Borehole Logs

BOREHOLE LOG

BOREHOLE (PJA)

Client		Nakheel														
Project		Proposed Crescent														
Location		The Palm Jebel Ali														
Ground Datum Level		2.36 m DMD														
Date Drilling Started		14/05/2007														
Date Drilling Completed		17/05/2007														
Equipment Type		Edeco Traveller T-30 Rotary Drilling Rig														
Drilling Fluid Used		Water/ Guargum														
R.Q.D. (%)	U.C.S. (kN/m ²)	S.P.T. (N)	Water Depth	Material model	Depth (m)	Legend	DESCRIPTION	Dry weight (dry)/kN/m ³	Wet weight (dry)/kN/m ³	Permeability in horizontal and vertical direction (m/day)	Young's modulus (E _{ref}) kN/m ²	Poisson's ratio (ν)	Cohesion (c _{ref}) kN/m ²	Friction angle (φ)	Dilatancy angle (ψ)	Type of material behaviour
		22		Mohr-Coulomb	3.0											
				Mohr-Coulomb	5.0		Made Ground, medium sense to dense, pale brown, slightly silt, fine to coarse sand	16.0	17.0	0.6	23000	0.35	0.0	33	3	Drained
		25		Mohr-Coulomb	10.0											
				Mohr-Coulomb	15.0		Light brown, silty, gravely, fine to medium sand with occasional fine to medium gravel and cemented pieces.	18.0	19.0	0.5	25000	0.35	1.0	35	5	Drained
40	4	>50		Mohr-Coulomb	20.0		Fresh to slightly weathered, thinly laminated, light brown, fine to medium grained, very weak to weak, calcareous SANDTONE .	22.0	22.0	0	5000000	0.30	50	25	0	Drained
				Mohr-Coulomb	25.0											
62	11			Mohr-Coulomb	30.0		Moderately to occasionally highly weathered brown grading to greenish grey, very weak to weak, conglomeratic, slightly sandy, carbonate SILTSTONE/ CALCISILTITE with some bands of conglomerate and sandstone.	23.0	23.0	0	9500000	0.25	54	28	0	Drained
					35.0											
					40.0											
					45.0											
					50.0											

Continued

BOREHOLE LOG

BOREHOLE (PJA)

Client		Nakheel														
Project		Proposed Crescent														
Location		The Palm Jebel Ali														
Ground Datum Level		2.36 m DMD														
Date Drilling Started		14/05/2007														
Date Drilling Completed		17/05/2007														
Equipment Type		Edeco Traveller T-30 Rotary Drilling Rig														
Drilling Fluid Used		Water/ Guargum														
R.O.D. (%)	U.C.S. (kN/m ²)	S.P.T. (N)	Water Depth	Material model	Depth (m)	Legend	DESCRIPTION	Dry weight (γ _{dry})/kN/m ³	Wet weight (γ _{wet})/kN/m ³	Permeability in horizontal and vertical direction (m/day)	Young's modulus (E _{en})/kN/m ²	Poisson's ratio (ν)	Cohesion (c _{ref})	Friction angle (φ)	Dilatancy angle (ψ)	Type of material behaviour
62	11			Mehr-Coulomb	55.0		Moderately to occasionally highly weathered brown grading to greenish grey, very weak to weak, conglomeratic, slightly sandy, carbonate SILTSTONE/ CALCISILTITE with some bands of conglomerate and sandstone.	23.0	23.0	0	9500000	0.25	54	28	0	Drained
87	17			Mehr-Coulomb	75.0		Slightly to moderately weathered, brown with frequent whitish clasts, medium to coarse grained, weak to moderately weak, locally very weak, sandy CONGLOMERATE comprised of fine to coarse gravel of assorted rock types with in a matrix of silty sand and few bands of silty sandstone.	23.5	23.5	0	14300000	0.20	57	30	0	Drained
					80.0		E.O.B									
					85.0											
					90.0											
					95.0											
					100.0											

BOREHOLE LOG

BOREHOLE (AB)

Client		Nakheel														
Project		Al Burj														
Location		Dubai Waterfront														
Ground Datum Level		2.65 m DMD														
Date Drilling Started		18/07/2008														
Date Drilling Completed		24/05/2008														
Equipment Type		Edeco Traveller T-30 Rotary Drilling Rig														
Drilling Fluid Used		Water/ Guargum														
R.Q.D. (%)	U.C.S. (kN/m ²)	S.P.T. (N)	Water Depth	Material model	Depth (m)	Legend	DESCRIPTION	Dry weight (dry)/kN/m ³	Wet weight (dry)/kN/m ³	Permeability in horizontal and vertical direction (m/day)	Young's modulus (E _{ref}) kN/m ²	Poisson's ratio (ν)	Cohesion (c _{ref}) kN/m ²	Friction angle (φ)	Dilatancy angle (ψ)	Type of material behaviour
		24		Mohr-Coulomb	5.0		Made Ground, consisting of light brown, silty, gravely, fine to medium sand with occasional fine to medium gravel and cemented pieces.	17.5	18.5	0.45	23520	0.35	1.0	34	4	Drained
38	3.5	>50		Mohr-Coulomb	6.0		Fresh to slightly weathered, thinly laminated, light brown, fine to medium grained, very weak to weak, calcareous SANDTONE .	21.0	21.0	0	4850000	0.30	48	24	0	Drained
58	10			Mohr-Coulomb	35.0		Moderately to occasionally highly weathered brown grading to greenish grey, very weak to weak, conglomeratic, slightly sandy, carbonate SILTSTONE/ CALCISILTITE with some bands of conglomerate and sandstone.	22.5	22.5	0	9320000	0.25	49	27	0	Drained

Continued

BOREHOLE LOG

BOREHOLE (AB)

Client		Nakheel														
Project		Al Burj														
Location		Dubai Waterfront														
Ground Datum Level		2.65 m DMD														
Date Drilling Started		18/07/2008														
Date Drilling Completed		24/05/2008														
Equipment Type		Edeco Traveller T-30 Rotary Drilling Rig														
Drilling Fluid Used		Water/ Guargum														
R.O.D. (%)	U.C.S. (kN/m ²)	S.P.T. (N)	Water Depth	Material model	Depth (m)	Legend	DESCRIPTION	Dry weight (γ _d)/kN/m ³	Wet weight (γ _w)/kN/m ³	Permeability in horizontal and vertical direction (m/day)	Young's modulus (E _{eq}) kN/m ²	Poisson's ratio (ν)	Cohesion (c _{ref})	Friction angle (φ)	Dilatancy angle (ψ)	Type of material behaviour
58	10			Mohr-Coulomb	55.0	X	Moderately to occasionally highly weathered brown grading to greenish grey, very weak to weak, conglomeratic, slightly sandy, carbonate SILTSTONE/ CALCISILTITE with some bands of conglomerate and sandstone.	22.5	22.5	0	9320000	0.25	49	27	0	Drained
					60.0	X										
62	12			Mohr-Coulomb	65.0	X	Slightly to moderately weathered, brown with frequent whitish clasts, medium to coarse grained, weak to moderately weak, locally very weak, sandy CONGLOMERATE comprised of fine to coarse gravel of assorted rock types with in a matrix of silty sand and few bands of silty sandstone.	23.5	23.5	0	14000000	0.20	55	30	0	Drained
					70.0	X										
					75.0	X										
61	11			Mohr-Coulomb	80.0	X	Moderately to occasionally highly weathered brown grading to greenish grey, very weak to weak, conglomeratic, slightly sandy, carbonate SILTSTONE/ CALCISILTITE with some bands of conglomerate and sandstone.	23.0	23.0	0	9400000	0.25	52	28	0	Drained
					85.0	X										
					90.0	X										
65	14			Mohr-Coulomb	95.0	X	Slightly to moderately weathered, brown with frequent whitish clasts, medium to coarse grained, weak to moderately weak, locally very weak, sandy CONGLOMERATE comprised of fine to coarse gravel of assorted rock types with in a matrix of silty sand and few bands of silty sandstone.	24.0	24.0	0	14300000	0.20	57	30	0	Drained
					100.0	X										

BOREHOLE LOG

BOREHOLE (AT)

Client		Tameer																								
Project		Anara Tower																								
Location		Al Sufouh Second																								
Ground Datum Level		3.26 m DMD																								
Date Drilling Started		20/06/2006																								
Date Drilling Completed		22/06/2006																								
Equipment Type		Edeco Traveller T-30 Rotary Drilling Rig																								
Drilling Fluid Used		Water/ Guargum																								
R.Q.D. (%)	U.C.S. (kN/m ²)	S.P.T. (N)	Water Depth	Material model	Depth (m)	Legend	DESCRIPTION	Dry weight (dry)/kN/m ³	Wet weight (dry)/kN/m ³	Permeability in horizontal and vertical direction (m/day)	Young's modulus (Eref) kN/m ²	Poisson's ratio (ν)	Cohesion (cref) kN/m ²	Friction angle (φ)	Dilatancy angle (ψ)	Type of material behaviour										
		24		Mohr-Coulomb	5.0		Made Ground, consisting of light brown, silty, gravely, fine to medium sand with occasional fine to medium gravel and cemented pieces.	17.5	18.5	0.45	23520	0.35	1.0	34	4	Drained										
38	3.5	>50		Mohr-Coulomb	10.0		Fresh to slightly weathered, thinly laminated, light brown, fine to medium grained, very weak to weak, calcareous SANDTONE .	21.0	21.0	0	4850000	0.30	48	24	0	Drained										
					15.0																					
					20.0		X																			
					25.0																					
58	10				35.0												Moderately to occasionally highly weathered brown grading to greenish grey, very weak to weak, conglomeratic, slightly sandy, carbonate SILTSTONE/ CALCISILTITE with some bands of conglomerate and sandstone.	22.5	22.5	0	9320000	0.25	49	27	0	Drained
					40.0																					
					45.0																					
					50.0																					

Continued

BOREHOLE LOG

BOREHOLE (AT)

Client		Tameer														
Project		Anara Tower														
Location		Al Sufouh Second														
Ground Datum Level		3.26 m DMD														
Date Drilling Started		20/06/2006														
Date Drilling Completed		22/06/2006														
Equipment Type		Edeco Traveller T-30 Rotary Drilling Rig														
Drilling Fluid Used		Water/ Guargum														
R.O.D. (%)	U.C.S. (kN/m ²)	S.P.T. (N)	Water Depth	Material model	Depth (m)	Legend	DESCRIPTION	Dry weight (γ _{dry})/kN/m ³	Wet weight (γ _w)/kN/m ³	Permeability in horizontal and vertical direction (m/day)	Young's modulus (E _{eq})/kN/m ²	Poisson's ratio (ν)	Cohesion (c _{ref})	Friction angle (φ)	Dilatancy angle (ψ)	Type of material behaviour
58	10			Mohr-Coulomb	55.0		Moderately to occasionally highly weathered brown grading to greenish grey, very weak to weak, conglomeratic, slightly sandy, carbonate SILTSTONE/ CALCISILTITE with some bands of conglomerate and sandstone.	22.5	22.5	0	9320000	0.25	49	27	0	Drained
					60.0											
					65.0											
					70.0											
62	12			Mohr-Coulomb	75.0		Slightly to moderately weathered, brown with frequent whitish clasts, medium to coarse grained, weak to moderately weak, locally very weak, sandy CONGLOMERATE comprised of fine to coarse gravel of assorted rock types with in a matrix of silty sand and few bands of silty sandstone.	23.5	23.5	0	14000000	0.25	55	30	0	Drained
					80.0											
					85.0											
61	11			Mohr-Coulomb	90.0		Moderately to occasionally highly weathered brown grading to greenish grey, very weak to weak, conglomeratic, slightly sandy, carbonate SILTSTONE/ CALCISILTITE with some bands of conglomerate and sandstone.	23.0	23.0	0	9400000	0.25	52	28	0	Drained
					95.0											
65	14			Mohr-Coulomb	95.0		Slightly to moderately weathered, brown with frequent whitish clasts, medium to coarse grained, weak to moderately weak, locally very weak, sandy CONGLOMERATE comprised of fine to coarse gravel of assorted rock types with in a matrix of silty sand and few bands of silty sandstone.	24.0	24.0	0	14300000	0.20	57	30	0	Drained
					100.0											

BOREHOLE LOG

BOREHOLE (JG)

Client		Jumerah Garden City														
Project		Towers, Villas and Canals														
Location		Al Satwa														
Ground Datum Level		4.30 m DMD														
Date Drilling Started		14/05/2006														
Date Drilling Completed		17/05/2006														
Equipment Type		Edeco Traveller T-30 Rotary Drilling Rig														
Drilling Fluid Used		Water/ Guargum														
R.Q.D. (%)	U.C.S. (kN/m ²)	S.P.T. (N)	Water Depth	Material model	Depth (m)	Legend	DESCRIPTION	Dry weight (dry)kN/m ³	Wet weight (dry)kN/m ³	Permeability in horizontal and vertical direction (m/day)	Young's modulus (E _{ref}) kN/m ²	Poisson's ratio (ν)	Cohesion (c _{ref}) kN/m ²	Friction angle (φ)	Dilatancy angle (ψ)	Type of material behaviour
		22		Mohr-Coulomb	4.0 5.0		Made Ground, medium sense to dense, pale brown, slightly silt, fine to coarse sand	16.0	17.0	0.6	23000	0.35	0.0	33	3	Drained
		25		Mohr-Coulomb	10.0 15.0		Light brown, silty, gravely, fine to medium sand with occasional fine to medium gravel and cemented pieces.	18.0	19.0	0.5	25000	0.35	1.0	35	5	Drained
40	4	>50		Mohr-Coulomb	20.0 25.0		Fresh to slightly weathered, thinly laminated, light brown, fine to medium grained, very weak to weak, calcareous SANDTONE .	22.0	22.0	0	5000000	0.30	50	25	0	Drained
62	11			Mohr-Coulomb	30.0 35.0 40.0 45.0 50.0		Moderately to occasionally highly weathered brown grading to greenish grey, very weak to weak, conglomeratic, slightly sandy, carbonate SILTSTONE/ CALCISILTITE with some bands of conglomerate and sandstone.	23.0	23.0	0	9500000	0.25	54	28	0	Drained

Continued

BOREHOLE LOG

BOREHOLE (JG)

Client		Jumerah Garden City														
Project		Towers, Villas and Canals														
Location		Al Satwa														
Ground Datum Level		4.30 m DMD														
Date Drilling Started		14/05/2006														
Date Drilling Completed		17/05/2006														
Equipment Type		Edeco Traveller T-30 Rotary Drilling Rig														
Drilling Fluid Used		Water/ Guargum														
R.O.D. (%)	U.C.S. (kN/m ²)	S.P.T. (N)	Water Depth	Material model	Depth (m)	Legend	DESCRIPTION	Dry weight (γ _{dry})/kN/m ³	Wet weight (γ _{wet})/kN/m ³	Permeability in horizontal and vertical direction (m/day)	Young's modulus (E _{ref}) kN/m ²	Poisson's ratio (ν)	Cohesion (c _{ref})	Friction angle (φ)	Dilatancy angle (ψ)	Type of material behaviour
62	11			Mohr-Coulomb	55.0		Moderately to occasionally highly weathered brown grading to greenish grey, very weak to weak, conglomeratic, slightly sandy, carbonate SILTSTONE/ CALCISILTITE with some bands of conglomerate and sandstone.	23.0	23.0	0	9500000	0.25	54	28	0	Drained
92	21			Mohr-Coulomb	70.0		Weak, reddish brown with molted buffwhite CONGLOMERATE, fine to medium garvels with sandy Silty matrix	24.0	24.0	0	15700000	0.17	59	30	0	Drained
87	17			Mohr-Coulomb	95.0		Slightly to moderately weathered, brown with frequent whitish clasts, medium to coarse grained, weak to moderately weak, locally very weak, sandy CONGLOMERATE comprised of fine to coarse gravel of assorted rock types with in a matrix of silty sand and few bands of silty sandstone.	23.5	23.5	0	14300000	0.20	57	30	0	Drained
					100.0											

BOREHOLE LOG

BOREHOLE (AC)

Client		Nakheel														
Project		Arabian Canal														
Location		Arabian Canal														
Ground Datum Level		55.18 m DMD														
Date Drilling Started		14/05/2008														
Date Drilling Completed		17/05/2008														
Equipment Type		Edeco Traveller T-30 Rotary Drilling Rig														
Drilling Fluid Used		Water/ Guargum														
R.Q.D. (%)	U.C.S. (kN/m ²)	S.P.T. (N)	Water Depth	Material model	Depth (m)	Legend	DESCRIPTION	Dry weight (dry)/kN/m ³	Wet weight (dry)/kN/m ³	Permeability in horizontal and vertical direction (m/day)	Young's modulus (E _{ref}) kN/m ²	Poisson's ratio (ν)	Cohesion (c _{ref}) kN/m ²	Friction angle (φ)	Dilatancy angle (ψ)	Type of material behaviour
		22		Mohr-Coulomb	3.0		Made Ground, medium sense to dense, pale brown, slightly silt, fine to coarse sand	16.0	17.0	0.6	23000	0.35	0.0	33	3	Drained
		25		Mohr-Coulomb	5.0		Light brown, silty, gravely, fine to medium sand with occasional fine to medium gravel and cemented pieces.	18.0	19.0	0.5	25000	0.35	1.0	35	5	Drained
					10.0											
40	4	>50		Mohr-Coulomb	15.0		Fresh to slightly weathered, thinly laminated, light brown, fine to medium grained, very weak to weak, calcareous SANDTONE .	22.0	22.0	0	5000000	0.30	50	25	0	Drained
					20.0											
62	11			Mohr-Coulomb	25.0		Moderately to occasionally highly weathered brown grading to greenish grey, very weak to weak, conglomeratic, slightly sandy, carbonate SILTSTONE/ CALCISILTITE with some bands of conglomerate and sandstone.	23.0	23.0	0	9500000	0.25	54	28	0	Drained
					30.0											
					35.0											
					40.0											
					45.0											
					50.0											

Continued

BOREHOLE LOG

BOREHOLE (AC)

Client		Nakheel														
Project		Arabian Canal														
Location		Arabian Canal														
Ground Datum Level		55.18 m DMD														
Date Drilling Started		14/05/2008														
Date Drilling Completed		17/05/2008														
Equipment Type		Edeco Traveller T-30 Rotary Drilling Rig														
Drilling Fluid Used		Water/ Guargum														
R.O.D. (%)	U.C.S. (kN/m ²)	S.P.T. (N)	Water Depth	Material model	Depth (m)	Legend	DESCRIPTION	Dry weight (γ _{dry})/kN/m ³	Wet weight (γ _{wet})/kN/m ³	Permeability in horizontal and vertical direction (m/day)	Young's modulus (E _{ref}) kN/m ²	Poisson's ratio (ν)	Cohesion (c _{ref})	Friction angle (φ)	Dilatancy angle (ψ)	Type of material behaviour
	62	11		Mohr-Coulomb	55.0 60.0 65.0 70.0 75.0 80.0 85.0 90.0 95.0 100.0	X	Moderately to occasionally highly weathered brown grading to greenish grey, very weak to weak, conglomeratic, slightly sandy, carbonate SILTSTONE/ CALCISILTITE with some bands of conglomerate and sandstone.	23.0	23.0	0	9500000	0.25	54	28	0	Drained

BOREHOLE LOG

BOREHOLE (TT)

Client		Tatweer														
Project		Tatwee Tower														
Location		Emirates Road														
Ground Datum Level		24.36 m DMD														
Date Drilling Started		14/08/2008														
Date Drilling Completed		17/08/2008														
Equipment Type		Edeco Traveller T-30 Rotary Drilling Rig														
Drilling Fluid Used		Water/ Guargum														
R.Q.D. (%)	U.C.S. (kN/m ²)	S.P.T. (N)	Water Depth	Material Model	Depth (m)	Legend	DESCRIPTION	Dry weight (dry)/kN/m ³	Wet weight (dry)/kN/m ³	Permeability in horizontal and vertical direction (m/day)	Young's modulus (E _{ref}) kN/m ²	Poisson's ratio (ν)	Cohesion (c _{ref}) kN/m ²	Friction angle (φ)	Dilatancy angle (ψ)	Type of material behaviour
		22		Mohr-Coulomb	5.0		Made Ground, medium sense to dense, pale brown, slightly silt, fine to coarse sand	16.0	17.0	0.6	23000	0.35	0.0	33	3	Drained
		25		Mohr-Coulomb	8.0		Light brown, silty, gravely, fine to medium sand with occasional fine to medium gravel and cemented pieces.	18.0	19.0	0.5	25000	0.35	1.0	35	5	Drained
40	4	>50		Mohr-Coulomb	10.0		Fresh to slightly weathered, thinly laminated, light brown, fine to medium grained, very weak to weak, calcareous SANDTONE .	22.0	22.0	0	5000000	0.30	50	25	0	Drained
					15.0											
					20.0											
					25.0											
62	11			Mohr-Coulomb	30.0		Moderately to occasionally highly weathered brown grading to greenish grey, very weak to weak, conglomeratic, slightly sandy, carbonate SILTSTONE/ CALCISILTITE with some bands of conglomerate and sandstone.	23.0	23.0	0	9500000	0.25	54	28	0	Drained
					35.0											
					40.0											
					45.0											
					50.0											

Continued

BOREHOLE LOG

BOREHOLE (TT)

Client		Tatweer																
Project		Tatwee Tower																
Location		Emirates Road																
Ground Datum Level		24.36 m DMD																
Date Drilling Started		14/08/2008																
Date Drilling Completed		17/08/2008																
Equipment Type		Edeco Traveller T-30 Rotary Drilling Rig																
Drilling Fluid Used		Water/ Guargum																
R.O.D. (%)	U.C.S. (kN/m ²)	S.P.T. (N)	Water Depth	Material model	Depth (m)	Legend	DESCRIPTION	Dry weight (γ _{dry})/kN/m ³	Wet weight (γ _w)/kN/m ³	Permeability in horizontal and vertical direction (m/day)	Young's modulus (E _{en}) kN/m ²	Poisson's ratio (ν)	Cohesion (c _{ref})	Friction angle (φ)	Dilatancy angle (ψ)	Type of material	behaviour	
	62	11		Mohr-Coulomb	55.0		Moderately to occasionally highly weathered brown grading to greenish grey, very weak to weak, conglomeratic, slightly sandy, carbonate SILTSTONE/ CALCISILTITE with some bands of conglomerate and sandstone.	23.0	23.0	0	9500000	0.25	54	28	0	Drained		
					60.0													
					65.0													
					70.0													
					75.0													
					80.0													
					85.0													
					90.0													
					95.0													
					100.0													

BOREHOLE LOG

BOREHOLE (JGC)

Client		Jumerah Garden City															
Project		Towers, Villas and Canals															
Location		Al Satwa															
Ground Datum Level		4.30 m DMD															
Date Drilling Started		14/05/2006															
Date Drilling Completed		17/05/2006															
Equipment Type		Edeco Traveller T-30 Rotary Drilling Rig															
Drilling Fluid Used		Water/ Guargum															
R.Q.D. (%)	U.C.S. (kN/m ²)	S.P.T. (N)	Water Depth	Material model	Depth (m)	Legend	DESCRIPTION	Dry weight (dry)/kN/m ³	Wet weight (dry)/kN/m ³	Permeability in horizontal and vertical direction (m/day)	Young's modulus (E _{ref}) kN/m ²	Poisson's ratio (ν)	Cohesion (c _{ref}) kN/m ²	Friction angle (φ)	Dilatancy angle (ψ)	Type of material	behaviour
		22		Mohr-Coulomb	4.0 5.0		Made Ground, medium sense to dense, pale brown, slightly silt, fine to coarse sand	16.0	17.0	0.6	23000	0.35	0.0	33	3	Drained	
40	4	>50		Mohr-Coulomb	10.0 15.0 20.0		Fresh to slightly weathered, thinly laminated, light brown, fine to medium grained, very weak to weak, calcareous SANDTONE .	22.0	22.0	0	5000000	0.30	50	25	0	Drained	
62	11			Mohr-Coulomb	25.0 30.0 35.0 40.0 45.0 50.0	XXXX	Moderately to occasionally highly weathered brown grading to greenish grey, very weak to weak, conglomeratic, slightly sandy, carbonate SILTSTONE/ CALCISILTITE with some bands of conglomerate and sandstone.	23.0	23.0	0	9500000	0.25	54	28	0	Drained	

Continued

BOREHOLE LOG

BOREHOLE (JGC)

Client		Jumerah Garden City														
Project		Towers, Villas and Canals														
Location		Al Satwa														
Ground Datum Level		4.30 m DMD														
Date Drilling Started		14/05/2006														
Date Drilling Completed		17/05/2006														
Equipment Type		Edeco Traveller T-30 Rotary Drilling Rig														
Drilling Fluid Used		Water/ Guargum														
R.O.D. (%)	U.C.S. (kN/m ²)	S.P.T. (N)	Water Depth	Material model	Depth (m)	Legend	DESCRIPTION	Dry weight (γ _{dry})/kN/m ³	Wet weight (γ _{wet})/kN/m ³	Permeability in horizontal and vertical direction (m/day)	Young's modulus (E _{ref}) kN/m ²	Poisson's ratio (ν)	Cohesion (c _{ref})	Friction angle (φ)	Dilatancy angle (ψ)	Type of material behaviour
62	11			Mohr-Coulomb	55.0	X	Moderately to occasionally highly weathered brown grading to greenish grey, very weak to weak, conglomeratic, slightly sandy, carbonate SILTSTONE/ CALCISILTITE with some bands of conglomerate and sandstone.	23.0	23.0	0	9500000	0.25	54	28	0	Drained
92	21			Mohr-Coulomb	70.0	X	Weak, reddish brown with molted buffwhite CONGLOMERATE, fine to medium garvels with sandy Silty matrix	24.0	24.0	0	15700000	0.17	59	30	0	Drained
87	17			Mohr-Coulomb	95.0	X	Slightly to moderately weathered, brown with frequent whitish clasts, medium to coarse grained, weak to moderately weak, locally very weak, sandy CONGLOMERATE comprised of fine to coarse gravel of assorted rock types with in a matrix of silty sand and few bands of silty sandstone.	23.5	23.5	0	14300000	0.20	57	30	0	Drained
					100.0	X										

BOREHOLE LOG

BOREHOLE (PJAc)

Client		Nakheel														
Project		Proposed Crescent														
Location		The Palm Jebel Ali														
Ground Datum Level		2.36 m DMD														
Date Drilling Started		14/05/2007														
Date Drilling Completed		17/05/2007														
Equipment Type		Edeco Traveller T-30 Rotary Drilling Rig														
Drilling Fluid Used		Water/ Guargum														
R.Q.D. (%)	U.C.S. (kN/m ²)	S.P.T. (N)	Water Depth	Material model	Depth (m)	Legend	DESCRIPTION	Dry weight (dry)/kN/m ³	Wet weight (dry)/kN/m ³	Permeability in horizontal and vertical direction (m/day)	Young's modulus (E _r) kN/m ²	Poisson's ratio (ν)	Cohesion (c _r) kN/m ²	Friction angle (φ)	Dilatancy angle (ψ)	Type of material behaviour
		22		Mohr-Coulomb	3.0											
					5.0											
					10.0		Made Ground, medium sense to dense, pale brown, slightly silt, fine to coarse sand	16.0	17.0	0.6	23000	0.35	0.0	33	3	Drained
40	4	>50		Mohr-Coulomb	15.0											
					20.0		Fresh to slightly weathered, thinly laminated, light brown, fine to medium grained, very weak to weak, calcareous SANDTONE .	22.0	22.0	0	5000000	0.30	50	25	0	Drained
					25.0											
62	11			Mohr-Coulomb	30.0		Moderately to occasionally highly weathered brown grading to greenish grey, very weak to weak, conglomeratic, slightly sandy, carbonate SILTSTONE/ CALCISILTITE with some bands of conglomerate and sandstone.	23.0	23.0	0	9500000	0.25	54	28	0	Drained
					35.0											
					40.0											
					45.0											
					50.0											

Continued

BOREHOLE LOG

BOREHOLE (PJAc)

Client		Nakheel														
Project		Proposed Crescent														
Location		The Palm Jebel Ali														
Ground Datum Level		2.36 m DMD														
Date Drilling Started		14/05/2007														
Date Drilling Completed		17/05/2007														
Equipment Type		Edeco Traveller T-30 Rotary Drilling Rig														
Drilling Fluid Used		Water/ Guargum														
R.O.D. (%)	U.C.S. (kN/m ²)	S.P.T. (N)	Water Depth	Material model	Depth (m)	Legend	DESCRIPTION	Dry weight (γ _{dry})/kN/m ³	Wet weight (γ _{wet})/kN/m ³	Permeability in horizontal and vertical direction (m/day)	Young's modulus (E _{en})/kN/m ²	Poisson's ratio (ν)	Cohesion (c _{ref})	Friction angle (φ)	Dilatancy angle (ψ)	Type of material behaviour
62	11			Mehr-Coulomb	55.0		Moderately to occasionally highly weathered brown grading to greenish grey, very weak to weak, conglomeratic, slightly sandy, carbonate SILTSTONE/ CALCISILTITE with some bands of conglomerate and sandstone.	23.0	23.0	0	9500000	0.25	54	28	0	Drained
87	17			Mehr-Coulomb	75.0		Slightly to moderately weathered, brown with frequent whitish clasts, medium to coarse grained, weak to moderately weak, locally very weak, sandy CONGLOMERATE comprised of fine to coarse gravel of assorted rock types with in a matrix of silty sand and few bands of silty sandstone.	23.5	23.5	0	14300000	0.20	57	30	0	Drained
					80.0		E.O.B									
					85.0											
					90.0											
					95.0											
					100.0											

BOREHOLE LOG

BOREHOLE (ACc)

Client		Nakheel																			
Project		Arabian Canal																			
Location		Arabian Canal																			
Ground Datum Level		55.18 m DMD																			
Date Drilling Started		14/05/2008																			
Date Drilling Completed		17/05/2008																			
Equipment Type		Edeco Traveller T-30 Rotary Drilling Rig																			
Drilling Fluid Used		Water/ Guargum																			
R.Q.D. (%)	U.C.S. (kN/m ²)	S.P.T. (N)	Water Depth	Material Model	Depth (m)	Legend	DESCRIPTION														
							Dry weight (dry)/kN/m ³	Wet weight (dry)/kN/m ³	Permeability in horizontal and vertical direction (m/day)	Young's modulus (E _{ref}) kN/m ²	Poisson's ratio (ν)	Cohesion (c _{ref}) kN/m ²	Friction angle (φ)	Dilatancy angle (ψ)	Type of material behaviour						
40	4	>50		Mohr-Coulomb	3.0		Fresh to slightly weathered, thinly laminated, light brown, fine to medium grained, very weak to weak, calcareous SANDTONE .														
					5.0																
					10.0				22.0	22.0	0	5000000	0.30	50	25	0	Drained				
					15.0																
					20.0																
					25.0																
92	21			Mohr-Coulomb	30.0		Weak, reddish brown with molted buffwhite CONGLOMERATE, fine to medium garvels with sandy Silty matrix	24.0	24.0	0	15700000	0.17	59	30	0	Drained					
62	11			Mohr-Coulomb	35.0		Moderately to occasionally highly weathered brown grading to greenish grey, very weak to weak, conglomeratic, slightly sandy, carbonate SILTSTONE/ CALCISILTITE with some bands of conglomerate and sandstone.	23.0	23.0	0	9500000	0.25	54	28	0	Drained					
85	13			Mohr-Coulomb	40.0		Weak, reddish brown with molted buffwhite CONGLOMERATE, fine to medium garvels with sandy Silty matrix	24.0	24.0	0	15700000	0.17	59	30	0	Drained					
62	11			Mohr-Coulomb	45.0		Moderately to occasionally highly weathered brown grading to greenish grey, very weak to weak, conglomeratic, slightly sandy, carbonate SILTSTONE/ CALCISILTITE with some bands of conglomerate and sandstone.	23.0	23.0	0	9500000	0.25	54	28	0	Drained					
					50.0																
Continued																					

BOREHOLE LOG

BOREHOLE (ACc)

Client		Nakheel														
Project		Arabian Canal														
Location		Arabian Canal														
Ground Datum Level		55.18 m DMD														
Date Drilling Started		14/05/2008														
Date Drilling Completed		17/05/2008														
Equipment Type		Edeco Traveller T-30 Rotary Drilling Rig														
Drilling Fluid Used		Water/ Guargum														
R.O.D. (%)	U.C.S. (kN/m ²)	S.P.T. (N)	Water Depth	Material model	Depth (m)	Legend	DESCRIPTION	Dry weight (γ _{dry})/kN/m ³	Wet weight (γ _w)/kN/m ³	Permeability in horizontal and vertical direction (m/day)	Young's modulus (E _{eq}) kN/m ²	Poisson's ratio (ν)	Cohesion (c _{ref})	Friction angle (φ)	Dilatancy angle (ψ)	Type of material behaviour
62	11			Mohr-Coulomb	55.0	XXXX	Moderately to occasionally highly weathered brown grading to greenish grey, very weak to weak, conglomeratic, slightly sandy, carbonate SILTSTONE/ CALCISILTITE with some bands of conglomerate and sandstone.	23.0	23.0	0	9500000	0.25	54	28	0	Drained
92	21			Mohr-Coulomb	60.0	XXXX	Weak, reddish brown with molted buffwhite CONGLOMERATE, fine to medium garvels with sandy Silty matrix	24.0	24.0	0	15700000	0.17	59	30	0	Drained
62	11			Mohr-Coulomb	70.0	XXXX	Moderately to occasionally highly weathered brown grading to greenish grey, very weak to weak, conglomeratic, slightly sandy, carbonate SILTSTONE/ CALCISILTITE with some bands of conglomerate and sandstone.	23.0	23.0	0	9500000	0.25	54	28	0	Drained
92	21			Mohr-Coulomb	75.0	XXXX	Weak, reddish brown with molted buffwhite CONGLOMERATE, fine to medium garvels with sandy Silty matrix	24.0	24.0	0	15700000	0.17	59	30	0	Drained
					80.0	XXXX										
62	11			Mohr-Coulomb	90.0	XXXX	Moderately to occasionally highly weathered brown grading to greenish grey, very weak to weak, conglomeratic, slightly sandy, carbonate SILTSTONE/ CALCISILTITE with some bands of conglomerate and sandstone.	23.0	23.0	0	9500000	0.25	54	28	0	Drained
					95.0	XXXX										
					100.0	XXXX										

BOREHOLE LOG

BOREHOLE (ABd)

Client		Nakheel														
Project		Al Burj														
Location		Dubai Waterfront														
Ground Datum Level		2.65 m DMD														
Date Drilling Started		18/07/2008														
Date Drilling Completed		24/05/2008														
Equipment Type		Edeco Traveller T-30 Rotary Drilling Rig														
Drilling Fluid Used		Water/ Guargum														
R.O.D. (%)	U.C.S. (kN/m ²)	S.P.T. (N)	Water Depth	Material model	Depth (m)	Legend	DESCRIPTION	Dry weight (γ _d)/kN/m ³	Wet weight (γ _w)/kN/m ³	Permeability in horizontal and vertical direction (m/day)	Young's modulus (E _{eq}) kN/m ²	Poisson's ratio (ν)	Cohesion (c _{ref})	Friction angle (φ)	Dilatancy angle (ψ)	Type of material behaviour
58	10			Mohr-Coulomb	55.0	X	Moderately to occasionally highly weathered brown grading to greenish grey, very weak to weak, conglomeratic, slightly sandy, carbonate SILTSTONE/ CALCISILTITE with some bands of conglomerate and sandstone.	22.5	22.5	0	9320000	0.25	49	27	0	Drained
					60.0	X										
62	12			Mohr-Coulomb	65.0	X	Slightly to moderately weathered, brown with frequent whitish clasts, medium to coarse grained, weak to moderately weak, locally very weak, sandy CONGLOMERATE comprised of fine to coarse gravel of assorted rock types with in a matrix of silty sand and few bands of silty sandstone.	23.5	23.5	0	1400000	0.20	55	30	0	Drained
					70.0	X										
					75.0	X										
61	11			Mohr-Coulomb	80.0	X	Moderately to occasionally highly weathered brown grading to greenish grey, very weak to weak, conglomeratic, slightly sandy, carbonate SILTSTONE/ CALCISILTITE with some bands of conglomerate and sandstone.	23.0	23.0	0	9400000	0.25	52	28	0	Drained
					85.0	X										
					90.0	X										
65	14			Mohr-Coulomb	95.0	X	Slightly to moderately weathered, brown with frequent whitish clasts, medium to coarse grained, weak to moderately weak, locally very weak, sandy CONGLOMERATE comprised of fine to coarse gravel of assorted rock types with in a matrix of silty sand and few bands of silty sandstone.	24.0	24.0	0	14300000	0.20	57	30	0	Drained
					100.0	X										

BOREHOLE LOG

BOREHOLE (ABd)

Client		Nakheel														
Project		Al Burj														
Location		Dubai Waterfront														
Ground Datum Level		2.65 m DMD														
Date Drilling Started		18/07/2008														
Date Drilling Completed		24/05/2008														
Equipment Type		Edeco Traveller T-30 Rotary Drilling Rig														
Drilling Fluid Used		Water/ Guargum														
R.Q.D. (%)	U.C.S. (kN/m ²)	S.P.T. (N)	Water Depth	Material model	Depth (m)	Legend	DESCRIPTION	Dry weight (dry)/kN/m ³	Wet weight (dry)/kN/m ³	Permeability in horizontal and vertical direction (m/day)	Young's modulus (E _{ref}) kN/m ²	Poisson's ratio (ν)	Cohesion (c _{ref}) kN/m ²	Friction angle (φ)	Dilatancy angle (ψ)	Type of material behaviour
		24		Mohr-Coulomb	5.0		Made Ground, consisting of light brown, silty, gravely, fine to medium sand with occasional fine to medium gravel and cemented pieces.	17.5	18.5	0.45	23520	0.35	1.0	34	4	Drained
38	3.5	>50		Mohr-Coulomb	6.0		Fresh to slightly weathered, thinly laminated, light brown, fine to medium grained, very weak to weak, calcareous SANDTONE .	21.0	21.0	0	4850000	0.30	48	24	0	Drained
					10.0											
					15.0											
					20.0											
					25.0											
					30.0											
58	10			Mohr-Coulomb	35.0		Moderately to occasionally highly weathered brown grading to greenish grey, very weak to weak, conglomeratic, slightly sandy, carbonate SILTSTONE/ CALCISILTITE with some bands of conglomerate and sandstone.	22.5	22.5	0	9320000	0.25	49	27	0	Drained
					40.0											
					45.0											
					50.0											

Continued

BOREHOLE LOG

BOREHOLE (TTd)

Client		Tatweer														
Project		Tatwee Tower														
Location		Emirates Road														
Ground Datum Level		24.36 m DMD														
Date Drilling Started		14/08/2008														
Date Drilling Completed		17/08/2008														
Equipment Type		Edeco Traveller T-30 Rotary Drilling Rig														
Drilling Fluid Used		Water/ Guargum														
R.Q.D. (%)	U.C.S. (kN/m ²)	S.P.T. (N)	Water Depth	Material Model	Depth (m)	Legend	DESCRIPTION	Dry weight (dry)/kN/m ³	Wet weight (dry)/kN/m ³	Permeability in horizontal and vertical direction (m/day)	Young's modulus (Eref) kN/m ²	Poisson's ratio (ν)	Cohesion (c _{ref}) kN/m ²	Friction angle (φ)	Dilatancy angle (ψ)	Type of material behaviour
		22		Mohr-Coulomb	5.0		Made Ground, medium sense to dense, pale brown, slightly silt, fine to coarse sand	16.0	17.0	0.6	23000	0.35	0.0	33	3	Drained
		25		Mohr-Coulomb	8.0		Light brown, silty, gravely, fine to medium sand with occasional fine to medium gravel and cemented pieces.	18.0	19.0	0.5	25000	0.35	1.0	35	5	Drained
40	4	>50		Mohr-Coulomb	15.0		Fresh to slightly weathered, thinly laminated, light brown, fine to medium grained, very weak to weak, calcareous SANDTONE .	22.0	22.0	0	5000000	0.30	50	25	0	Drained
62	11			Mohr-Coulomb	20.0		Moderately to occasionally highly weathered brown grading to greenish grey, very weak to weak, conglomeratic, slightly sandy, carbonate SILTSTONE/ CALCISILTITE with some bands of conglomerate and sandstone.	23.0	23.0	0	9500000	0.25	54	28	0	Drained
92	21			Mohr-Coulomb	30.0		Weak, reddish brown with molted buffwhite CONGLOMERATE, fine to medium garvels with sandy Silty matrix	24.0	24.0	0	15700000	0.17	59	30	0	Drained
					35.0											
					40.0											
					45.0											
					50.0											

Continued

BOREHOLE LOG

BOREHOLE (TTd)

Client		Tatweer														
Project		Tatwee Tower														
Location		Emirates Road														
Ground Datum Level		24.36 m DMD														
Date Drilling Started		14/08/2008														
Date Drilling Completed		17/08/2008														
Equipment Type		Edeco Traveller T-30 Rotary Drilling Rig														
Drilling Fluid Used		Water/ Guargum														
R.O.D. (%)	U.C.S. (kN/m ²)	S.P.T. (N)	Water Depth	Material model	Depth (m)	Legend	DESCRIPTION	Dry weight (γ _{dry})/kN/m ³	Wet weight (γ _w)/kN/m ³	Permeability in horizontal and vertical direction (m/day)	Young's modulus (E _{eq}) kN/m ²	Poisson's ratio (ν)	Cohesion (c _{ref})	Friction angle (φ)	Dilatancy angle (ψ)	Type of material behaviour
62	11			Mohr-Coulomb	55.0		Moderately to occasionally highly weathered brown grading to greenish grey, very weak to weak, conglomeratic, slightly sandy, carbonate SILTSTONE/ CALCISILTITE with some bands of conglomerate and sandstone.	23.0	23.0	0	9500000	0.25	54	28	0	Drained
92	21			Mohr-Coulomb	60.0		Weak, reddish brown with molted buffwhite CONGLOMERATE, fine to medium garvels with sandy Silty matrix	24.0	24.0	0	15700000	0.17	59	30	0	Drained
					65.0											
					70.0											
					75.0											
62	11			Mohr-Coulomb	80.0		Moderately to occasionally highly weathered brown grading to greenish grey, very weak to weak, conglomeratic, slightly sandy, carbonate SILTSTONE/ CALCISILTITE with some bands of conglomerate and sandstone.	23.0	23.0	0	9500000	0.25	54	28	0	Drained
					85.0											
					90.0											
					95.0											
					100.0											

BOREHOLE LOG

BOREHOLE (ABe)

Client		Nakheel														
Project		Al Burj														
Location		Dubai Waterfront														
Ground Datum Level		2.65 m DMD														
Date Drilling Started		18/07/2008														
Date Drilling Completed		24/05/2008														
Equipment Type		Edeco Traveller T-30 Rotary Drilling Rig														
Drilling Fluid Used		Water/ Guargum														
R.Q.D. (%)	U.C.S. (kN/m ²)	S.P.T. (N)	Water Depth	Material model	Depth (m)	Legend	DESCRIPTION	Dry weight (dry)/kN/m ³	Wet weight (dry)/kN/m ³	Permeability in horizontal and vertical direction (m/day)	Young's modulus (E _{ref}) kN/m ²	Poisson's ratio (ν)	Cohesion (c _{ref}) kN/m ²	Friction angle (φ)	Dilatancy angle (ψ)	Type of material behaviour
		24		Mohr-Coulomb	5.0		Made Ground, consisting of light brown, silty, gravely, fine to medium sand with occasional fine to medium gravel and cemented pieces.	17.5	18.5	0.45	23520	0.35	1.0	34	4	Drained
		25		Mohr-Coulomb	6.0		Light brown, silty, gravely, fine to medium sand with occasional fine to medium gravel and cemented pieces.	18.0	19.0	0.5	25000	0.35	1.0	35	5	Drained
38	3.5	>50		Mohr-Coulomb	15.0		Fresh to slightly weathered, thinly laminated, light brown, fine to medium grained, very weak to weak, calcareous SANDTONE .	21.0	21.0	0	4850000	0.30	48	24	0	Drained
58	10			Mohr-Coulomb	35.0		Moderately to occasionally highly weathered brown grading to greenish grey, very weak to weak, conglomeratic, slightly sandy, carbonate SILTSTONE/ CALCISILTITE with some bands of conglomerate and sandstone.	22.5	22.5	0	9320000	0.25	49	27	0	Drained

Continued

BOREHOLE LOG

BOREHOLE (ABe)

Client		Nakheel														
Project		Al Burj														
Location		Dubai Waterfront														
Ground Datum Level		2.65 m DMD														
Date Drilling Started		18/07/2008														
Date Drilling Completed		24/05/2008														
Equipment Type		Edeco Traveller T-30 Rotary Drilling Rig														
Drilling Fluid Used		Water/ Guargum														
R.O.D. (%)	U.C.S. (kN/m ²)	S.P.T. (N)	Water Depth	Material model	Depth (m)	Legend	DESCRIPTION	Dry weight (γ _{dry})/kN/m ³	Wet weight (γ _w)/kN/m ³	Permeability in horizontal and vertical direction (m/day)	Young's modulus (E _{eq}) kN/m ²	Poisson's ratio (ν)	Cohesion (c _{ref})	Friction angle (φ)	Dilatancy angle (ψ)	Type of material behaviour
58	10			Mohr-Coulomb	55.0	X	Moderately to occasionally highly weathered brown grading to greenish grey, very weak to weak, conglomeratic, slightly sandy, carbonate SILTSTONE/ CALCISILTITE with some bands of conglomerate and sandstone.	22.5	22.5	0	9320000	0.25	49	27	0	Drained
62	12			Mohr-Coulomb	60.0	X	Slightly to moderately weathered, brown with frequent whitish clasts, medium to coarse grained, weak to moderately weak, locally very weak, sandy CONGLOMERATE comprised of fine to coarse gravel of assorted rock types with in a matrix of silty sand and few bands of silty sandstone.	23.5	23.5	0	1400000	0.20	55	30	0	Drained
				Mohr-Coulomb	65.0	X										
				Mohr-Coulomb	70.0	X										
61	11			Mohr-Coulomb	75.0	X	Moderately to occasionally highly weathered brown grading to greenish grey, very weak to weak, conglomeratic, slightly sandy, carbonate SILTSTONE/ CALCISILTITE with some bands of conglomerate and sandstone.	23.0	23.0	0	9400000	0.25	52	28	0	Drained
				Mohr-Coulomb	80.0	X										
				Mohr-Coulomb	85.0	X										
65	14			Mohr-Coulomb	90.0	X	Slightly to moderately weathered, brown with frequent whitish clasts, medium to coarse grained, weak to moderately weak, locally very weak, sandy CONGLOMERATE comprised of fine to coarse gravel of assorted rock types with in a matrix of silty sand and few bands of silty sandstone.	24.0	24.0	0	14300000	0.20	57	30	0	Drained
				Mohr-Coulomb	95.0	X										
				Mohr-Coulomb	100.0	X										

BOREHOLE LOG

BOREHOLE (ACe)

Client		Nakheel														
Project		Arabian Canal														
Location		Arabian Canal														
Ground Datum Level		55.18 m DMD														
Date Drilling Started		14/05/2008														
Date Drilling Completed		17/05/2008														
Equipment Type		Edeco Traveller T-30 Rotary Drilling Rig														
Drilling Fluid Used		Water/ Guargum														
R.Q.D. (%)	U.C.S. (kN/m ²)	S.P.T. (N)	Water Depth	Material Model	Depth (m)	Legend	DESCRIPTION	Dry weight (dry)kN/m ³	Wet weight (dry)kN/m ³	Permeability in horizontal and vertical direction (m/day)	Young's modulus (E) kN/m ²	Poisson's ratio (ν)	Cohesion (c) kN/m ²	Friction angle (φ)	Dilatancy angle (ψ)	Type of material behaviour
		22		Mohr-Coulomb	3.0		Made Ground, medium sense to dense, pale brown, slightly silt, fine to coarse sand	16.0	17.0	0.6	23000	0.35	0.0	33	3	Drained
		25		Mohr-Coulomb	5.0		Light brown, silty, gravely, fine to medium sand with occasional fine to medium gravel and cemented pieces.	18.0	19.0	0.5	25000	0.35	1.0	35	5	Drained
					10.0											
		>50		Mohr-Coulomb	15.0		Fresh to slightly weathered, thinly laminated, light brown, fine to medium grained, very weak to weak, calcareous SANDTONE .	22.0	22.0	0	5000000	0.30	50	25	0	Drained
40	4				20.0											
		21		Mohr-Coulomb	25.0		Weak, reddish brown with molted buffwhite CONGLOMERATE, fine to medium garvels with sandy Silty matrix	24.0	24.0	0	15700000	0.17	59	30	0	Drained
		11		Mohr-Coulomb	30.0		Moderately to occasionally highly weathered brown grading to greenish grey, very weak to weak, conglomeratic, slightly sandy, carbonate SILTSTONE/ CALCISILTITE with some bands of conglomerate and sandstone.	23.0	23.0	0	9500000	0.25	54	28	0	Drained
62					35.0											
		21		Mohr-Coulomb	40.0		Weak, reddish brown with molted buffwhite CONGLOMERATE, fine to medium garvels with sandy Silty matrix	24.0	24.0	0	15700000	0.17	59	30	0	Drained
					45.0											
					50.0											

Continued

BOREHOLE LOG

BOREHOLE (ACe)

Client		Nakheel														
Project		Arabian Canal														
Location		Arabian Canal														
Ground Datum Level		55.18 m DMD														
Date Drilling Started		14/05/2008														
Date Drilling Completed		17/05/2008														
Equipment Type		Edeco Traveller T-30 Rotary Drilling Rig														
Drilling Fluid Used		Water/ Guargum														
R.O.D. (%)	U.C.S. (kN/m ²)	S.P.T. (N)	Water Depth	Material model	Depth (m)	Legend	DESCRIPTION	Dry weight (γ _{dry})/kN/m ³	Wet weight (γ _w)/kN/m ³	Permeability in horizontal and vertical direction (m/day)	Young's modulus (E _{ref}) kN/m ²	Poisson's ratio (ν)	Cohesion (c _{ref})	Friction angle (φ)	Dilatancy angle (ψ)	Type of material behaviour
62	11			Mohr-Coulomb	55.0		Moderately to occasionally highly weathered brown grading to greenish grey, very weak to weak, conglomeratic, slightly sandy, carbonate SILTSTONE/ CALCISILTITE with some bands of conglomerate and sandstone.	23.0	23.0	0	9500000	0.25	54	28	0	Drained
92	21			Mohr-Coulomb	60.0		Weak, reddish brown with molted buffwhite CONGLOMERATE, fine to medium garvels with sandy Silty matrix	24.0	24.0	0	15700000	0.17	59	30	0	Drained
					65.0											
62	11			Mohr-Coulomb	70.0											
					75.0		Moderately to occasionally highly weathered brown grading to greenish grey, very weak to weak, conglomeratic, slightly sandy, carbonate SILTSTONE/ CALCISILTITE with some bands of conglomerate and sandstone.	23.0	23.0	0	9500000	0.25	54	28	0	Drained
					80.0											
					85.0											
					90.0											
					95.0											
					100.0											

BOREHOLE LOG

BOREHOLE (Creek)

Client		Creek														
Project		Creek														
Location		Creek														
Ground Datum Level		2.36 m DMD														
Date Drilling Started		14/05/2005														
Date Drilling Completed		17/05/2005														
Equipment Type		Edeco Traveller T-30 Rotary Drilling Rig														
Drilling Fluid Used		Water/ Guargum														
R.Q.D. (%)	U.C.S. (kN/m ²)	S.P.T. (N)	Water Depth	Material model	Depth (m)	Legend	DESCRIPTION	Dry weight (ρ _{dry})kN/m ³	Wet weight (ρ _{wet})kN/m ³	Permeability in horizontal and vertical direction (m/day)	Young's modulus (E _{ref}) kN/m ²	Poisson's ratio (ν)	Cohesion (c _{ref}) kN/m ²	Friction angle (φ)	Dilatancy angle (ψ)	Type of material behaviour
		22		Mohr-Coulomb	5.0 6.0		Made Ground, medium sense to dense, pale brown, slightly silt, fine to coarse sand	16.0	17.0	0.6	23000	0.35	0.0	33	3	Drained
		25		Mohr-Coulomb	10.0 15.0 20.0	X X X X X	Light brown, silty, gravely, fine to medium sand with occasional fine to medium gravel and cemented pieces.	18.0	19.0	0.5	25000	0.35	1.0	35	5	Drained
40	4	>50		Mohr-Coulomb	25.0		Fresh to slightly weathered, thinly laminated, light brown, fine to medium grained, very weak to weak, calcareous SANDTONE .	22.0	22.0	0	5000000	0.30	50	25	0	Drained
40	4	>50		Mohr-Coulomb	30.0		Fresh to slightly weathered, thinly laminated, light brown, fine to medium grained, very weak to weak, calcareous SANDTONE .	22.0	22.0	0	5000000	0.30	50	25	0	Drained
62	11			Mohr-Coulomb	35.0 40.0 45.0 50.0		Moderately to occasionally highly weathered brown grading to greenish grey, very weak to weak, conglomeratic, slightly sandy, carbonate SILTSTONE/ CALCISILTITE with some bands of conglomerate and sandstone.	23.0	23.0	0	9500000	0.25	54	28	0	Drained

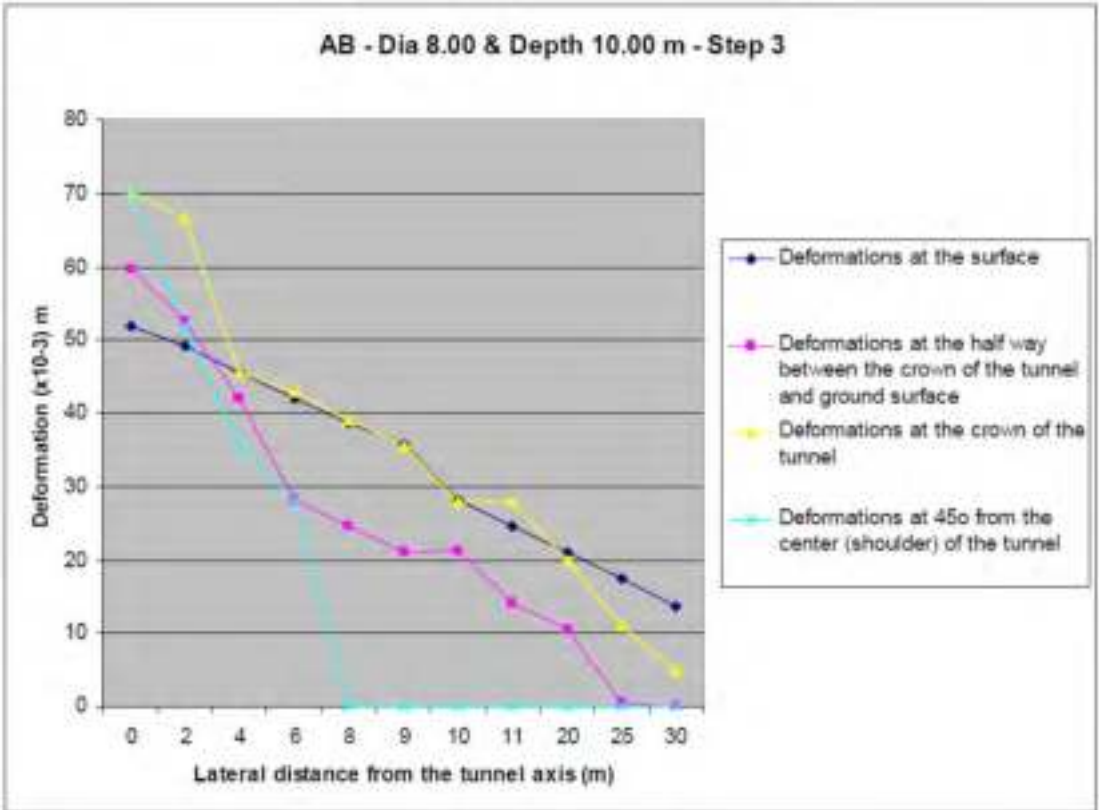
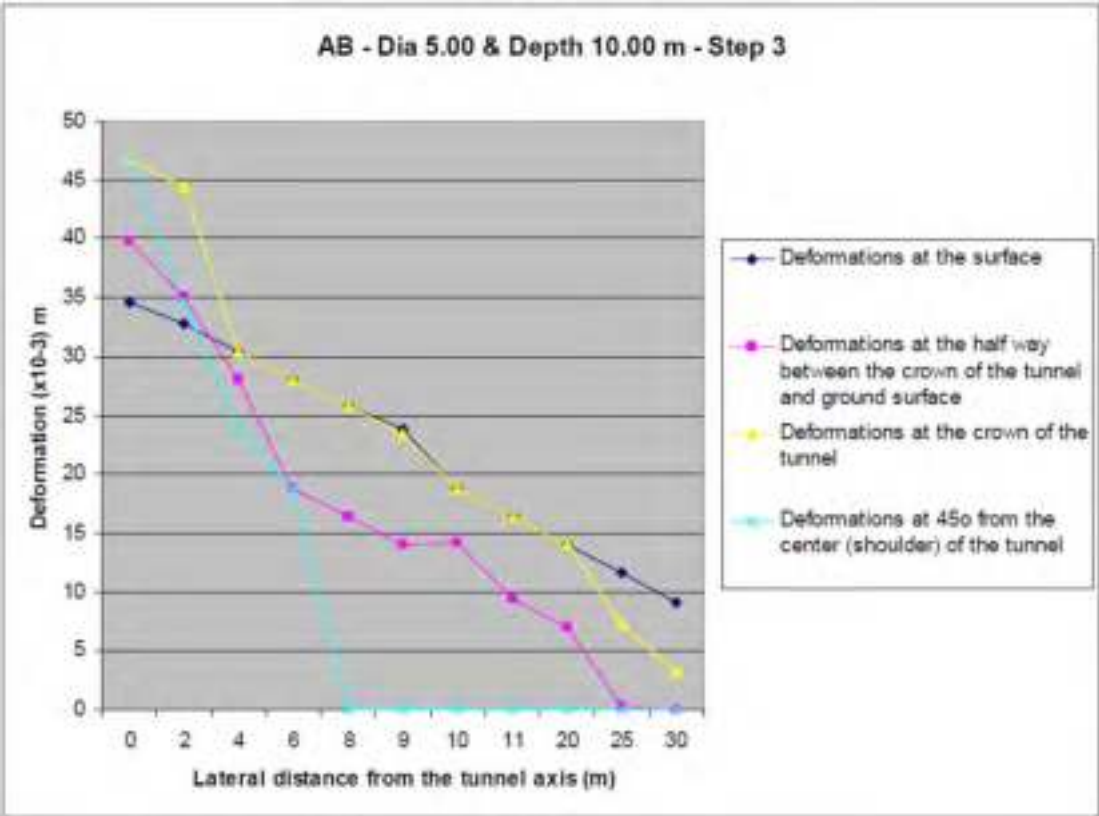
Continued

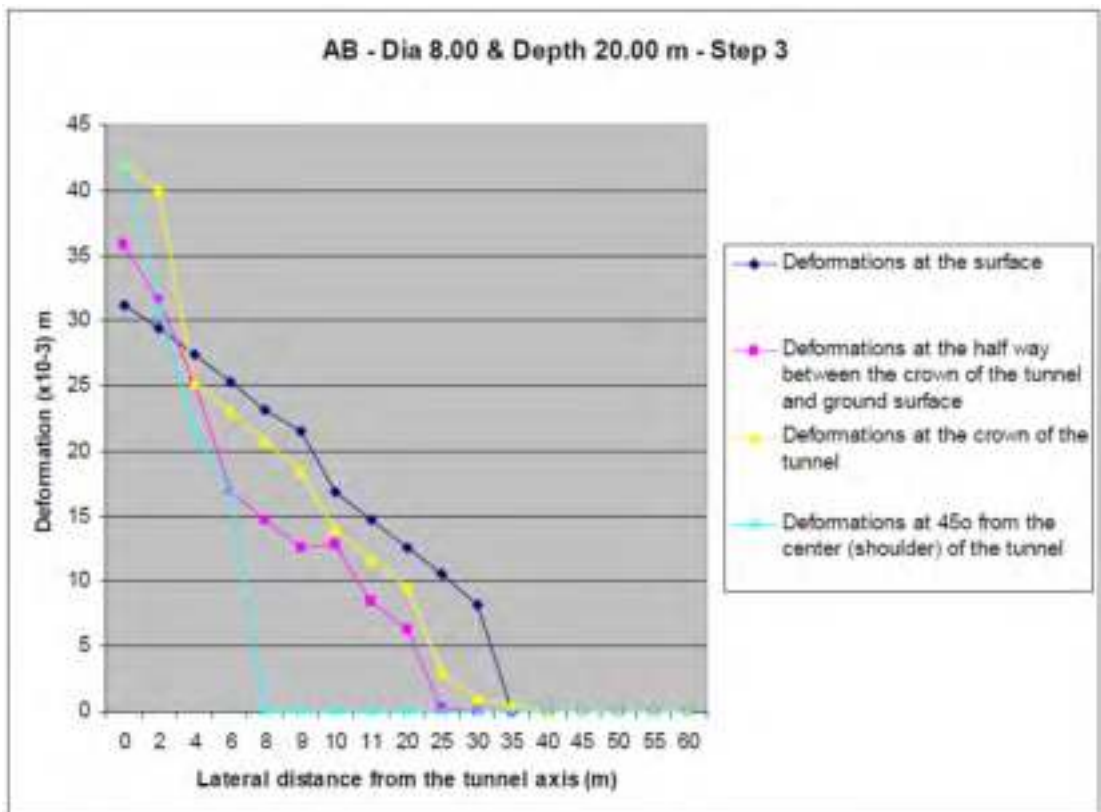
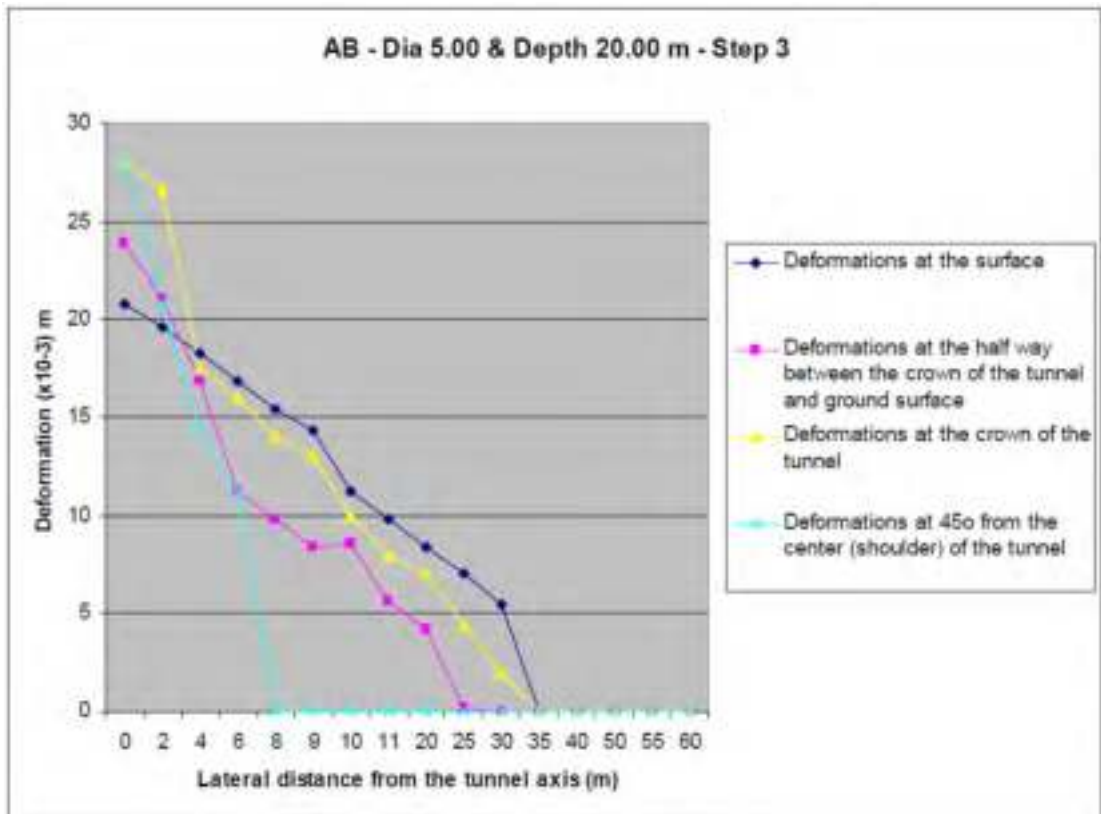
BOREHOLE LOG

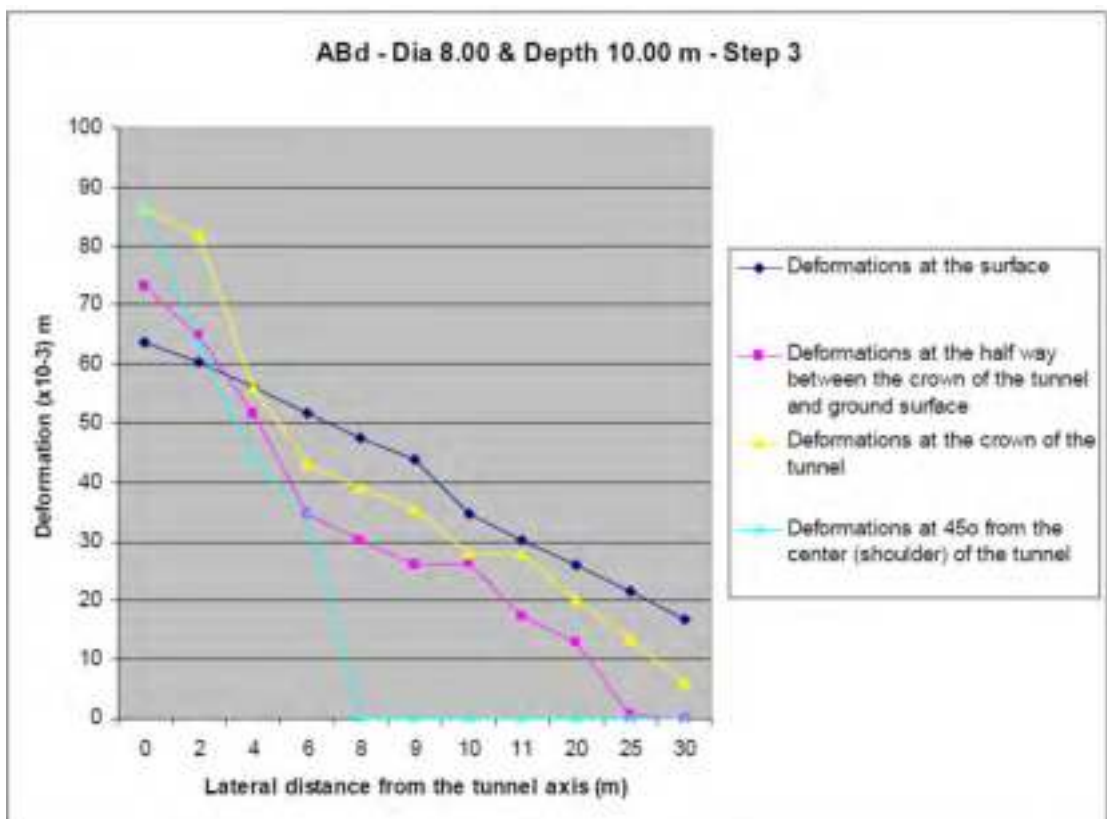
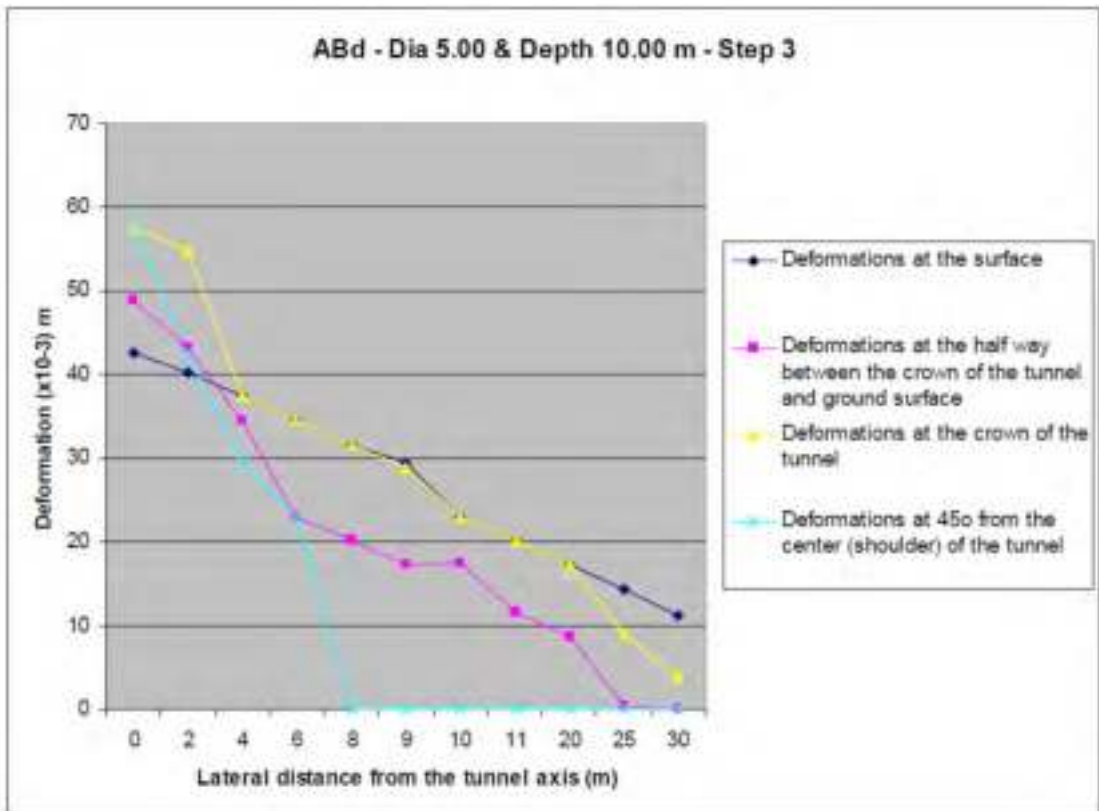
BOREHOLE (Creek)

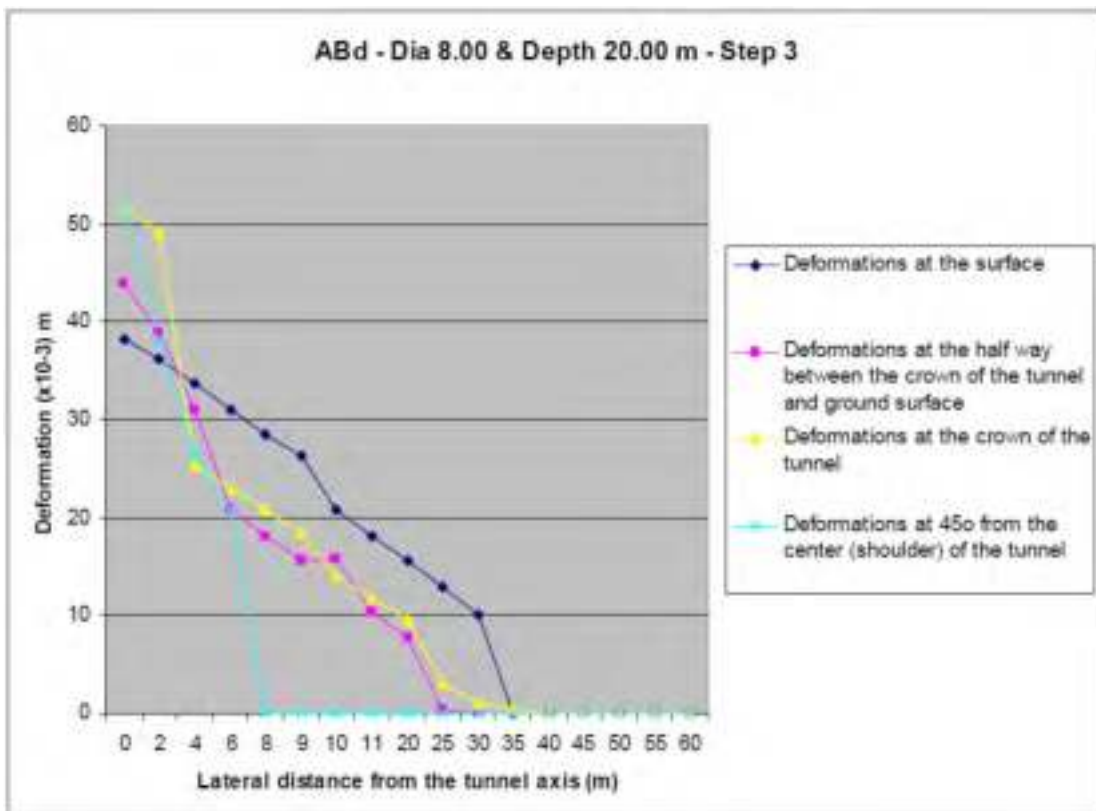
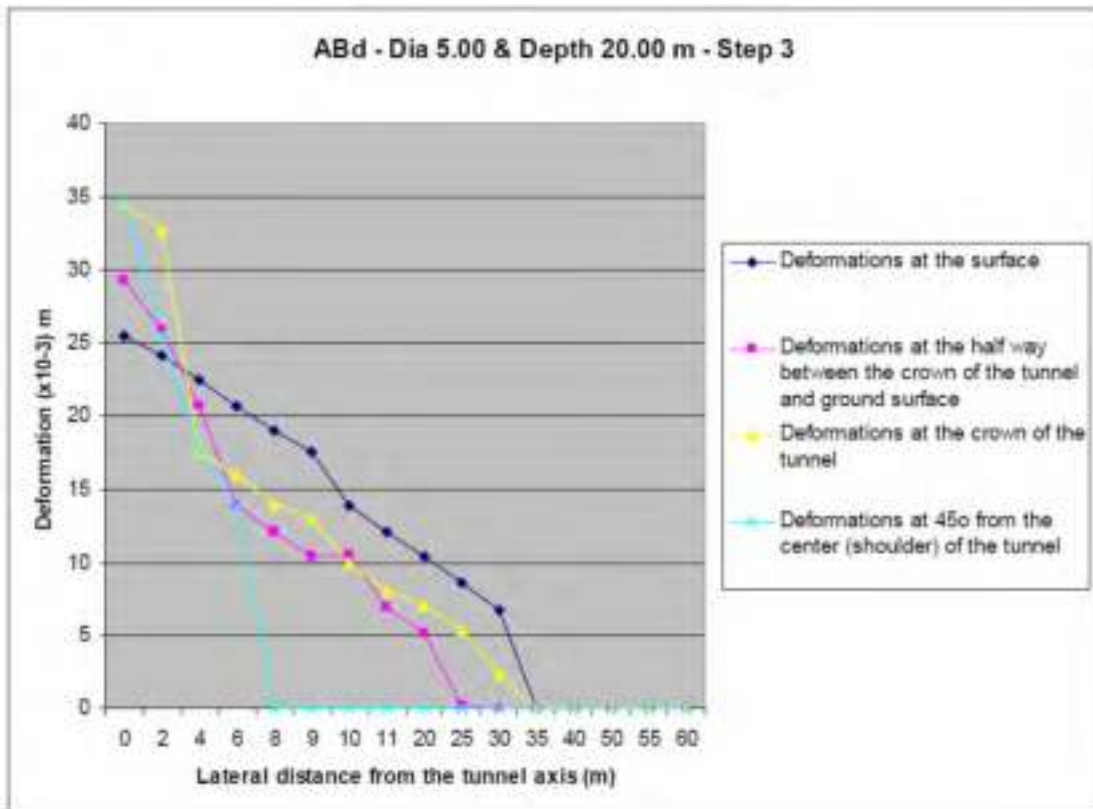
Client		Creek															
Project		Creek															
Location		Creek															
Ground Datum Level		2.36 m DMD															
Date Drilling Started		14/05/2005															
Date Drilling Completed		17/05/2005															
Equipment Type		Edeco Traveller T-30 Rotary Drilling Rig															
Drilling Fluid Used		Water/ Guargum															
R.O.D. (%)	U.C.S. (kN/m ²)	S.P.T. (N)	Water Depth	Material model	Depth (m)	Legend	DESCRIPTION	Dry weight (γ _{dry})/kN/m ³	Wet weight (γ _{wet})/kN/m ³	Permeability in horizontal and vertical direction (m/day)	Young's modulus (E _{ref})/kN/m ²	Poisson's ratio (ν)	Cohesion (c _{ref})	Friction angle (φ)	Dilatancy angle (ψ)	Type of material behaviour	
62	11			Mohr-Coulomb	55.0	X	Moderately to occasionally highly weathered brown grading to greenish grey, very weak to weak, conglomeratic, slightly sandy, carbonate SILTSTONE/ CALCISILTITE with some bands of conglomerate and sandstone.	23.0	23.0	0	9500000	0.25	54	28	0	Drained	
					60.0	X											
					65.0	X											
					70.0	X											
					75.0	X											
					80.0	X	E.O.B										
					85.0	X											
					90.0	X											
					95.0	X											
					100.0	X											

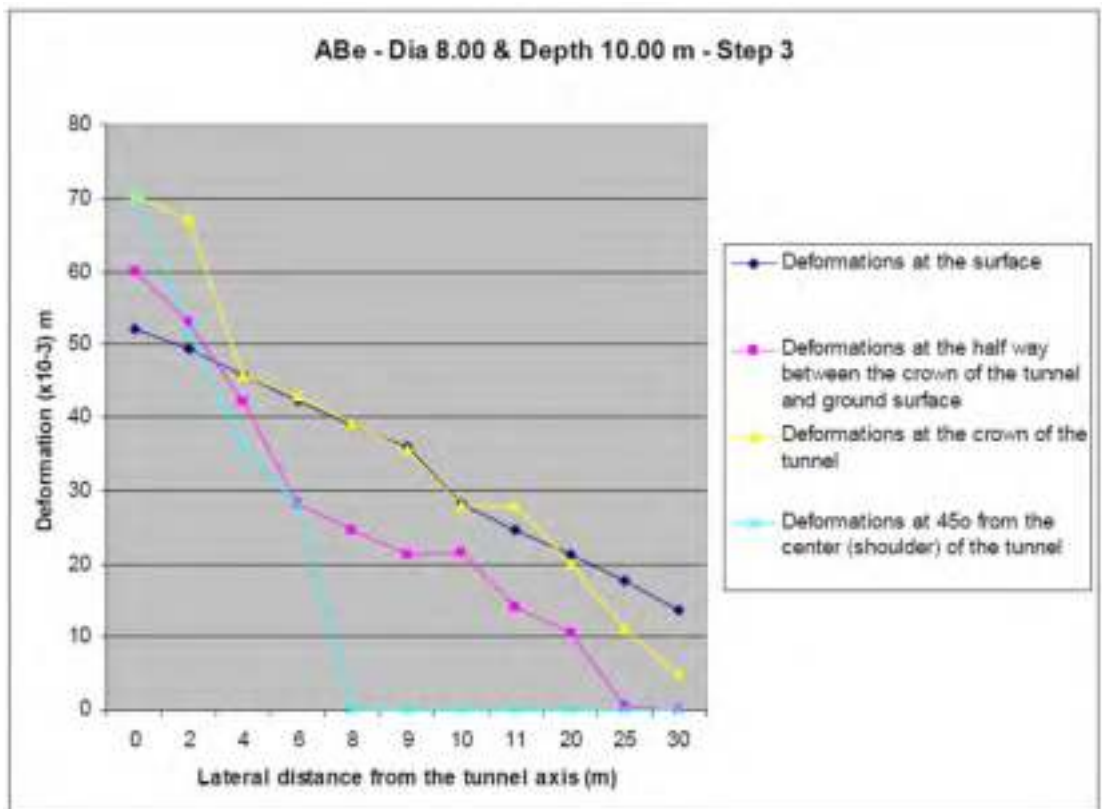
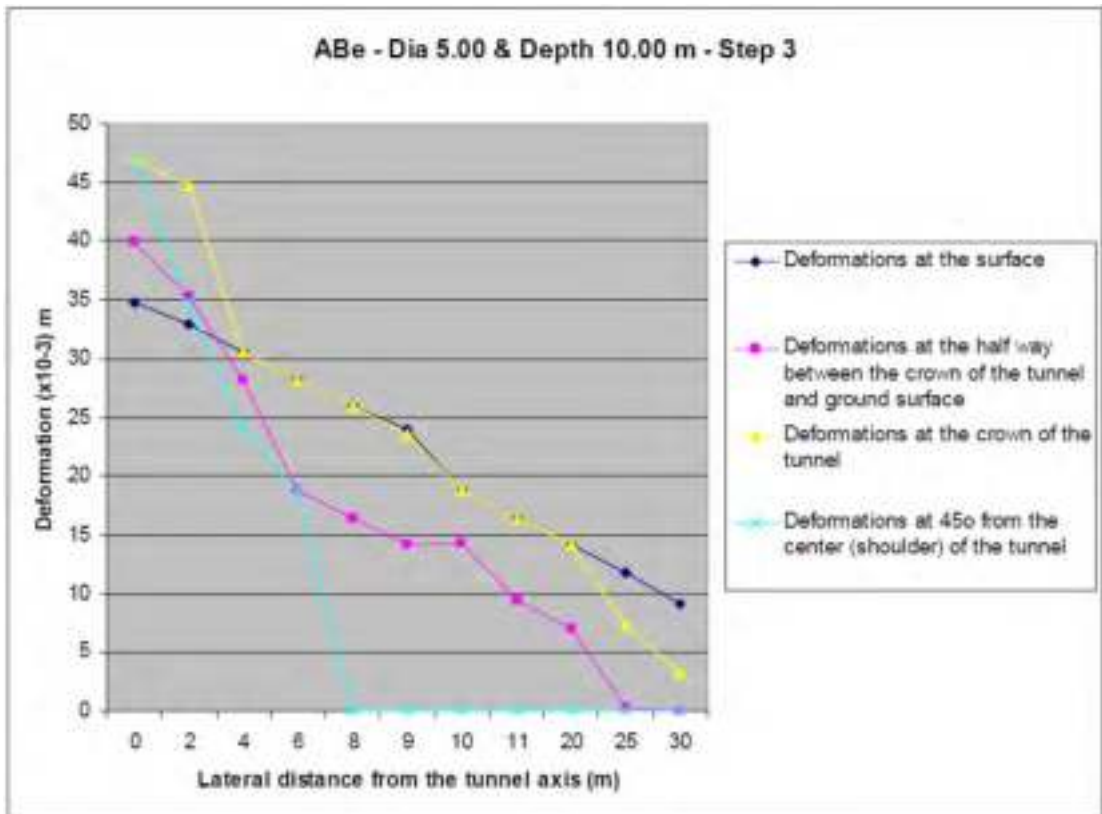
Appendix B
Deformation plots for all combinations

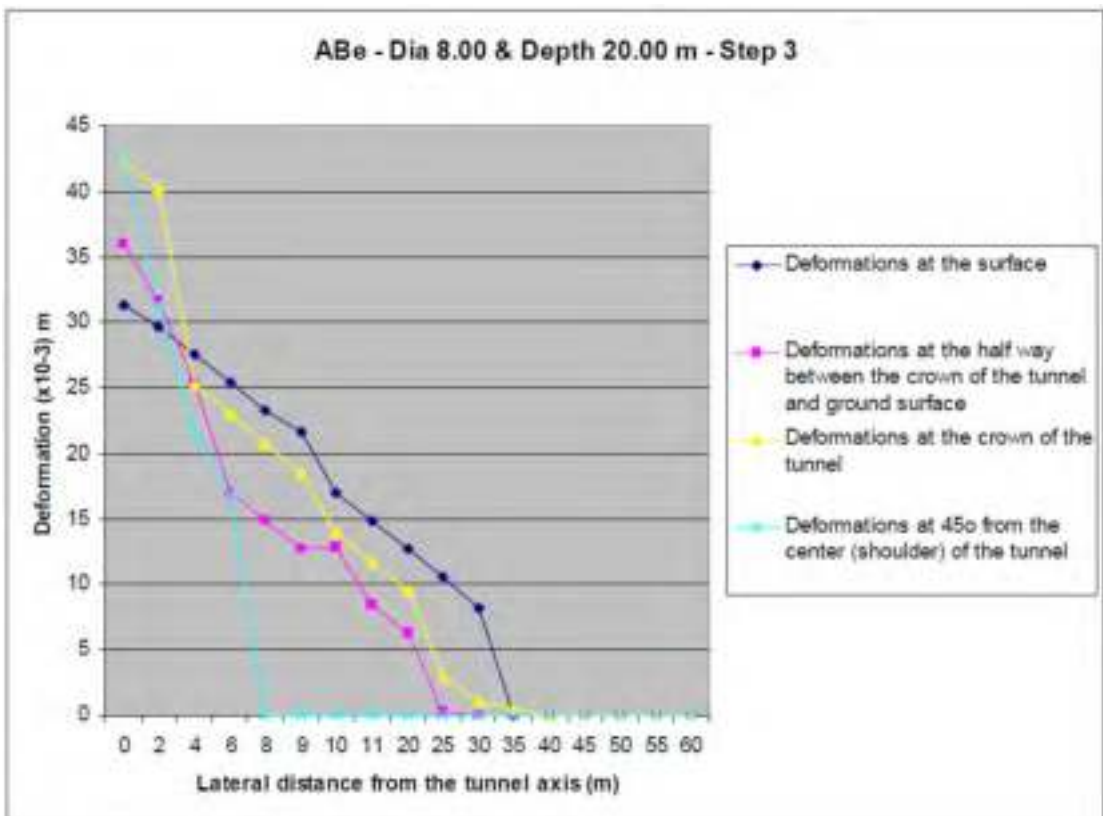
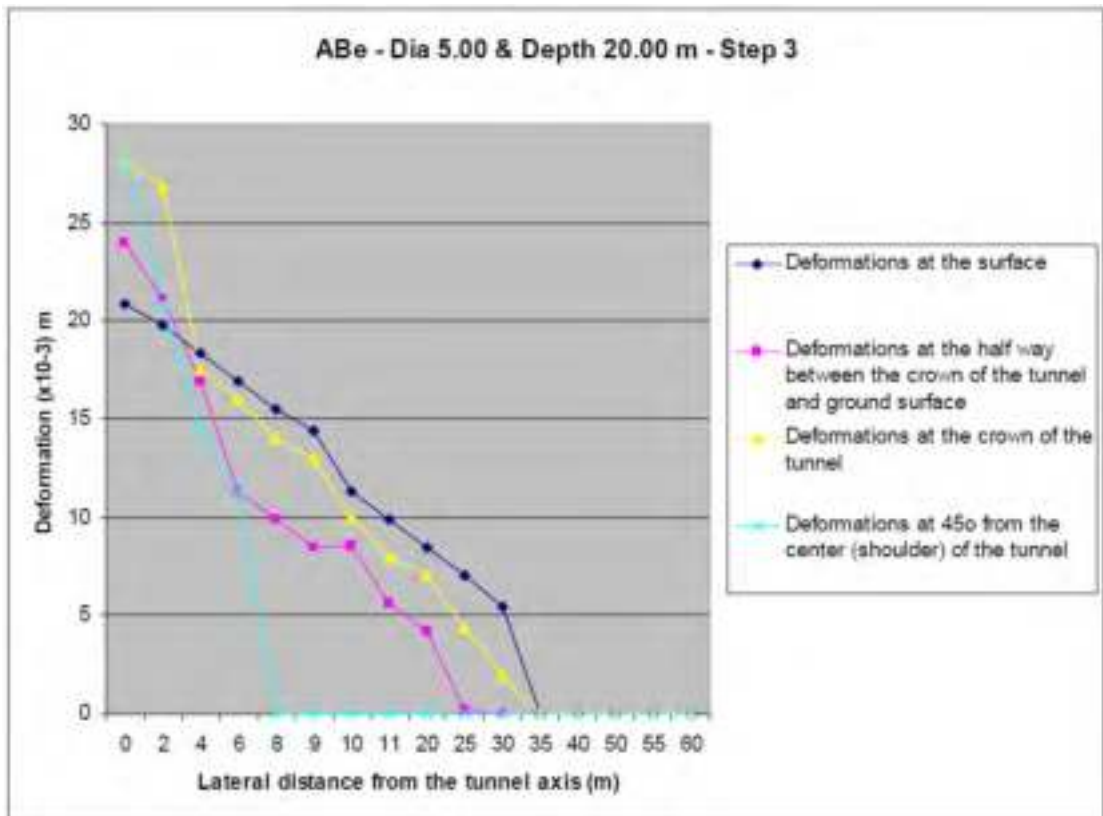


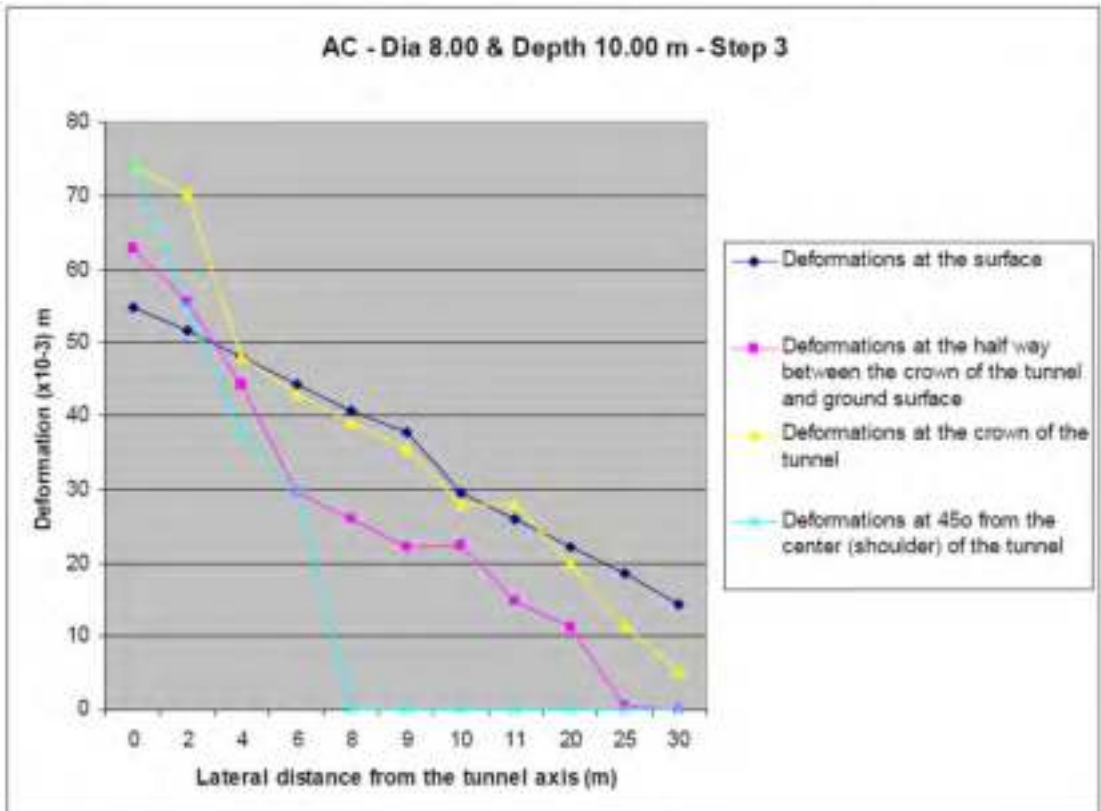
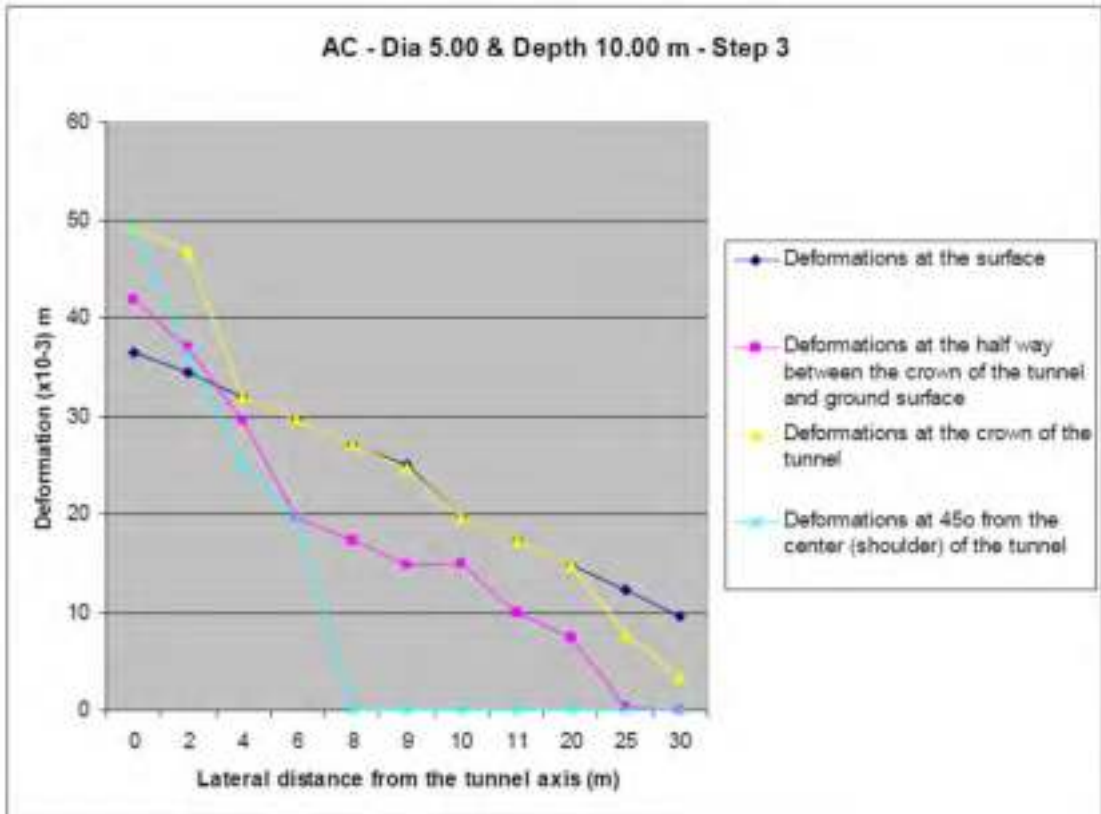


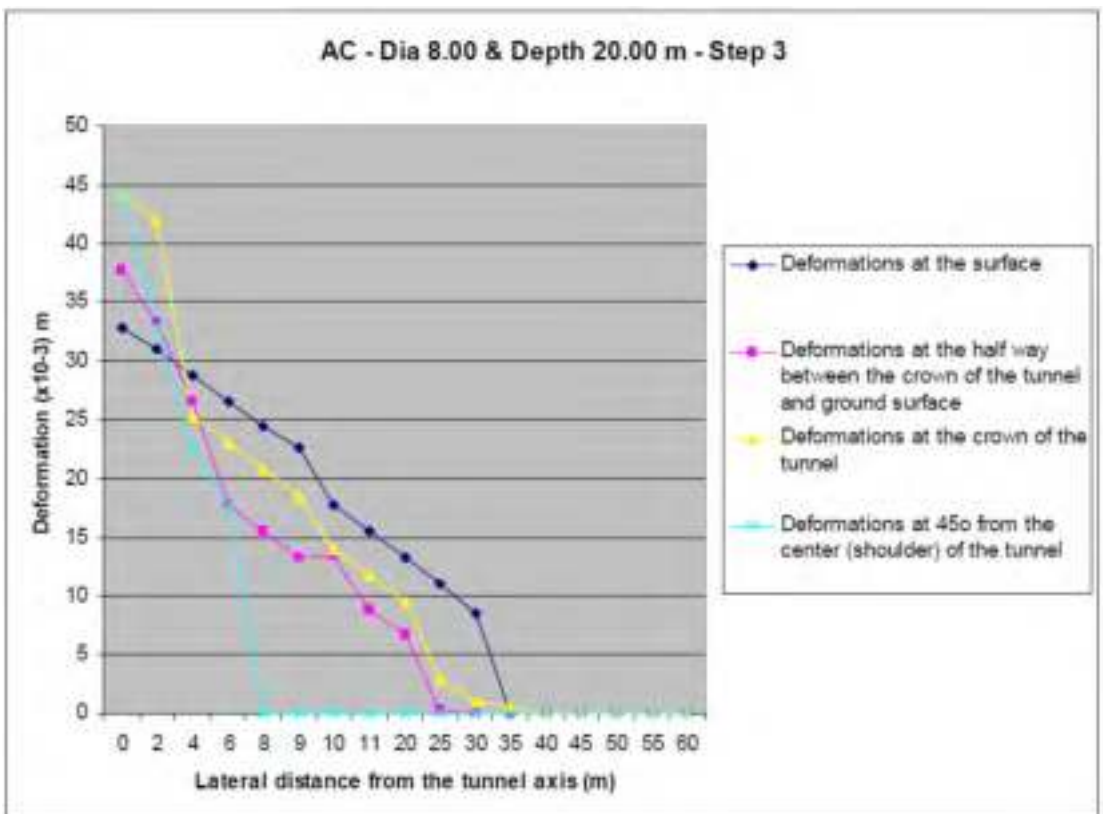
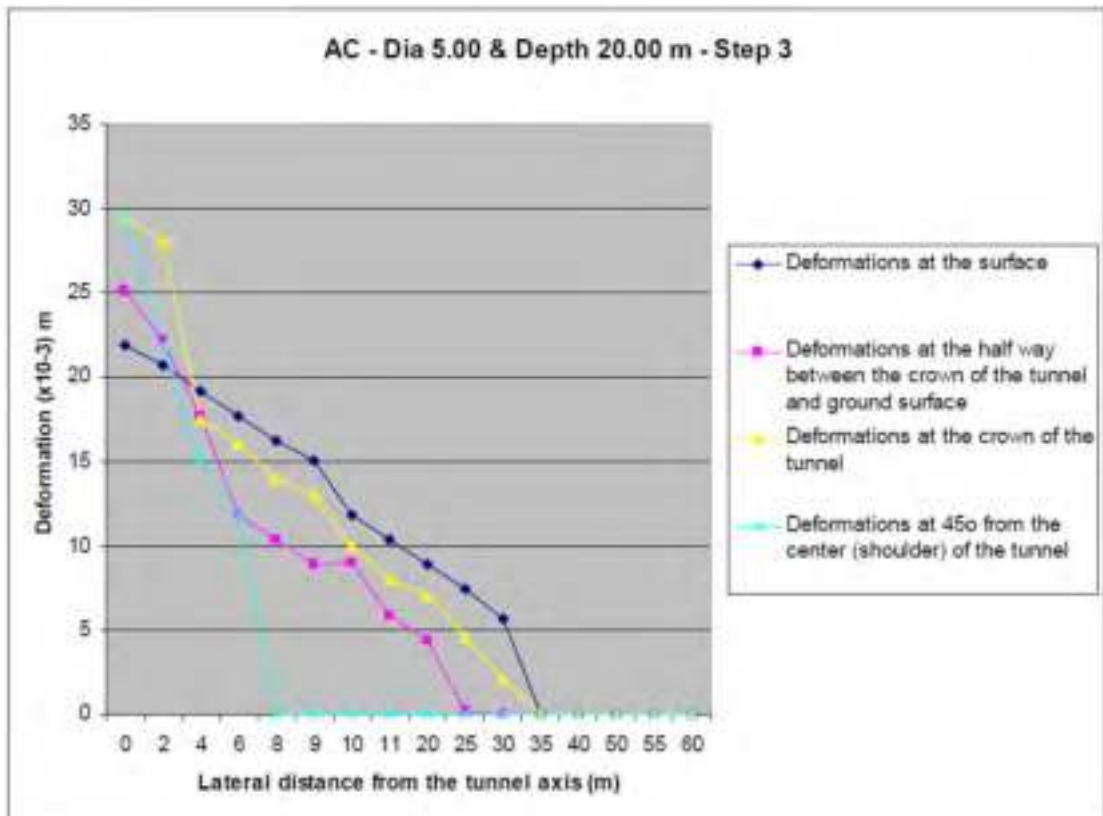


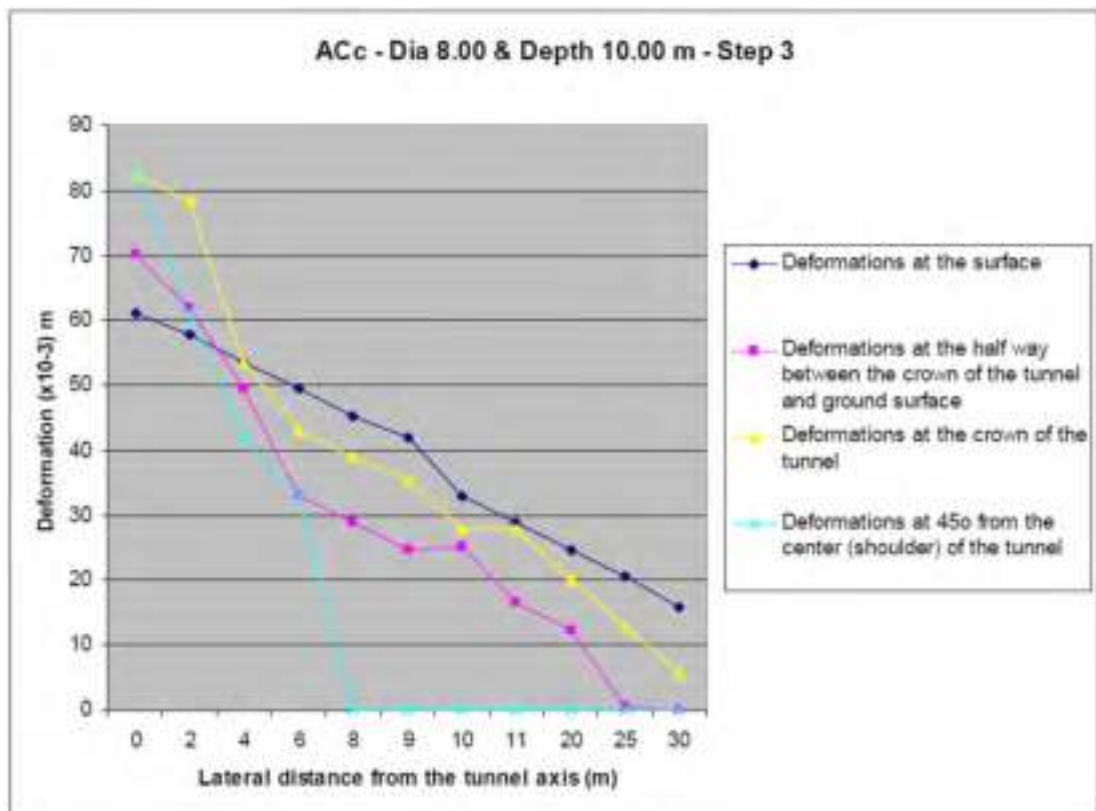
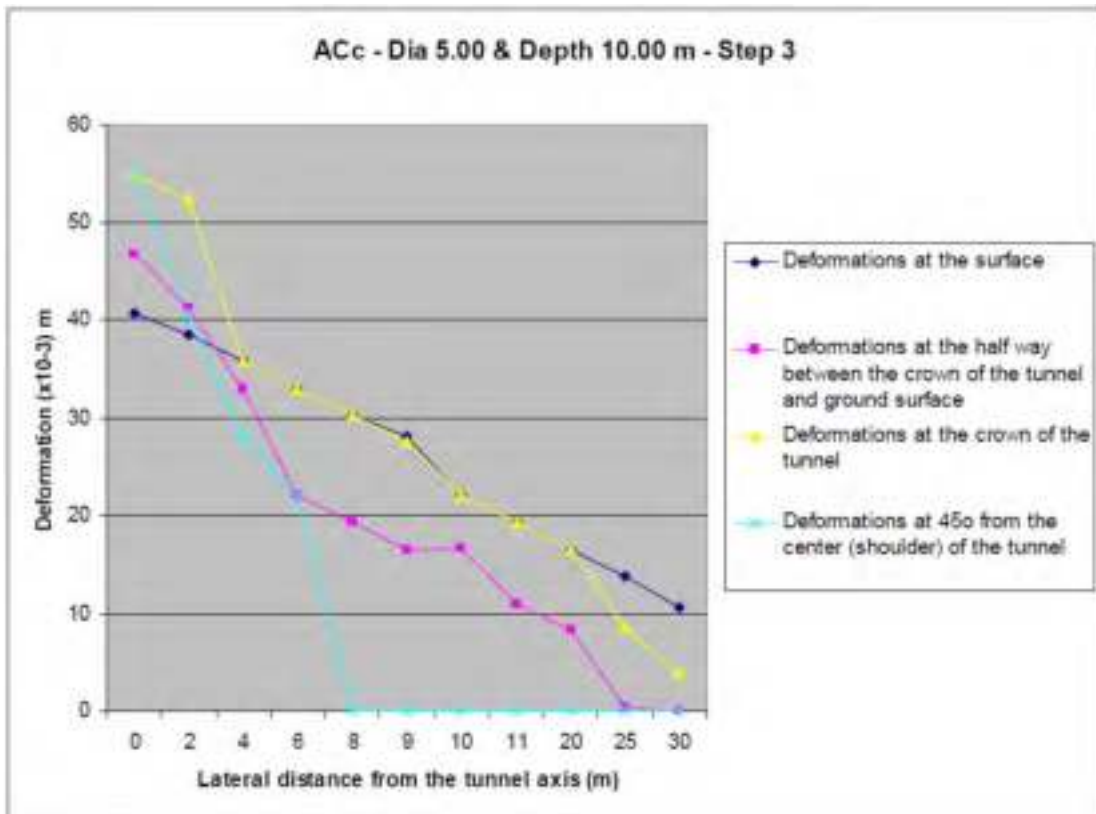


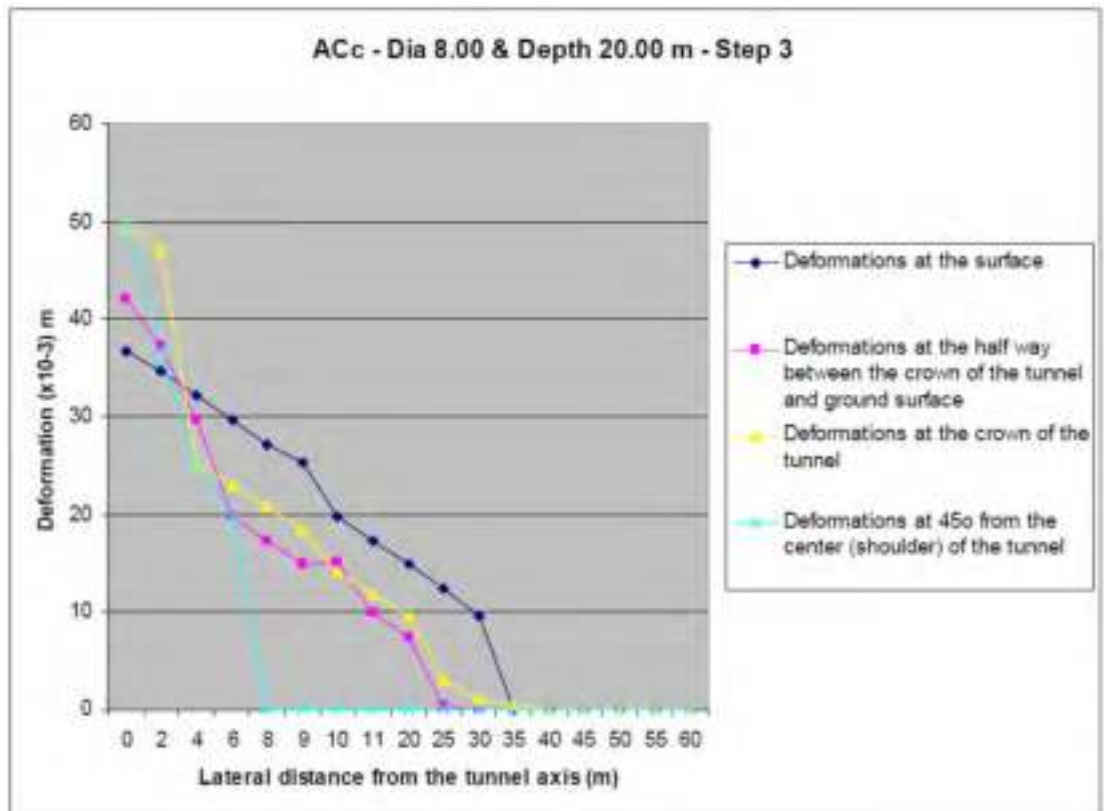
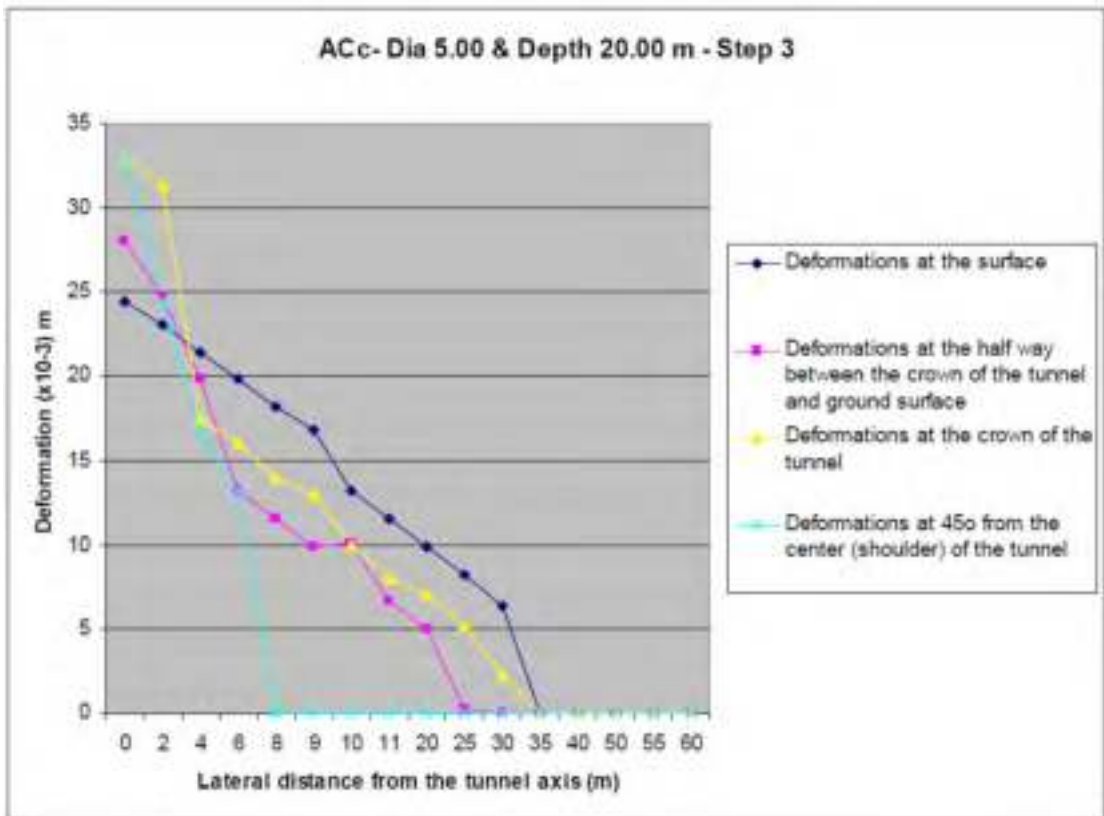


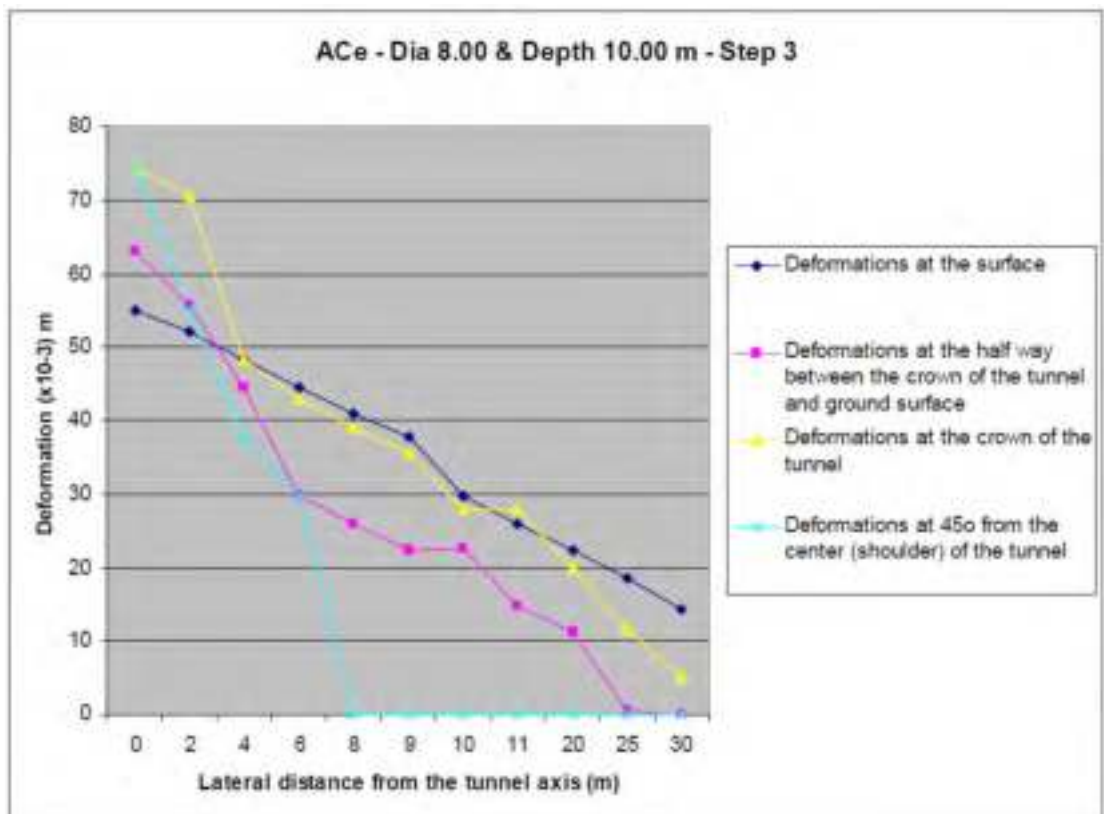
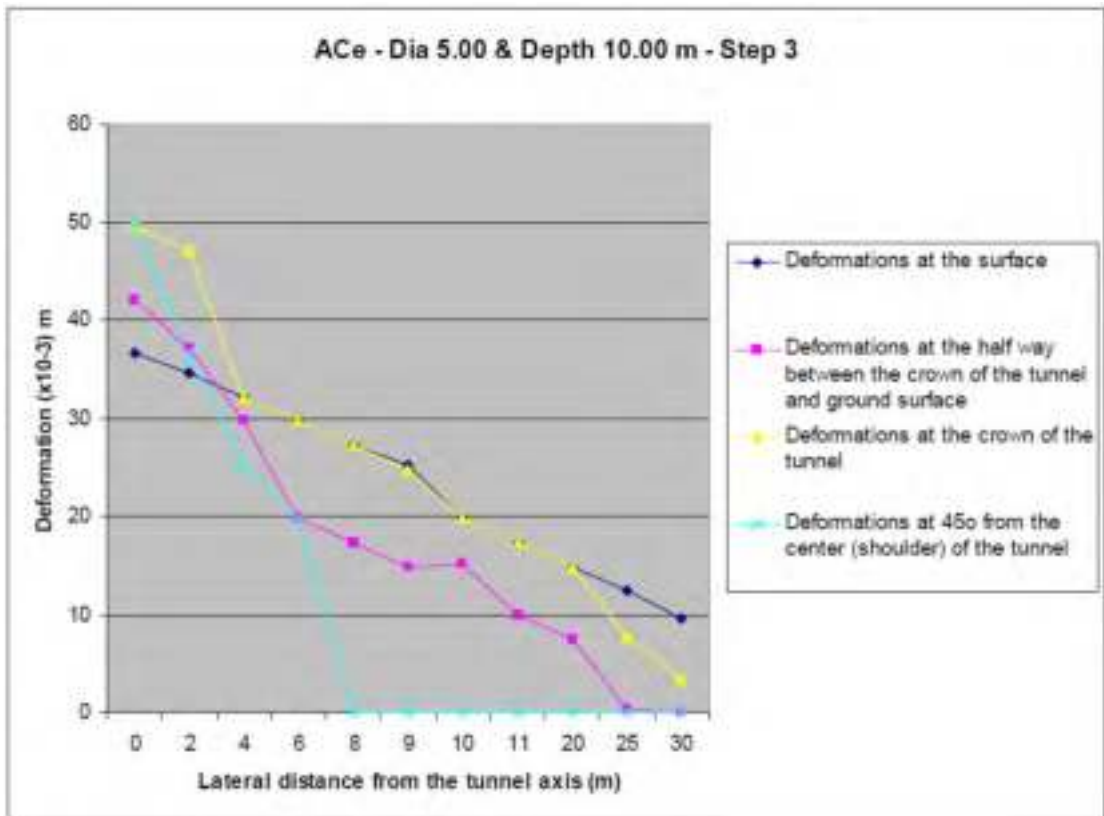


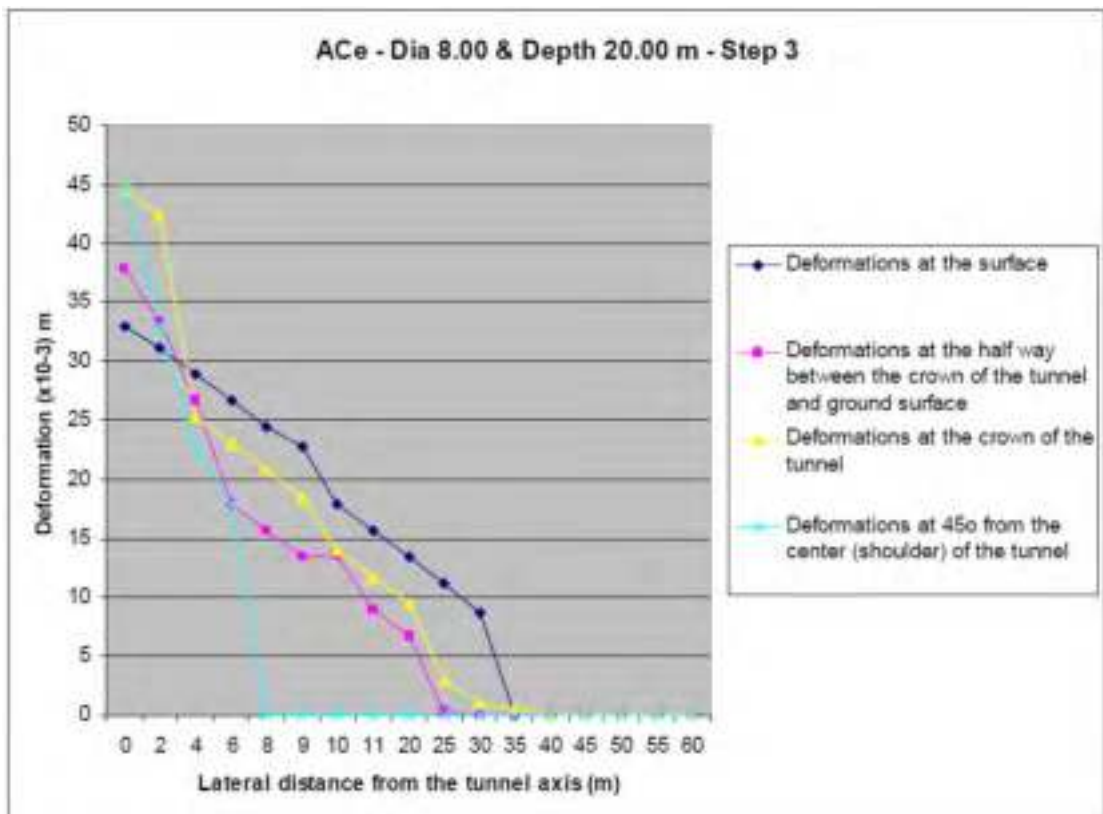
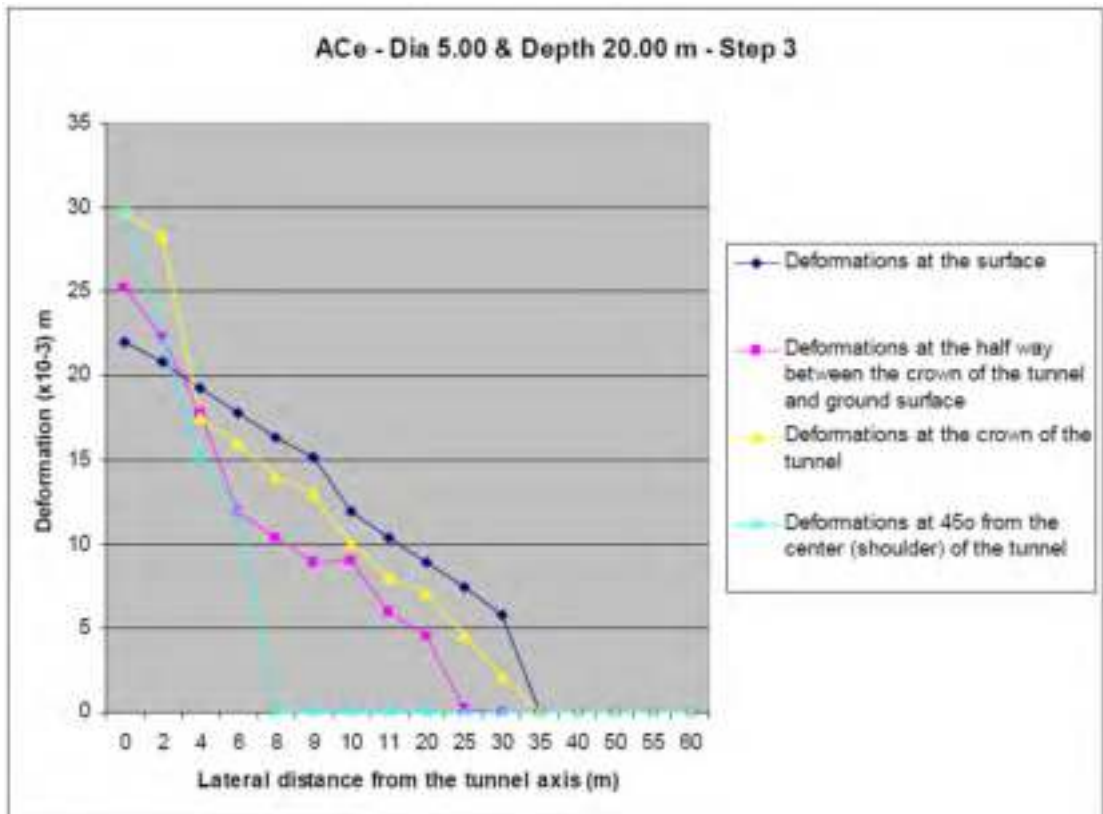


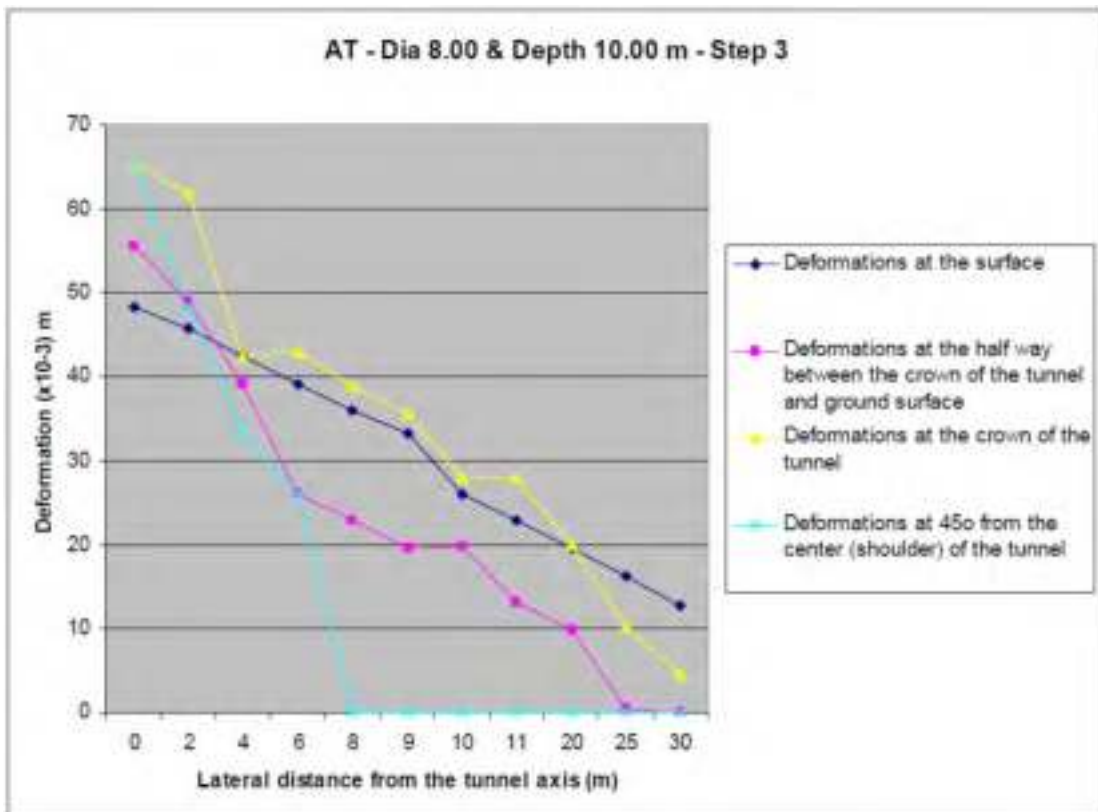
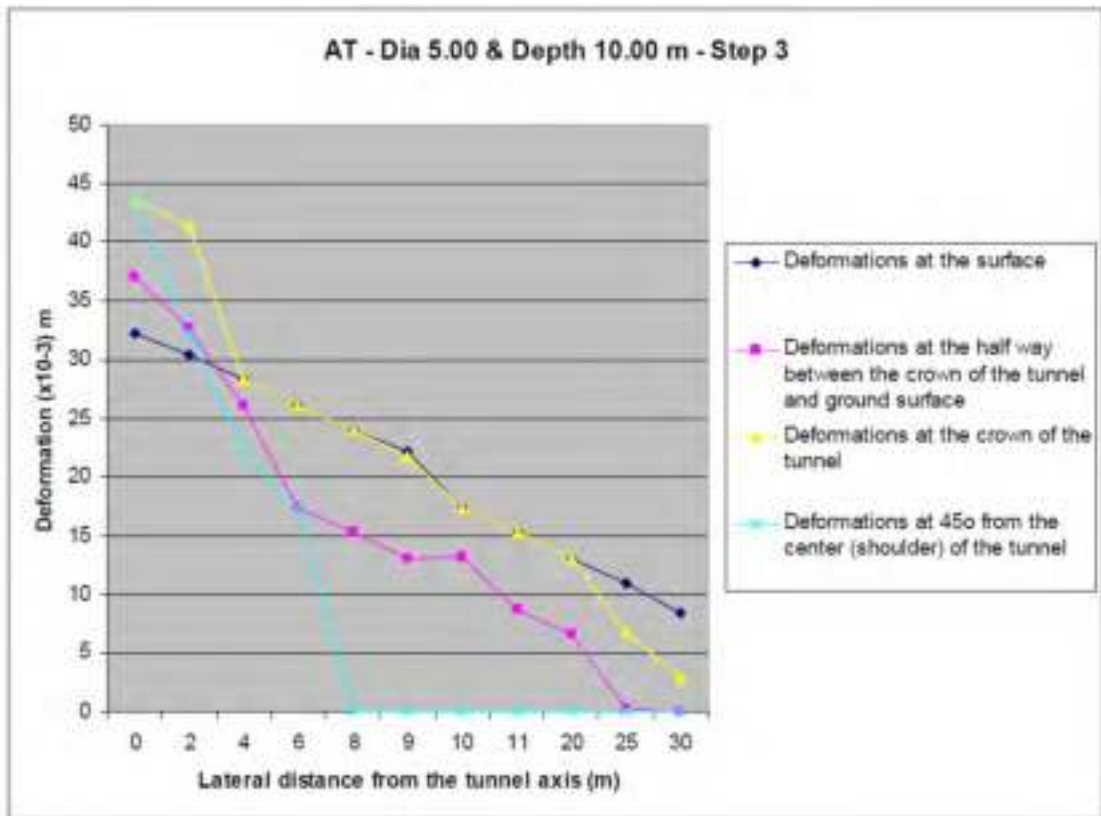


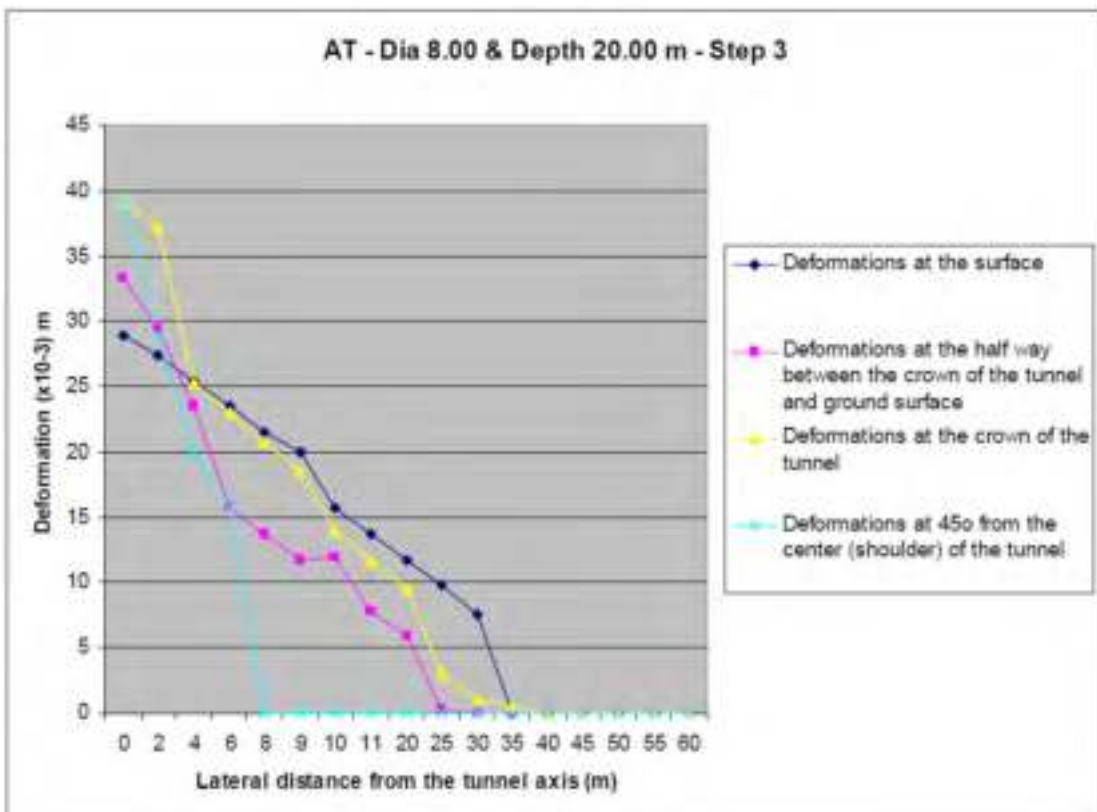
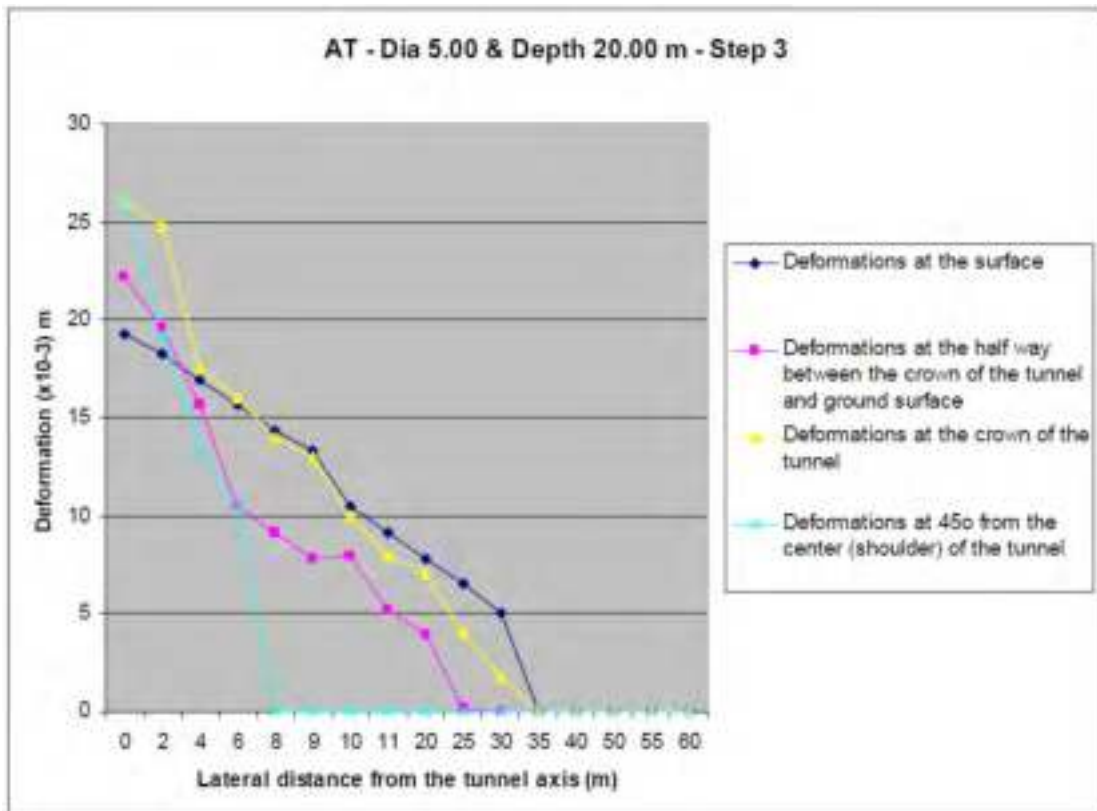


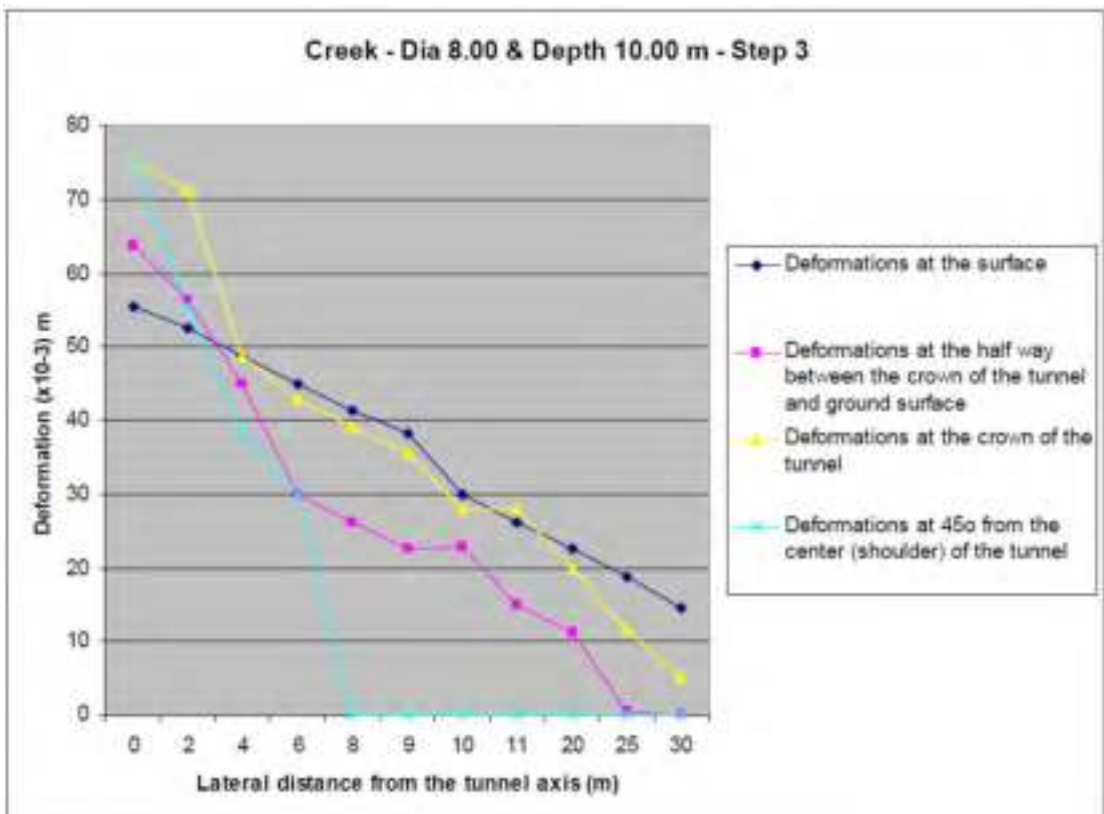
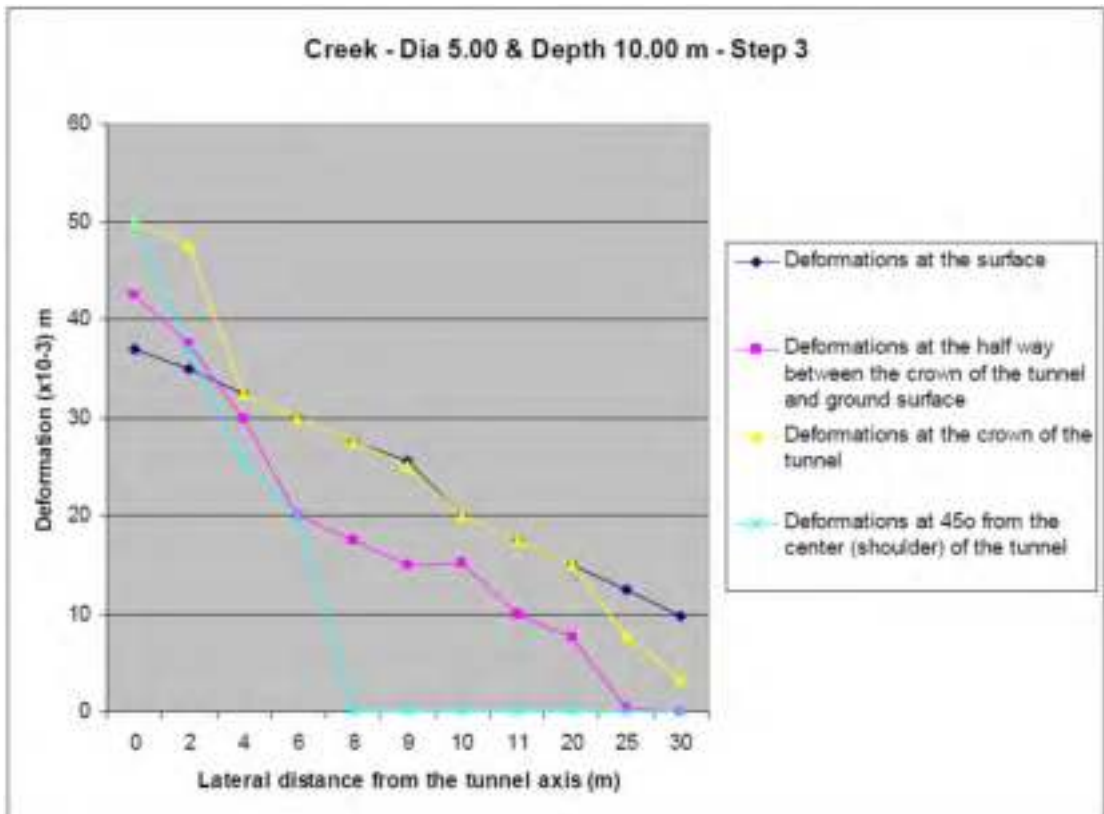


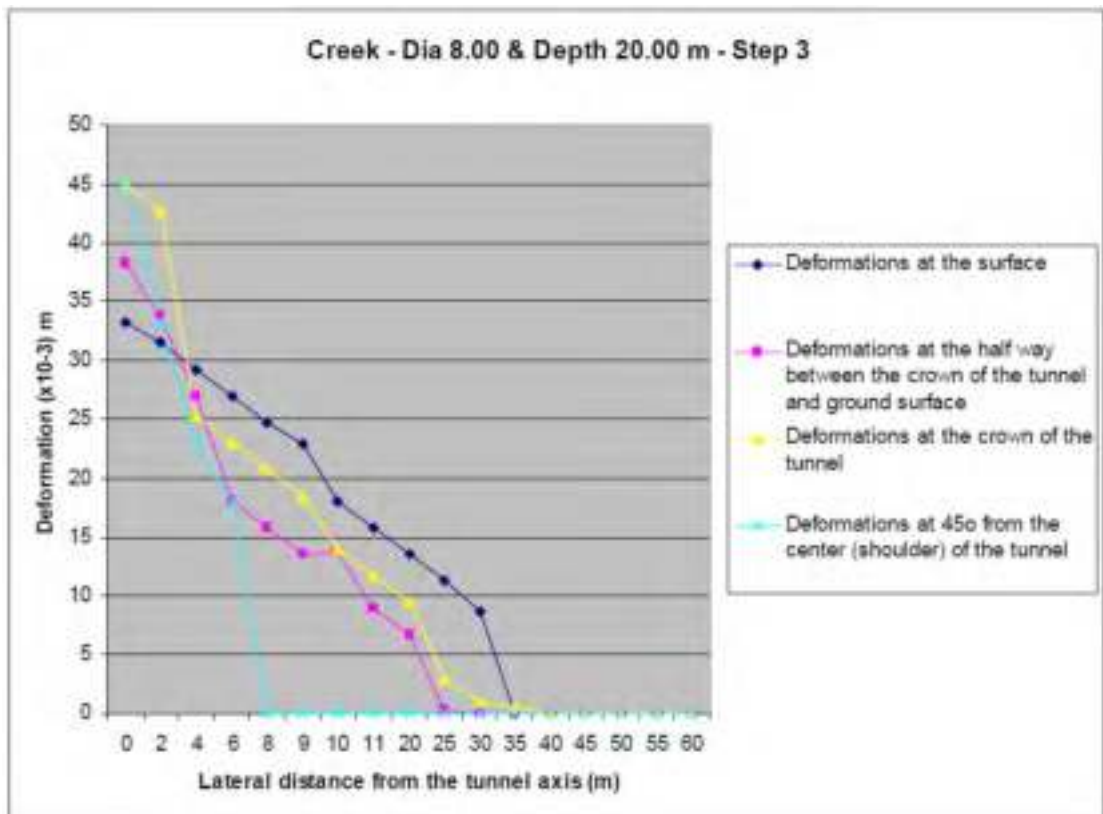
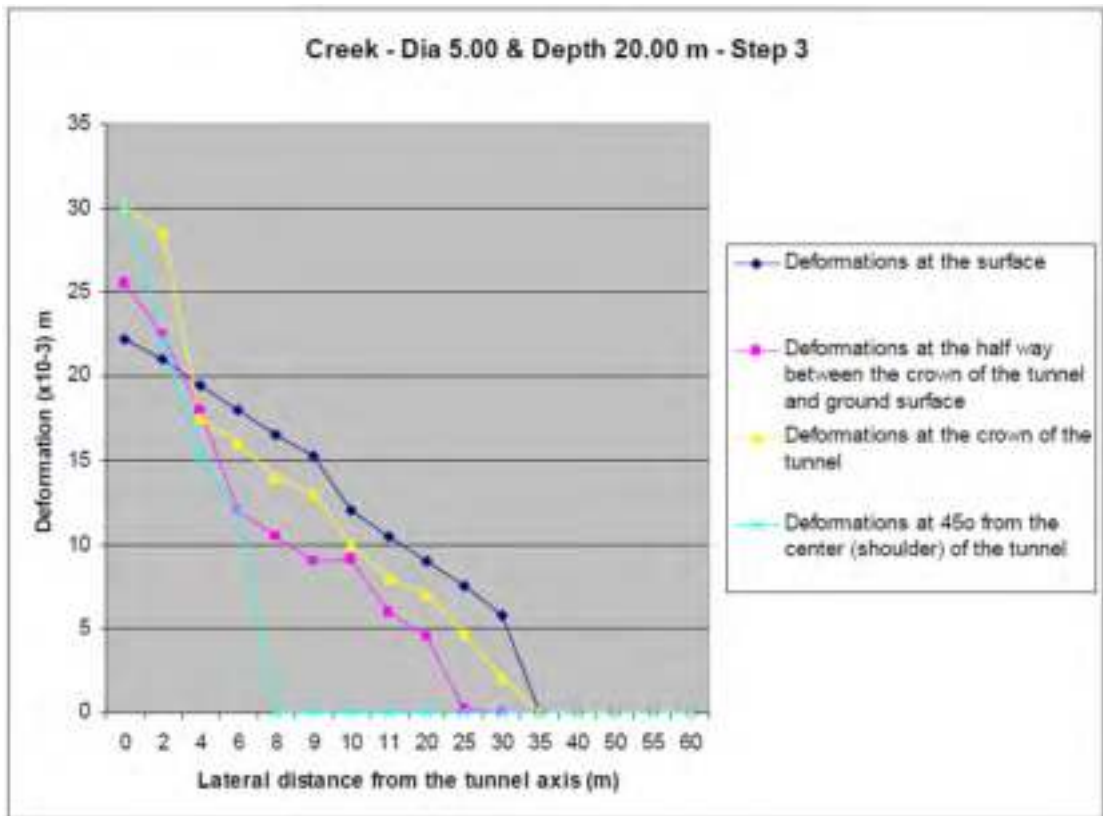


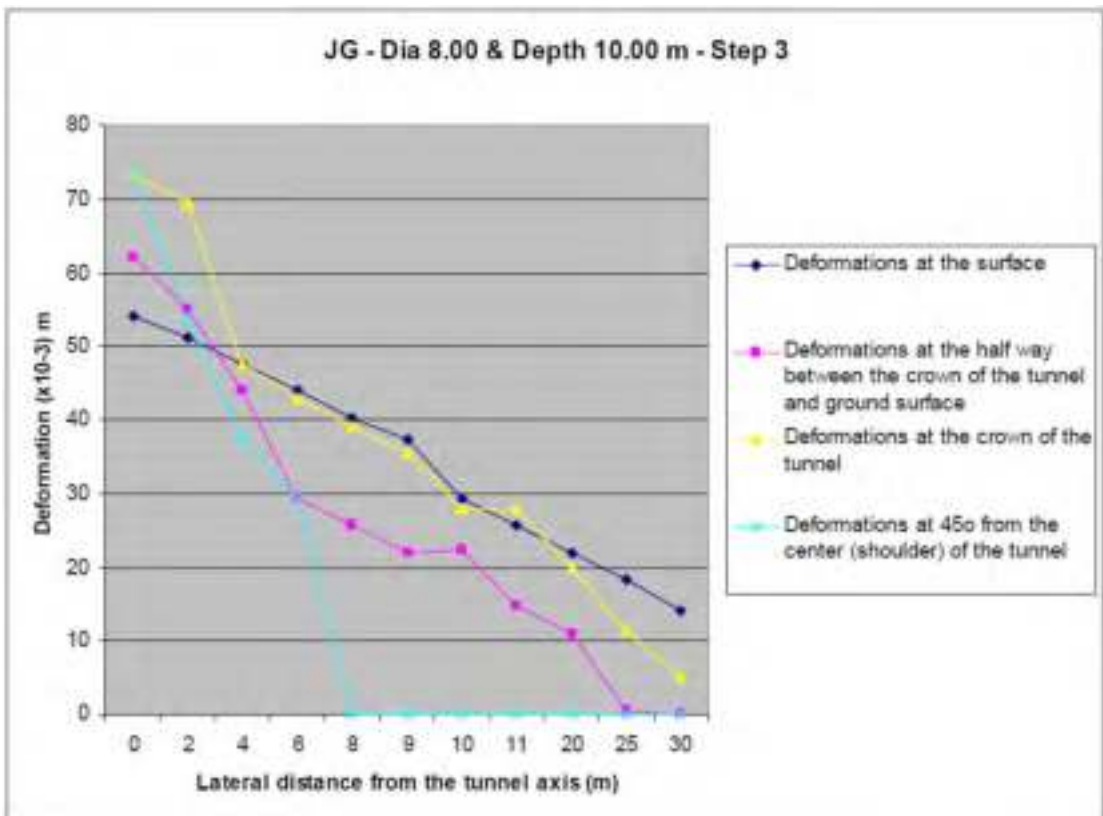
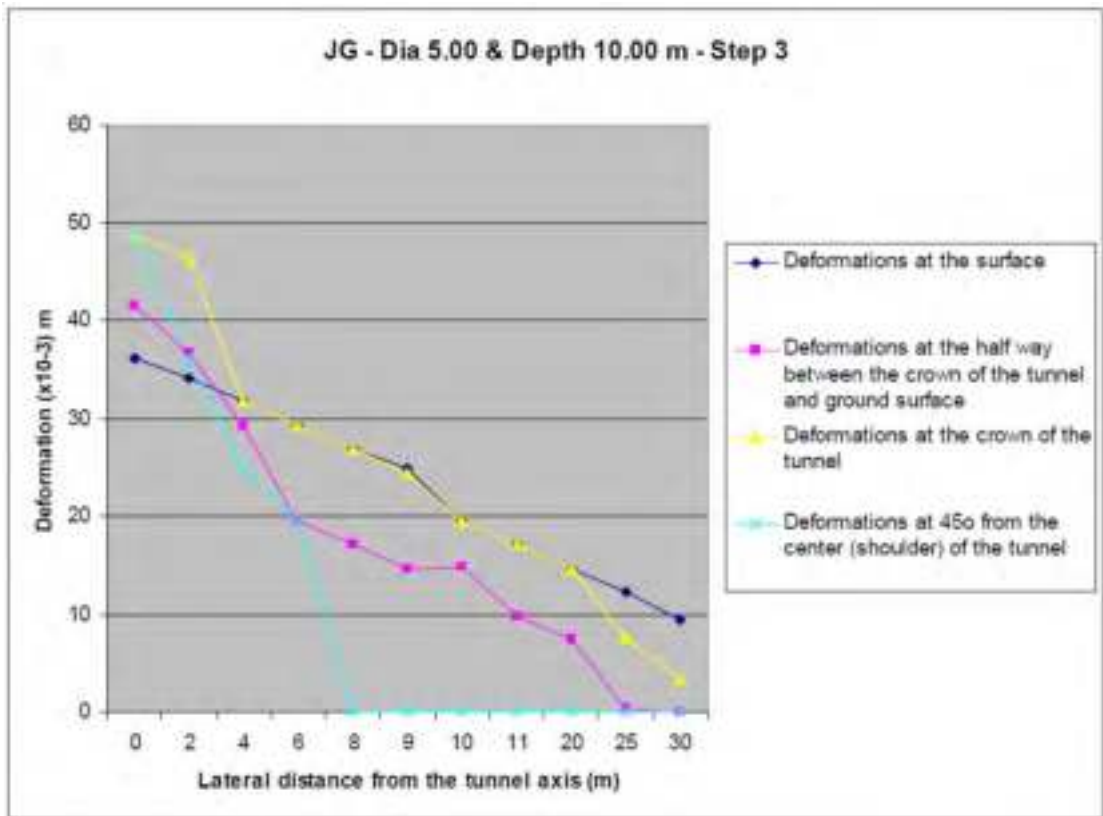


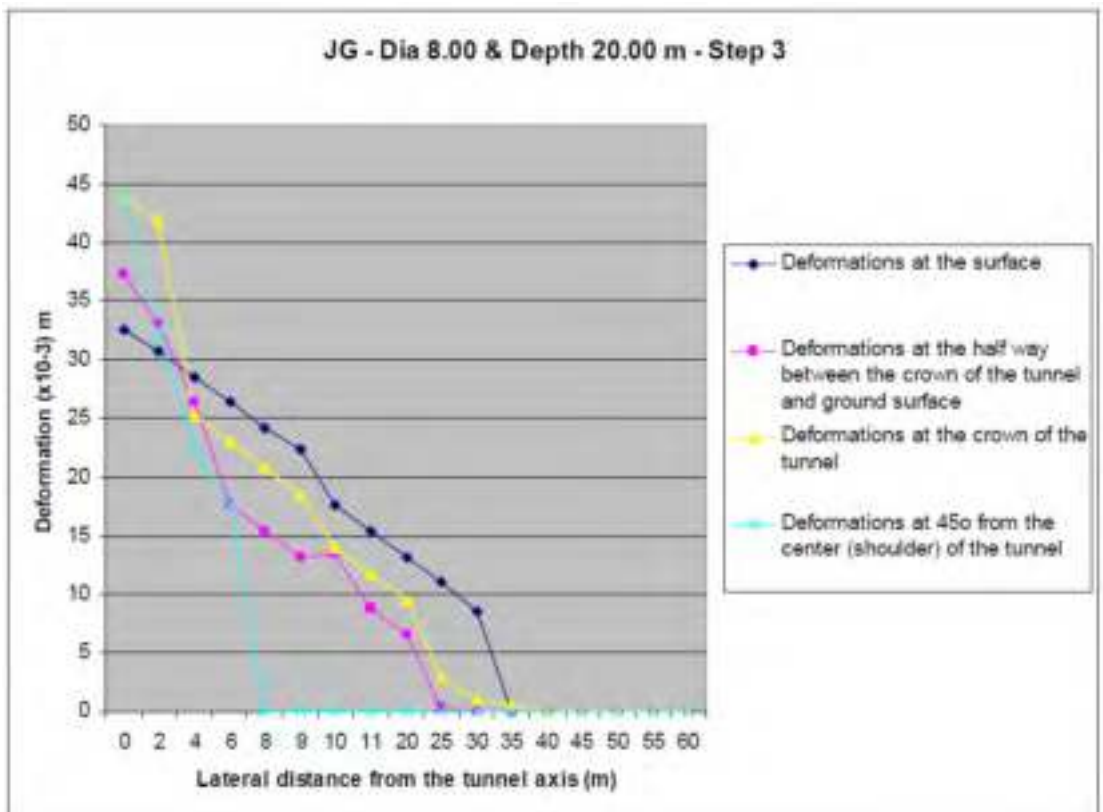
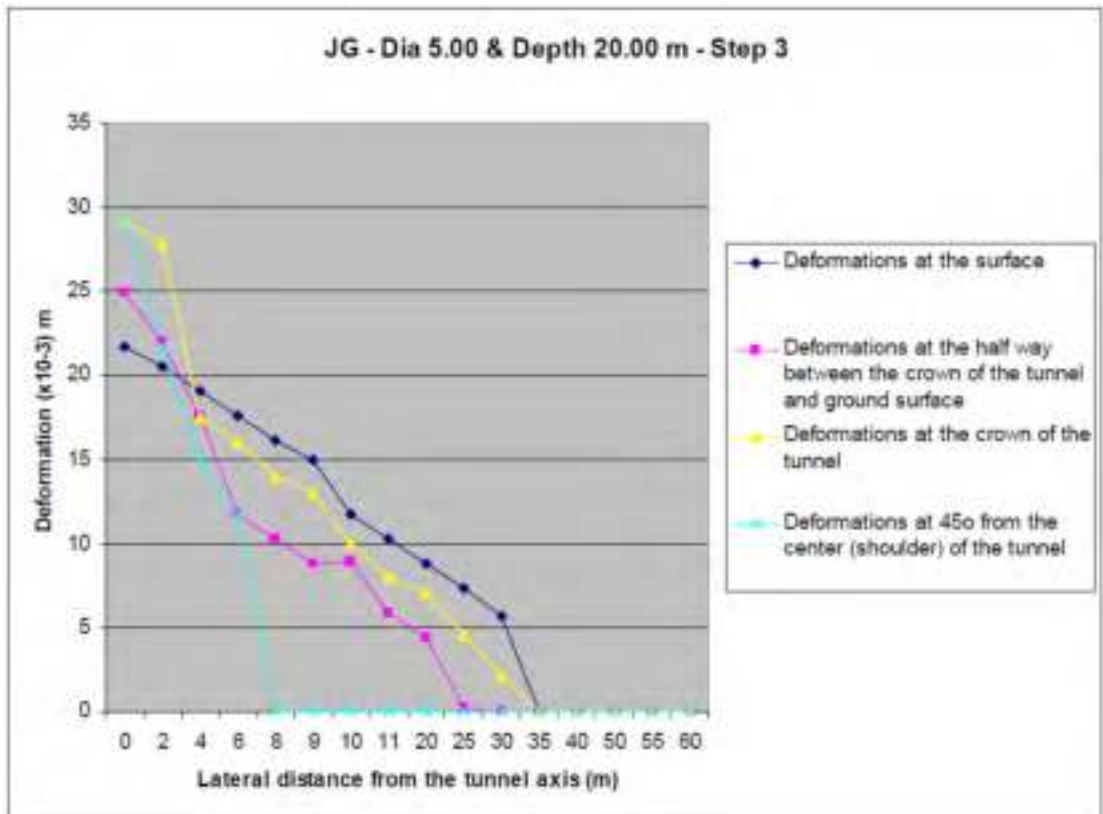


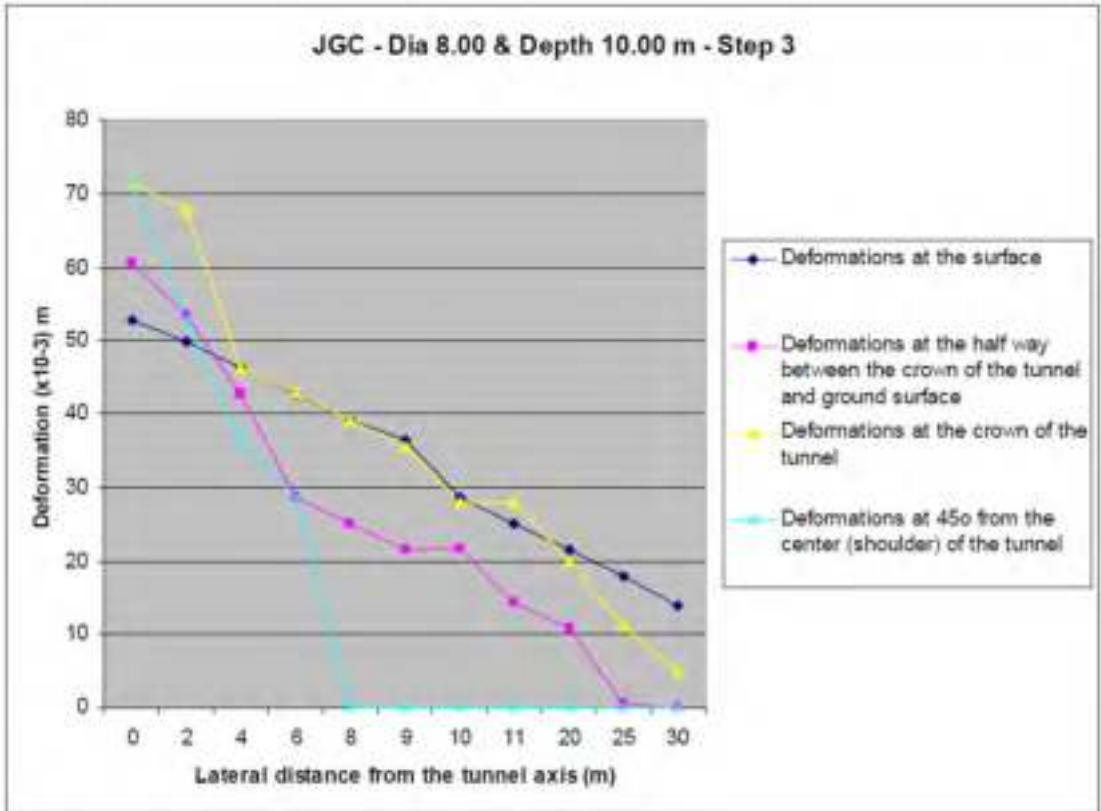
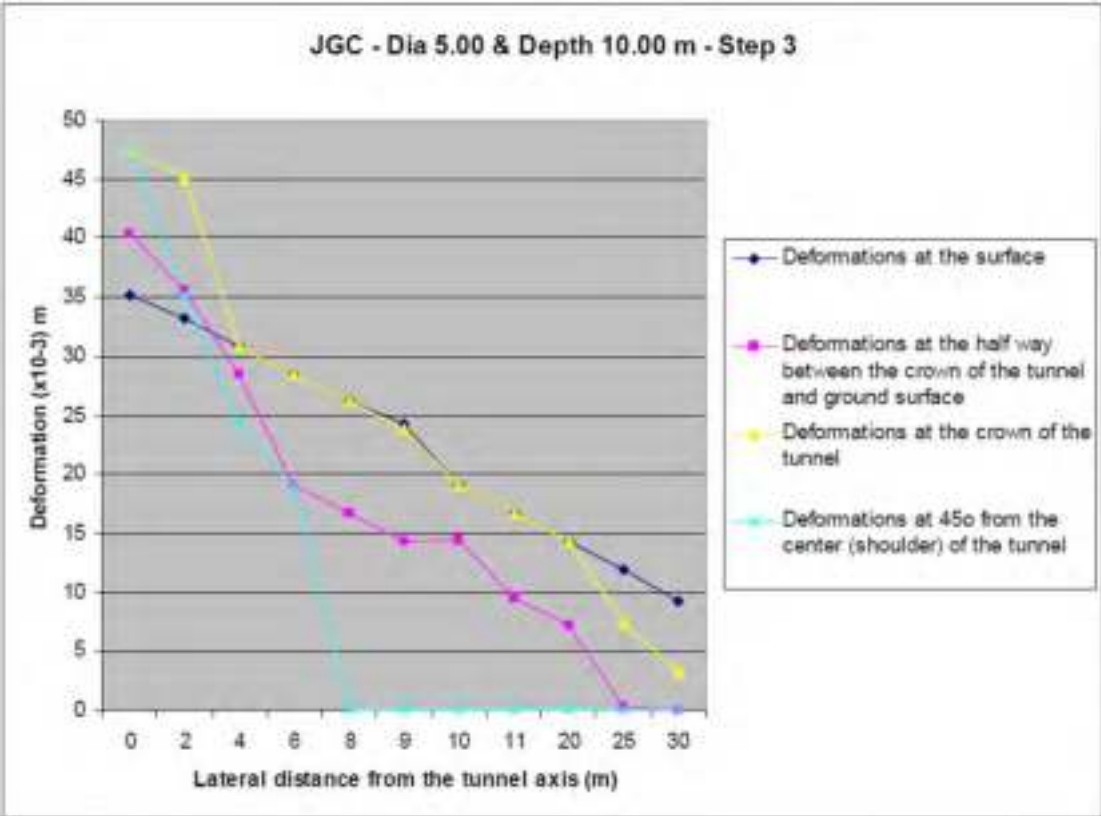


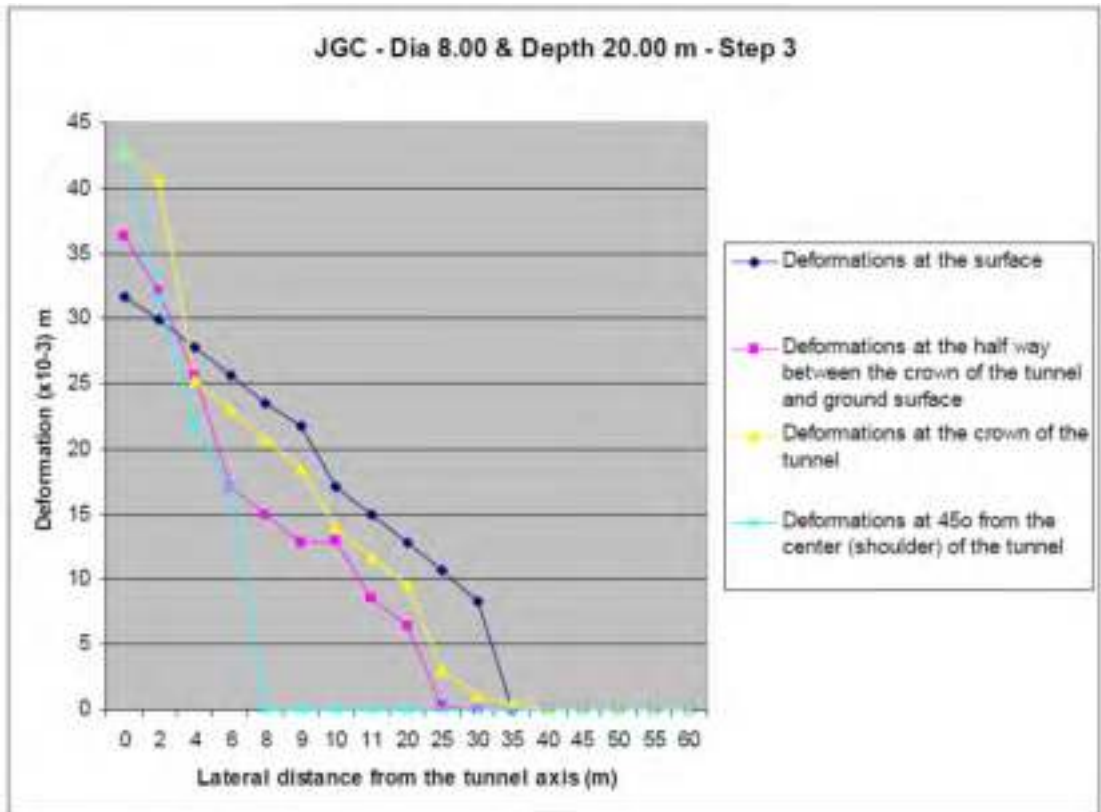
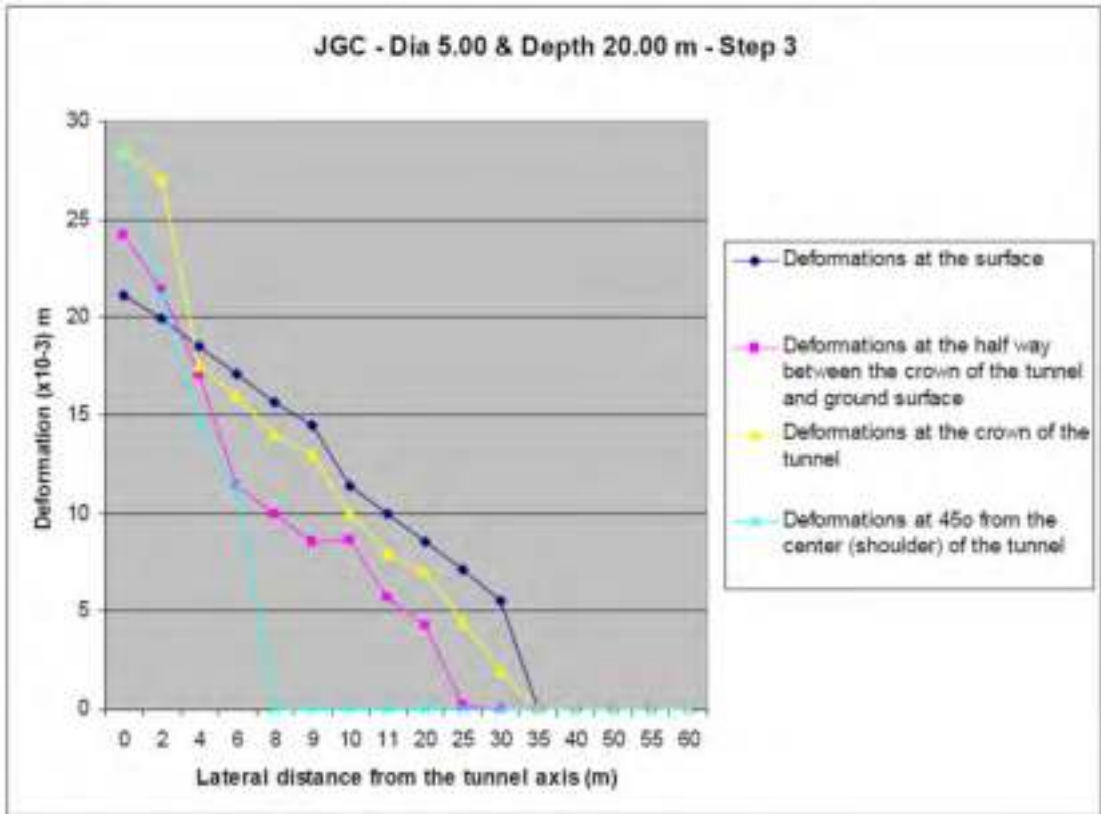


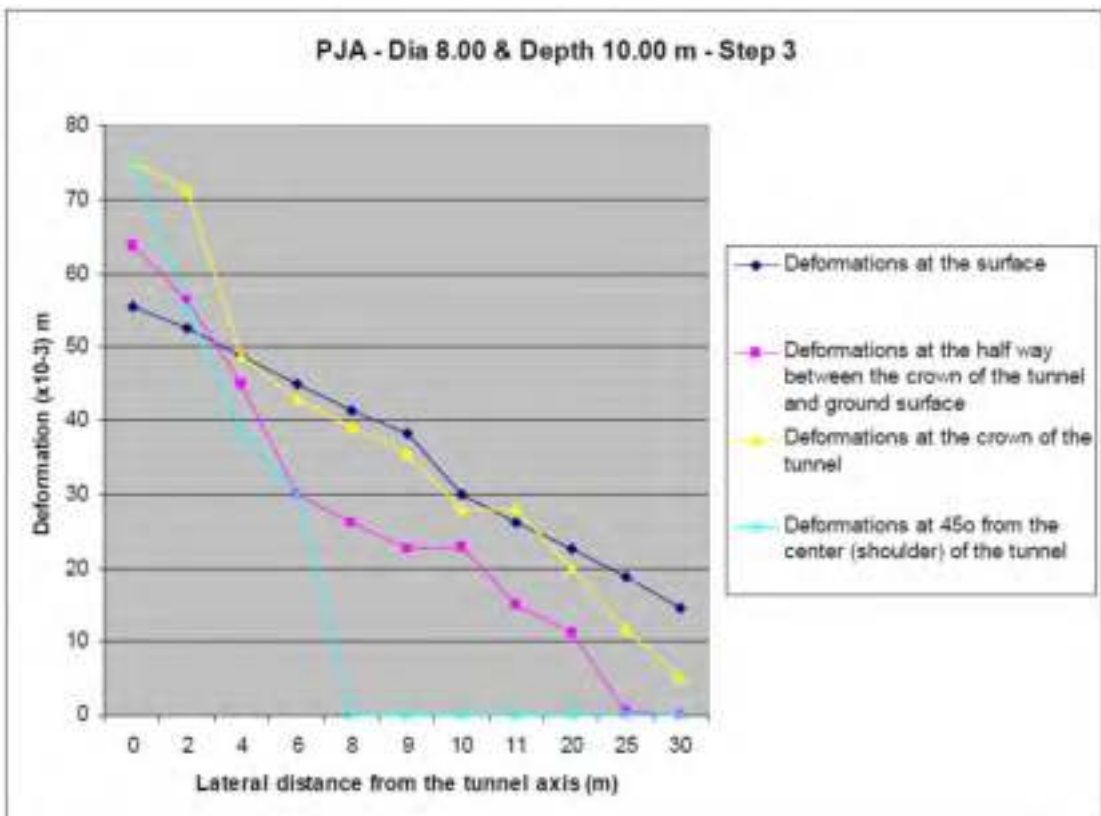
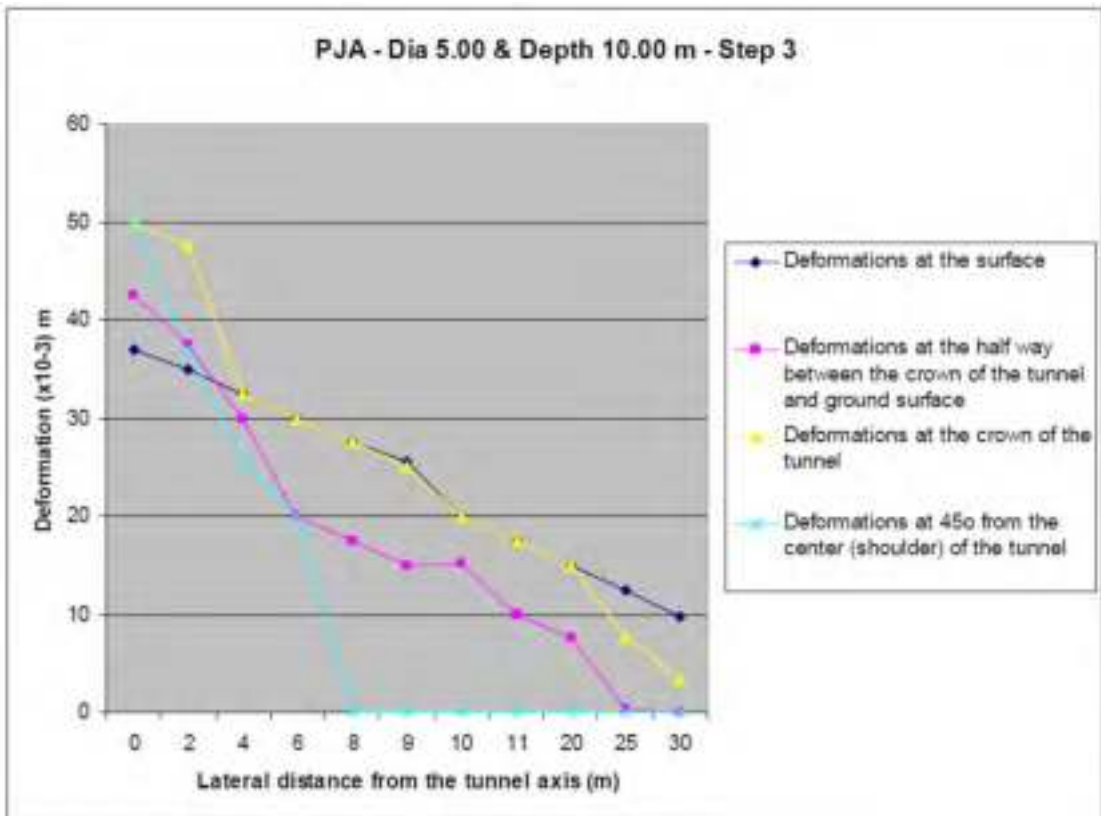


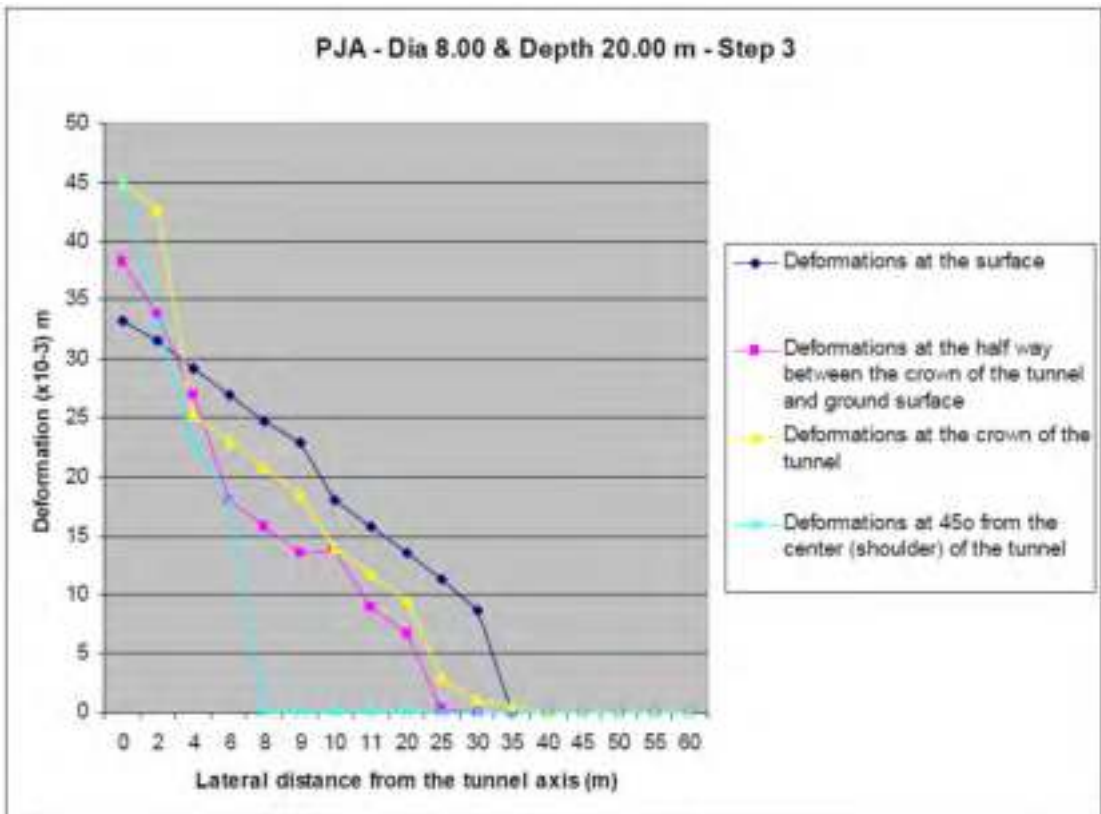
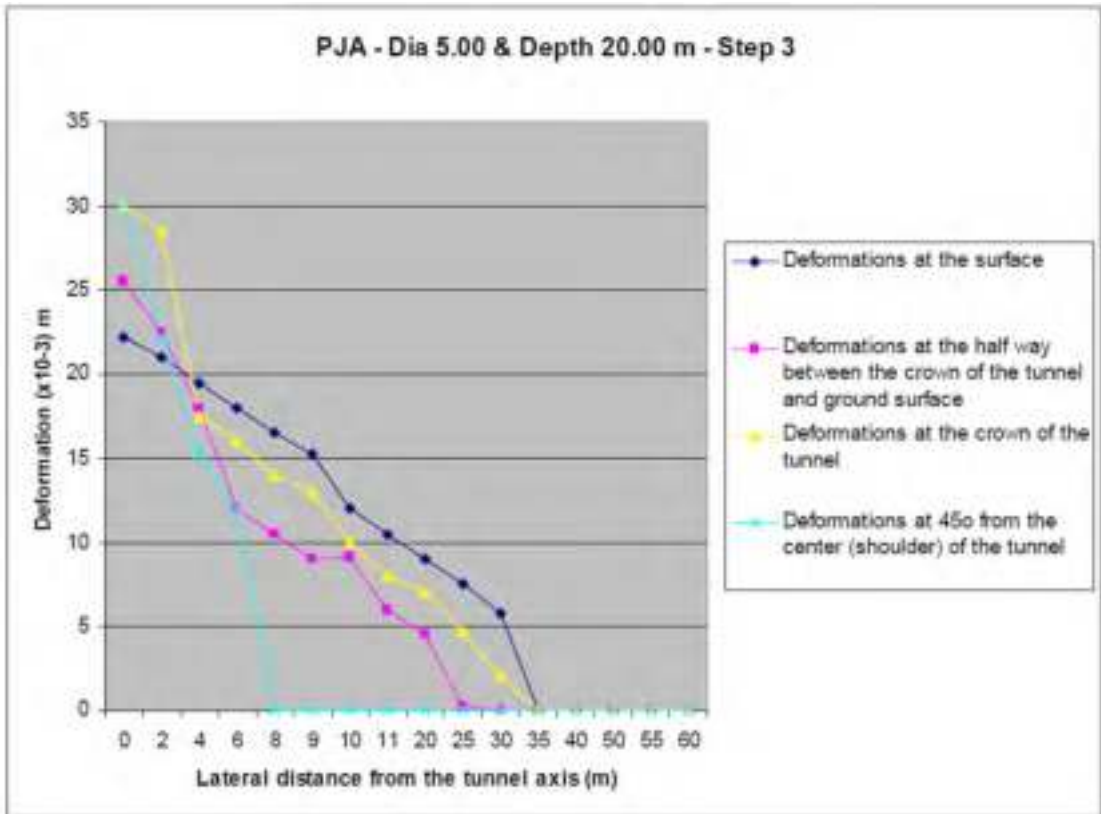


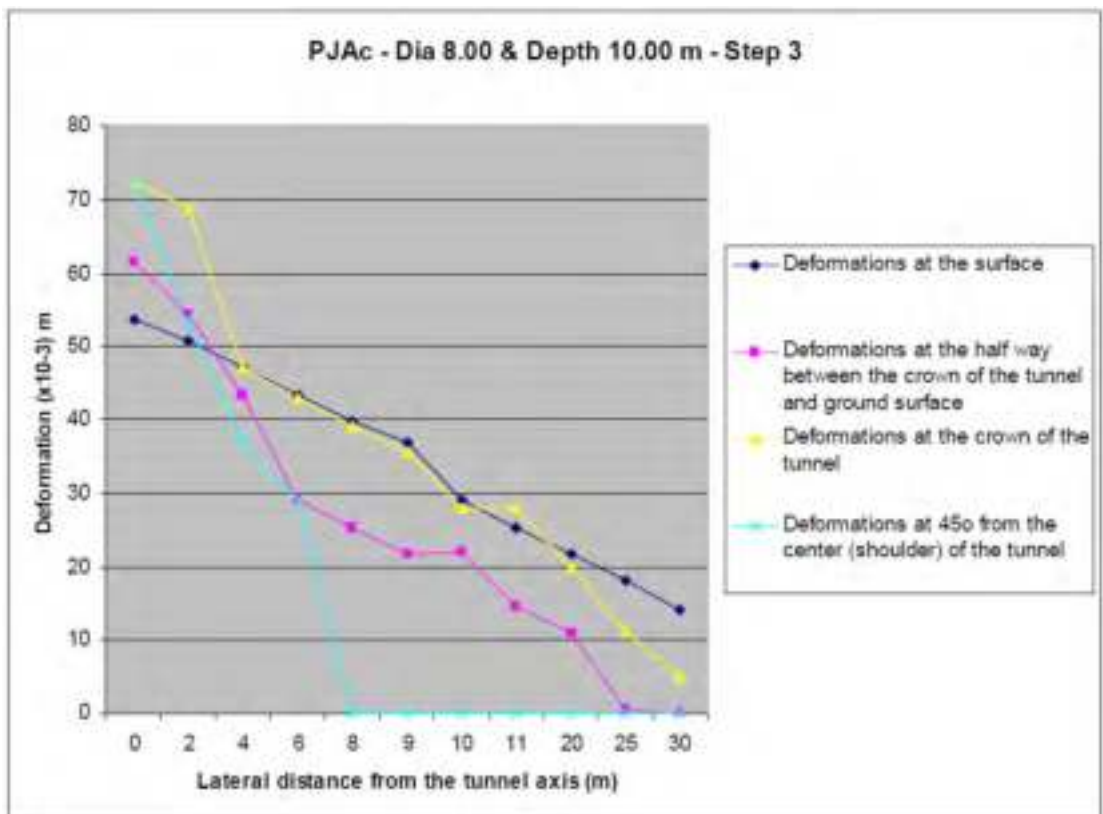
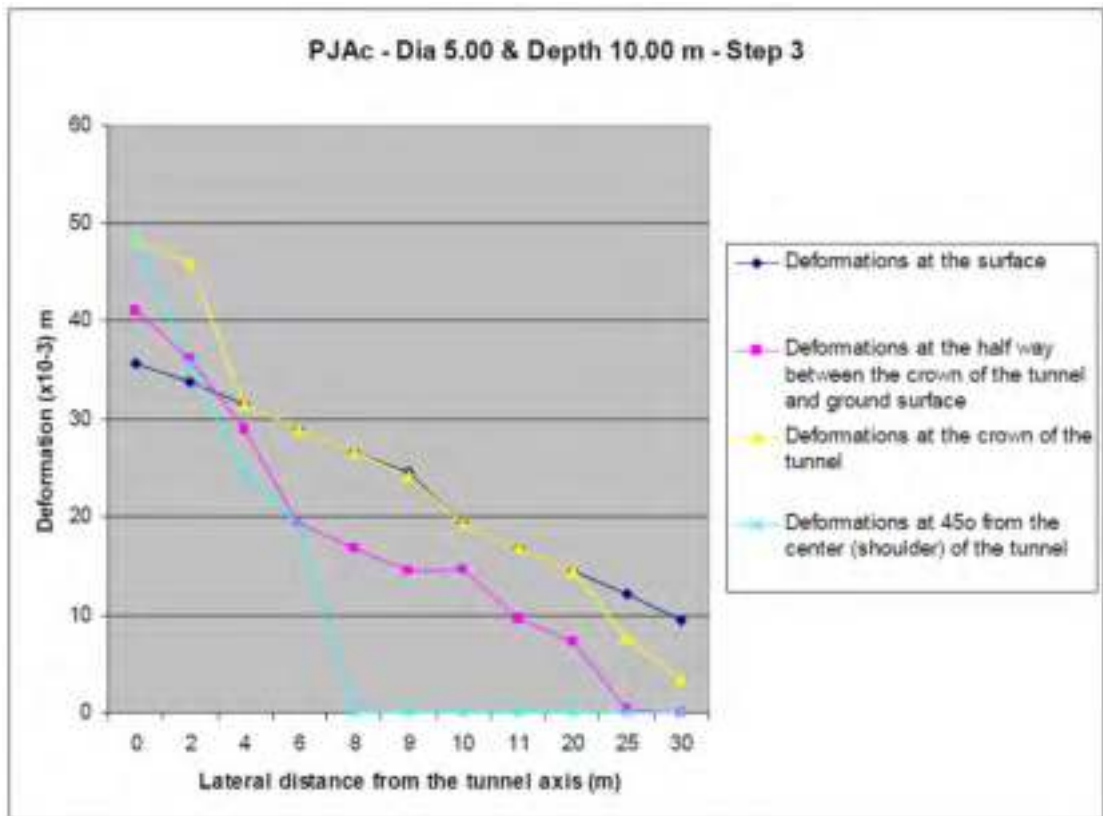


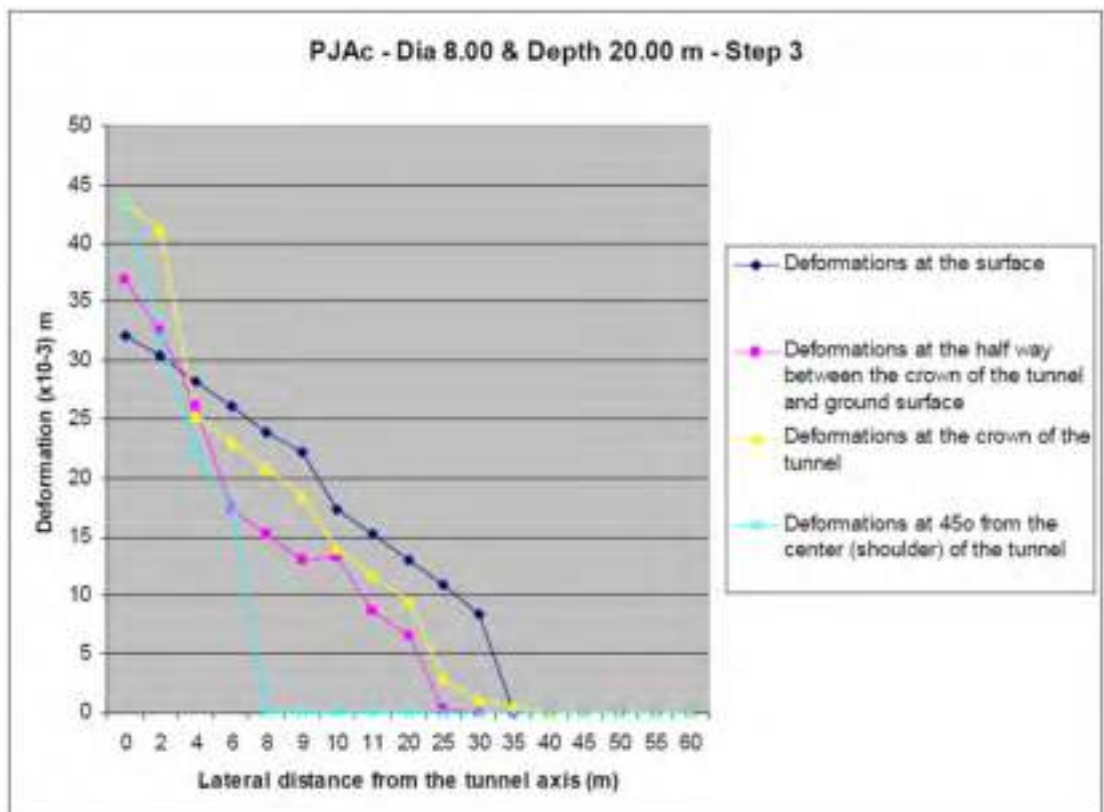
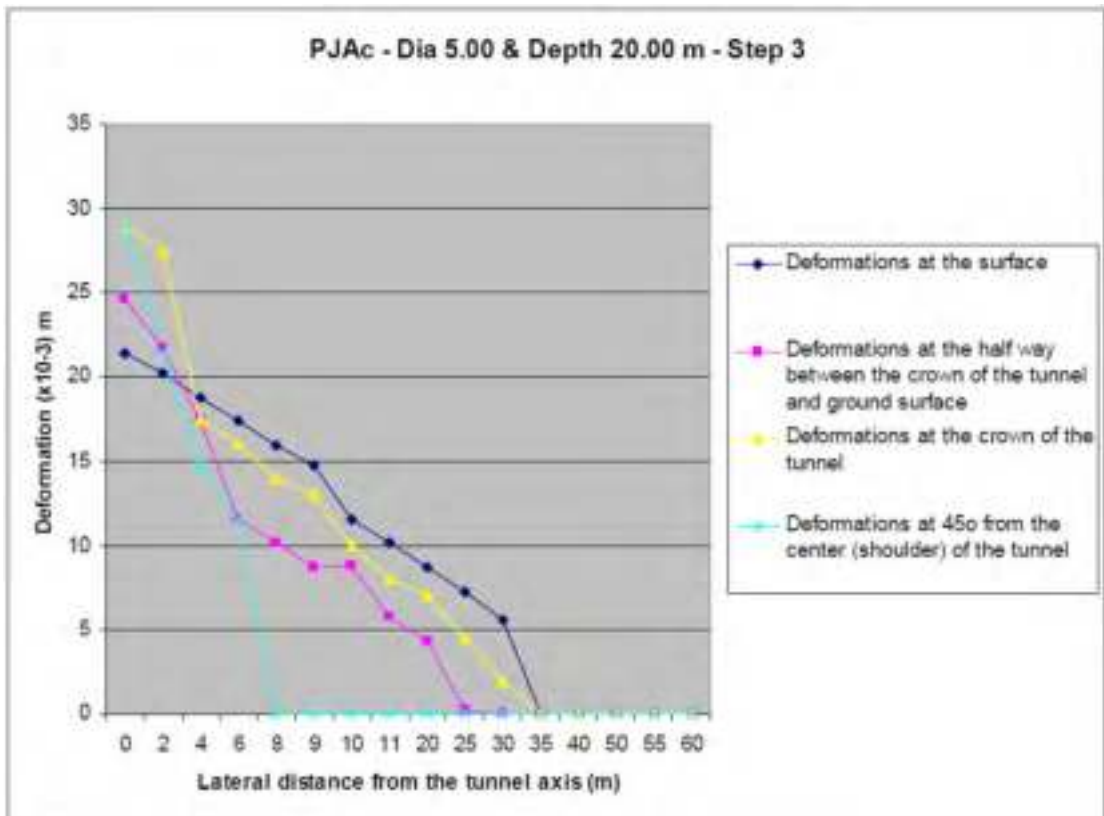


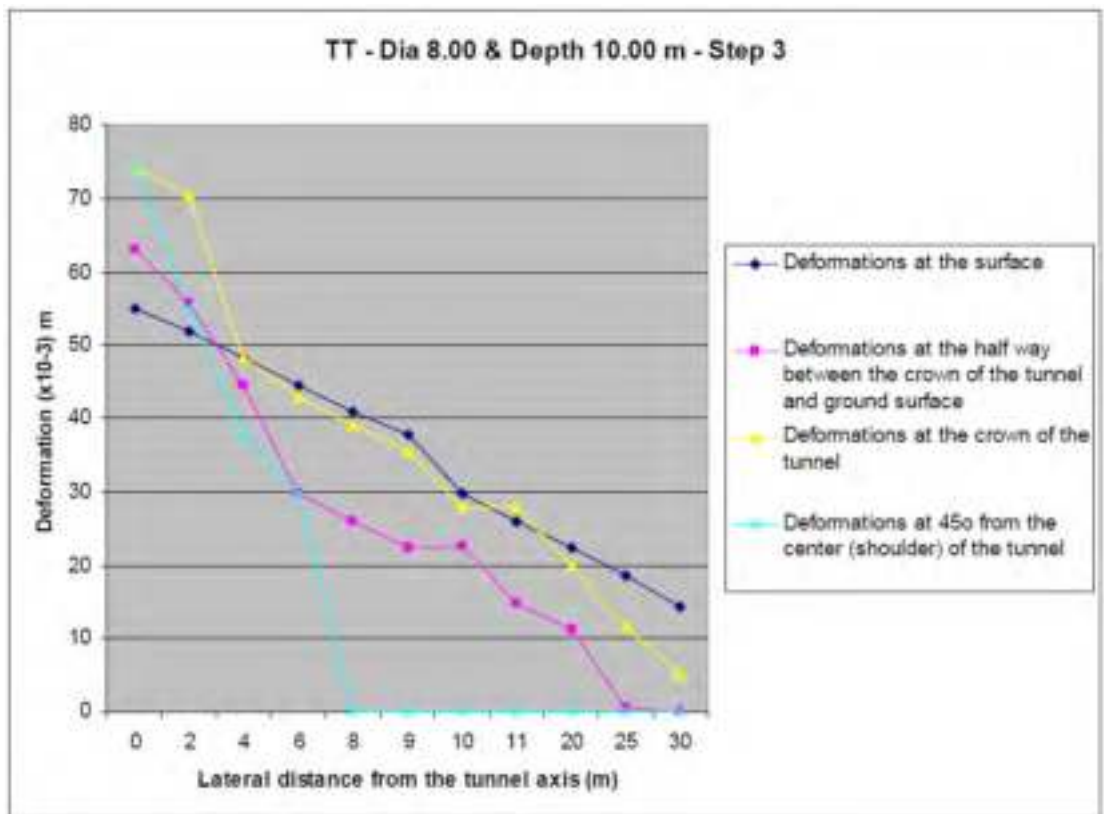
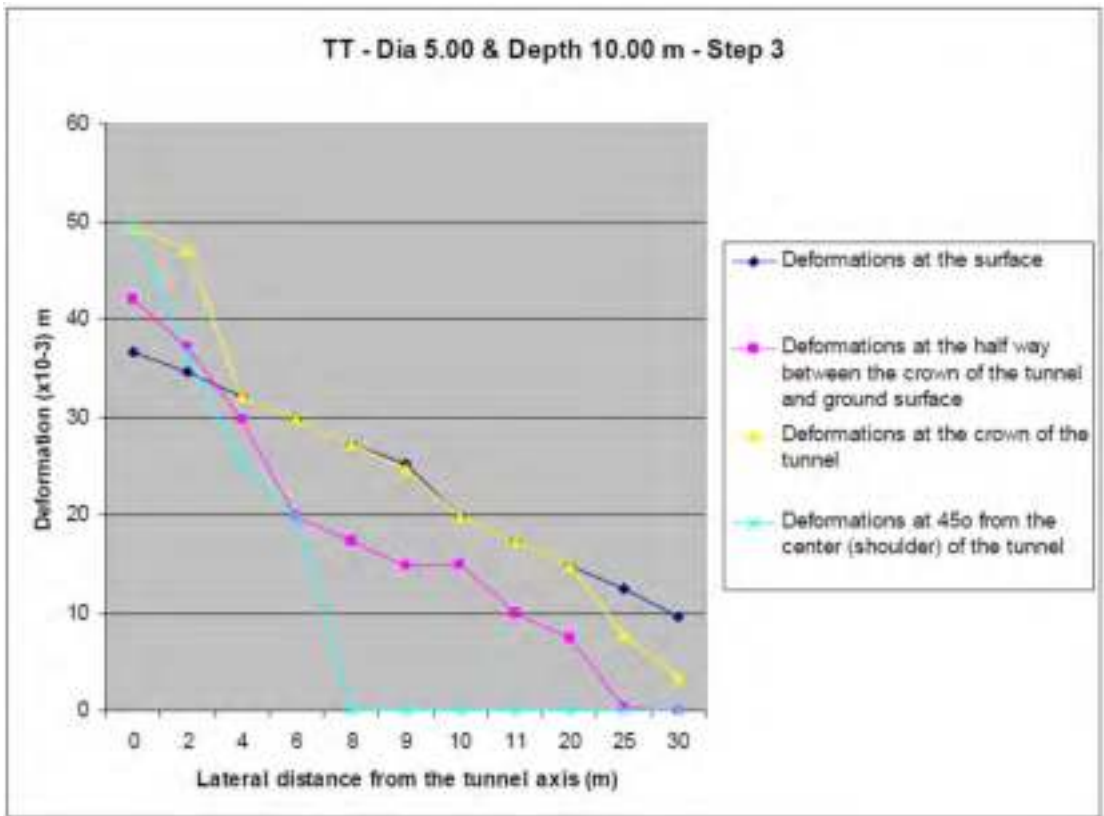


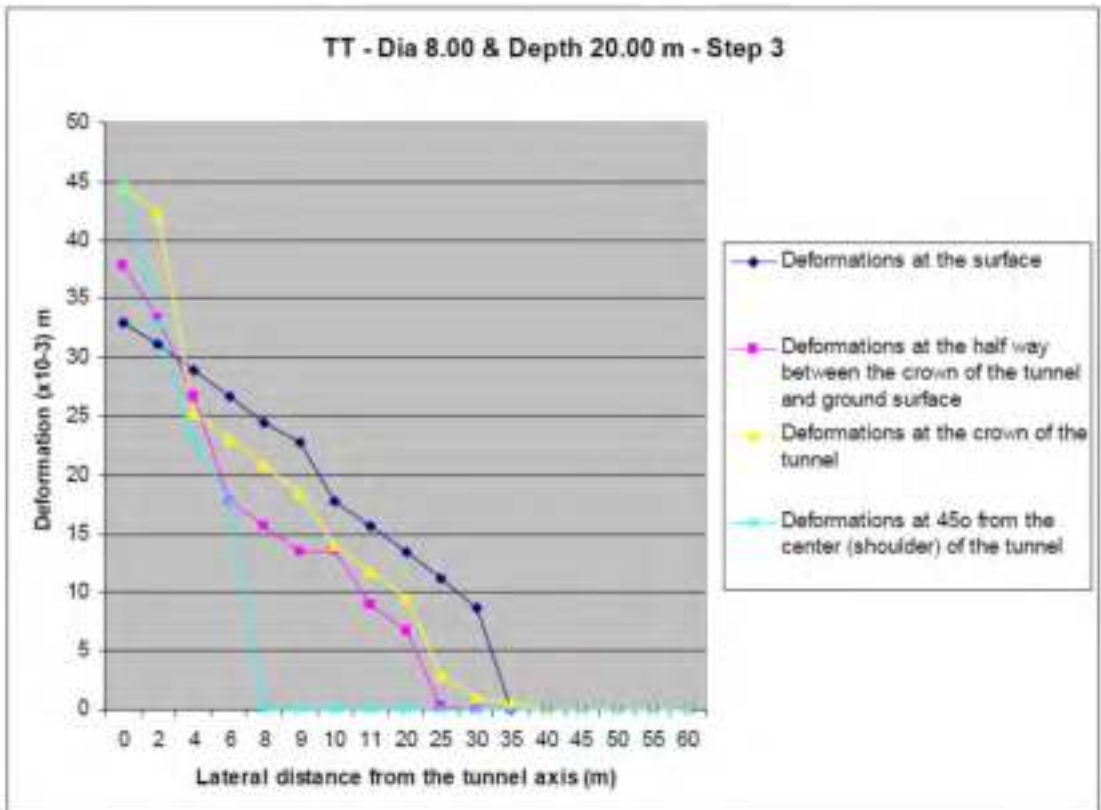
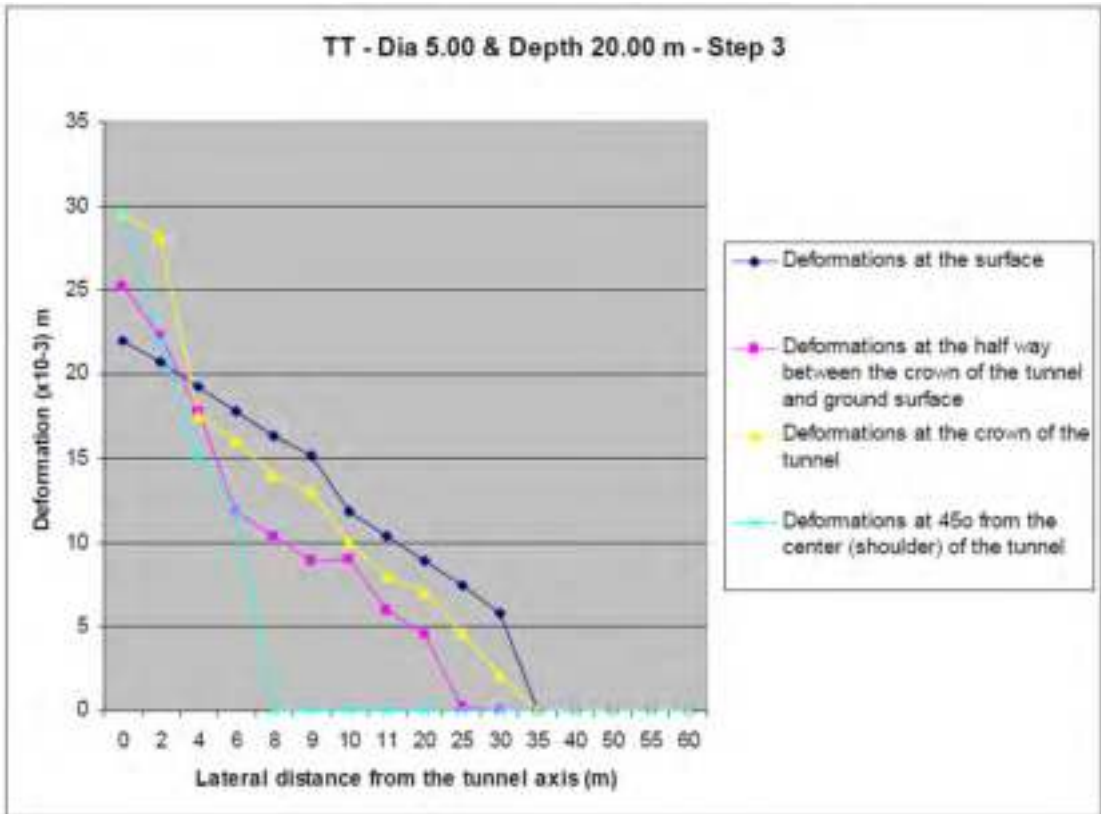


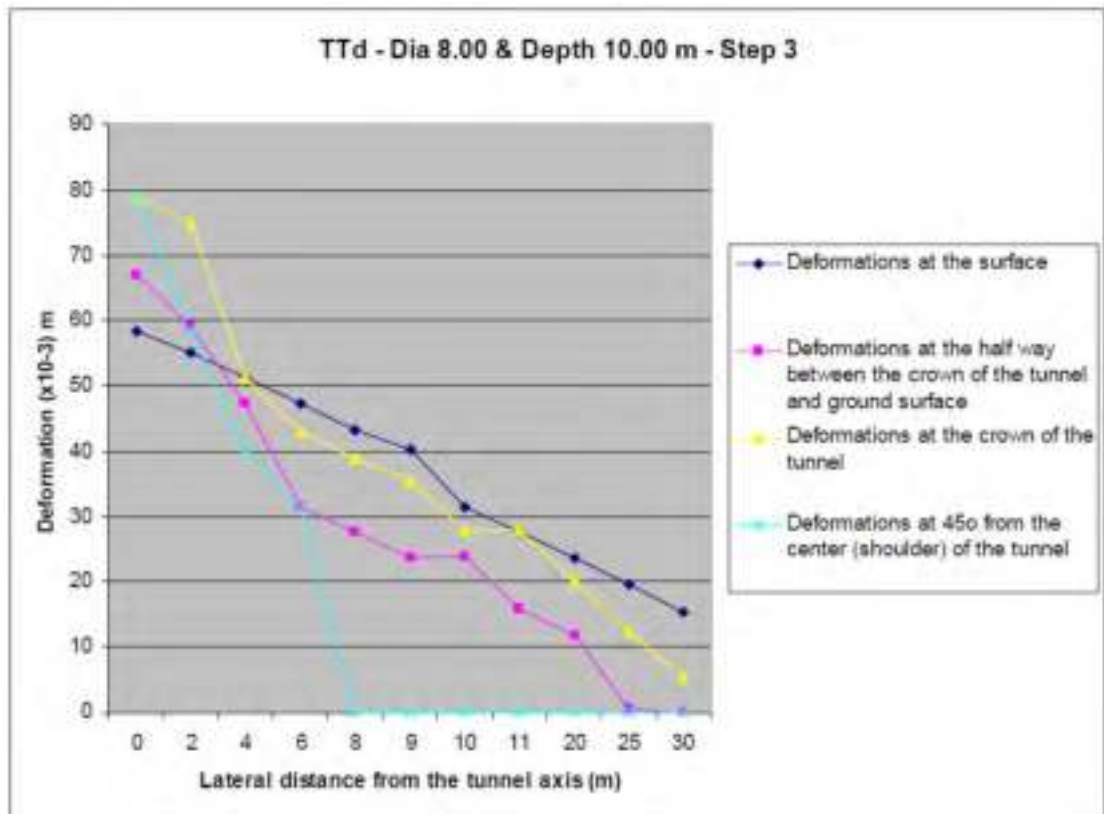
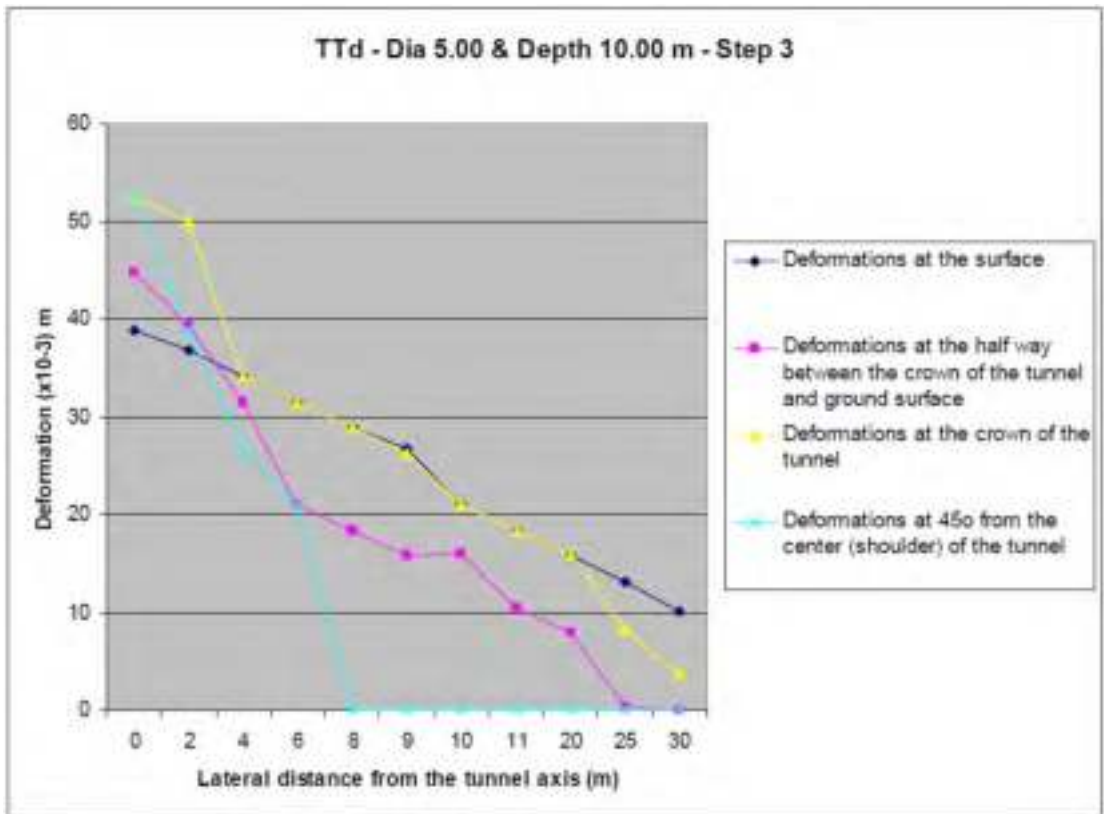


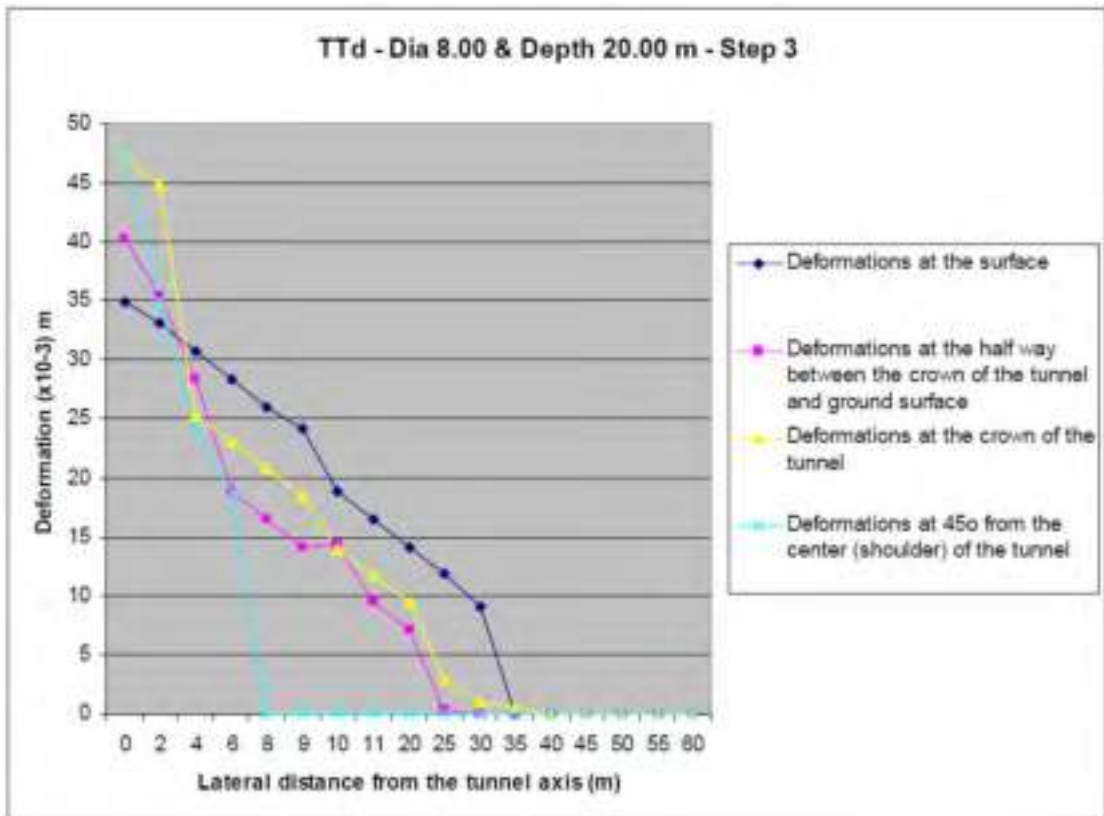
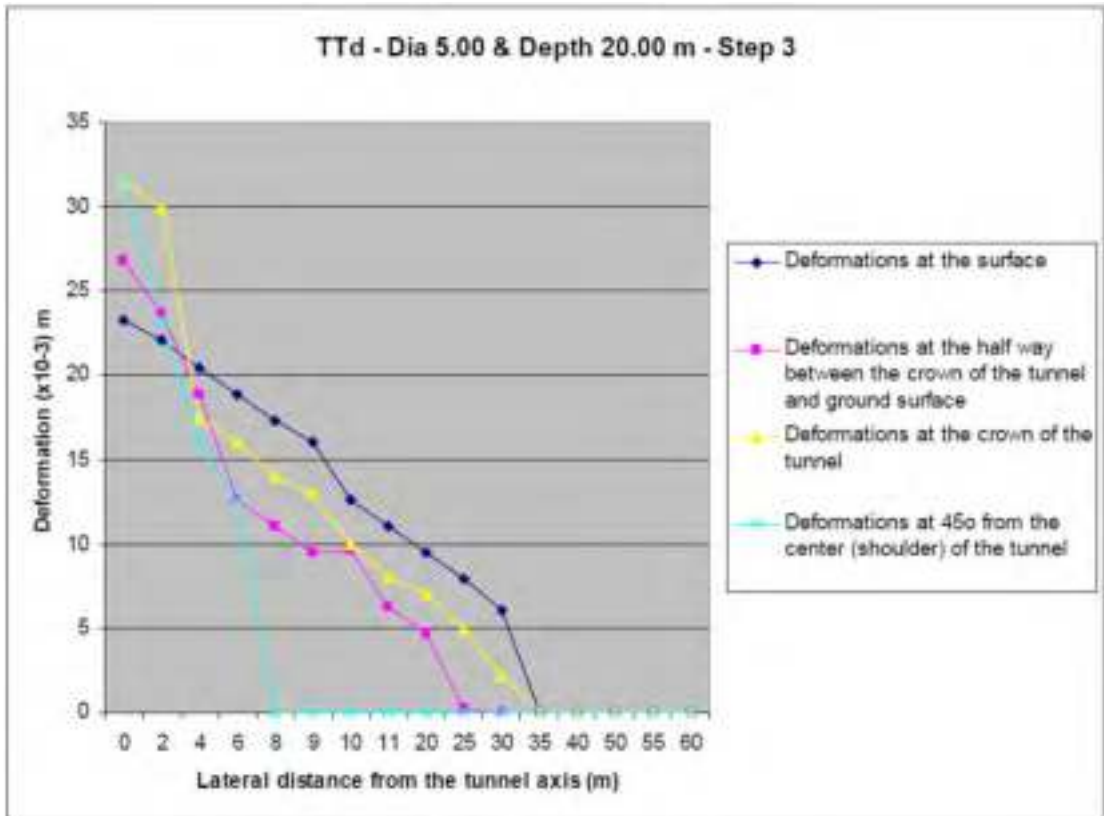






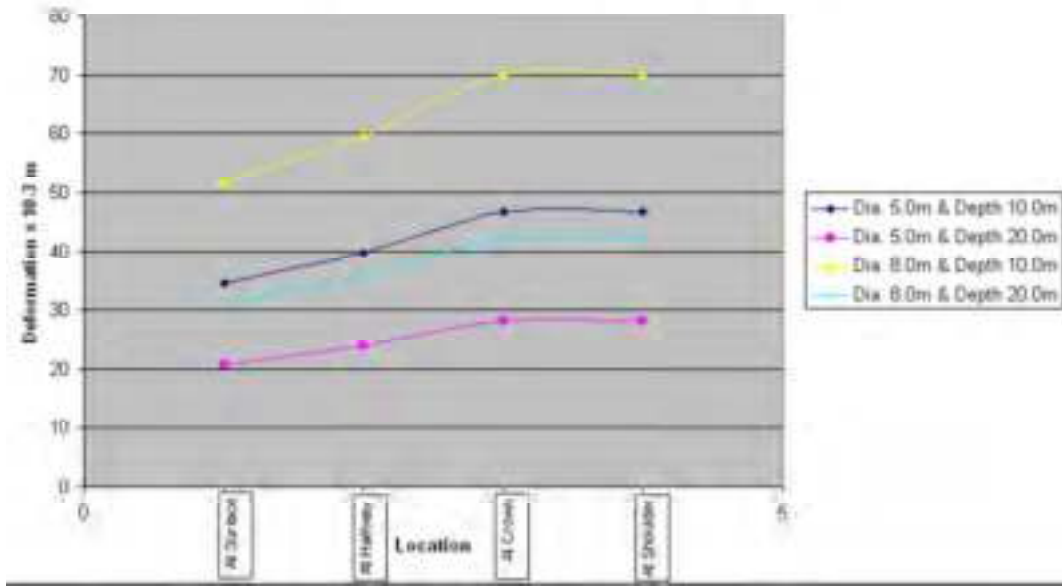




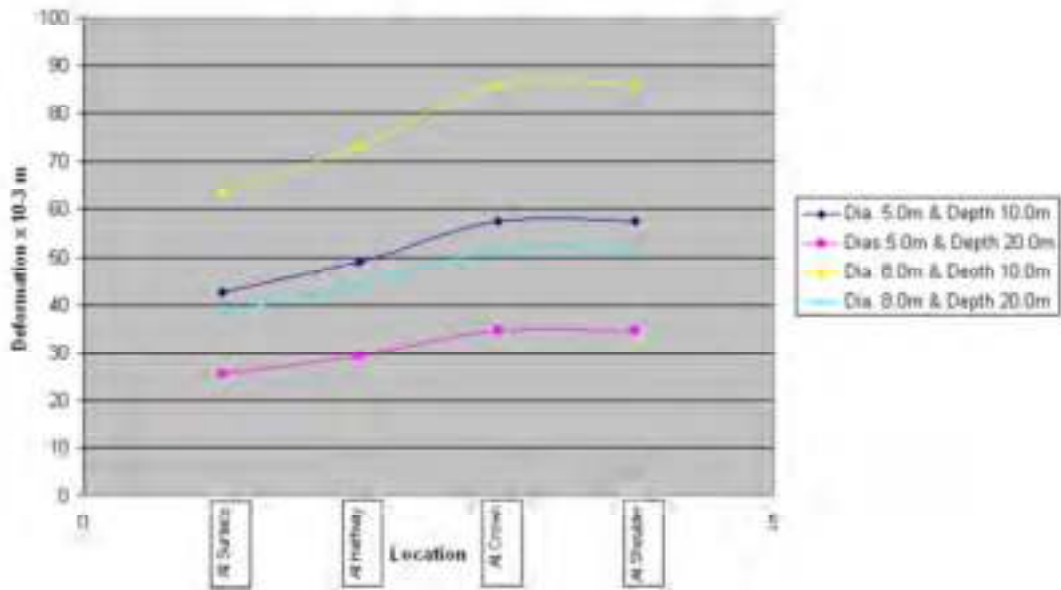


Appendix C
Combination of diameters and depths

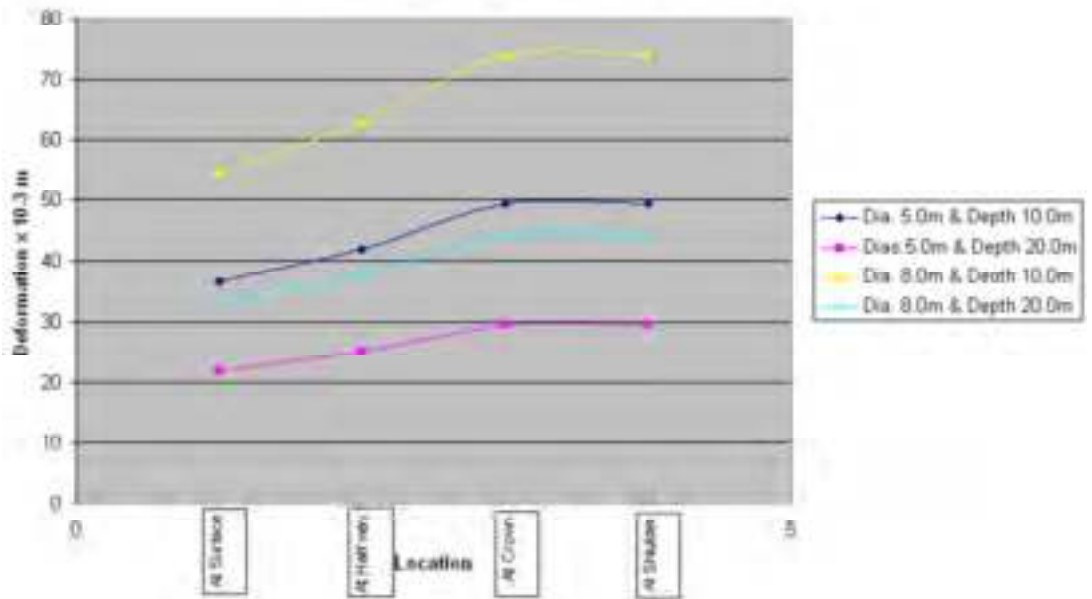
Maximum values of Deformation at Site AB



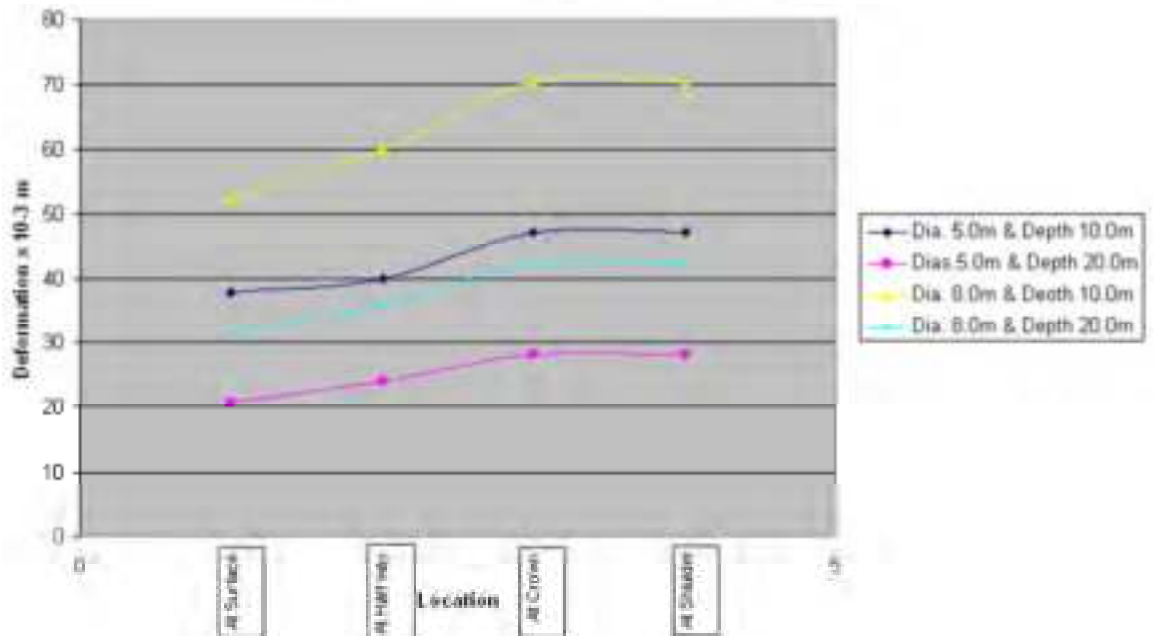
Maximum values of Deformation at Site ABd



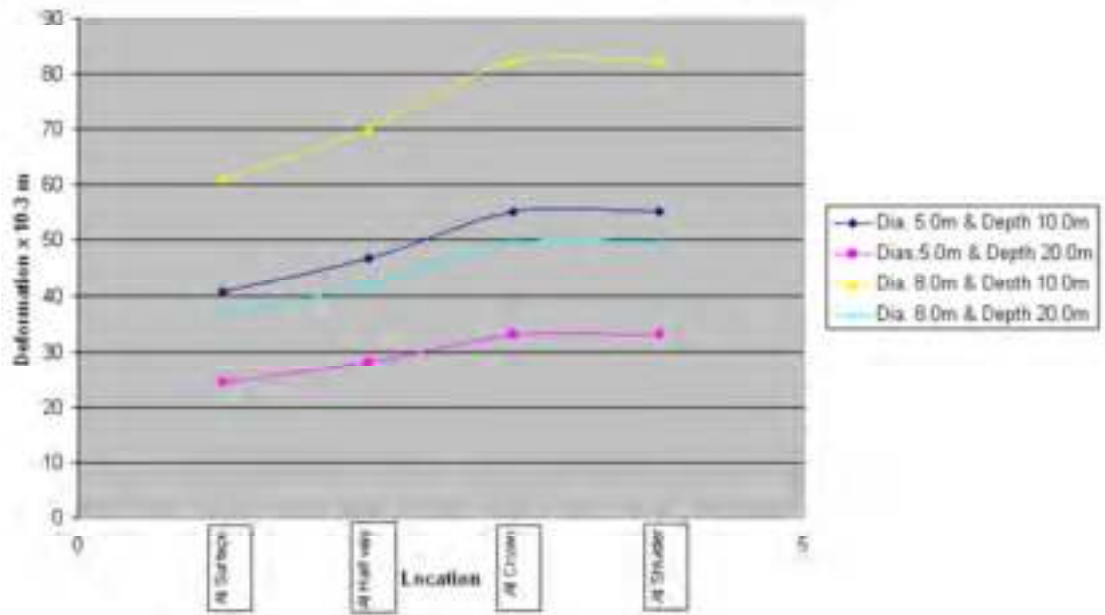
Maximum values of Deformation at Site AC



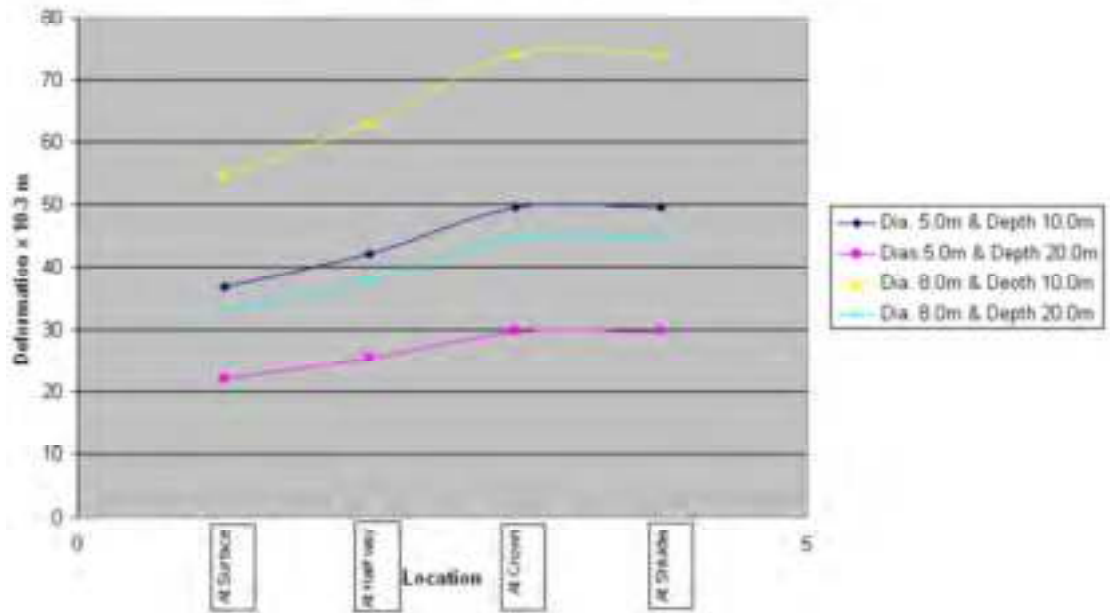
Maximum values of Deformation at Site ABe



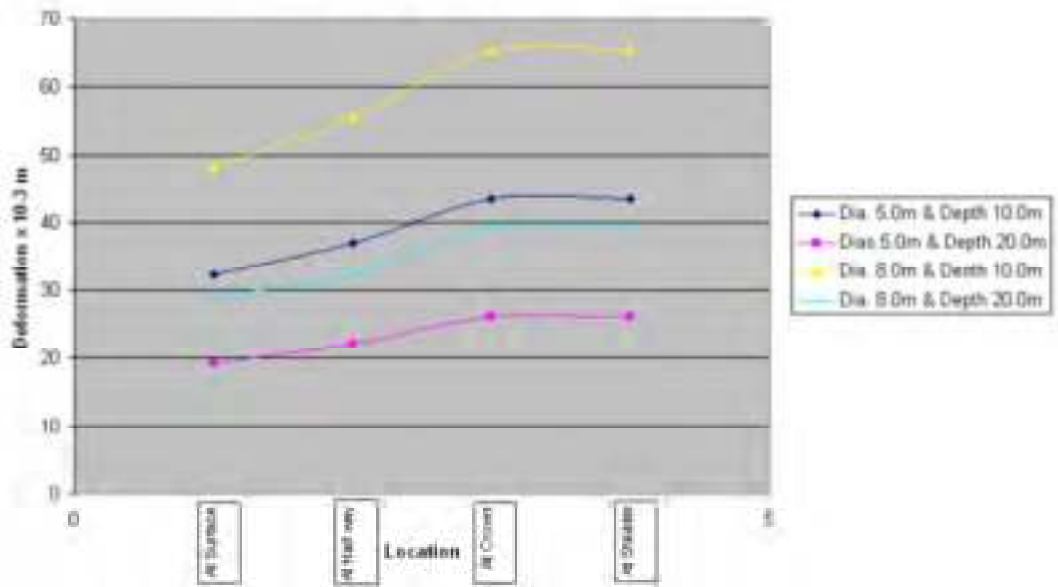
Maximum values of Deformation at Site ACc



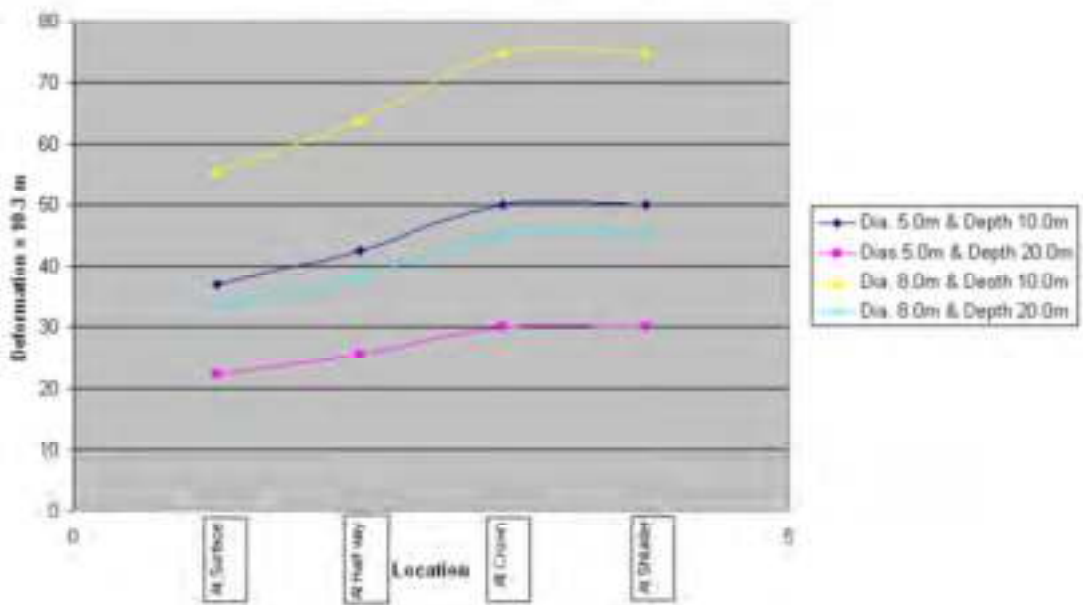
Maximum values of Deformation at Site ACe



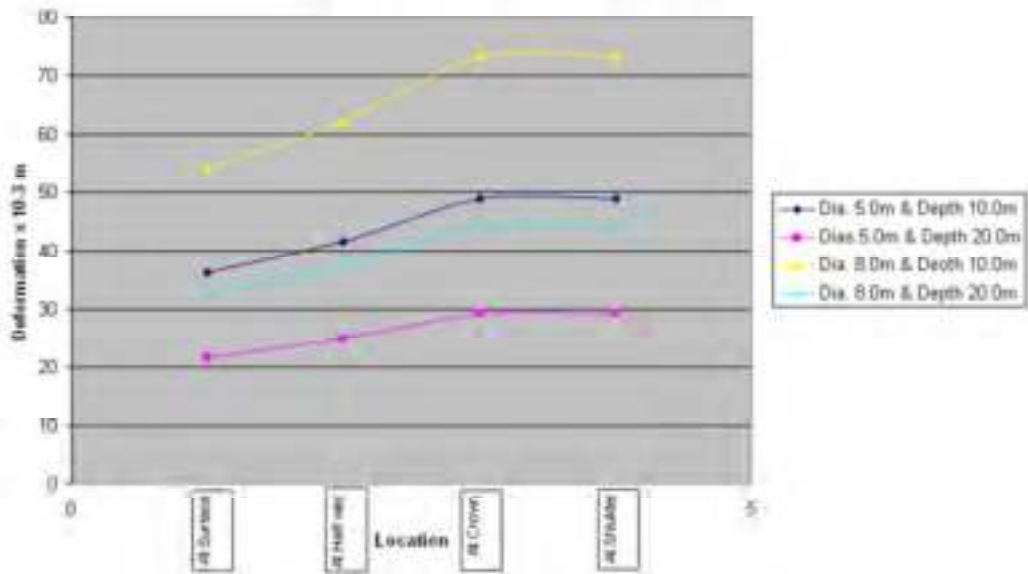
Maximum values of Deformation at Site AT



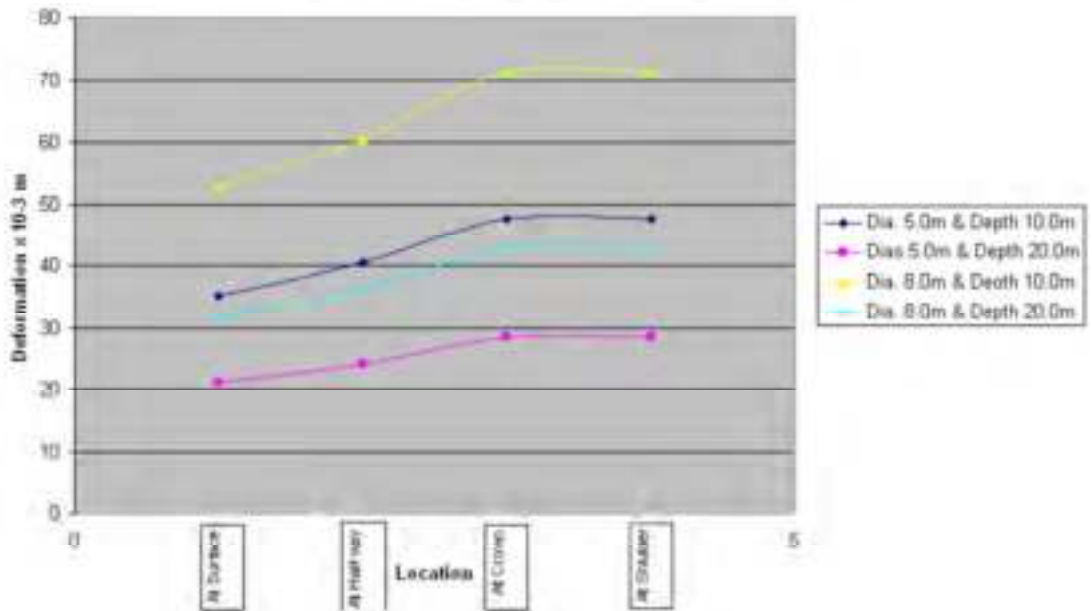
Maximum values of Deformation at Site Creek



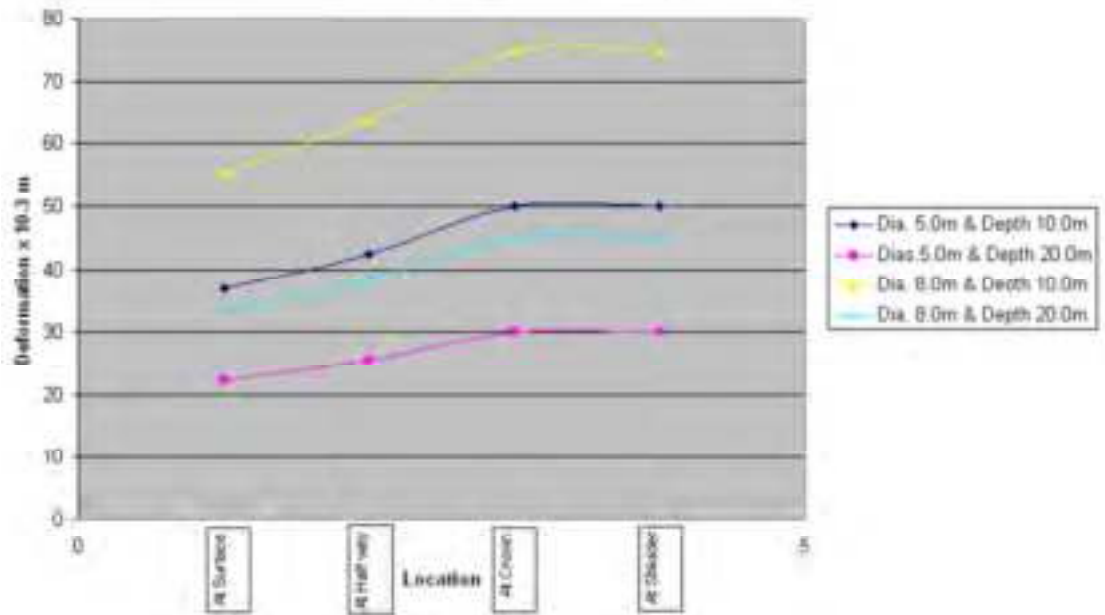
Maximum values of Deformation at Site JG



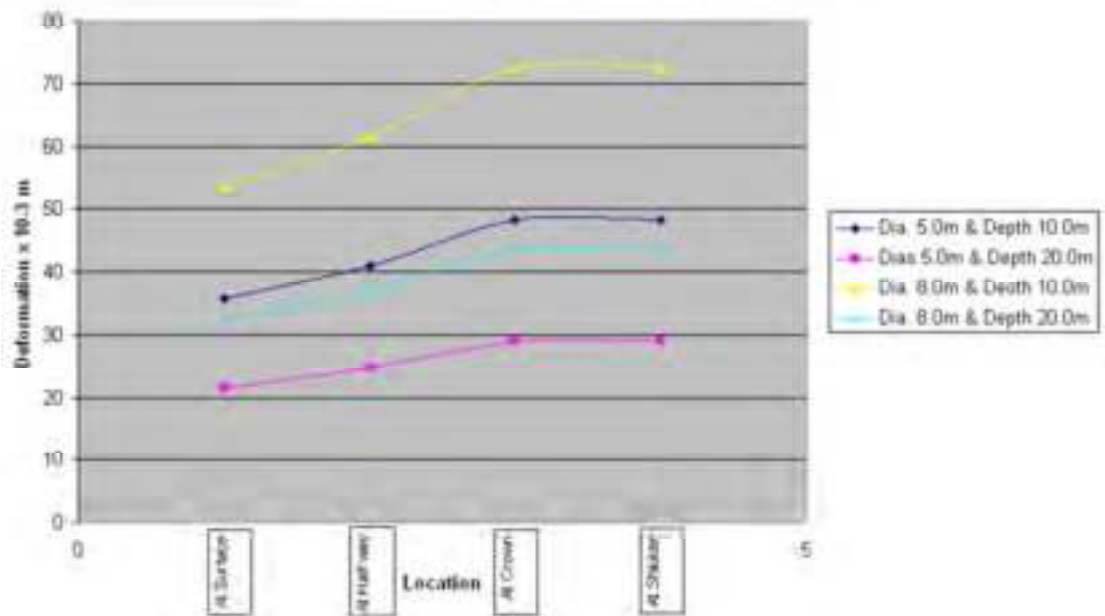
Maximum values of Deformation at Site JGc



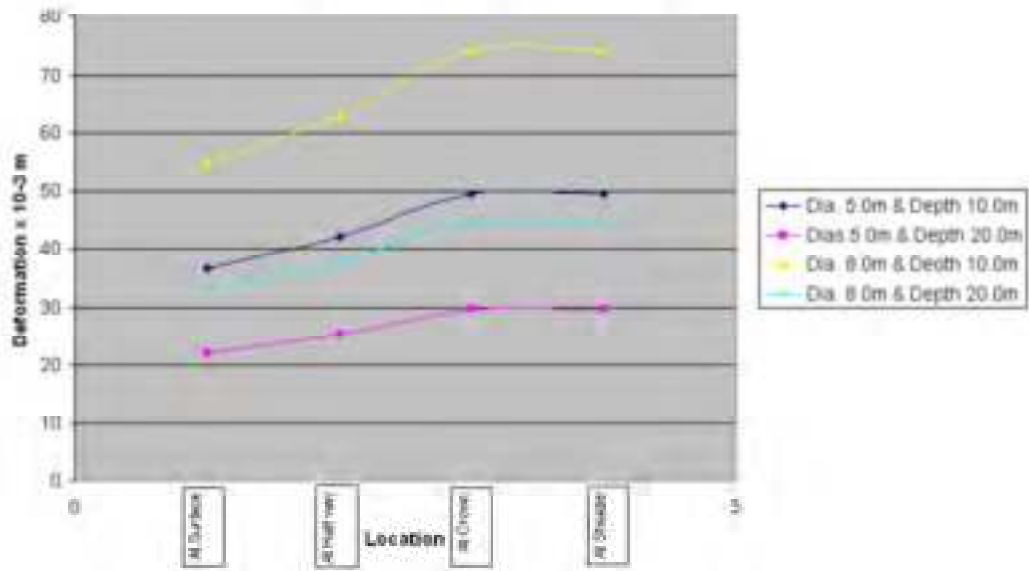
Maximum values of Deformation at Site PJA



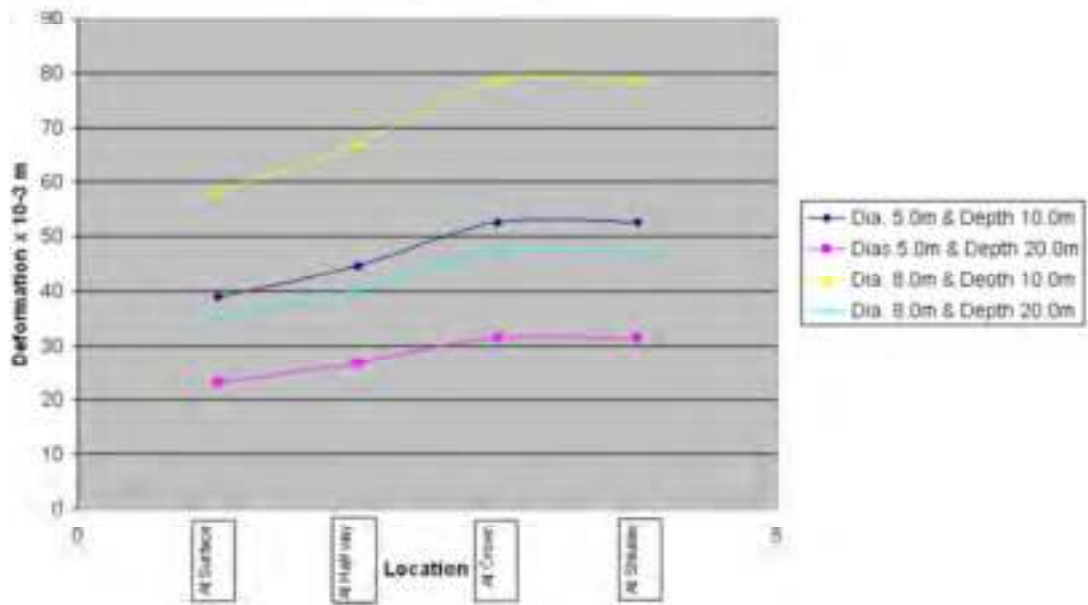
Maximum values of Deformation at Site PJAc



Maximum values of Deformation at Site TT



Maximum values of Deformation at Site TTd



Vita

Nasser Al Hai was born in the Dubai, United Arab Emirates on May 29, 1981. He graduated in the secondary level in Dubai High School in 1999. While taking up Civil Engineering Program from Higher College of Technology in college, he worked as a Junior Structural Engineer in RMJM and as a Civil Engineer at Hyder in his junior year (2003). In 2004, he graduated in the Higher Diploma with distinction. In 2005, he worked as Deputy Structural Engineer in Jebel Ali Free Zone Authority (JAFZA) and was also able to establish a pre-stressed company called Tensachai. In 2006, he was promoted Structural Engineer Manager. He also created an engineering consultancy firm called DEC Dynamic Engineering Consultancy on the same year. In 2007, he obtained a Bachelor's Degree in Applied Engineering Science Management HCT, and again graduated with flying colors.

In 2008, Mr. Al Hai joined Trakhees in the Port Custom Freezone Corporation (PCFC) and worked as Head of Building Permit, Infrastructure and Marine. In 2011, he founded a holding company called Al Hai Investment Group. Currently, he is associated with Construction Management and Contracting Company (CMCC). A man who does not run out of energy and does not tire of studying, he was able to earn another course, Master's Degree in Civil Engineering at the American University of Sharjah.